SOLUTION-PROCESSABLE RANDOM COPOLYESTERS CONTAINING PERYLENEBISIMIDE AND OLIGO(*P*-PHENYLENEVINYLENE) BY REACTIVE BLENDING

THESIS SUBMITTED TO THE

UNIVERSITY OF PUNE

FOR THE DEGREE OF

DOCTOR OF PHILOSOPHY

IN CHEMISTRY

BY

KUMARI NISHA S.

RESEARCH SUPERVISOR

DR. S. K. ASHA

POLYMER SCIENCE AND ENGINEERING DIVISION

CSIR-NATIONAL CHEMICAL LABORATORY

PUNE-411008

INDIA

MARCH 2014

Dedicated to My Parents

For their endless love and encouragement…

DECLARATION

I hereby declare that the research work embodied in the thesis entitled "***Solution-Processable Random Copolyesters containing Perylenebisimide and Oligo(p-pheneylenevinylene) by Reactive Blending***" has been carried out by me at Polymer Science and Engineering Division of CSIR-National Chemical Laboratory, Pune under the supervision of Dr. S. K. Asha. I also affirm that this work is original and has not been submitted in part or full, for any other degree or diploma to this or any other University or Institution.

Kumari Nisha S

Date: 27-03-2014 Kumari Nisha S.

Polymer Science & Engineering Division
CSIR-National Chemical Laboratory
Council of Scientific & Industrial Research
Dr. Homi Bhabha Road
Pune-411008, India

Dr. S. K. Asha
Scientist
Tel: 91-20-25902062; Fax: 91-20-25902615
E-mail: sk.asha@ncl.res.in

CERTIFICATE

This is to certify that the work embodied in the thesis entitled "***Solution-Processable Random Copolyesters containing Perylenebisimide and Oligo(p-pheneylenevinylene) by Reactive Blending***" has been carried out by **Kumari Nisha S.** under my supervision at Polymer Science and Engineering Division of CSIR-National Chemical Laboratory, Pune and the same has not been submitted elsewhere for any other degree.

Dr. S. K. Asha

(Research Supervisor)

ACKNOWLEDGEMENT

I am ever grateful to my research guide Dr. Asha S. K. for her constant encouragement and wise counsel was of immense value to me in completing this research work. I am always and ever thankful for her moral support during my Ph.D. I do sincerely acknowledge the freedom rendered by her in the laboratory for the independent thinking, planning and execution of research. Without her encouragement and constant guidance, I could not finish my doctoral degree.

I sincerely acknowledge Dr. M. Jayakannan, for his constant inspiration, helpful discussions and suggestions, and support throughout my Ph.D work that helped me a lot.

I am grateful to Dr. Sourav Pal, Director, NCL, Pune, for availing me all the laboratory facilities to do my research. I acknowledge with thanks the timely innovative suggestions given by Dr. Sivaram, Dr. Krishnamoorthy, Dr. Nithyanandhan, Dr. Satish Ogale and Dr. Wadgaonkar.

I would like to thank my all friends from NCL and IISER, especially, Rekha, Kaushal, Nagesh, Ghanashyam, Chinmay, Shekhar, Senthil, Prajitha, Saibal, Swapnil, Sandeep, Sarabjot, Vidhya, Jinish, Balamurugan, Mahima, Smita, Pramod, Ananthraj, Bapu, Narsimha, Rajendra, Bhagyashree, Vikas, Nilesh, Sonashree, Mehak and Tameez for their love, care and support which made my life memorable at NCL, Pune. I would also take this opportunity to show my sincere thanks to those who have immensely helped me at some point of time during my research. Mr. Menon, Mrs. Poorvi, Mr. Saroj, Ketan, Rounak, Yogesh, Mohan Raj, Arul, Meha and Amruta are also acknowledged.

I would like to express my warmest thanks to all my friends at NCL, especially Pragati, Bindhu, Deepa, Vinisha and Roshna chechi. My special mention goes to few more friends namely Leena chechi and Thushara chechi for their moral support in some tough situations in my life during Ph.D.

I would like to acknowledge Council of Scientific and Industrial Research (CSIR) for financial assistance and CSIR-NCL for all the laboratory facilities.

I take this opportunity to express my love and gratitude to my parents for everything I achieved in my life. Special thanks to my brother and sister (Liji chechi) for all the love and support. Last, but not least, to my dear husband, thank you for your encouragement, love and support extended to me for the successful completion of this research work.

CONTENTS

Abbreviations

η_{inh}	Inherent viscosity
$\chi 2$	Chi-square
τ	Decay time
α	Pre-exponential factor
Φ	Fluorescence quantum yield
A	Acceptor
AFM	Atomic force microscopy
BHJ	Bulk heterojunction
CHDM	1,4-cyclohexanedimethanol
$CDCl_3$	Deuterated chloroform
1D	One-dimensional
D	Donor
DCM	Dichloromethane
DMAc	N,N-Dimethylacetamide
DMCD	1,4-Dimethylcyclohexane dicarboxylate
DMF	N,N-Dimethylformamide
DSC	Differntial scanning colorimetry
FT-IR	Fourier transform infrared
g	Gram
HCl	Hydrochloric acid
HBr	Hydrobromic acid

MALDI-TOF	Matrix-assisted laser desorption ionization-time of flight
MCH	Methylcyclohexane
mg	Milligram
MHz	Megahertz
mL	Millilitre
mmol	Millimole
Mn	Number average molecular weight
Mw	Weight average molecular weight
NBI	Naphthalenebisimide
nm	Nanometer
NMR	Nuclear magnetic resonance
OD	Optical density
ODCB	Ortho-dichlorobenzene
OFET	Organic field effect transistor
OLED	Organic light-emitting diode
OPV	Oligo(*p*-pheneylenevinylene)
OPVs	Organic photovoltaics
OSC	Organic solar cell
P3HT	Poly(3-hexyl thiophene)
PBI	Perylenebisimide
PC	Bisphenol A polycarbonate
PCBM	Phenyl-C_{61}-butyric acid methyl ester

PCCD	Poly(1,4-cyclohexanedimethylene-1,4-cyclohexanedicarboxylate)
PDI	Polydispersity index
PDP	Pentadecyl phenol
PL	Photoluminescence
PLLA	Poly(L-lactic acid)
PPV	Poly(*p*-pheneylenevinylene)
PTCDI	Perylenetetracarboxylicbisanhydride
RI	Refractive index
SEC	Size exclusion chromatography
SEM	Scanning electron microscope
Tc	Crystallization temperature
T_g	Glass transition temperature
TGA	Thermogravimetric analysis
THF	Tetrahydrofuran
T_m	Melting temperature
TMS	Tetramethylsilane
TEM	Transmission electron microscopy
TFA	Trifluoroaceticacid
UV	Ultraviolet
WXRD	Wide angle X-ray diffraction

PREFACE

Ease of synthesis and film forming ability or ease of processability are very important properties that are highly desirable in organic semiconducting materials. Reasonably high molecular weight is a pre-requisite for polymeric semiconducting materials to attain this goal of easy processability. But unlike acrylic or vinylic polymers where this is true, in main chain semiconducting polymers, the π-π stacking interaction of the aromatic core results in reduced solubility and hence reduced solution processability. The π-π stacking interaction is a major hurdle to develop film forming polymers especially for n-type semiconducting materials like perylenebisimides. Perylene and naphthalene bisimides (PBI/NBI) have been attracting considerable attention as good n-type organic semiconductors because of its outstanding photophysical properties, thermal stability and ability to self-organize. Although a number of PBI main-chain polymers have been reported, most of them are only soluble in special solvents such as concentrated sulphuric acid or m-cresol, mainly due to the strong π-π stacking interaction. Another important bottleneck in the development of suitable polymeric materials for photovoltaic applications is the lack of an easy synthetic process whereby donor and acceptor incorporated polymers can be developed. An alternate method would be to blend acceptor molecules like perylenebisimide derivatives with donor polymers like poly(*p*-phenylenevinylene) (PPV) or polythiophene (PT) so as to obtain spin coatable films, but this method suffers from phase separation problems.

M. Jayakannan et.al investigated the reactive blending of bisphenol A polycarbonate (**PC**) with [poly(1,4-cyclohexylenedimethylene-1,4-cyclohexanedicarboxylate)] (**PCCD**) via a new high-temperature solution-blending methodology. This high-temperature solution-blending involved dissolving **PC** and **PCCD** in minimum amounts of a high boiling solvent like ortho-dichlorobenzene (ODCB) and heating at high temperature (150-185°C) in presence of a transesterification catalyst. They showed that ester-carbonate interchange occurred via transesterification in these blends. Using model reactions they showed that both alcoholysis and transesterification were amenable under these reactive blending conditions. We were motivated to apply this methodology to incorporate suitably functionalized semiconducting materials – both donor and acceptor type, on commercially available polyesters backbone.

This thesis has been divided in to four major sections:

1. Synthesis of a series of random donor-acceptor copolymer incorporating oligo(*p*-phenylenevinylene) (OPV) and perylenebisimide (PBI) by a facile one-pot high-temperature solution-blending approach.
2. Study the chirality induced self-assembly of linear π-conjugated systems like oligo(*p*-phenylenevinylene) in solid state.
3. Development of a novel luminescent flexible film and nanofibers for advanced photonic applications.
4. Study the photo-induced energy transfer and photo-induced charge separation in the donor-acceptor polyesters.

This thesis work has been organized in six chapters. Chapter-1 start with a brief introduction to organic semiconductors and their application in organic devices. Detailed literature surveys on different types of organic semiconductors which are commonly used in electronic devices, their properties and limitations have been discussed. This chapter provides literature survey on the self-assembly of π-conjugates in solid state and one-dimensional (1D) self-assembly of organic molecules and their application in electronic devices. The energy- and electron-transfer process in donor-acceptor system is discussed. Towards the end, reactive blending has been discussed as an important approach for synthesizing new polymer for scale-up and commercialization.

In the second chapter, a high-temperature solution-blending process has been used to synthesize a series of copolymers incorporating varying mole ratios of perylenebisimide (PBI) into the backbone of an engineering thermoplastic polyester [Poly(1,4-cyclohexylenedimethylene-1,4-cyclohexanedicarboxylate)] (**PCCD**). A random donor-acceptor copolymer incorporating oligo(*p*-phenylenevinylene) (OPV) and PBI was also synthesized. The chemical incorporation of these chromophores into the polyester backbone was proved by carrying out the melt polycondensation from the monomers 1,4-cyclohexanedimethanol (CHDM) and 1,4-dimethylcyclohexane dicarboxylate (DMCD) with varying mole ratios of terminal hydroxyl functionalized PBI and OPV derivatives. Polymers synthesized using high-temperature solution-blending approach possessed the required thin film processability. The structural differences between the polymer synthesized by high-temperature solution-bending and melt polycondensation were studied.

The third chapter describes the synthesis and self-assembly of a series of copolyesters incorporating varying mol ratios of an achiral oligo(*p*-phenylenevinylene) (OPV) into the backbone of a chiral poly(L-lactic acid) (**PLLA**) via high-temperature solution-blending. Absorption, emission and lifetime-decay studies showed that OPV chromophore was highly aggregated in the solid state. Circular dichroism (CD) spectroscopy, scanning electron microscopy (SEM) and atomic force microscopy (AFM) studies revealed that the **PLLA-OPV** copolyester formed self-assembled architecture in which the helical organization of the achiral OPV segments was dictated by the chiral **PLLA** segments. The observed CD signal and AFM image accounted for right-handed helical self-assembly of OPV chromophore in the solid state. These results confirmed the effect of chiral **PLLA** segment on tuning the OPV chromophore packing and supramolecular chirality in molecular aggregates. The methodology illustrated here provides opportunities for the design of a new class of hierarchical self-assembled architectures based on organic π-conjugated materials and the manipulation of their optical properties. Strong blue and green fluorescent nanofibers of copolyester incorporating OPV chromophore were successfully constructed by electrospinning technique.

The fourth chapter deals with the synthesis of a series of high molecular weight random copolyesters of **PLLA** and **PCCD** incorporating varying mol ratios of perylenebisimide (PBI) into the backbone of **PLLA** and **PCCD** via high-temperature solution-blending. The polymers were characterized by ^{1}H NMR spectroscopy and size exclusion chromatography (SEC) and their bulk properties were investigated by differential scanning calorimetry (DSC) and wide-angle X-ray diffraction (WXRD). These polymers showed good solubility in common organic solvents and formed free-standing transparent and flexible films. Bright red photoluminescence was observed for all these films upon irradiation with ultraviolet radiation. The photophysical properties were studied using steady-state UV-vis absorption and fluorescence spectroscopy in solution as well as in solid state. Strong red fluorescent nanofibers of these polymers were successfully constructed by electrospinning technique. The nanofiber fabricated from random copolyester incorporating both OPV and PBI exhibited blue, green and red emission upon excitation at different wavelengths. The luminescent colour of the nanofibers can thus be tuned by the suitable choice of chromophores. The approach described here is easily adoptable for a wide range of

π-conjugated chromophores to achieve the goal of easy fabrication to 1D nanostructure with strong photoluminescence.

In the fifth chapter, novel copolyesters consisting of oligo(*p*-phenylenevinylene) (OPV) as donor (D) and perylenebisimide (PBI) as acceptor (A) were synthesized by melt polycondensation. Photo-induced energy transfer and photo-induced charge separation in these polyesters were studied in solution as well as in the solid state. Selective excitation of OPV moiety resulted in the energy transfer efficiency of > 90% from OPV to PBI chromophore in the solution state. The photo-induced energy transfer process in solution state was supported by fluorescence lifetime decay studies. The HOMO and LUMO values of polyesters were calculated from cyclic voltammetry. A strong fluorescence quenching (~ 100 %) of both chromophores in solid state indicated an efficient photo-induced charge transfer after photoexcitation of either donor or acceptor. Reactive blend of donor/acceptor copolyester was also prepared by the transesterification reaction between donor and acceptor alone copolyesters. The energy transfer efficiency from donor to acceptor moiety upon selective excitation of donor chromophore in the donor/acceptor copolyester blend was four times higher compared to a physical mixture of donor and acceptor alone copolyesters, which gives the direct proof for the transesterification reaction in polyester/polyester reactive blending.

The last chapter summarizes the outcome of research work carried out in the Ph.D. thesis.

Chapter 1

Introduction and Literature Survey

1.1. General Introduction to Organic Semiconductors

Organic electronics has emerged as a vibrant field of research and development, and technology.[1-6] An organic semiconductor is an organic material with semiconductor properties, that is, with an electrical conductivity between that of insulators and metals. This means the traditional (semi)conducting inorganic materials such as silicon, copper or metal oxides are replaced by organic materials (small molecules, oligomers or polymers). In comparison to the inorganic counterparts, organic materials possess reduced conducting properties, but they exhibit a lot of advantages that enable novel applications, such as organic devices on flexible or transparent foils.[7, 8] The fabrication of organic devices is simple: the organic material is deposited on top of a transparent electrode and eventually a cathode is evaporated. The final device is extremely thin and thus lightweight. Generally there are two competing processing technologies: (1) gas-phase deposition (such as thermal evaporation of small molecules) and (2) solution-based methods (such as printing of "organic inks"). Whereas the first method allows for easy processing of several materials on top of each other, the second promises cost-effective and fast production.[8, 9] Organic electronics is still a young field of technology including devices such as organic field effect transistors (OFETs), organic solar cells (OSC) or organic light-emitting diodes (OLEDs). These devices enable new applications and design possibilities, for example in the field of portable electronics, large area lighting, flexible displays or energy production.

1.2. Organic photovoltaic Materials

The need to develop inexpensive renewable energy sources stimulates scientific research for efficient, low-cost photovoltaic devices.[10] Currently, most commercial solar cells are made from a refined, highly purified silicon crystal, similar to the material used in the manufacture of integrated circuits and computer chips (wafer silicon). The high cost of these silicon solar cells and their complex production process has generated interest in developing alternative photovoltaic technologies.[11] Organic solar cell technology is a promising candidate for the solar energy conversion compared to its inorganic counterparts due to its low cost, light weight, and potential use in flexible devices.[10-15] Like inorganic PVs, organic devices are made by creating interfaces of an electron-rich material (p-type) with an electron-poor material (n-type). The bulk heterojunction (BHJ) solar cell has become one of the most successful device structures developed to date. In this device structure, the blend of donor and

acceptor or donor-acceptor polymer is used as active layer. The chemical structure of various conjugated polymers and oligomers commonly used in organic solar cell have been summarized in the scheme 1.1.[8]

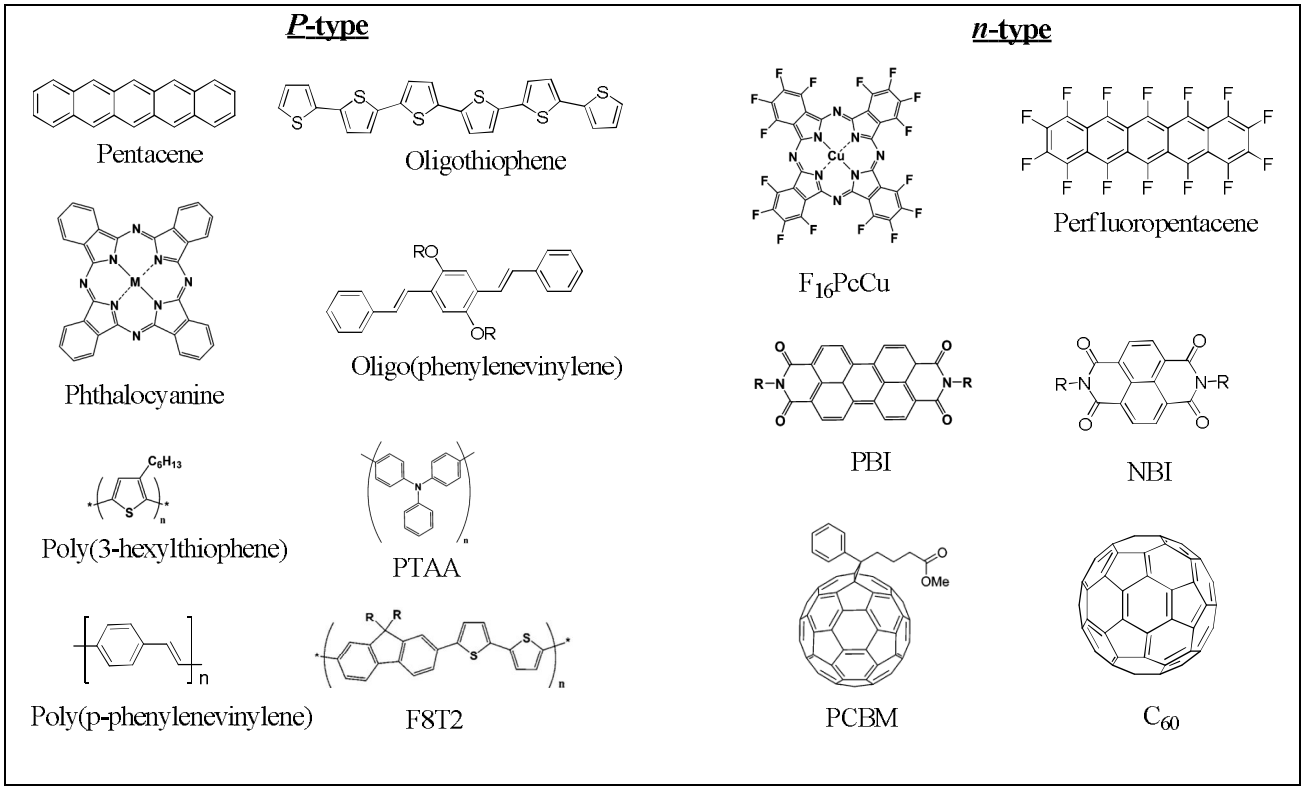

Scheme 1.1. *Various conjugated polymers and oligomers used in organic solar cells (Adapted from Chem. Rev.* ***2007****, 107, 1324-1338).*

Important representatives of hole conducting semiconductors are phthalocyanines, pentacene, oligothiophene, oligofluorene, oligo(phenylenevinylene), derivatives of thiophene chains such as poly(3-hexyl thiophene), derivatives of phenylenevinylene backbones such as poly[2-methoxy-5-(3,7-dimethyloctyloxy)]-1,4-phenylenevinylene) (MDMO-PPV) and derivatives of fluorene backbones such as (poly(9,9′-dioctylfluorene-co-bis- N,N′-(4-butylphenyl-1,4-phenylenediamine) (PFB) etc.[8] Much of the focus has been on the development of p-type semiconductors that have seen a dramatic rise in performance over the last decade. Much less attention has been devoted to electron transporting materials. The reported n-type organic semiconductors are PCBM (phenyl-C_{61}-butyric acid methyl ester), perylenebisimide, naphthalanebisimide and perfluoropentacene etc. The most used acceptor material in organic solar cells is PCBM, which is soluble in organic solvents.[16, 17] The success

of PCBM as a champion acceptor for OSCs is due to its ability to accept electrons from semiconducting polymers at ultrafast time scales, and the nano-scale interpenetrating network that it forms with these polymers. However, PCBM suffers from disadvantages including high energy costs for material production and poor absorption in the visible spectrum. Perylene and naphthalene bisimides (PBI/NBI) have been attracting considerable attention as good n-type organic semiconductors because of its out-standing photophysical properties, thermal stability, and ability to self-organize.[18-23]

1.3. Operating principles of organic solar cell

This section will deal with the material and device requirement for one of the organic photovoltaic device i.e solar cell.[24, 25] The process of conversion of light into electricity by an organic solar cell can be described by the following steps: absorption of a photon leading to the formation of an excited state, that is, the bound electron-hole pair (exciton) creation; exciton diffusion to a region where exciton dissociation, that is, charge separation occurs; and charge transport within the organic semiconductor to the respective electrodes.[8] The photo-induced charge transfer from poly(*p*-pheneylenevinylene) (PPV) (donor) to C_{60} (acceptor) is depicted schematically in figure 1.1 together with the energetic description.

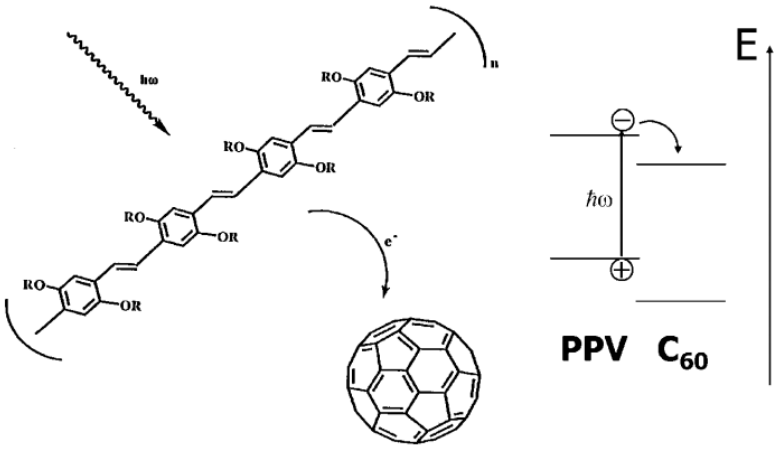

***Figure 1.1**. Illustration of the photo-induced charge transfer (left) with a sketch of the energy level scheme (right). After excitation in the PPV polymer, the electron is transferred to the C_{60} due to its higher electron affinity (Adapted from J. Mater. Res. **2004**, 19, 1924-1945).*

Donor and acceptor molecules must be well-mixed in bulk heterojunctions on the length scale of 10-20 nm in each domain because exciton recombination significantly increases when the domain sizes of the donor or acceptor materials exceed the exciton

diffusion length.[26, 27] The charge carrier mobilities of crystalline organic semiconductors are higher than amorphous semiconductors because of strong π-π interactions.[28, 29] But, the photovoltaic properties of crystalline conjugated polymers with higher carrier mobilities are not always good due to macrophase separation of the active layers during post-fabrication treatment process.[30, 31] Active layers consist of conjugated polymers as donors and fullerenes as acceptors often form complicated morphologies that typically arise from limited polymer:fullerene miscibility, resulting in phase-separated polymer and fullerene-rich domains.[32, 33] An active layer incorporating phase-separated domains in a solar cell can affect the device performance because these domains provide not only interfaces for charge separation of photogenerated excitons but also percolation pathways for charge carrier transport to the respective electrodes. The former requires a fine dispersion of fullerene units in the polymer, due to the short exciton diffusion length in the polymer (≤ 10 nm), while the latter requires fullerene domain to form complementary interpenetrating networks for charge transport to the respective electrodes to avoid charge recombination.[34]

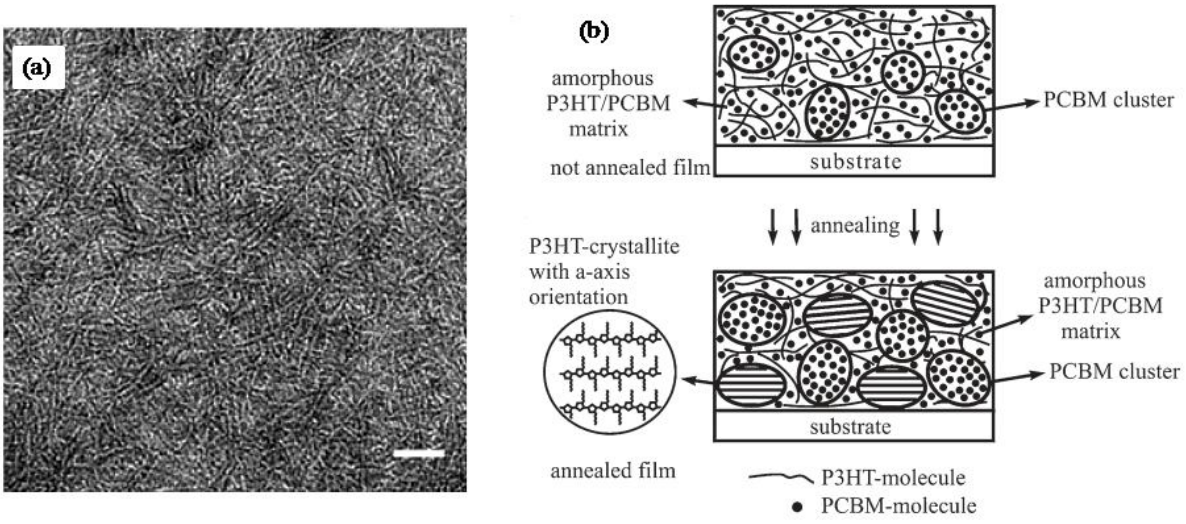

Figure 1.2*. (a) Bright-field TEM image of a thermally annealed P3HT:PCBM film. The scale bar is 200 nm (Adapted from Nano Lett.* ***2009****, 9, 507-513); (b) schematic drawings of the hierarchical structure in the nanometer-scale morphology in pristine and annealed P3HT:PCBM films (Adapted from Adv. Mater.* ***2009****, 21, 1323-1338).*

Figure 1.2 (a) shows the bright-field TEM image of an annealed regioregular poly(3-hexyl thiophene) (P3HT):PCBM photoactive layer; the P3HT fibers and PCBM-rich domains are clearly discernable as bright and dark regions, respectively, because of their different densities.[32] Figure 1.2 (b) shows a schematic drawing of a hierarchical P3HT:PCBM

microstructure.[33] In a pristine film, the fullerene moieties can disperse individually or form aggregated domains intercalated between P3HT lamellae and amorphous polymer chains. The sizes of the aggregated fullerene and P3HT lamellae domains show increase after thermal annealing. One way to overcome these drawbacks is by covalently linking the donor (D) and acceptor (A) in a single polymer chain.[35-38] The covalent bond enables a predefined control over the characteristic distance between donor and acceptor and thereby the extent of phase separation.

Polymers are attractive for organic photovoltaics because thin films of these materials can be obtained through simple solution techniques such as drop casting, spin-coating and ink printing etc. But the mobilities are usually lower than the small molecules due to the poor molecular ordering and low crystallinity obtained by the solution techniques.[39-41] Therefore, apart from designing suitable chemical structures, self-organization of molecules in the solid state remains a major challenge before π-conjugated organic materials can be utilized for actual application in molecular electronics.

1.4. Self-assembly of Organic Semiconductors

Self-assembled supramolecular structures of π-conjugated molecular building blocks are a promising class of materials to improve the solid-state organization of future optoelectronic materials.[42-45] Over the past decade, several noncovalent interactions such as hydrogen bonding, electrostatic interactions, π-π stacking, dipolar interactions, chirality, and so forth, have been identified as enabling the construction of various hierarchical architecture from specially engineered small molecule building blocks.[46-49] Oligofluorenes, oligothiophenes, oligophenylenes and oligophenylenevinylenes were reported for chiral self-organization in π-conjugated materials.[50-52] High luminescent characteristics, thermal and optical stability, film forming tendency and solubility in organic solvents make oligo(*p*-phenylenevinylene) (OPV) chromophore very unique compared to other 'p' type π-conjugates.[53, 54]

The self organization of oligo(*p*-phenylenevinylene) (OPV) chromophore via hydrogen bonding, π-π stacking and metal-ion interactions etc has been reported and the resultant structure were tested successfully as active layer in electronic devices.[55, 56] Meijer and co-workers have made significant contributions to the helical self-assembly of π-conjugated oligomers derived from phenylenevinylenes, where the chirality of the attached side chains was translated to the conjugated oligomer backbone at a supramolecular level.[57,

[58] They reported the synthesis and characterization of three hydrogen-bonded oligo(*p*-phenylenevinylene)s, **OPV3**, **OPV4**, and **OPV5**, that differed in conjugation length [figure 1.3 (a)].[58] All three compounds possessed chiral side chains, long aliphatic chains, and an ureido-s-triazine hydrogen bonding unit. ^{1}H NMR and photophysical measurements showed that the OPV oligomers grew hierarchically in an apolar solvent; initially, dimers were formed by hydrogen bonds that subsequently developed into stacks by π-π interactions of the phenylenevinylene backbone with induced helicity via the chiral side chains [figure 1.3 (b)].

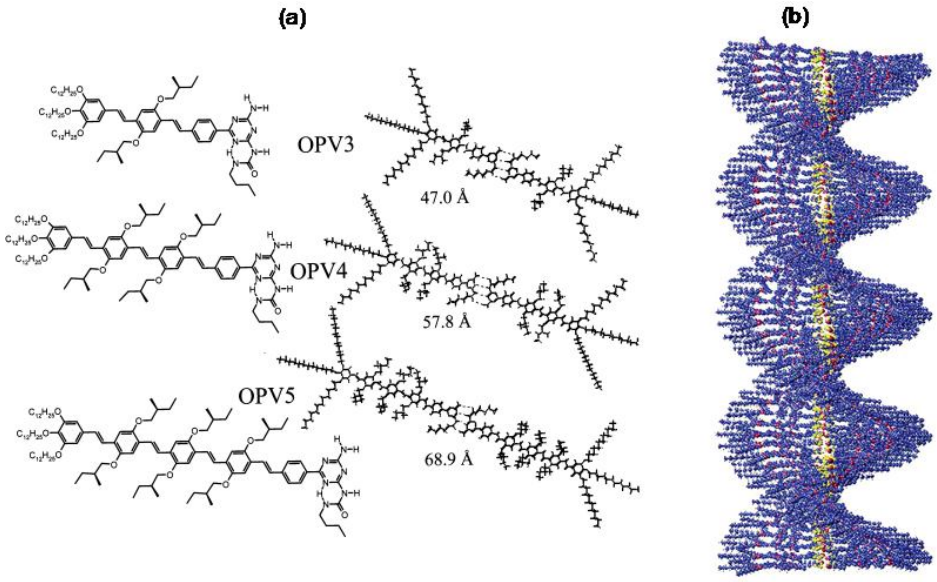

***Figure 1.3**. (a) Molecular structures of **OPV3**, **OPV4**, and **OPV5** as calculated by molecular dynamics and subsequent energy minimization at 300 K for 50 ps; (b) self-assembled helical columnar architectures at low temperatures simulated for stacked **OPV4** dimers (Adapted from J. Am. Chem. Soc. **2003**, 125, 15941-15949).*

Ajayaghosh and co-workers described the hierarchical growth of left-handed helical nanostructures of chiral oligo(*p*-phenylenevinylene)s (OPVs).[59] Three different OPVs with remote chiral handles, **C-OPV1**, **C-OPV2**, and **C-OPV3** were prepared and the structures of the molecules are shown in figure 1.4 (a). **C-OPV2**, with hexadecyl side chains, was able to form stable aggregates in solution (as evident from optical studies). **C-OPV1**, with dodecyl side chains, was found to be a better gelator than **C-OPV2**, and formed a yellow fluorescent gel in nonpolar solvents, such as dodecane, heptane, and cyclohexane [figure 1.4 (b)]. However, **C-OPV3**, which is substituted with six chiral side chains, failed to form a gel in any of the solvents. AFM analysis of the **C-OPV1** gel from dodecane (6.5×10^{-3} M) clearly showed the formation of entangled left-handed-helical coiled-coil fibers of 50-100 nm in

diameter [figure 1.4 (c)]. Careful analysis of a single fiber showed the morphology of a left-handed coiled-coil rope of approximately 90 nm width and 11 nm height [figure 1.4 (d)]. These observations point towards a hierarchical self-organization of the **C-OPV1** into coiled-coil aggregates of nanometer dimensions.

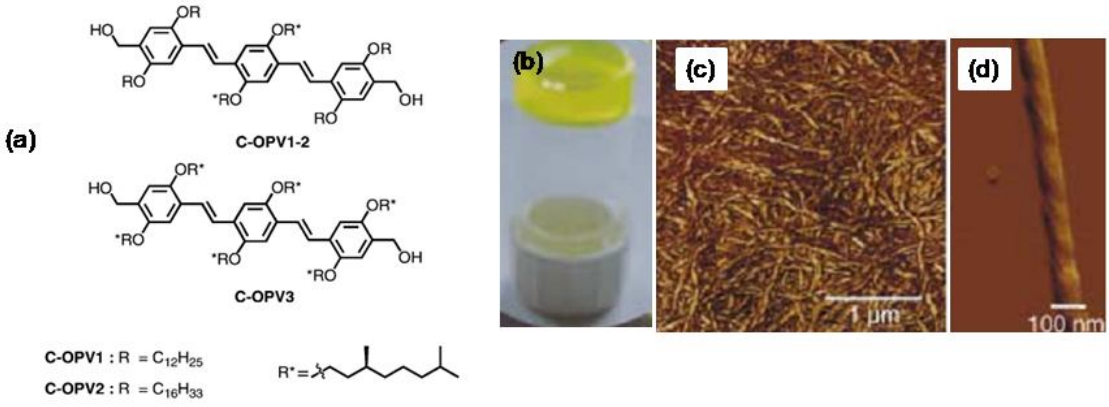

Figure 1.4*. (a) Structures of chiral OPV derivatives; (b) photograph of the gel from* ***C-OPV1*** *in dodecane solution (6 x* 10^{-3} *M); (c) dense network of helical fibers and (d) single left-handed coiled-coil rope of the* ***C-OPV1*** *(Adapted from Angew. Chem. Int. Ed.* ***2004****, 43, 3421-3425).*

A different approach towards helical system is to use host-guest chemistry to induce tunable chirality to the achiral host by specific recognition of appropriate chiral guest molecules. S. J. George and co-workers reported the adenosine phosphate induced one-dimensional (1D) self-assembly and the resultant supra-molecular chirality of naphthalenebiimide (NBI) amphiphiles i.e. **NDPA-Amph** and **NDPA-Bola** [figure 1.5 (a)].[60] Extensive studies on molecular phosphate sensors suggested that the dipicolylethylenediamine-zinc complex (DPA-Zn) motif can specifically bind to various adenosine phosphates with high association constants.[61] Hence they designed NBI amphiphiles substituted with DPA-Zn motifs, in order to promote guest induced self-assembly and chiral induction through specific binding interactions. The binding of multivalent chiral phosphates resulted in high chiral order, as evident from the excitonic, bisignated circular dichroism signals, in the resulting NBI assemblies. Transmission Electron Microscopy (TEM) imaging of **NDPA-Amph** (70% water in THF, 7 x 10^{-5} M) assemblies with 0.5 equivalents of ADP, stained with uranyl acetate showed the formation of 1D nanofibers with a uniform diameter of 8 nm [figure 1.5 (b) and (c)]. TEM analysis of **NDPA-Bola/ADP** co-assemblies revealed the formation of fibers with 4 nm diameter, suggesting

that they were constructed from single NBI π-stacked columns with bound adenosine phosphates on both DPA-Zn sites.

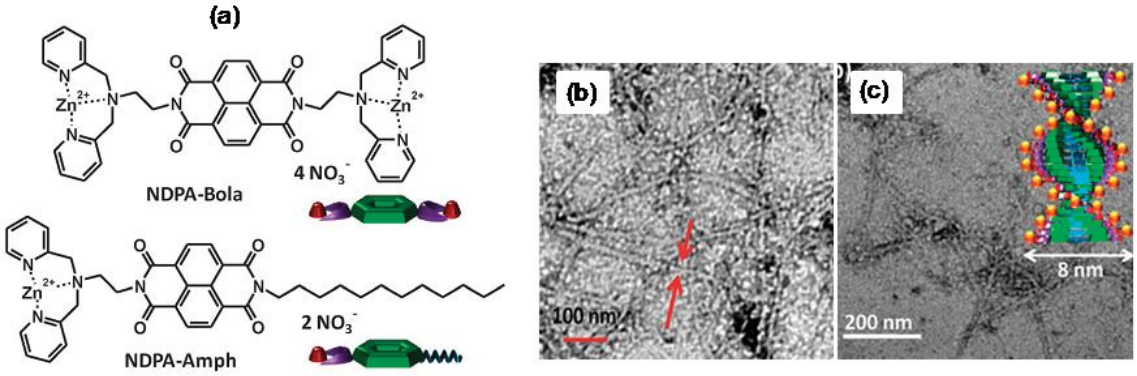

Figure 1.5*. (a) Molecular structures of* ***NDPA-Bola*** *and* ***NDPA-Amph****; (b) and (c) TEM images (7 x 10^{-5} M solution) of* ***NDPA-Amph****/0.5 equivalents of ADP (70% water in THF). Inset of (c) shows the schematic of the corresponding helical stack (Adapted from Chem. Commun.* ***2012****, 48, 10948-10950).*

Another category that has received lot of attention is the helical self-assembly of the achiral π-conjugated oligomers by the chiral peptide segments.[62-64] R. J. Kumar and co-workers determined the ability of semiconductors templated by α-helical polypeptides to form higher order structures and the charge carrier properties of the supramolecular assemblies.[64] L-lysine was functionalized with a sexithiophene organic semiconductor unit via iterative Suzuki couping and the click reaction. The resultant amino acid was incorporated into a homopolypeptide by ring-opening polymerization of an amino acid N-carboxyanhydride and the structure of the polymer is shown in figure 1.6. Spectroscopic investigation of the polypeptide revealed that it adopted an α-helical secondary structure in organic solvents that underwent hierarchical self-assembly to form higher order structures as shown in figure 1.6. In cyclohexane, the polymer formed organogels at 2% (w/v). Organic photovoltaic and organic field effect transistor devices were fabricated by deposition of the PCBM blended active layer from chlorobenzene at concentrations shown to induce self-assembly of the polymer. Compared with control compounds, these devices showed significantly greater hole mobility, short circuit current, and efficiency.

Though, supra-molecular assemblies have been obtained by different approaches, all of them are synthetically challenging. Hence, construction of highly ordered solid state

structures of π-conjugates by using a simple approach is still a challenging problem to be addressed.

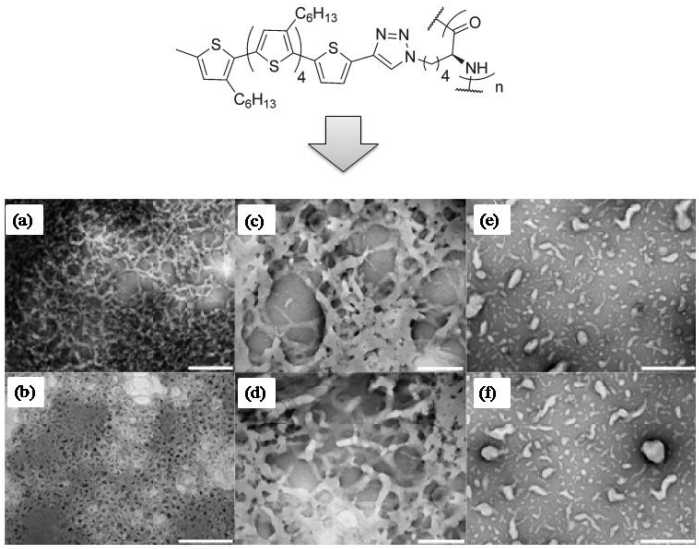

Figure 1.6*. Self-organization of polymer as visualized by negative staining (uranyl acetate in EtOH) TEM of samples deposited from solutions in cyclohexane; (a)-(d) 2.1 x 10^{-5} M; (e) and (f) 1.0 x 10^{-5} M. Scale bar (a), (b): 500 nm; (c), (d): 200 nm; (e), (f): 500 nm (Adapted from J. Am. Chem. Soc.* ***2011****, 133, 8564-8573).*

1.5. Highly Fluorescent 1D Nanostructures of Organic Semiconductors

Inorganic nanowires have been extensively investigated for the linear optical properties, which can potentially be employed in various nanodevice applications including laser, waveguide, and polarized emission.[65-67] The same research has been much less advanced for the organic counterparts.[68] The device application concerned with the linear optical properties, particularly those based on fluorescence emission, demands that the organic nanomaterials thus fabricated be highly fluorescent.[69, 70] Although various small molecules, oligomers and conjugated polymers have been fabricated into 1D nanostructure, most of the π -conjugated molecules lose their strong fluorescence upon being assembled into the solid state.[71-73] The challenge is thus to find building-block molecules that are not only suited for fabrication into 1D structure but also, enable strong fluorescence in the solid state.

Several classes of organic materials with high p-type charge carrier mobility have been known for long time; their n-type counterparts have become available only recently. Perylenebisimides (PBI) is the basis for a class of n-type chromophores exhibiting relatively

high electron mobility, large molar absorption coefficients, fluorescence quantum yield as well as good thermal and photochemical stabilities.[18-20] L. Zang and co-workers reported the fabrication of ultralong nanobelts (>0.3 mm) from an asymmetric perylenebisimide derivative, shown in figure 1.7 (a).[74] The polyoxyethylene side-chain attachment made the molecule highly soluble in hydrophilic solvents such as ethanol. Self-assembly of the nanobelts of this molecule was performed through a solvent exchange processing, in which the molecules were transferred from a "good" solvent (such as ethanol) into a "poor" solvent (such as H_2O) where the molecules had limited solubility and therefore self-assembled into 1D nanobelts via molecular stacking. Figure 1.7 (b) shows the ultralong nanobelt structure obtained from the self-assembly of this molecule in a 1:1 water:ethanol solvent and figure 1.7 (d) shows the emission photograph taken for the nanobelt suspension (under irradiation of 366 nm UV light), where the fluorescence was quenched as expected.

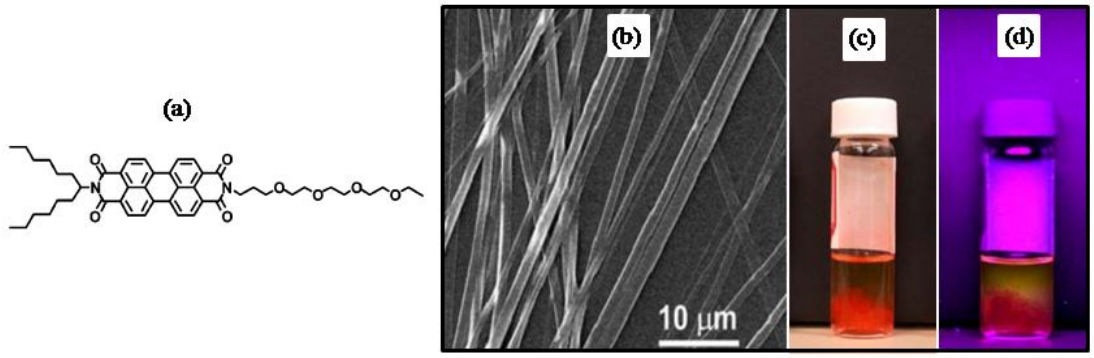

Figure 1.7*. (a) Molecular structures of perylenebisimide derivative; (b) SEM image showing the belt morphology and uniform size of the nanobelts; (c) photograph taken for the nanobelts formed and suspended in 1:1 water:ethanol; (d) the emission photograph taken for the same samples under irradiation of a 366 nm UV light (Adapted from J. Am. Chem. Soc.* ***2007****, 129, 7234-7235).*

F. Würthner and co-workers synthesized a highly fluorescent perylenebisimide based organogelator (**PBI1**), shown in figure 1.8.[75] UV/Vis studies revealed more pronounced aggregation in apolar solvents like MCH due to intermolecular π-π stacking and hydrogen bonding interactions. On the other hand, in polar solvents like acetone and dioxane, participation of the solvent molecules in hydrogen bonding significantly reduced the aggregation propensity but enforced the gel formation at higher concentrations [figure 1.8 (a)]. Although highly fluorescent organogels can feasibly be fabricated from the PBIs modified with substituents at the bay positions, the twisted conformation of the PBI backbone

distorted the π-π stacking, thus preventing the formation of well-defined nanowires in straight geometry suited for nanodevices fabrication [figure 1.8 (b) and (c)].

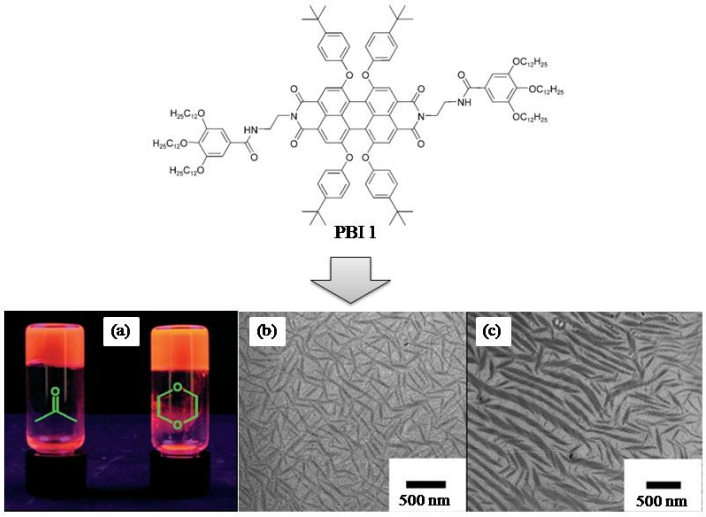

***Figure 1.8**. (a) Photographs of **PBI1** in different solvents under a UV lamp (366 nm); (b) and (c) TEM images of **PBI1** in MCH (1 x 10^{-4} M) and acetone (1 x 10^{-3} M) respectively (Adapted from Chem. Eur. J. **2008**, 14, 8074-8078).*

Strong fluorescent nanofibers have recently been fabricated from a half-hydrolyzed PBI modified with branched side-chains in appropriate size (e.g., hexylheptyl) as shown in figure 1.9.[76] This molecule possessed a structure that provided a good balance between the molecular stacking and the fluorescence yield of the materials thus assembled. The former prefers a molecular structure with minimal steric hindrance (usually referring to a small or linear side chain), while the latter favors bulky, branched side chains that may distort the π-π stacking to afford increased fluorescence (by enhancing the low-energy excitonic transition) for the molecular assembly. Figure 1.9 (a) shows the scanning electron microscopy (SEM) image of the nanofibers fabricated from this molecule through a vapor-diffusion (slow solvent exchange) process. The average diameter of the nanofibers is ~350 nm as determined by zoom-in SEM imaging as shown in figure 1.9 (b). These nanofibers demonstrated strong fluorescence with yield ~15% as depicted in the fluorescence microscopy images [figure 1.9 (c) and (d)], implying a distorted molecular stacking that is usually observed for the PBIs modified with branched side chains. However, the nanofibers fabricated were highly curved and entangled together, probably because of the asymmetric structure of the molecules. Although the entangled nanofibers demonstrated potential applications in fluorescence

sensing of gaseous reagents, the curved shape made them less suited for application in 1D confined optical nanodevice.

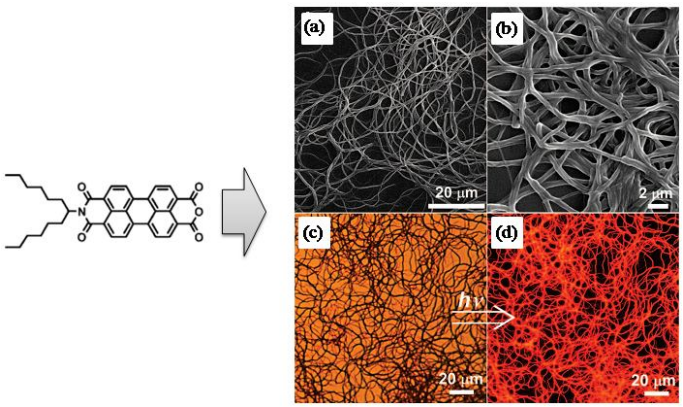

***Figure 1.9**. (a) SEM image of the nanofibril film deposited on a glass slide; (b) zoom-in SEM image of the nanofibril film; (c) and (d) bright-field and fluorescence optical microscopy image of a nanofibril film respectively (Adapted from Nano Lett. **2008**, 8, 2219-2223).*

L. Zang and co-workers recently reported the fabrication of well-defined nanobelts from the flip-flap stacking of a cyclohexyl substituted molecule, **CH-PTCDI**, as shown in figure 1.10 (a).[77] The nanobelts demonstrated long, straight belt-like morphology with length of hundreds of micrometers and width of 250-1500 nm [figure 1.10 (b)]. In contrast to the weak fluorescence emission (with quantum yield <1%) previously observed for the self-assembled materials of PBIs, which mostly adopted the translated stacking, these nanobelts demonstrated dramatically increased emission (with quantum yield of ca. 17%), which could easily be imaged with a fluorescence microscope [figure 1.10 (c)]. The increased fluorescence of these new nanobelts is attributed to the flip-flap stacking mode, which was believed to be effective for enhancing the fluorescence by strengthening the low-energy excitonic transition.

Even though well-defined highly fluorescent 1D nanostructure has been recently fabricated from various symmetric and asymmetric PBIs, there is no such 1D self-assembly reported for PBI based polymers. PBI small molecules possess specific electronic and optical properties due to their well-defined chemical structure. However, the material properties of small molecules are generally secondary to those of their polymeric analogues, since entanglements of macromolecular chains, which are responsible for the typical polymer properties, are lacking. Hence more intellectual input is required for developing fluorescent

1D nanostructure from PBI based polymers which would be really promising for many applications.

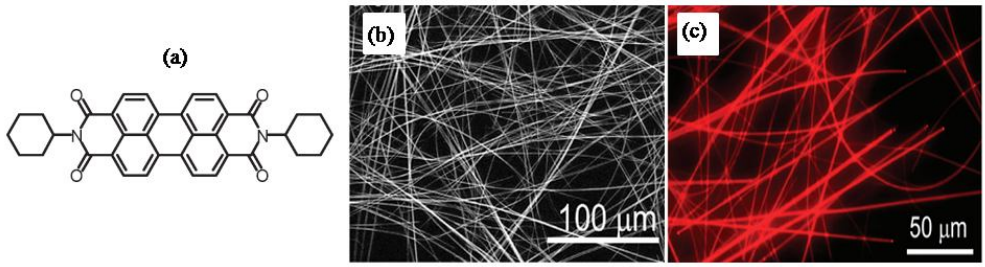

***Figure 1.10**. Molecular structure of **CH-PTCDI**; (b) large area SEM image showing the long nanobelts deposited on a glass slide; (c) fluorescence microscopy image of nanobelts cast on glass slide (Adapted from Chem. Mater. **2009**, 21, 2930-2934).*

1.6. Photo-induced Energy- and Electron-Transfer in Donor-Acceptor System

Energy- and electron-transfer processes between a donor and an acceptor play a fundamental role in most of the applications such as OLEDs and solar cells as well as in basic biological process such as photosynthesis.[78-82] Therefore, a systematic design and study of tailor-made donor-bridge-acceptor (DBA) model systems are required for understanding these key processes. Photo-induced energy transfer between donor and acceptor was studied as early as 1940.[83, 84] The nonradiative energy transfer due to dipole-dipole interactions in donor-acceptor mixtures and bridged systems within a range of about 10 nm can be explained by Förster transfer. Here, the rate of energy transfer (k_T) is extremely dependent on the distance R between the moieties ($k_T \propto R^{-6}$). Photo-induced electron transfer was also reported in different types of donor-acceptor systems.

Thelakkat and co-workers have reported the photo-induced energy- and electron-transfer in DBA molecule containing tetraphenylbenzidine (TPD) and perylenebisimide (PBI).[85] The structure of the molecule is shown in figure 1.11. The energy transfer efficiencies in DBA determined using different methods such as (i) decrease in donor lifetime, (ii) decrease in donor fluorescence intensity, and (iii) increase in acceptor fluorescence intensity lie close to >90%. The schematic representation of the photo-induced energy- and electron-transfer observed in DBA molecule is shown in figure 1.11 (d) and (e).

In figure 1.11 (d), the energy is transferred from the excited D to A and figure 1.11 (e) depicts one of the possible channels of concurring charge-transfer processes after the direct excitation of A. The influence of linking D and A on the energy transfer process from D to A was investigated by comparing the fluorescence spectra of DBA and a blend of donor (TPD) and acceptor (PBI). They found that the fluorescence lifetime of pure donor, donor in the presence of acceptor, and donor in DBA decreases from 0.85 to 0.57 ns and finally to extremely short values of even below 80 ps, respectively. Thus, the linkage of D and A has a drastic influence on energy transfer dynamics in DBA.

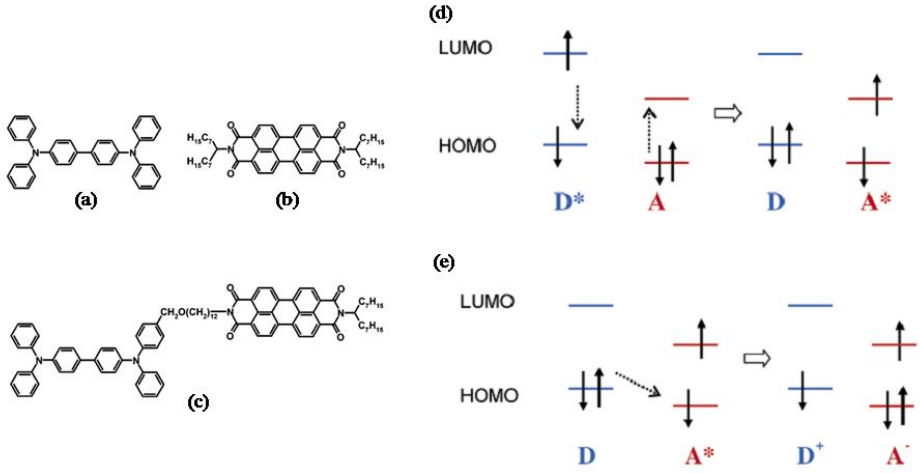

Figure 1.11. *Chemical structures of (a) tetraphenylbenzidine (TPD), (b) perylenebisimide (PBI), (c) DBA molecule containing tetraphenylbenzidine and perylenebisimide; (d) Energy transfer from donor to acceptor after excitation of the donor at 349 nm and (e) one possible channel of electron transfer and fluorescence quenching of acceptor after direct excitation of acceptor at 525 nm (Adapted from Chem. Mater.* ***2007****, 19, 88-94).*

Both oligo(*p*-phenylenevinylene) (OPV) and perylenebisimide (PBI) chromophores have been utilized in bulk-heterojunction like solar cell configurations as donor and acceptor materials, but their combination has received little attention.[86-91] E. W. Meijer and co-workers have synthesized two copolymers consisting of alternating oligo(*p*-phenylenevinylene) (OPV) donor and perylenebisimide (PBI) acceptor chromophores by using a Suzuki polycondensation reaction.[92] The copolymers differed by the length of the saturated spacer that connected the OPV and PBI units, as shown in scheme 1.2. Photo-induced singlet energy transfer and photo-induced charge separation in these polychromophores have been studied in solution and in the solid state via photoluminescence and femtosecond pump-probe spectroscopy. In both polymers, a photo-induced electron transfer occurs within a few picoseconds after excitation of the OPV or the PBI chromophore. The differences in rate

constants for the electron- and energy-transfer processes were discussed on the basis of correlated quantum-chemical calculations and in terms of conformational preferences and folding of the two polymers. In solution, the lifetime of the charge-separated state is longer than in the films where geminate recombination is much faster.

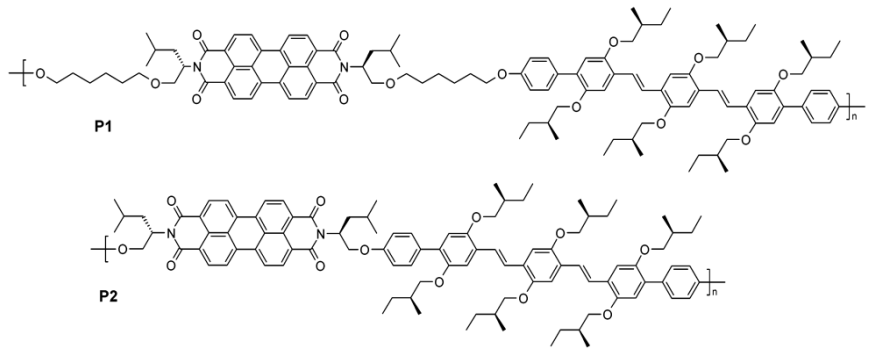

***Scheme 1.2**. The Structure of alternating copolymers containing OPV and PBI (**P1** and **P2**).*

R. A. J. Janssen and co-workers have synthesized two new donor-acceptor copolymers that consist of an enantiomerically pure oligo(*p*-phenylenevinylene) main chain with dangling perylenebisimides by using a Suzuki cross-coupling polymerization as shown in scheme 1.3.[93] Absorption and circular dichroism spectroscopy revealed that the transition dipole moments of the donor in the main chain and the dangling acceptor moieties of the copolymers were coupled and in a helical orientation in solution, even at elevated temperatures. A strong fluorescence quenching of both chromophores indicated an efficient photo-induced charge transfer after photo-excitation of either donor or acceptor. The formation and recombination kinetics of the charge-separated state were investigated in detail with femtosecond and near-steady-state photo-induced absorption spectroscopy. The optical characteristics indicated a short distance and appreciable interaction between the electron-rich donor chain and the dangling electron-poor acceptor chromophores.

Although research on the photo-induced energy- and electron-transfer in copolymer containing OPV and PBI chromophores have been done, the systematic study of the factors influencing the photo-induced energy- and electron-transfer in OPV-PBI copolymer is a missing link in the literature.

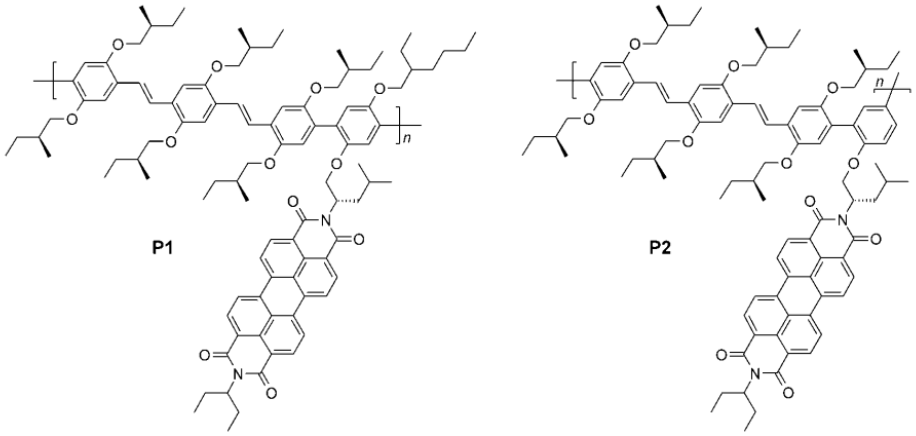

***Scheme 1.3**. The structure of copolymers containing OPV and PBI chromophores (**P1** and **P2**).*

1.7. Reactive Blending

The important bottleneck in the development of suitable polymeric materials for photovoltaic applications is the lack of an easy synthetic process. The technology of polymer blends has been one of the major areas of research and development in polymer science in the past three decades. The advantages of polymer blends versus developing new polymeric structures have been well-documented.[94-96] The ability to combine existing polymers into new compositions offers the advantage of reduced research and development expense compared to the development of new monomers and polymers to yield a similar property profile. An additional advantage is the much lower capital expense involved with scale-up and commercialization. Another specific advantage of polymer blends versus new monomer/polymer composition is that blends can often offer property profile combinations not easily obtained with new polymeric structures. An inherent property of condensation polymers is their ability to react with each other.[97-99] The presence of groups like ester, amide, urethane, and other similar types, as well as carboxylic, amine, etc., groups in the polymers makes the post reaction possible. Interchange reactions take place at elevated temperatures (most frequently in the melt) between functional groups belonging to molecules with different degree of polymerization or different chemical compositions. Most prominent examples are polyesters, polycarbonates and polyamides, where interchange reactions are best studied and understood.[97-99]

Polyesters and polycarbonates are mostly used for engineering thermoplastics because of their excellent mechanical and thermal properties. Bisphenol A polycarbonate (**PC**)/polyester blends are among the most widely studied polymer blend systems industrially and academically. Because **PC** and polyester have common ester linkages in the backbone, ester-carbonate exchange (transesterification) occurs during their high-temperature melt blending. M. Jayakannan and P. Anilkumar investigated the reactive blending of bisphenol A polycarbonate (**PC**) with poly(1,4-cyclohexanedimethylene-1,4-cyclohexanedicarboxylate) (**PCCD**) using a new high-temperature solution-blending methodology.[100] The blending was carried out at very high concentrations at high temperatures. This approach had many advantages over conventional melt blending, such as independence from the polymer properties (T_g, T_m, and T_c and crystallization temperature) and flow behaviors. The ester-carbonate exchange reaction in the blends was studied with ^{1}H NMR and Fourier transform infrared (FT-IR). The ester-carbonate exchange reaction in the **PC**/**PCCD** blends leads to four major types of new linkages, two corresponding to new esters and two corresponding to new carbonates, as shown in scheme 1.4. Model blending reactions based on acidolysis, alcoholysis, and transesterification reactions were carried out to study the effect of **PCCD** end groups on **PC**/**PCCD** reactive blending. These model reactions revealed that the reactive blending was affected by both alcoholysis and transesterification, whereas acidolysis was absent. This may be due to the poor nucleophilicity of aliphatic acids toward the aromatic polycarbonates.

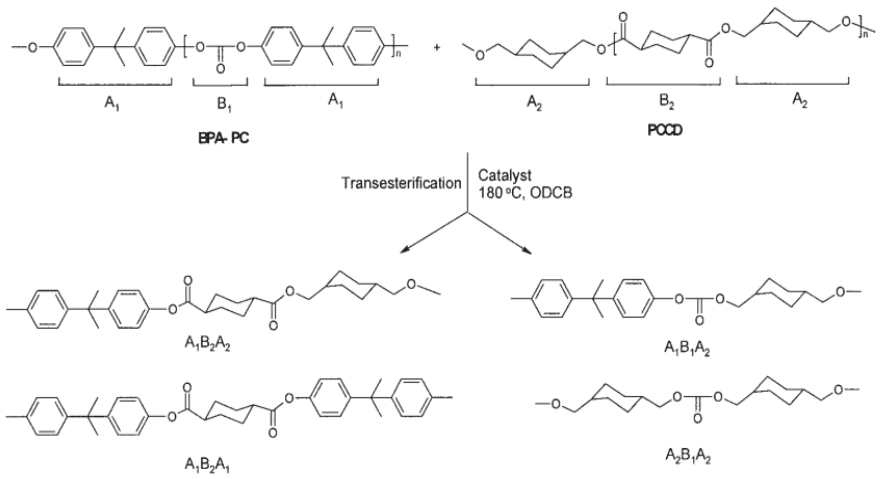

Scheme 1.4. *Ester-carbonate exchange reaction in the reactive blending of bisphenol A polycarbonate (**BPA-PC**) with **PCCD** (Adapted from J. Polym. Sci. Part A: Polym. Chem. **2004**, 42, 3996-4008).*

1.8. Conclusions and Aims of the Thesis

Ease of synthesis and film-forming ability or ease of processability is very important properties that are highly desirable in organic semiconducting materials. Reasonably high molecular weight is a prerequisite for polymeric semiconducting materials to attain this goal of easy processability. However, unlike acrylic or vinylic polymers where this is true, in main-chain semiconducting polymers, the π-π stacking interaction of the aromatic core results in reduced solubility and hence reduced solution processability. The π-π stacking interaction is a major hurdle to develop film-forming polymers especially for n-type semiconducting materials like perylene and naphthalene bisimides (PBI/NBI). Therefore, the synthesis of high molecular weight solution processable semiconducting polymers by using a simple approach is very challenging. This thesis work is focused on design and development of new solution processable semiconducting polymers and their supramolecular organization in the solid state. The important aspects of the thesis are:

1. Demonstrate a successful strategy for the synthesis of donor-acceptor semiconducting polymers.
2. Chirality induced helical self-assembly of π-conjugated material has been studied.
3. A simple approach for the fabrication of highly fluorescent semiconducting polymer into 1D elongated fiber over a large scale has been developed.
4. The photo-induced energy- and electron-transfer in random copolyester containing oligo (*p*-phenylenevinylene) and perylenebisimide were investigated.

In the second chapter, we have demonstrated a successful strategy for the incorporation of fluorescent chromophores such as OPV and PBI into the backbone of poly(1,4-cyclohexylenedimethylene-1,4-cyclohexanedicarboxylate)] (**PCCD**). These polymers possessed the required thin film processability for potential application in organic photovoltaic devices. The third chapter deals with chiral polyester induced solid state helical self-assembly of oligo(*p*-phenylenevinylene) (OPV) chromophore. In the fourth chapter, synthesis of highly fluorescent n-type organic semiconducting material, which could be fabricated into well-defined nanofibers over a large scale, was investigated. The fifth chapter describes the synthesis of novel copolyesters containing OPV and PBI chromophore by melt polycondensation. Photoinduced energy- and electron-transfer in these polyesters were studied in solution as well as in the solid state. Finally, the overall conclusion of the thesis has been summarized.

1.9. References

1) Kelley, T. W.; Baude, P. F.; Gerlach, C.; Ender, D. E.; Muyres, D.; Haase, M. A.; Vogel, D. E.; Theiss, S. D. *Chem. Mater*. **2004**, *16*, 4413-4422.
2) Zhaoab, X.; Zhan, X. *Chem. Soc. Rev*. **2011**, *40*, 3728-3743.
3) Baude, P. F.; Ender, D. A.; Haase, M. A.; Kelley, T. W.; Muyres, D. V.; Theiss, S. D. *Appl. Phys. Lett.* **2003**, *82*, 3964-3966.
4) Kim, Y. H.; Park, S. K.; Moon, D. G.; Kim, W. K.; Han, J. I. *Jpn. J. Appl. Phys*. **2004**, *43*, 3605-3608.
5) Nomoto, K.; Hirai, N. H.; Yoneya, N.; Kawashima, N.; Noda, M.; Wada, M.; Kasahara, J. *IEEE Trans. Electron. Devices* **2005**, *52*, 1519-1526.
6) Braga, D.; Horowitz, G. *Adv. Mater*. **2009**, *21*, 1473-1486.
7) Sariciftci, N. S.; Smilowitz, L.; Heeger, A. J.; Wudl, F. *Science* **1992**, *258*, 1474-1476.
8) Günes, S.; Neugebauer, H.; Sariciftci, N. S. *Chem. Rev*. **2007**, *107*, 1324-1338.
9) Allard, S.; Forster, M.; Souharce, B.; Thiem, H.; Scherf, U. *Angew. Chem. Int. Ed.* **2008**, *47*, 4070-4098.
10) Tang, C. W. *Appl. Phys. Lett.* **1986**, *48*, 183-185.
11) Choy, W. C. H. *Organic Solar Cells: Materials and Device Physics*; Springer, **2013**.
12) Krebs, F. C. *Polymeric solar Cells: Materials, Design, Manufacture*; DEStech Publications, **2010**.
13) Brabec, C. J.; Dyakonov, V.; Parisi, J.; Sariciftci, N. S. *Organic Photovoltaics: Concepts and Realization;* Springer, **2003**.
14) Pagliaro, M.; Palmisano, G.; Ciriminna, R. *Flexible Solar Cells*; Wiley-VCH, **2008**.
15) McEvoy, A. J; Castñer, L.; Markvart, T. *Solar Cells: Materials, Manufacture and Operation*; Elsevier, **2012**.
16) Langa, F.; Nierengarten, J. *Fullerenes: Principles and Applications*; The Royal Society of Chemistry, **2007**.
17) Yao, J.; Wilkins, C. L. *J. Org. Chem.* **1995**, *60*, 532-538.
18) Horowitz, B. G.; Kouki, F.; Spearman, P.; Fichou, D.; Nogues, C.; Pan, X.; Garnier, F. *Adv. Mater*. **1996**, *8*, 242-245.
19) Würthner, F. *Chem. Commun*. **2004**, 1564-1579.

20) Jones, B. A.; Ahrens, M. J.; Yoon, M.; Facchetti, A.; Marks, T. J.; Wasielewski, M. R. *Angew. Chem. Int. Ed*. **2004**, *43*, 6363-6366.

21) Rachford, A. A.; Goeb, S.; Castellano, F. N. *J. Am. Chem. Soc*. **2008**, *130*, 2766-2767.

22) Guoqiang, R.; Eilaf, A.; Jenekhe, S. A. *Adv. Energy Mater*. **2011**, *1*, 946-953.

23) Schmidt-Mende, L.; Fechtenkötter, A.; Müllen, K.; Moons, E.; Friend, R. H.; MacKenzie, J. D. *Science* **2001**, *293*, 1119-1122.

24) Hoppea, H.; Sariciftci, N. S. *J. Mater. Res.* ***2004****, 19, 1924-1945.*

25) Sun, S.; Sariciftci, N. S, Organic Photovoltaics: Mechanism, Materials, and Devices; CRC Press**, 2005**.

26) Kim, J. S.; Lee, J. H.; Park, J. H; Kim, J. K.; Cho, K. *Adv. Mater*. **2010**, *22*, 1355-1360.

27) Zhokhavets, U.; Erb, T.; Gobsch, G.; Sariciftci, N. S. *Thin Solid Films* **2006**, *496*, 679-682.

28) Ong, B. S.; Wu, Y.; Liu, P.; Gardner, S. *J. Am. Chem. Soc*. **2004**, *126*, 3378-3379.

29) Becerril, H. A.; Miyaki, N.; Tang, M. L.; Mondal, R.; Sun, Y. -S.; Mayer, A. C.; Parmer, J. E.; McGehee, M. D.; Bao, Z. *J. Mater. Chem*. **2009**, *19*, 591-593.

30) Lloyd, M. T.; Mayer, A. C.; Subramanian, S.; Mourey, D. A.; Herman, D. J.; Bapat, A. V.; Anthony, J. E.; Malliaras, G. G. *J. Am. Chem. Soc*. **2007**, *129*, 9144-9149.

31) Thompson, B. C.; Kim, B. J.; Kavulak, D. F.; Sivula, K.; Mauldin, C.; Fŕechet, J. M. J. *Macromolecules* **2007**, *40*, 7425-7428.

32) van Bavel, S. S.; Sourty, E.; de With, G.; Loos,, J. *Nano Lett.* **2009**, *9*, 507-513.

33) Dennler, G.; Scharber, M. C.; Brabec, C. J. *Adv. Mater.* **2009**, *21*, 1323-1338.

34) Nelson, J.; Kwiatkowski, J. J.; Kirkpatrick, J.; Frost, J. M. *Acc. Chem. Res.* **2009**, *42*, 1768-1778.

35) Zhang, Q.; Cirpan, A.; Russell, T. P.; Emrick, T. *Macromolecules* **2009**, *42*, 1079-1082.

36) Sommer, M.; Hüttner, S.; Steiner, U.; Thelakkat, M. *Appl. Phys. Lett.* **2009**, *95*, 183308.

37) Marder, S. R.; Lee, K, -S. *Photoresponsible Polymers-II;* Springer, **2008**.

38) Zhang, Z.; Wang, J. *J. Mater. Chem.* **2012**, *22*, 4178-4187.

39) Hüttner, S.; Sommer, S.; Thelakkat, M. *Appl. Phys. Lett.* **2008**, *92*, 093302.

40) Zhan, X.; Tan, Z.; Domercq, B.; An, Z.; Zhang, X.; Barlow, S.; Li, Y.; Zhu, D.; Kippelen, B.; Marder, S. R.; *J. Am. Chem. Soc*. **2007**, *129*, 7246-7247.

41) Holliday, S.; Donaghey, J. E.; McCulloch, I. *Chem. Mater*. **2014**, *26*, 647-663.

42) Kraft, A.; Grimsdale, A. C.; Holmes, A. B. *Angew. Chem. Int. Ed*. **1998**, *37*, 402-428.

43) Zgierski, M. Z.; Fujiwara, T.; Lim, E. C. *Acc. Chem. Res*. **2010**, *43*, 506-517.

44) Chen, G.; Jiang, M.; *Chem. Soc. Rev*. **2011**, *40*, 2254-2266.

45) Hoeben, F. J. M.; Jonkheijm, P.; Meijer, E. W.; Schenning, A. P. H. J. *Chem. Rev.* **2005**, *105*, 1491-1546.

46) Engelkamp, H.; Middelbeek, S.; Nolte, R. J. M. *Science* **1999**, *284*, 785-788.

47) Oda, R.; Huc, I.; Schmutz, M.; Candau, S. J.; MacKintosh, F. C. *Nature* **1999**, *399*, 566-569.

48) Sakai, N.; Matile, S. *Chem. Commun*. **2003**, 2514-2523.

49) Sautter, A; Schmid, D. G.; Jung, G.; Würthner, F. *J. Am. Chem. Soc*. **2001**, *123*, 5424-5430.

50) Geng, Y.; Trajkovska, A.; Katsis, D.; Ou, J. J.; Culligan, S. W.; Chen, S. H. *J. Am. Chem. Soc.* **2002**, *124*, 8337-8347.

51) Digennaro, A.; Wennemers, H.; Joshi, G.; Schmid, S.; Mena-Osteritz, E. *Chem. Commun.* **2013**, *49*, 10929-10931.

52) García, F.; Aparicio, F.; Marenchino, M.; Campos-Olivas, R.; Sánchez, L. *Org. Lett.* **2010**, *12*, 4264-4267.

53) Jørgensen, M.; Krebs, F. C. *J. Org. Chem*. **2004**, *69*, 6688-6696.

54) Guerlin, A.; Dumur, F.; Miomandre, F.; Wantz, G.; Mayer, C. R. *Org. Lett*. **2010**, *12*, 2382-2385.

55) Ajayaghosh, A; Praveen, V. K. *Acc. Chem. Res*. **2007**, *40*, 644-656.

56) Kimura, M.; Miki, N.; Adachi, N.; Tatewaki, Y.; Ohtaa, K.; Shirai, H. *J. Mater. Chem.* **2009**, *19*, 1086-1092.

57) Schenning, A. P. H. J.; Jonkheijm, P.; Peeters, E.; Meijer, E. W. *J. Am. Chem. Soc.* **2001**, *123*, 409-416.

58) Jonkheijm, P.; Hoeben, F. J. M.; Kleppinger, R.; Herrikhuyzen, J. V.; Schenning, A. P. H. J. *J. Am. Chem. Soc.* **2003**, *125*, 15941-15949.

59) George, S. J.; Ajayaghosh, A.; Jonkheijm, P.; Schenning, A. P. H. J; Meijer, E. W. *Angew. Chem. Int. Ed*. **2004**, *43*, 3421-3425.

60) Kumar, M.; Jonnalagadda, N.; George, S. J. *Chem. Commun*. **2012**, *48*, 10948-10950.

61) Kim, S. K.; Lee, D. H.; Hong, J. -I; Yoon, J. *Acc. Chem. Res*. **2009**, *42*, 23-31.

62) Klok, H. -A.; Rösler, A.; Götz, G.; Mena-Osteritzc, E.; Bäuerle, P. *Org. Biomol. Chem*. **2004**, *2*, 3541-3544.

63) Harrington, D. A.; Behanna, H. A.; Tew, G. N.; Claussen, R. C.; Stupp, S. I. *Chem. Biol*. **2005**, *12*, 1085-1091.

64) Kumar, R. J.; MacDonald, J. M.; Singh, T. B.; Waddington, L. J.; Holmes, A. B. *J. Am. Chem. Soc.* **2011**, *133*, 8564-8573.

65) Xia, Y.; Yang, P.; Sun, Y.; Wu, Y.; Mayers, B.; Gates, B.; Yin, Y.; Kim, F.; Yan, H. *Adv. Mater*. **2003**, *15*, 353-389.

66) Huang, M. H.; Mao, S.; Feick, H.; Yan, H.; Wu, Y.; Kind, H.; Weber, E.; Russo, R.; Yang, P. *Science* **2001**, *292*, 1897-1899.

67) Law, M.; Sirbuly, D. J.; Johnson, J. C.; Goldberger, J.; Saykally, R. J.; Yang, P. *Science* **2004**, *305*, 1269-1273.

68) Zang, L.; Che, Y.; Moore, J. S. *Acc. Chem. Res.* **2008**, *41*, 1596-1608.

69) Zhao, Y. S.; Fu, H.; Hu, F.; Peng, A.; Yang, W.; Yao, J. *Adv. Mater*. **2008**, *20*, 79-83.

70) Zhao, Y. S.; Peng, A.; Fu, H.; Ma, Y.; Yao, *J. Adv. Mater*. **2008**, *20*, 1661-1665.

71) Jenekhe, S. A.; Osaheni, J. A. *Science* **1994**, *265*, 765-768.

72) Langhals, H.; Krotz, O.; Polborn, K.; Mayer, P. *Angew. Chem. Int. Ed*. **2005**, *44*, 2427-2428.

73) Cornil, J.; Beljonne, D.; Calbert, J.-P.; Bredas, J.-L. *Adv. Mater*. **2001**, *13*, 1053-1067.

74) Che, Y.; Datar, A.; Balakrishnan, K.; Zang, L. *J. Am. Chem. Soc.* **2007**, *129*, 7234-7235.

75) Li, X. -Q.; Zhang, X.; Ghosh, S.; Würthner, F. *Chem. Eur. J*. **2008**, *14*, 8074-8078.

76) Che, Y.; Yang, X.; Loser, S.; Zang, L. *Nano Lett*. **2008**, *8*, 2219-2223.

77) Che, Y.; Yang, X.; Balakrishnan, K.; Zuo, J.; Zang, L. *Chem. Mater*. **2009**, *21*, 2930-2934.

78) Wasielewski, M. R. *Chem. Rev.* **1992**, *92*, 435-461.

79) Guldi, D. M. *Chem. Soc. Rev*. **2002**, *31*, 22-36.

80) Yu, G.; Gao, J.; Hummelen, J. C.; Wudl, F.; Heeger, A. J. *Science* **1995**, *270*, 1789-1791.

81) Günes, S.; Neugebauer, H.; Sariciftci, N. S. *Chem. Rev*. **2007**, *107*, 1324-1338.

82) Alam, M. M.; Jenekhe, S. A. *Chem. Mater.* **2004,** *16*, 4647-4656.

83) Speiser, S. *Chem. Rev*. **1996**, *96*, 1953-1976.

84) Lakowicz, J. R. *Principles of Fluorescence Spectroscopy*; Springer, **2010**.

85) Bauer, P.; Wietasch, H.; Lindner, S. M.; Thelakkat, M. *Chem. Mater*. **2007**, *19*, 88-94.

86) Marcos Ramos, A.; Rispens, M. T.; Van Duren, J. K. J.; Hummelen, J. C.; Janssen, R. A. J. *J. Am. Chem. Soc*. **2001**, *123*, 6714-6715.

87) Angadi, M. A.; Gosztola, D.; Wasielewski, M. R. *J. Appl. Phys.* **1998**, *83*, 6187-6189.

88) Dittmer, J. J.; Marseglia, E. A.; Friend, R. H. *Adv. Mater.* **2000**, *12*, 1270-1274.

89) Nierengarten, J.-F.; Eckert, J.-F.; Nicoud, J.-F.; Ouali, L.; Krasnikov, V.; Hadziioannou, G. *Chem. Commun.* **1999**, 617-618.

90) Peeters, E.; Van Hal, P. A.; Knol, J.; Brabec, C. J.; Sariciftci, N. S.; Hummelen, J. C.; Janssen, R. A. J. *J. Phys. Chem. B* **2000**, *104*, 10174-10190.

91) El-ghayoury, A.; Schenning, A. P. J. H.; Van Hal, P. A.; Van Duren, J. K. J.; Janssen, R. A. J.; Meijer, E. W. *Angew. Chem. Int. Ed.* **2001**, *40*, 3660-3663.

92) Neuteboom, E. E.; Meskers, S. C. J.; Van Hal, P. A.; van Duren, J. K. J.; Meijer, E. W.; Janssen, R. A. J.; Dupin, H.; Pourtois, G.; Cornil, J.; Lazzaroni, R.; Brėdas, J. -L.; Beljonne, D. *J. Am. Chem. Soc.* **2003**, *125*, 8625-8638.

93) Neuteboom, E. E.; van Hal, P. A.; Janssen, R. A. J. *Chem. Eur. J.* **2004**, *10*, 3907-3918.

94) Utracki, L. A. *Commercial Polymer Blends*; Springer, **1998**.

95) Robeson, L. M. *Polymer Blends: A Comprehensive Review*; Hanser Publishers, **1994**.

96) Utracki, L. A. *Polymer Blends Handbook*; Harwood Academic Publishers, **2000**.

97) Fakirov, S. *Transreactions in Condensation Polymers*; Wiley-VCH, **1999**.

98) Immirzi, B.; Malinconico, M.; Orsello, G.; Portofino, S.; Volpe, M. G. *J. mater. Sci.* **1999**, *34*, 1625-1639.

99) Legros, A.; Carreau, P. J.; Favis, B. D. *Polymer*, **1994**, *35*, 758-764.

100) Jayakannan, M.; AnilKumar, P. *J. Polym. Sci. Part A: Polym. Chem.* **2004**, *42*, 3996-4008.

Chapter 2

A facile one-pot Reactive Solution Blending Approach for Main Chain Donor-Acceptor Polymeric Materials

Chapter 2

A facile one-pot Reactive Solution Blending Approach for Main Chain Donor-Acceptor Polymeric Materials

A high-temperature solution-blending process has been used to synthesize a series of copolymers incorporating varying mole ratios of perylenebisimide (PBI) into the backbone of an engineering thermoplastic polyester [poly(1,4-cyclohexylenedimethylene-1,4-cyclohexanedicarboxylate)] (**PCCD**). A random donor-acceptor copolymer incorporating oligo(*p*-phenylenevinylene) (OPV) and PBI was also synthesized. The chemical incorporation of these chromophores into **PCCD** was confirmed by carrying out the melt polycondensation using 1,4-cyclohexanedimethanol (CHDM) and 1,4-dimethylcyclohexane dicarboxylate (DMCD) with hydroxyl functionalized PBI and OPV derivatives. Higher extent of incorporation of PBI (35 mole %) could be achieved using the blending approach retaining solubility, film forming ability and higher molecular weights. The PBI polymers produced using the two different approaches exhibited structural variations. The polymers formed from the solution blending approach had a semicrystalline nature with blocks of **PCCD** separating the PBI units; whereas those produced using the melt condensation route were amorphous polymers. This structural variation was reflected in their photophysical properties also with the reactive solution blended polymers exhibiting higher fluorescence quantum yields. These results demonstrate the easy incorporation of suitably functionalized donor and acceptor moieties into a completely aliphatic polyester backbone to produce free standing films of hitherto non-processable polymers.

2.1. Introduction

The ongoing interest in organic semiconducting materials is driven by the scientific challenges they present as well as by the promise of real-world applications in a multitude of products such as plastic/flexible displays, sensors, and RF-ID tags, as recently reviewed. [1-10] Furthermore, recent developments in organic-based light-emitting diodes (OLEDs), photovoltaics (OPVs), and field-effect transistors (OFETs) have opened up many new and exciting challenges and opportunities in the field of thin-film optoelectronics.[11] Most organic conducting materials can be described as p-type semiconductors, in which holes in the valence band are the majority charge carriers. Perylene and naphthalene bisimides (PBI/NBI) have been attracting considerable attention as good n-type organic semiconductors because of the outstanding photophysical properties, thermal stability, and ability to self-organize.[12-16] The ultimate promise of organic semiconductors is in inexpensive, large-area and solution-processed electronics. Therefore, semiconductors could be tailored to have improved solubility and film-forming properties. One of the major challenges confronting the field of organic electronics has been the development of solution processable and film-forming electron-transporting (n-type) organic semiconductors for thin film device structures. Although a number of PBI main-chain polymers have been reported, most of them are not solution processable due to strong π-π stacking interactions.[17, 18] Recently, the strategy of incorporating donor (D) and acceptor (A) units into the polymer backbone has proven to be very effective in improving device performances by taking advantage of intermolecular donor and acceptor interactions.[19-21] A number of alternating D-A conjugated polymers have been designed and investigated for optoelectronic materials. The development of new D-A polymers are synthetically challenging and the final D-A copolymer would rarely possess the required thin film processability.

The covalent incorporation of small molecular weight active molecules into polymeric matrixes represents an interesting strategy with numerous useful applications.[22-24] Melt transesterification is a common route to prepare polyesters and it requires high vacuum, high reaction temperature and proper catalysts.[23, 24] Considerable interest has arisen in the reactive blending of polymers containing active functional groups in the polymer chains during the melt-mixing process in recent years.[25] The materials produced through reactive blending are homogeneous, more compatible, and less sensitive to long-term phase separation.[26] Polyesters are mostly used for engineering thermoplastics because of their excellent thermal

and mechanical properties. Among them, **PCCD** [Poly(1,4-cyclohexylenedimethylene-1,4-cyclohexanedicarboxylate)] has attracted more attention in the plastic industry because of their outstanding properties such as resistance to UV radiation and their chemical resistance.[27] Jayakannan et.al investigated the reactive blending of bisphenol A polycarbonate (**PC**) with **PCCD** via a new high-temperature solution-blending methodology.[28] This high-temperature solution-blending involved dissolving **PC** and **PCCD** in minimum amounts of a high boiling solvent like ortho-dichlorobenzene (ODCB) and heating it to high temperature (150- 185°C) in presence of a transesterification catalyst. They showed that ester-carbonate interchange occurred via transesterification in these blends. Using model reactions they showed that both alcoholysis and transesterification were amenable under these reactive blending conditions.

We were motivated to apply this methodology to incorporate suitably functionalized semiconducting materials – both donor and acceptor type, on a polyester backbone. An aliphatic hydroxyl functionalized pentadecylphenol (PDP) substituted symmetric perylene bisimide derivative was developed as the n-type semiconducting material, which was incorporated in varying mole ratios into an aliphatic polyester backbone based on **PCCD** using the solution blending approach. The success of this methodology was crosschecked by synthesizing the same copolymer via the usual melt polycondensation approach also. The structure and properties of the semiconducting polymers developed using both approaches were compared using ^{1}H NMR, UV-Vis absorption and emission studies. An aliphatic hydroxyl functionalized oligo(*p*-phenylenevinylene) (OPV) derivative was also synthesized and it was incorporated into the **PCCD** backbone thereby proving the versatility of this approach. A random copolyester incorporating both the acceptor (PBI) and donor (OPV) moieties was also developed and the energy transfer from donor to acceptor was studied using fluorescence quenching studies. The transesterification by reactive solution blending approach described here is easily adoptable for a wide range of suitably derivatised donor or acceptor molecules resulting in tunable photophysical properties with film forming ability.

2.2. Experimental Methods

2.2.1. Materials: PCCD was donated by GE plastics. Perylene-3,4,9,10-tetracarboxylic dianhydride (PTCDA), 3-pentadecylphenol, zinc acetate, imidazole, 1,4-cyclohexanedimethanol (CHDM) (cis + trans), 1,4-dimethylcyclohexane dicarboxylate

(DMCD) (cis + trans), titanium(IV) butoxide [$Ti(OBu)_4$], 4-methoxyphenol, 2-ethylhexylbromide, triethylphosphite, 4-hydroxybenzaldehyde, potassium-tert-butoxide and ortho-dichlorobenzene (ODCB) were purchased from Aldrich and used without further purifications. HBr in glacial acetic acid, paraformaldehyde, potassium carbonate, potassium iodide, dimethyl sulfoxide, N,N-dimethylformamide (DMF), tetrahydrofuran (THF), 2-chloroethanol and all other solvents were purchased locally and purified with standard procedures.

2.2.2. Instrumentation: ^{1}H NMR spectra were recorded using a Bruker Avance 200 MHz spectrometer. Chemical shifts (δ) are reported in ppm at 25 ^oC using $CDCl_3$ as solvent with a small amount of tetramethylsilane (TMS) as internal standard. The mass spectral analysis of monomer was carried out using a Voyager-De-STR MALDI-TOF (Applied Biosystems, Framingham, MA, USA) instrument equipped with 337 nm pulsed nitrogen laser used for desorption and ionization. The molecular weight of synthesized polymers was determined using size exclusion chromatography (SEC). SEC measurements were carried on a Polymer Laboratories PL-GPC-220 at 25 ^oC using chloroform (Merck) as the mobile phase. The analysis was carried out at a flow rate of 1 mL/min using a set of three PLgel columns and a refractive index (RI) detector. Columns were calibrated with polystyrene standards and the molecular weights reported were with respect to polystyrene. The inherent viscosity (η_{inh}) of the polymers was measured for 0.5 wt % polymer solutions in mixture of phenol/1,1,2,2-tetrachloroethane (60/40) as solvent. UV/Vis spectra were recorded using a Perkin-Elmer Lambda-35 UV/Vis spectrometer and fluorescence measurements were performed using a Fluorolog HORIBA Jobin Yvon fluorescence spectrophotometer having a 450 W xenon lamp. Solid state photoluminescence spectra were recorded using the front face scan mode with the same Fluorolog spectrofluorimeter. The fluorescence quantum yields of PBI polymer were determined in $CHCl_3$ using rhodamine 6G in ethanol (Φ = 0.95) as the standard by exciting at 490 nm and OPV polymer were determined in $CHCl_3$ using quinine sulphate in 0.1M H_2SO_4 (Φ = 0.54) as the standard by exciting at 360 nm. The thermal stability of the polymers was analyzed using a Perkin-Elmer thermogravimetric analyzer under nitrogen atmosphere from 50 to 800 ^oC at 10 ^oC/ min. Differntial scanning colorimetry (DSC) was performed using TA Q10 differential scanning calorimeter at heating rate of 10 ^oC/min. WXRD were recorded using Phillips x'pertpro powder X-ray diffractometer using Cu Kα radiation, and the spectra were recorded in the range of 2θ = 5-50°. Electrochemical properties of polymers were studied using a BAS-Epsilon potentiostat.

2.2.3. Synthesis

Synthesis of Per-PDP-Diol: Per-PDP-Diol was synthesized from 4-amino-3-pentadecylphenol and PTCDA by following the literature procedure.[29]

Synthesis of Per-PDP-2-Diol: Per-PDP-Diol (1.00 g, 1 mmol), K_2CO_3 (0.69 g, 5 mmol) and a trace of KI were dissolved in 100 mL dry DMF under nitrogen atmosphere. Heated the mixture at 80 ^oC for 1 h. 2-Chloroethanol (0.40 g, 5 mmol) was added at 0 ^oC and the mixture was again heated at 80 ^oC for 48 h. The reaction mixture was then cooled to room temperature and precipitated by adding 2N HCl and washed with water. The precipitate was filtered off and dried in an oven at 60 °C in vacuum (0.5 mm Hg). Yield = 77%; ^1H NMR (200 MHz, $CDCl_3$) δ ppm: 8.75 (m, 8H, perylene **H**), 7.00 (m, 6H, Ar**H**–PDP), 4.16 (t, 4H, Ar–O–C**H**$_2$–CH_2–OH), 4.02 (t, 4H, Ar–O–CH_2–C**H**$_2$–OH), 2.41 (t, 4H, Ar–C**H**$_2$–), 1.76 (aliphatic –O**H**), 1.55 (m, 4H, Ar–CH_2–C**H**$_2$–), 1.19 (m, 48H, aliphatic –C**H**$_2$–), 0.85 (t, 6H, terminal –C**H**$_3$); MALDI-TOF (dithranol matrix): m/z calcd for $C_{70}H_{86}N_2O_8$: 1083.44; found: 1086.02.

Synthesis of copolyesters of PCCD incorporating PBI through high-temperature solution-blending rout (BPer-x-PCCD): PCCD (2.24 g, 8 mmol) was dissolved in ODCB (5 mL) by heating to 150 °C in an oil bath. To the solution, Per-PDP-2-Diol (2.16 g, 2 mmol) was added (for **BPer-13-PCCD**). The mixture was stirred continuously for 12 h using an overhead mechanical stirrer at a constant rate of 100 rpm. To the solution, $Ti(OBu)_4$ (34 mg, 1 mol %) solution in ODCB was added and the reactive blending was continued with stirring at 180 °C for 24 h. The product was cooled, dichloromethane (DCM) was added, and the polymer solution was poured into methanol. The resultant material was filtered and subjected to solvent extraction using acetone to remove unreacted Per-PDP-2-Diol that would be physically trapped in the polymer voids. The polymer was dried in oven at 60 ^oC in vacuum (0.5 mm Hg). Yield = 61.36%; ^1H NMR (200 MHz, $CDCl_3$) δ ppm: 8.74 (perylene **H**), 6.98 (Ar**H**–PDP), 4.47 (–CH_2–C**H**$_2$–O–CO–), 4.23 (–C**H**$_2$–CH_2–O–CO–), 3.98 (cis –C**H**$_2$– in **PCCD**), 3.89 (trans –C**H**$_2$– in **PCCD**), 2.5–0.5 (cyclic–**H** in **PCCD** + aliphatic **H** in PDP).

A similar procedure was employed to synthesize the **BPer-x-PCCD** series of polyesters by change in the molar ratio of Per-PDP-2-Diol in the feed from 2 to 50 mol%.

Synthesis of copolyesters of PCCD incorporating PBI through melt polycondensation rout (MCPer-x): DMCD (2.00 g, 10 mmol), CHDM (1.29 g, 9 mmol) and Per-PDP-2-Diol (1.08 g, 1 mmol) were weighed into a tubular glass reactor (for **MCPer-10**). The reaction mixture was melted at 160 ^{o}C, cooled and $Ti(OBu)_4$ (3.4 mg, 0.1 mol % of diester) solution in ODCB was added to the mixture. The reaction was heated from 160 to 180 ^{o}C over 2 h with stirring 100 rpm and then from 180 to 230 ^{o}C over 2 h, allowing methanol to distil. Vacuum was applied and the pressure was gradually reduced to 0.4 mm Hg over 20 min, while the temperature was raised from 230 to 250 ^{o}C. The reaction was continued at 250 ^{o}C for 2 h. The product was cooled, DCM was added, and the polymer solution was poured into methanol. The resultant material was filtered and subjected to solvent extraction using acetone to remove unreacted PerPDP-2-Diol that would be physically trapped in the polymer voids. The polymer was dried in oven at 60 ^{o}C in vacuum (0.5 mm Hg). Yield = 65.45%; ^{1}H NMR (200 MHz, $CDCl_3$) δ ppm: 8.74 (perylene **H**), 6.98 (Ar**H**–PDP), 4.47 (–CH_2–C**H**$_2$–O–CO–), 4.23 (–C**H**$_2$–CH_2–O–CO–), 3.98 (cis –C**H**$_2$– in **PCCD**), 3.89 (trans –C**H**$_2$– in **PCCD**), 3.66 (–CO–O–C**H**$_3$ end group), 2.5–0.5 (cyclic–**H** in **PCCD** + aliphatic **H** in PDP).
A similar procedure was employed to synthesize the **MCPer-x** series of polyesters by change in the molar ratio of Per-PDP-2-Diol in the feed from 2 to 50 mol%.

Synthesis of OPV-2-Diol: The bisphosphonate ylide and 4-(2-hydroxyethoxy)benzaldehyde were synthesized by following the literature procedure.[30] Potassium-tert-butoxide (0.45 g, 0.004 mol) dissolved in 15 mL of dry THF was added to the mixture of bisphosphonate ylide (1.07 g, 0.002 mol) and 4-(2-hydroxyethoxy)benzaldehyde (0.66 g, 0.004 mol) at 0 ^{o}C and the contents were stirred under nitrogen for 24 h at 30 ^{o}C. The contents were poured into water to obtain a yellow powder which was dissolved in chloroform, washed with water, brine, and dried using anhydrous Na_2SO_4. The red sticky solid was further purified by passing through a silica gel column using ethyl acetate and hexane (60/40 v/v) as eluant. Yield = 60.83%; ^{1}H NMR (200 MHz, CDCl3) δ ppm: 7.60–6.80 (m, 14H, Ar–**H** and vinylic **H**), 4.20–3.80 (m, 13H, ArOC**H**$_2$–, ArOCH_2–C**H**$_2$–and ArOC**H**$_3$), 1.90–0.70 (m, 15H, aliphatic); MALDI-TOF (dithranol matrix): m/z calcd for $C_{35}H_{44}O_6$: 560.74; found: 561.10 [M+1]; elemental analysis calcd (%): C 74.97, H 7 .91; found: C 74.49, H 7.69.

Synthesis of random copolyester of PCCD incorporating OPV chromophore through high-temperature solution-blending rout (BOPV-4-PCCD): PCCD (2.66 g, 9.5 mmol) was dissolved in ODCB (5 mL) by heating to 150 °C in an oil bath. To the solution, OPV-2-Diol (0.28 g, 0.5 mmol) was added. The mixture was stirred continuously for 12 h using an

overhead mechanical stirrer at a constant rate of 100 rpm. To the solution, $Ti(OBu)_4$ (34 mg, 1 mol %) solution in ODCB was added and the reactive blending was continued with stirring at 180 °C for 24 h. The product was cooled, DCM was added, and the polymer solution was poured into methanol. The resultant material was filtered and the polymer was dried in oven at 60 ^oC in vacuum (0.5 mm Hg). Yield = 77.55%; ^1H NMR (200 MHz, $CDCl_3$) δ ppm: 7.60–6.8 (Ar–**H** and vinylic **H**), 4.43 (–CH_2–C**H**$_2$–O–CO–R), 4.25–3.7 (ArOC**H**$_2$–, ArOC**H**$_3$, cis and trans –C**H**$_2$– in **PCCD**), 2.50–0.50 (aliphatic **H** in OPV unit + cyclic–**H** in **PCCD**).

Synthesis of random copolyester of PCCD incorporating OPV chromophore through melt polycondensation (MCOPV-4): DMCD (2.00 g, 10 mmol), CHDM (1.37 g, 9.5 mmol) and OPV-2-Diol (0.28 g, 0.5 mmol) were weighed into a tubular glass reactor. The reaction mixture was melted in a salt bath at 160 ^oC, cooled and Ti(IV) butoxide (3.4 mg, 0.1 mol % of diester) solution in ODCB was added to the mixture. The reaction was heated from 160 to 180 ^oC over 2 h with stirring 100 rpm and then from 180 to 230 ^oC over 2 h, allowing methanol to distil. Vacuum was applied and the pressure was gradually reduced to 0.4 mm Hg over 20 min, while the temperature was raised from 230 to 253 ^oC. The reaction was continued at 253 ^oC for 2 h. The product was cooled, DCM was added, and the polymer solution was poured into methanol. The resultant material was filtered and dried in oven at 60 ^oC in vacuum (0.5 mm Hg). Yield = 76.99%; ^1H NMR (200 MHz, $CDCl_3$) δ ppm: 7.60–6.80 (Ar–**H** and vinylic **H**), 4.43 (–CH_2–C**H**$_2$–O–CO–R), 4.25–3.70 (ArOC**H**$_2$–, ArOC**H**$_3$, cis and trans –C**H**$_2$– in **PCCD**), 2.50–0.85 (aliphatic **H** in OPV unit + cyclic–**H** in **PCCD**).

Synthesis of random copolyester of PCCD incorporating both OPV and PBI chromophores through high-temperature solution-blending rout (BPer-3-OPV-5-PCCD): PCCD (2.52 g, 9 mmol) was dissolved in ODCB (5mL) by heating to 150 °C in an oil bath. To the solution, OPV-2-Diol (0.28 g, 0.5 mmol) and Per PDP-2-Diol (0.54 g, 0.5 mmol) was added. The mixture was stirred continuously for 12 h using an overhead mechanical stirrer at a constant rate of 100 rpm. To the solution, $Ti(OBu)_4$ (34 mg, 1 mol %) solution in ODCB was added and the reactive blending was continued with stirring at 180 °C for 24 h. The product was cooled, DCM was added, and the polymer solution was poured into methanol. The resultant material was filtered and the polymer was dried in oven at 60 ^oC in vacuum (0.5 mm Hg). Yield = 74.85%; ^1H NMR (200 MHz, $CDCl_3$) δ ppm: 8.74 (perylene **H**), 7.60–6.80 (Ar**H**–PDP, Ar–**H** and vinylic **H** in OPV unit), 4.43 (–CH_2–C**H**$_2$–O–CO–),

4.25–3.70 (ArOC**H**$_2$–, ArOC**H**$_3$, cis and trans –C**H**$_2$– in **PCCD**), 2.50–0.50 (cyclic–**H** in **PCCD** + aliphatic **H** in PDP + aliphatic **H** in OPV unit).

Synthesis of random copolyester of PCCD incorporating both OPV and PBI chromophores through melt polycondensation (MCPer-3-OPV-4): DMCD (2.00 g, 10 mmol), CHDM (1.30 g, 9 mmol), OPV-2-Diol (0.28 g, 0.5 mmol) and Per-PDP-2-Diol (0.54 g, 0.5 mmol) were weighed into a tubular glass reactor. The reaction mixture was melted in a salt bath at 160 ^{o}C, cooled and Ti(IV) butoxide (3.4 mg, 0.1 mol % of diester) solution in ODCB was added to the mixture. The reaction was heated from 160 to 180 ^{o}C over 2 h with stirring 100 rpm and then from 180 to 230 ^{o}C over 2 h, allowing methanol to distil. Vacuum was applied and the pressure was gradually reduced to 0.4 mm Hg over 20 min, while the temperature was raised from 230 to 250 ^{o}C. The reaction was continued at 250 ^{o}C for 2 h. The product was cooled, DCM was added, and the polymer solution was poured into methanol. The resultant material was filtered and dried in oven at 60 ^{o}C in vacuum (0.5 mm Hg). Yield = 76.46%; ^{1}H NMR (200 MHz, $CDCl_3$) δ ppm: 8.74 (perylene **H**), 7.60–6.80 (Ar**H**–PDP, Ar–**H** and vinylic **H** in OPV unit), 4.43 (–CH$_2$–C**H**$_2$–O–CO–), 4.25–3.70 (ArOC**H**$_2$–, ArOC**H**$_3$, cis and trans –C**H**$_2$ – in PCCD), 3.66 (–CO–O–C**H**$_3$ end group), 2.50–0.50 (cyclic–**H** in PCCD + aliphatic **H** in PDP + aliphatic **H** in OPV unit).

2.3. Results and Discussions

2.3.1. Synthesis and Characterization of Monomers and Polymers

The hydroxyl functionalized pentadecylphenol substituted perylenebisimide derivative (Per-PDP-2-Diol) was synthesized through the 2-chloroethanol coupling of Per-PDP-Diol as shown in scheme 2.1. The synthesis of Per-PDP-Diol is reported elsewhere.[29] Similarly, the hydroxyl functionalized OPV derivative (OPV-2-Diol) was synthesized as shown in scheme 2.2. The bisphosphonate ylide was synthesized as reported in literature.[30] The Wittig-Horner coupling of the ylide with 4-(2-hydroxyethoxy)benzaldehyde was carried out in dry THF to obtain the OPV-2-Diol. The structures of monomers were confirmed by ^{1}H NMR and MALDI-TOF spectra, which is shown in figure 2.1.

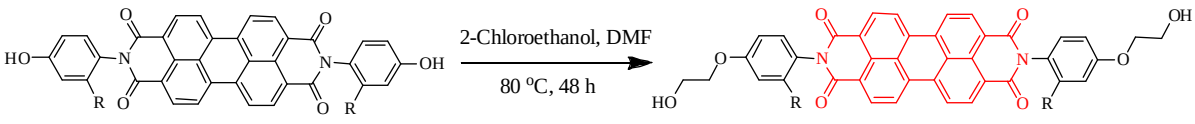

Scheme 2.1. *Synthesis of Per-PDP-2-Diol by the 2-chloroethanol coupling of Per-PDP-Diol.*

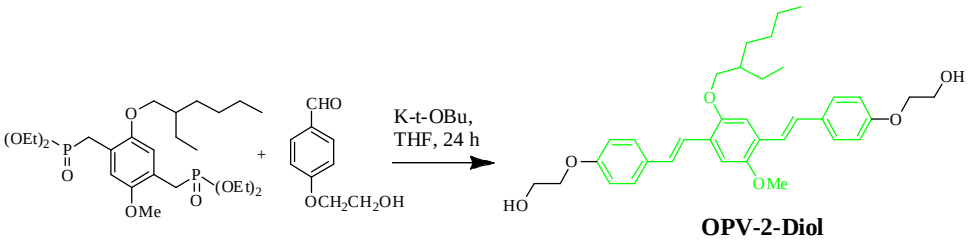

Scheme 2.2. *Synthesis of OPV-2-Diol by Wittig-Horner reaction.*

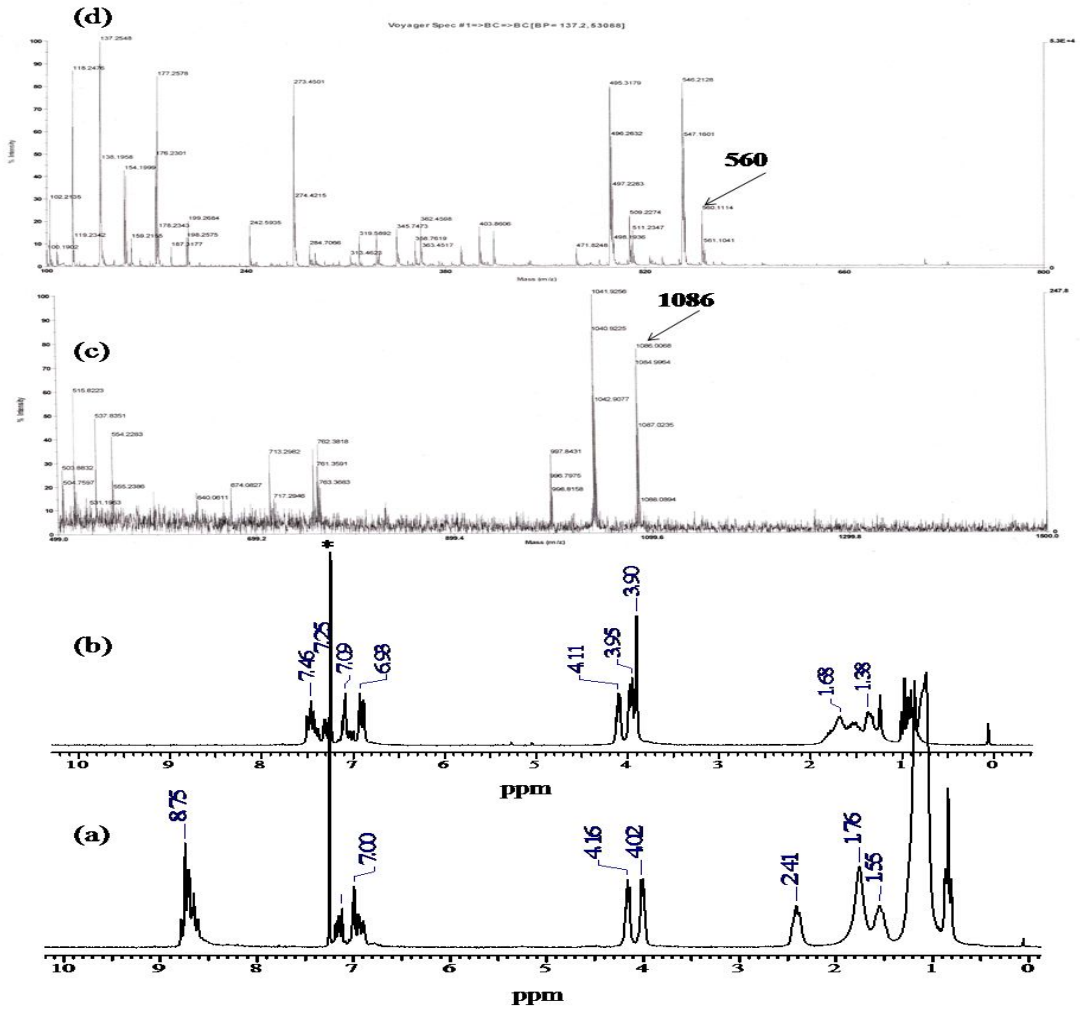

Figure 2.1. *^{1}H NMR spectra of (a) Per-PDP-2-Diol and (b) OPV-2-Diol recorded in $CDCl_3$; MALDI-TOF of (c) Per-PDP-2-Diol and (d) OPV-2-Diol.*

The high-temperature solution-blending of Per-PDP-2-Diol (acceptor) or OPV-2-Diol (donor) with **PCCD** was carried out by dissolving the hydroxyl functionalized acceptor or donor in minimum amount of a high boiling solvent like ODCB and heating in presence of 1 mol % of transesterification catalyst $Ti(OBu)_4$, as shown in scheme 2.3. ODCB was chosen as the solvent because of its inert nature towards transesterification and high boiling point. The blending was carried out in a cylindrical glass reactor at 180 ^oC for 24 h with constant stirring using mechanical stirrer, under continuous nitrogen flow. For workup, the polymer was dissolved in DCM and precipitated into methanol and further subjected to solvent extraction using acetone to remove unreacted monomers. The copolyesters obtained by the blending approach were named as **BPer-x-PCCD** or **BOPV-x-PCCD** where x represented the actual mole % incorporation calculated from integration of ^1H NMR signal.

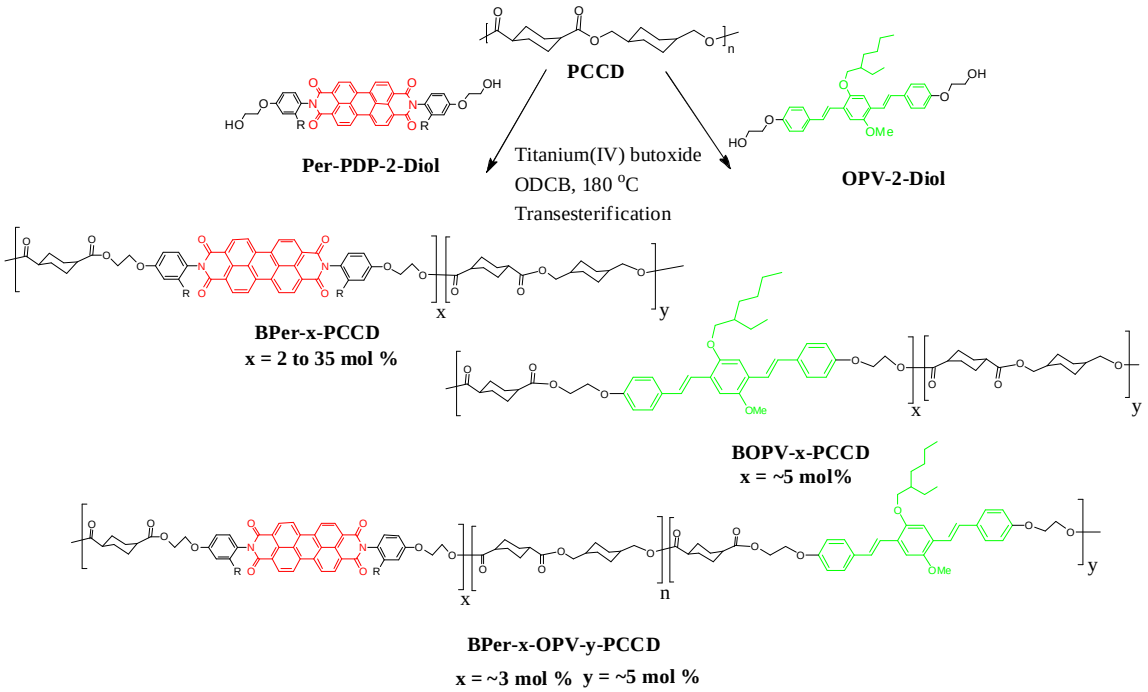

Scheme 2.3. *Synthetic route for high-temperature solution-blending of Per-PDP-2-Diol and OPV-2 Diol with Poly(1,4-cyclohexylenedimethylene-1,4-cyclohexane dicarboxylate).*

Table 2.1 gives the sample name, amount of hydroxyl functionalized PBI or OPV taken in the feed, the actual incorporation determined using ^1H NMR, molecular weight determined using SEC in $CHCl_3$ using polystyrene standards, the inherent viscosity measured in the mixture of phenol and 1,1,2,2-tetrachloroethane (60/40 v/v), the 10 % weight loss temperature obtained from TGA, the glass transition temperature (T_g) obtained from DSC as well as the yield of the various copolyesters. A copolyester incorporating OPV was

synthesized by taking 5 mol % OPV-2-Diol in the feed. Random copolyester incorporating both OPV and PBI chromophores was also synthesized using the blending approach by taking 5 mol % each of the Per-PDP-2-Diol and OPV-2-Diol in the feed. The structure of all the copolyesters synthesized using the high-temperature solution-blending approach is shown in scheme 2.3.

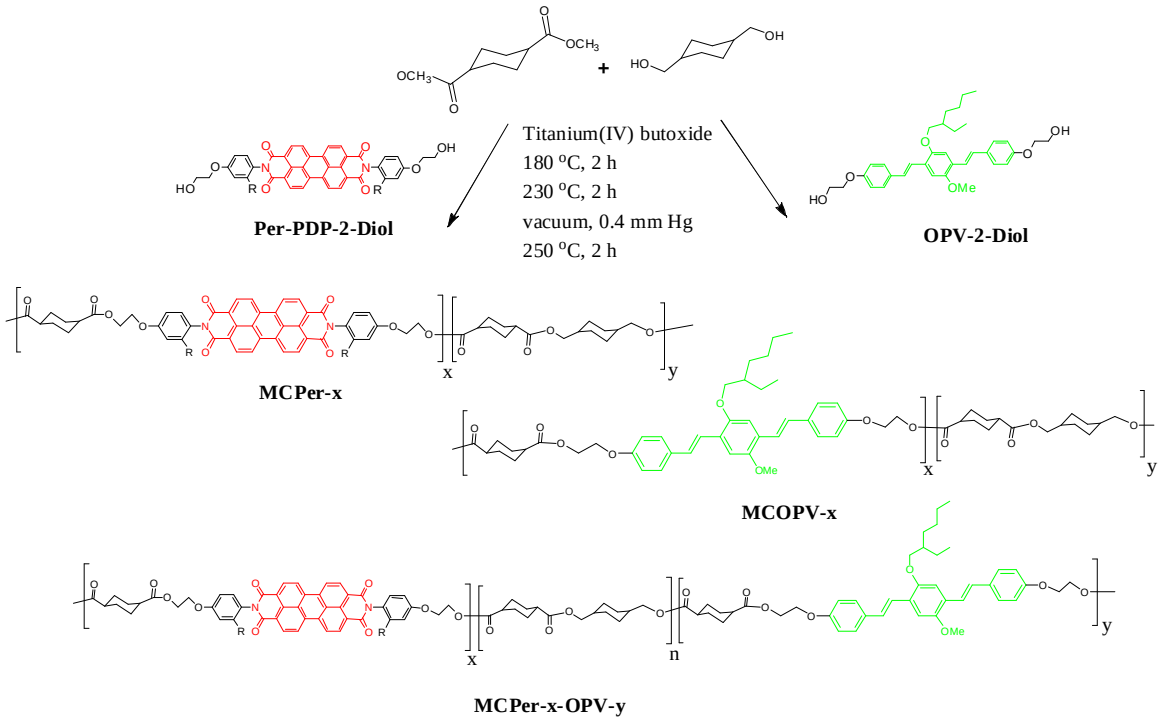

Scheme 2.4. *Melt condensation polymerization of Per-PDP-2-Diol/OPV-2-Diol, DMCD and CHDM.*

The covalent incorporation of either the PBI or OPV unit into the **PCCD** backbone was structurally confirmed by carrying out the melt condensation of the Per-PDP-2-Diol or OPV-2-Diol with 1,4-cyclohexanedimethanol (CHDM) and 1,4-dimethylcyclohexane dicarboxylate (DMCD) following literature procedure as shown in scheme 2.4.[31] 0.1 mol % of $Ti(OBu)_4$ dissolved in ODCB was added as the catalyst. The melt condensation was carried out in a cylindrical glass reactor in a two step process. The first step was at atmospheric pressure with a temperature ramp and continuous nitrogen flow to remove the methanol that was eliminated, while the second step was under dynamic vacuum (0.4 mm Hg) at 250 ^{o}C. Finally the polymers were dissolved in DCM and precipitated into methanol. The copolyesters obtained by the melt condensation approach were named as **MCPer-x** or **MCOPV-x** where x represented the mole % incorporation. The feed, actual incorporation and the polymer characterization data for the melt condensation copolyester series are given in

table 2.2. The percentage of the monomer DMCD was kept fixed at 100 mol % and that of Per-PDP-2-Diol: CHDM was varied from 100:0 to 0:100. The OPV copolyester was synthesized by taking 5 mol % OPV-2-Diol in the feed, whereas for the random copolyester incorporating both PBI and OPV, 5 mol % each of the acceptor and donor moieties were taken in the feed.

Table 2.1. *Feed, actual incorporation from ^{1}H NMR, molecular weight, viscosity data, degradation temperature and yield of polymers by high-temperature solution-blending approach.*

Sample	Feed ratio (PCCD : PBI/ OPV)	Composition (PCCD: PBI/OPV) (from ^{1}H NMR) (mol %)	Mw (g/mol)	PDI	η_{inh} (dL/ g)[a]	T_g (^{o}C)	T_D (^{o}C)[b]	Yield (%)[c]
PCCD	-	-	58000	1.7	0.89	69	389	-
BPer-2-PCCD	98:2	98.8: 1.2	51900	1.88	0.69	69	407	68
BPer-3-PCCD	95:5	96.9:3.1	32600	1.74	0.49	69	403	67
BPer-6-PCCD	90:10	94.0:6.0	30600	2.2	0.53	-	397	67
BPer-13-PCCD	80:20	87.5:12.5	26000	2.6	0.27	-	385	61
BPer-21-PCCD	70:30	79.0:21.0	15200	1.7	0.23	-	388	53
BPer-35-PCCD	50:50	65.0:35.0	13000	1.9	0.13	-	391	48
BOPV-4-PCCD	95:5	96:4	34800	2.3	0.43	69	430	78

a. Inherent viscosity measured for 0.5 wt % polymer solutions in mixture of phenol/1,1,2,2-tetrachloroethane (60/40) as solvent at 30 ^{o}C.
b. Temperature represents 10% weight loss in TGA measurements at heating rate of 10 ^{o}C/min under nitrogen.
c. Yield of the precipitated and solvent extracted sample.

Table 2.2. *Feed, actual incorporation from ^1H NMR, molecular weight, viscosity data, degradation temperature and yield of polymers synthesized by melt condensation approach.*

Sample	Feed Ratio (DMCD: CHDM: PBI/ OPV)	Composition (PCCD: PBI/OPV) (from ^1H NMR) (mol %)	Mw (g/ mol)	PDI	η_{inh} (dL/ g)[b]	T_g (^oC)[c]	T_D (^oC)[c]	Yield (%)[d]
MC-PCCD	100:100:0	-	20500	1.8	0.31	42	396	82
MCPer-2	100:98:2	98.4:1.6	58300	2.3	0.57	46	399	64
MCPer-4	100: 95:5	95.8:4.2	36800	2.1	0.42	38	393	66
MCPer-10	100: 90:10	90.2:9.8	20800	2.2	0.28	36	396	65
MCPer-17	100: 80:20	82.7:17.3	9200	1.3	0.24	-	411	51
MCPer-28	100:70:30	71.6:28.4[a]	12000[a]	1.6	-	-	399	46
MCPer-43	100:50:50	57.4:42.6[a]	8700[a]	1.5	-	-	418	45
MCPer-100	100:0:100	-	-	-	-	-	436	43
MCOPV-4	100:95:5	96:4	62700	2.8	0.43	50	426	77
MCPer-3-OPV-4	100:90:5:5	93:3:4	19200	2.3	0.30	42	405	76

a. Determined for the soluble fraction
b. Inherent viscosity measured for 0.5 wt % polymer solutions in mixture of phenol/1,1,2,2-tetrachloroethane (60/40) as solvent at 30 ^oC.
c. Temperature represents 10% weight loss in TGA measurements at heating rate of 10 ^oC/min under nitrogen.
d. Yield of the precipitated sample.

The structures of polymers were confirmed by ^1H NMR and molecular weights were determined using size exclusion chromatography (SEC). Figure 2.2 compares the ^1H NMR

spectra of **PCCD** and Per-PDP-2-Diol with that of the copolyester obtained by both blending (**BPer-6-PCCD**) and melt condensation (**MCPer-10**) approach. The ^{1}H NMR spectrum of **PCCD** showed two doublets at 3.98 and 3.89 ppm corresponding to the cis- and trans-isomeric protons in the ester linkage –COO-C**H$_2$** and the peaks from 2.5 to 0.9 ppm corresponded to the protons in the cycloaliphatic rings in PCCD [figure 2.2 (a)]. For Per-PDP-2-Diol, the aromatic protons appeared at 8.75 ppm for the eight protons of the perylene aromatic ring (labelled 'd') and at 7.00 ppm corresponding to the six protons of the PDP ring (labelled 'e'), the – Ar-O-C**H$_2$**-C**H$_2$**-OH protons appeared at 4.16 and 4.02 ppm (labelled 'f' and 'g') respectively. In the 6 mol % perylene blend with **PCCD** [figure 2.2 (c)] the –C**H$_2$**-C**H$_2$**-OH peak from Per-PDP-2-Diol shifted upfield from 4.02 to 4.47 ppm and 4.16 to 4.23 ppm respectively upon formation of the new ester linkage. The formation of the new trans-ester linkage involving PBI was confirmed by the shift of the **–**C**H$_2$**-OH proton in the proton NMR spectra, which transformed into the new –C**H$_2$**-O-COR linkage. This was additionally confirmed by the same shift observed for the copolyester of Per-PDP-2-Diol with DMCD and CHDM [**MCPer-10**; figure 2.2 (d)]. The ^{1}H NMR spectra for commercial **PCCD** [figure 2.2 (a)] showed the presence of two sets of doublets around 3.48 and 3.55 ppm (encircled in figure). This corresponded to the methylene protons of the C**H$_2$**OH end groups.[32] The polyesters obtained by the blending approach also showed [see encircled in figure 2.2 (c)] this doublet. The polyester prepared by the melt condensation route showed a singlet at 3.66 ppm also in some cases [figure 2.2 (d), by asterisk] which corresponded to the methyl ester (-CO-O-C**H$_3$**) end groups from the DMCD component.[32]

Figure 2.3 compares the ^{1}H NMR spectra of OPV-2-Diol with that for **BOPV-4-PCCD**. Similar to the observation with the perylene based copolyester, in the OPV polyester also, transesterification resulted in the formation of new trans-ester linkage confirmed by the shift of the **–**C**H$_2$**-OH proton of OPV-2-Diol from 3.90 to 4.43 ppm to the new –C**H$_2$**-O-COR linkage at 4.43 ppm. Figure 2.3 also shows the ^{1}H NMR spectra of the donor-acceptor copolyester **BPer-3-OPV-5-PCCD**. The new transester linkage corresponding to both perylene as well as OPV overlapped and was observed at the same position at 4.43 ppm. But the aromatic protons corresponding to 8 protons of perylene at 8.74 ppm and six protons of OPV at 7.45 ppm clearly provided the proof for incorporation of both units using the blend as well as melt condensation approach.

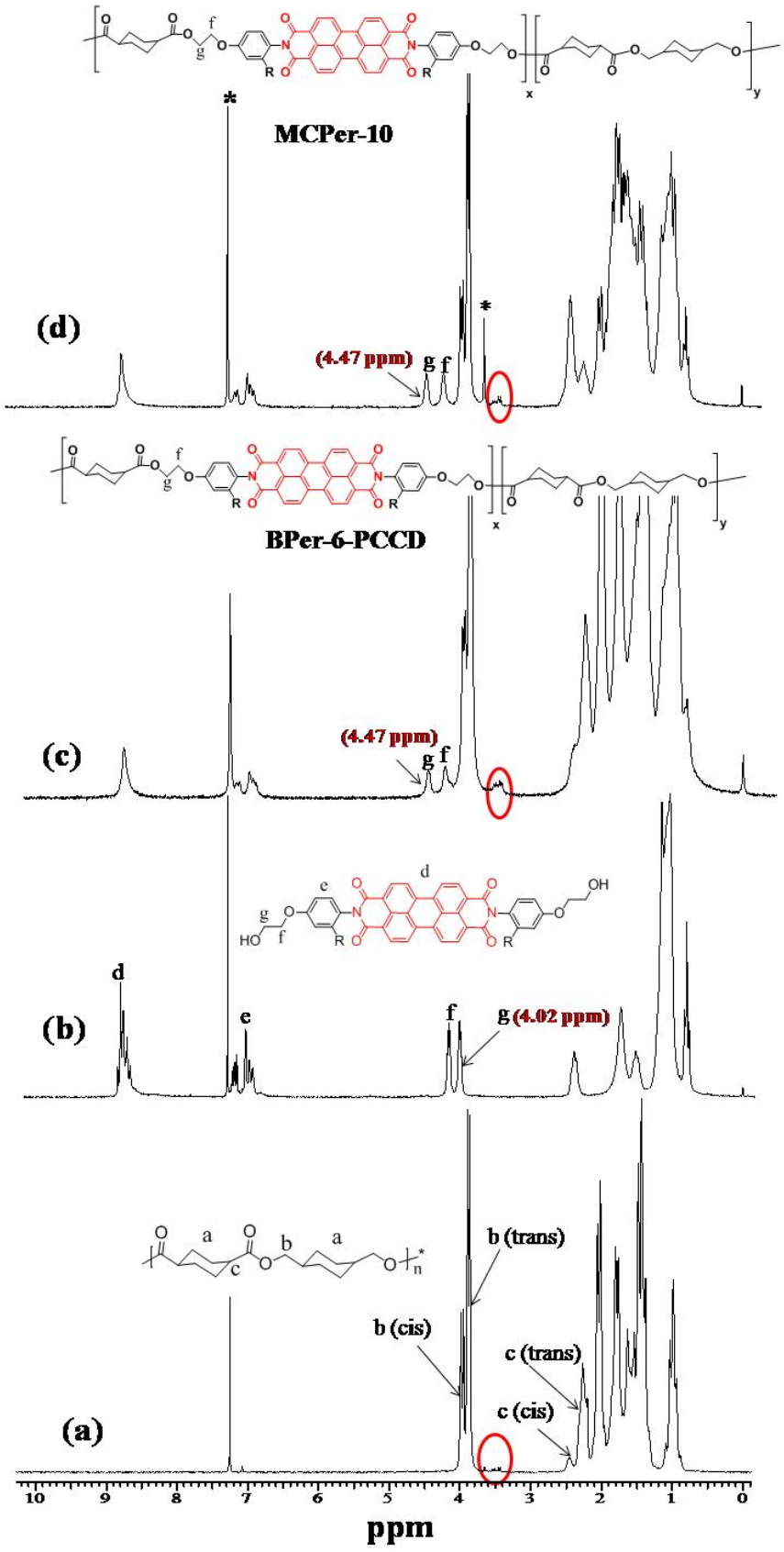

Figure 2.2. *Stack plot of* ^{1}H *NMR spectra of* ***PCCD****, Per-PDP-2-Diol and copolymer* ***BPer-6-PCCD*** *and* ***MCPer-10****.*

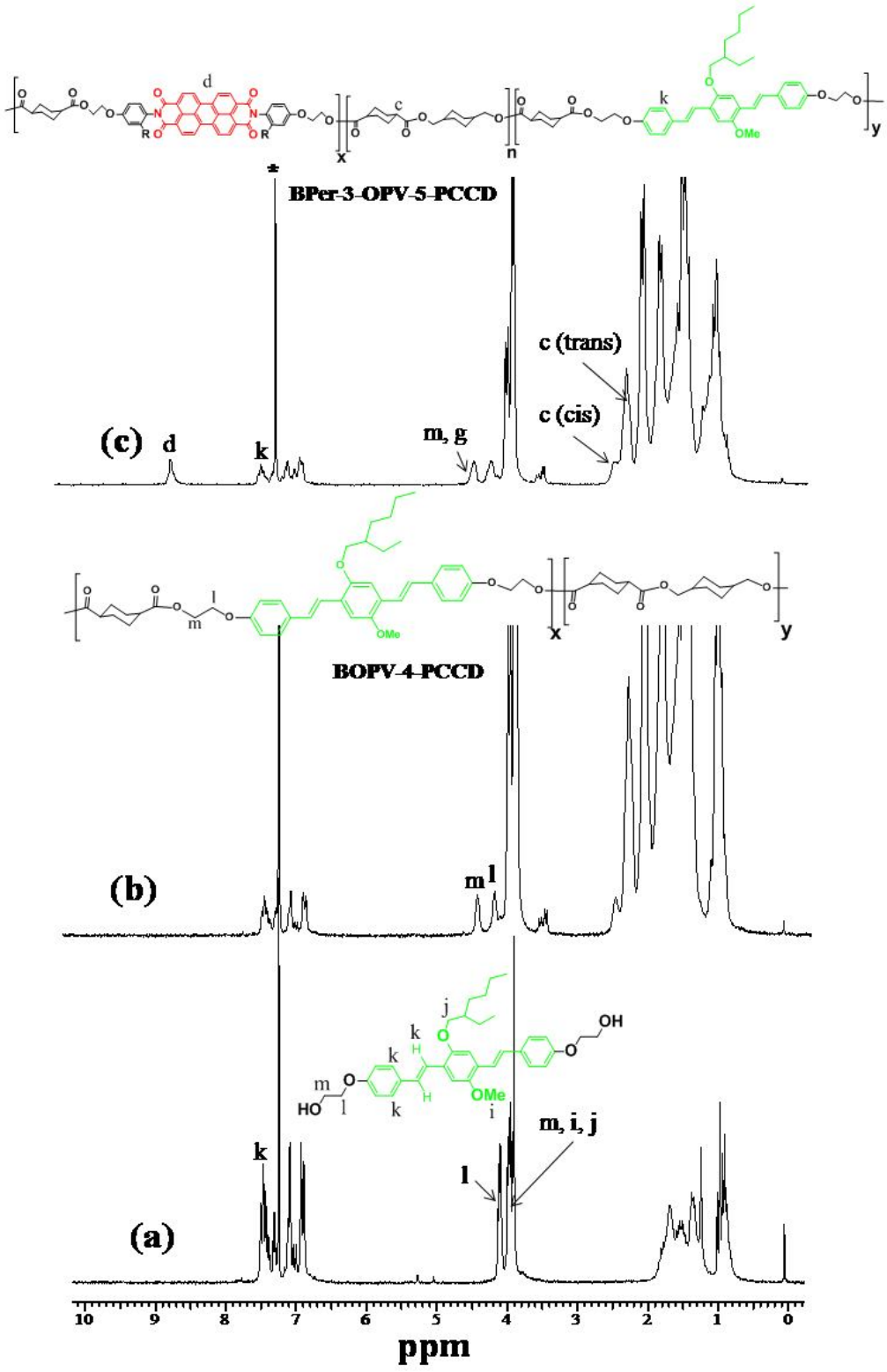

Figure 2.3. *Stack plot of [1]H NMR spectra of OPV-2-Diol, copolymer* ***BOPV-4-PCCD*** *and donor-acceptor random copolymer* ***BPer-3-OPV-5-PCCD****.*

The incorporation of the perylene or OPV in the different copolyesters were calculated from the [1]H NMR spectra by comparing the integration of peaks corresponding to

the perylene aromatic protons (labelled 'd') with that of the **PCCD** 'b' protons or OPV aromatic protons (labelled 'k') with that of the **PCCD** protons. In the copolyester containing both perylene and OPV, the aromatic units and the two protons corresponding to the cis and trans cycloaliphatic ring of **PCCD** (labelled 'c') were used to calculate the extent of incorporation of the donor and acceptor with respect to **PCCD**. Thus, the mol % of perylene incorporated in the blend series was determined as 1.2, 3.1, 6.0, 12.5, 21.0 and 35.0 mol % corresponding to feed taken for 2, 5, 10, 20, 30 and 50 mol % respectively. Although 50 mol % of Per-PDP-2-Diol was taken in the feed for the solution blending approach, the actual incorporation determined from ^{1}H NMR was only 35 mol%. Beyond this the molecular weight of the obtained polymer was drastically reduced, so higher incorporation of perylene beyond 35 mol% was not pursued using the solution blending approach.

The mol % of PBI incorporated in the melt condensation series was determined as 1.6, 4.2, 9.8, 17.3, 28.4 and 42.6 mol % corresponding to feed taken for 2, 5, 10, 20, 30 and 50 mol % respectively which are given in table 2.1 and table 2.2. Beyond 20 mol % of Per-PDP-2-Diol in the feed, the polymer solubility reduced very much. The incorporation and molecular weight for the last two entries, i.e. 30 and 50 mol % in the feed were that of the soluble fraction only. The 100 mole % polymer of PBI with DMCD alone was an insoluble rock, and so was not considered for any further characterization. Thus, the limitation of the melt condensation approach was the insolubility of the polyesters having more than 20 mol % incorporation of the rigid perylene units. On the other hand, with the high-temperature solution-blending approach, upto 35 mol % incorporation of perylene could be achieved with reasonably good molecular weight and without losing out on solubility and processability. But the advantage of the melt condensation route was that for the same mol % perylene taken in the feed, more incorporation occurred in this route compared to solution blending.

Figure 2.4 shows the plot of actual mole % incorporation against the feed intake in the case of PBI based copolyesters synthesized using the two approaches – solution blending and melt condensation. The difference in perylene incorporation between the two approaches became more prominent at higher perylene content in the feed. Similarly, the incorporation of OPV was determined to be 4 mol % for a feed intake of 5 mol % in both blend as well as melt condensation route. For 5 mol % each of OPV and PBI in the feed, random copolyesters incorporated more OPV compared to perylene using either approach as seen from the higher incorporation of OPV compared to PBI.

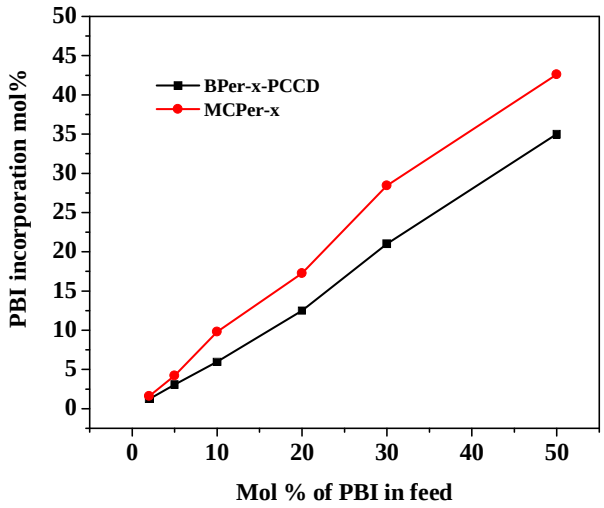

Figure 2.4. *Mole % incorporation of PBI in the copolyesters as a function of Per-PDP-2-Diol taken in feed by solution blending as well as melt condensation approach.*

2.3.2. Molecular Weights of Polymers

The polymers were soluble in common chlorinated solvents such as DCM and chloroform at room temperature. The molecular weights of the polymers were determined by SEC in $CHCl_3$ using polystyrene standards. Figure 2.5 (a) shows the size exclusion chromatogram for the polyesters prepared by the solution blending approach plotted along with that of the parent **PCCD** polymer (dotted line). The copolyesters all eluted slowly compared to **PCCD** indicating their lower molecular weights which was a consequence of the chopping of the polymer chains to incorporate the perylene. On the other hand, in the melt condensation approach, small incorporation of rigid units like perylene or OPV resulted in an increase in the molecular weight [figure 2.5 (b)]. For instance the Mw of **PCCD** synthesized via melt condensation was 20,500 whereas a 2 mol % incorporation of Per-PDP-2-Diol resulted in copolyester with Mw 58,300. Comparing ~ 5 mol % incorporation of perylene versus OPV, **MCOPV-4** exhibited higher Mw of 62,700 whereas Mw of **MCPer-4** was 36,800.

Figure 2.5 (c) compares the effect of increased incorporation of Per-PDP-2-Diol upon Mw for copolymers produced by the solution blending and melt condensation approaches. For similar perylene incorporation, the molecular weight was higher for the copolyesters produced via solution blending approach. The solution blending approach was conducted with commercial **PCCD** (Mw: 58,000) which had a considerably higher molecular weight

compared to the laboratory prepared **PCCD** (Mw: 20,500). The advantage of the solution blending approach over the melt condensation route was the ability to incorporate higher mol % of the n-type semiconducting perylenebisimide unit (35 mol %) with high molecular weight (Mw: 6,900 and Mw: 13,000) and still remain completely soluble in common organic solvents like chloroform. In contrast, the polymers from the melt condensation approach, the maximum perylenebisimide incorporation which allowed complete solubility in $CHCl_3$ was only 17 mol % (Mw: 9,200). Table 2.1 and 2.2 also gives the solution viscosity measured in a solvent mixture of phenol/1,1,2,2-tetrachloroethane of composition (60/40) for all the polymers. For instance, the η_{inh} of **PCCD** synthesized by melt condensation approach was 0.31, which nearly doubled to 0.57 upon incorporation of < 2 mole % PBI and to 0.43 upon incorporation of ~ 4 mole % of OPV. The commercial **PCCD** had a very high η_{inh} of 0.89. Upon incorporation of more PBI, the η_{inh} reduced drastically to ~ 0.13 for ~ 35 mole % PBI incorporation.

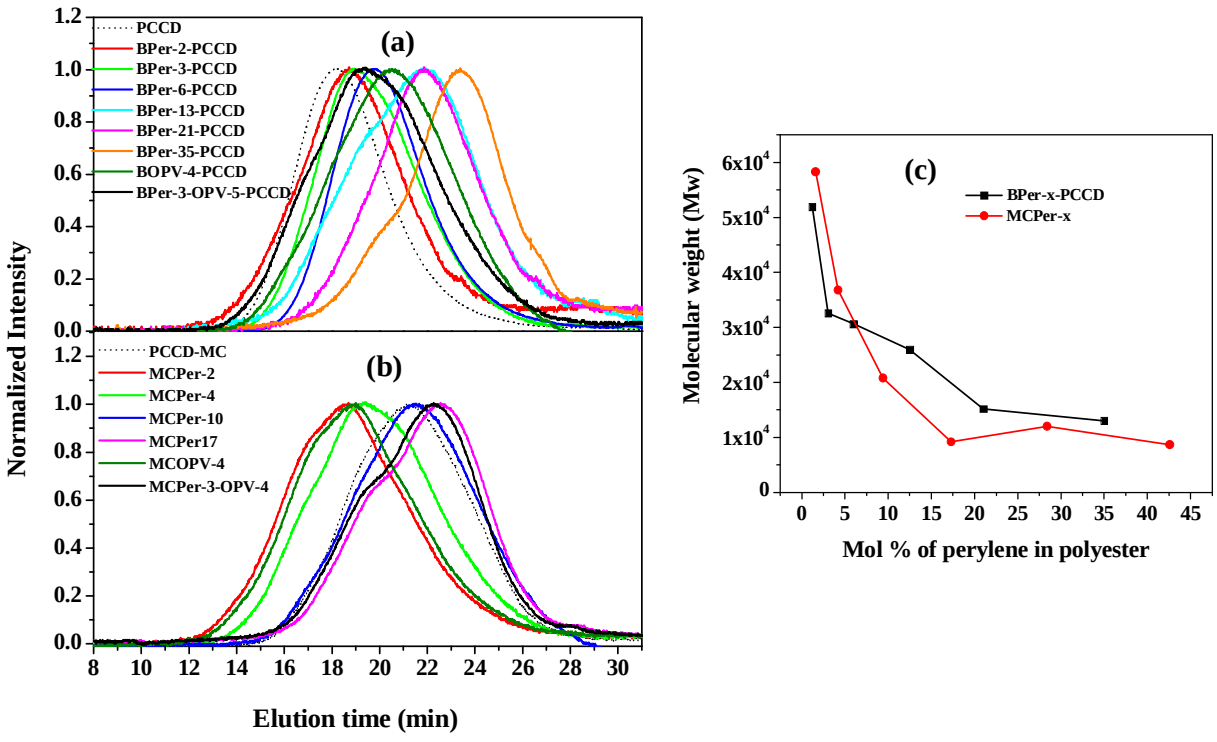

Figure 2.5. *SEC of copolyesters produced by the (a) solution blending approach and (b) melt condensation approach recorded in chloroform using polystyrene as standard; (c) plot comparing the molecular weight (M_w) of copolyesters produced by solution blending as well as melt condensation approach as a function of increased incorporation of perylene.*

2.3.3. Thermal Properties of Polyesters

Figure 2.6 shows the TGA analysis for both series of polymers. The 10 % weight loss temperature is given in the tables 2.1 and 2.2. The incorporation of rigid units like perylene or OPV improved the thermal stability of the copolymers and they were all thermally stable up to 380 ^{o}C.

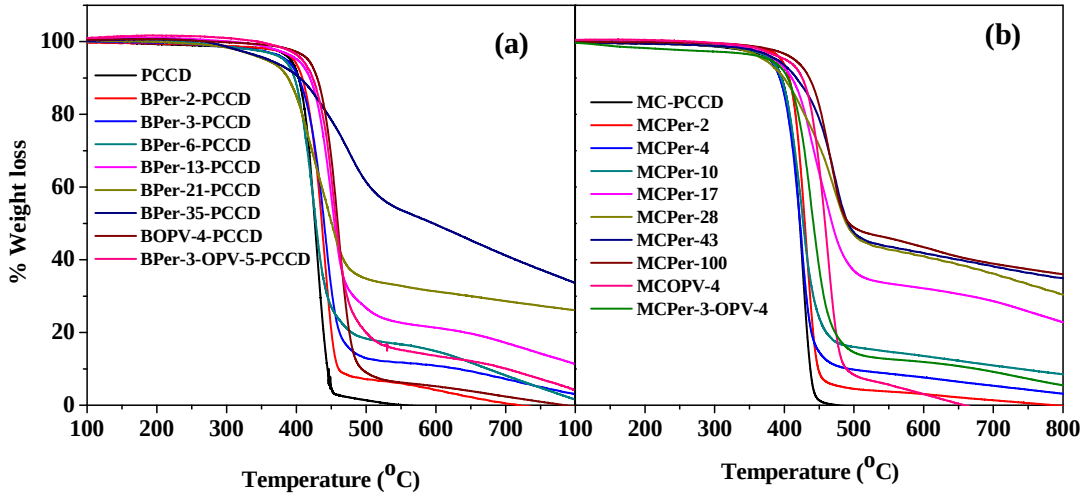

Figure 2.6. *TGA thermograms of* ***PCCD****, Per-PDP-2-Diol, OPV-2-Diol and copolyesters produced by (a) solution blending approach and (b) melt condensation polymerization.*

Figure 2.7 (a) compares the second heating DSC thermogram of commercial **PCCD** and laboratory synthesized **PCCD**. The former exhibited a T_g around 69 ^{o}C, an exothermic crystallization at 115 ^{o}C followed by a melting at 218 ^{o}C.[33] On the other hand, the thermogram of the laboratory synthesized **PCCD** was very different. It showed a much lower value for T_g ~ 42 ^{o}C and did not exhibit any other transitions. The reason for this difference lies in the stereochemistry of the 1,4-cyclohexylene rings in the final polymer.[33] Commercial **PCCD** and laboratory synthesised **PCCD** are developed using DMCD having different trans content, 90 % and 50 % respectively. Higher the trans content, higher is the ability of the polymer to crystallize.[33] Thus commercial **PCCD** is a semicrystalline polymer whereas the laboratory synthesized **PCCD** was amorphous. The Per-PDP-2Diol did not show a melting transition upon heating till 350 ^{o}C, whereas the OPV-2-Diol melted at 108 ^{o}C [see figure 2.7 (b)].

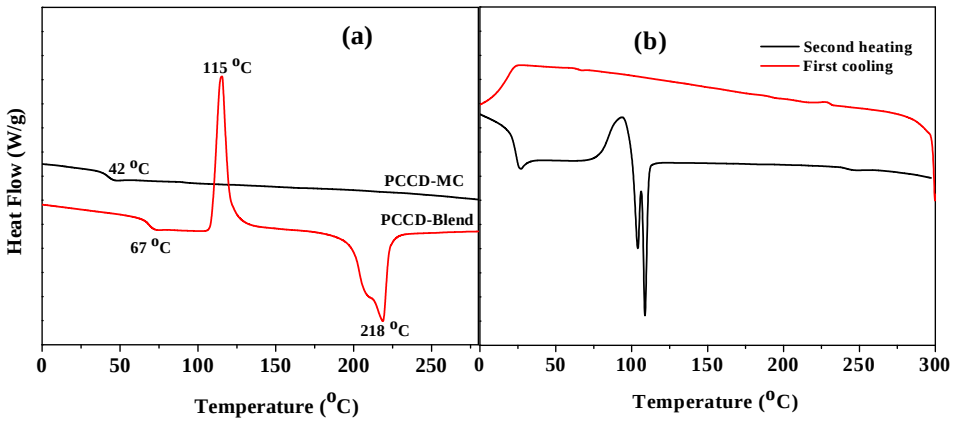

Figure 2.7. *DSC thermograms of (a)* ***PCCD-Blend****,* ***PCCD-MC*** *and (b) OPV-2-Diol at heating rate of 10 °C/min.*

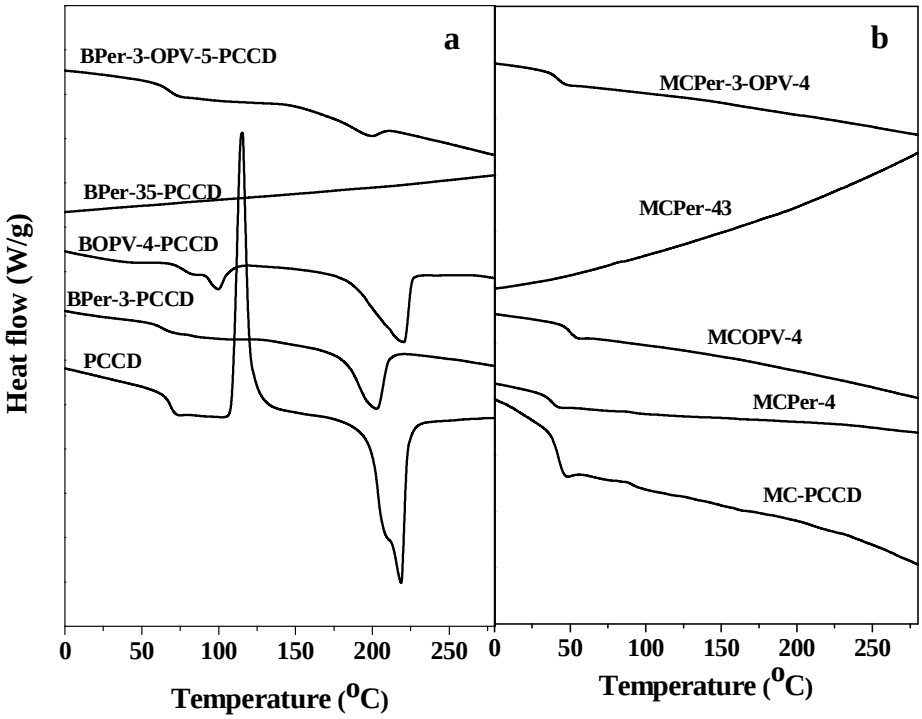

Figure 2.8. *DSC thermograms of polymers produced by (a) solution blending approach and (b) melt condensation.*

Figure 2.8 shows the stack plot of the second heating scans in the DSC thermograms of the copolyesters with ~ 5 mol % perylene or OPV, the donor-acceptor random copolymer, the copolymer with the highest perylene incorporation (35 mol % via blending and 43 mol % via melt condensation) and **PCCD** obtained using both solution blending and melt condensation routes. A T_g and melting transition were clearly observable in all cases except for the highest incorporation of perylene in the copolymers produced by solution blending

approach (values of T_g are given in tables 2.1 and 2.2). In contrast, the copolymers produced by melt condensation approach were characterized by only a T_g as they were amorphous polymers. The T_g value increased from 42 °C for laboratory synthesized **PCCD** to 46 °C for **MCPer-2** and 50 °C for **MCOPV-4** indicating the increased stiffness upon incorporation of rigid PBI or OPV units into the cycloaliphatic backbone.

2.3.4. Wide-angle X-ray Diffraction (WXRD)

The two series of polymers produced by solution blending and melt condensation approach were analyzed for their bulk packing using wide angle X-ray diffraction (WXRD) in the range of 2θ = 5-50° at room temperature (25 °C). Figure 2.9 shows the WXRD patterns of **PCCD** along with that of two copolymers at low PBI incorporation obtained using the solution blending as well as melt condensation approaches. The peak position as well as pattern of the commercial **PCCD** and low PBI incorporated polymer samples by solution blending indicated evidence for ordered organization in the same crystalline phase comparable to literature reports.[33] On the other hand, the **PCCD** and copolymers produced by melt condensation showed distinct differences in the WXRD pattern. The copolymers showed broad featureless patterns indicating absence of crystallinity.

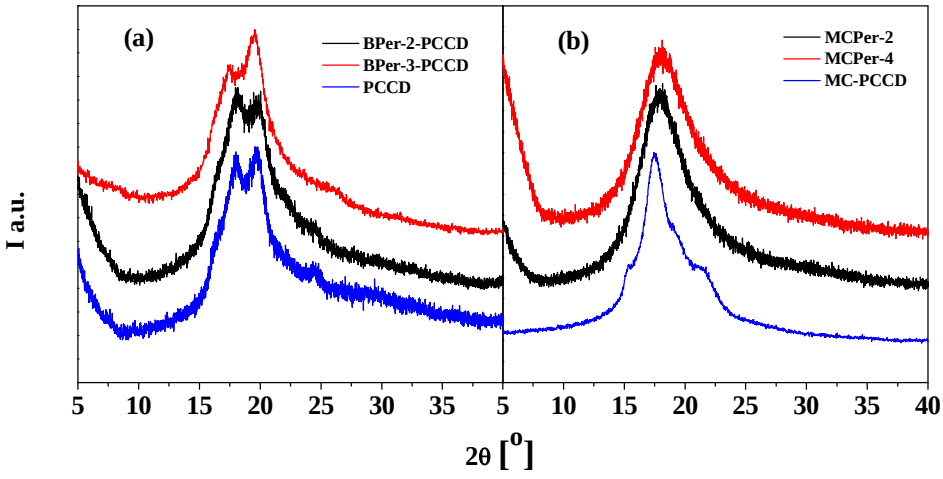

Figure 2.9. *WXRD traces of copolyesters produced by the (a) solution blending and (b) melt condensation approach.*

2.3.5. Optical Properties of Polymers

The optical properties of the polymers were investigated by UV-Vis and fluorescence spectroscopy in both solution and solid state. The copolyesters of perylene showed the typical absorption of perylene with peaks in the range of 400-530 nm, corresponding to the 0–0, 0–1, 0–2, and 0–3 electronic transitions in chloroform.[34] Emission from the copolymers was studied by exciting at the absorption wavelength of 490 nm. Figure 2.10 (a) and (b) compares the normalized absorption and emission of **BPer-3-PCCD** in chloroform as well as in film state spin-coated from chloroform solution. The absorption spectrum in the solid state was broad and the ratios of peak intensities were different compared to that in solution indicating aggregation.[34] In solution, typical emission of perylenebisimides with peak maxima at 535, 578, 625 nm was observed whereas in the solid state, perylene monomer emission at 535 nm was hugely suppressed and a red shifted intense broad aggregate emission was observed at 616 nm.[34]

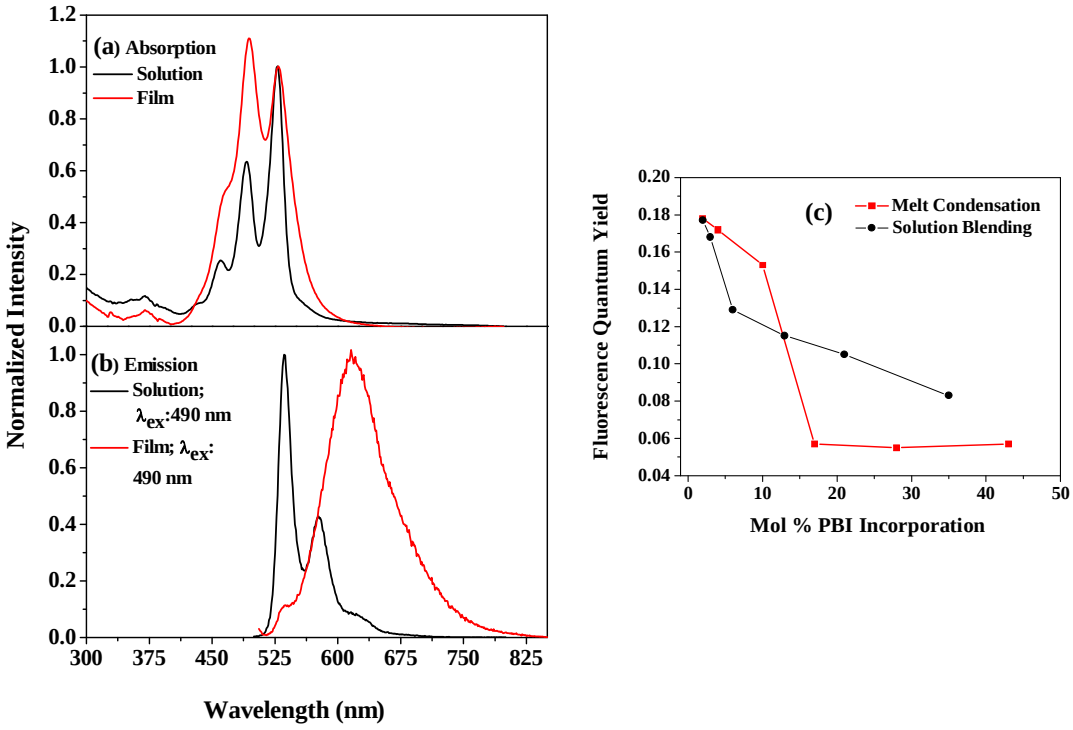

Figure 2.10. *Normalized (a) absorption and (b) emission of* ***BPer-3-PCCD*** *prepared by high temperature blending in the solution (chloroform) as well as in film spin-coated from chloroform; (c) plot comparing the fluorescence quantum yield (Φ_{FL}) as a function of PBI incorporation for the two series of PBI copolyesters obtained by melt condensation and solution blending.*

Table 2.3 gives the fluorescence quantum yield data for all the copolymers along with that of the starting fluorophores – Per-PDP-2-Diol and OVP-2-Diol. Per-PDP-2-Diol exhibited only weak fluorescence which got enhanced upon its esterification in polymer backbone. Thus the Φ_{FL} increased from 0.057 for Per-PDP-2-Diol to 0.18 in the 2 mol % perylene incorporated polymer **BPer-2-PCCD**. As perylene incorporation increased a decrease in fluorescence quantum yield was observed which could be attributed to aggregation induced quenching.[35]

Table 2.3. *Photophysical properties Per-PDP-2-Diol, OPV-2-Diol and polymers prepared by solution blending in $CHCl_3$ solution.*

Sample (In CHCl3)	Absorption peak λ (nm)	Emission λ_{max} (nm)	Quantum yield $\phi_{Perylene}$ [c]	Quantum yield ϕ_{OPV} [d]
Per-PDP-2-Diol	527	535[a]	0.057	-
BPer-2-PCCD	527	535[a]	0.177	-
BPer-3-PCCD	527	535[a]	0.168	-
BPer-6-PCCD	527	535[a]	0.129	-
BPer-13-PCCD	527	535[a]	0.115	-
BPer-21-PCCD	527	535[a]	0.105	-
BPer-35-PCCD	527	535[a]	0.083	-
OPV-2-Diol	394	445[b]	-	0.20
BOPV-4-PCCD	390	445,470[b]	-	0.50
BPer-3-OPV-5-PCCD	390,527	445,[b] 535[a]	0.14	0.22

a. Excitation at 490 nm
b. Excitation at 390 nm
c. The fluorescence quantum yields for PBI polymers were obtained upon excitation at 490 nm and were measured using rhodamine-6G in ethanol as a standard.
d. The fluorescence quantum yields for OPV polymers were obtained upon excitation at 360 nm and were measured using 0.1OD quinine sulphate solution at 360 nm in 0.1M H_2SO_4 solution.

Figure 2.10 (c) compares the decrease in fluorescence quantum yield for the perylene copolyesters synthesized using the two routes – melt condensation and solution blending. It

can be seen from the figure that although the emission quantum yield reduced with increasing PBI incorporation, the polymers produced by the solution blending approach exhibited higher quantum yields compared to those prepared by the melt condensation route having similar perylene incorporation. This indicated different extents of aggregation of perylene in the polymers produced using the two routes. The statistically random incorporation of perylene during the melt condensation process resulted in perylene aggregation beyond 10 mole % incorporation. On the other hand, the transesterification method of perylene incorporation during solution blending resulted in polymers where the PBI units were segmented by blocks of **PCCD** units, which reduced their aggregation and thereby imparting higher fluorescence quantum yields. This structural difference of the polymers was also evident in their DSC thermograms which showed that the polymers produced by solution blending were more crystalline (contributed by crystalline **PCCD** domains) compared to those produced by melt condensation approach which were all amorphous.

Figure 2.11 shows the normalized absorption and emission spectra of **BOPV-4-PCCD** recorded in chloroform as well as in film spin-coated from chloroform solution. The OPV copolyester exhibited absorption maximum at 390 nm and emission maximum at 445 nm with a shoulder peak at 470 nm in chloroform.[36] The solid state emission was red shifted with a peak maximum at 480 nm due to the aggregation of OPV units in the polymer.[37]

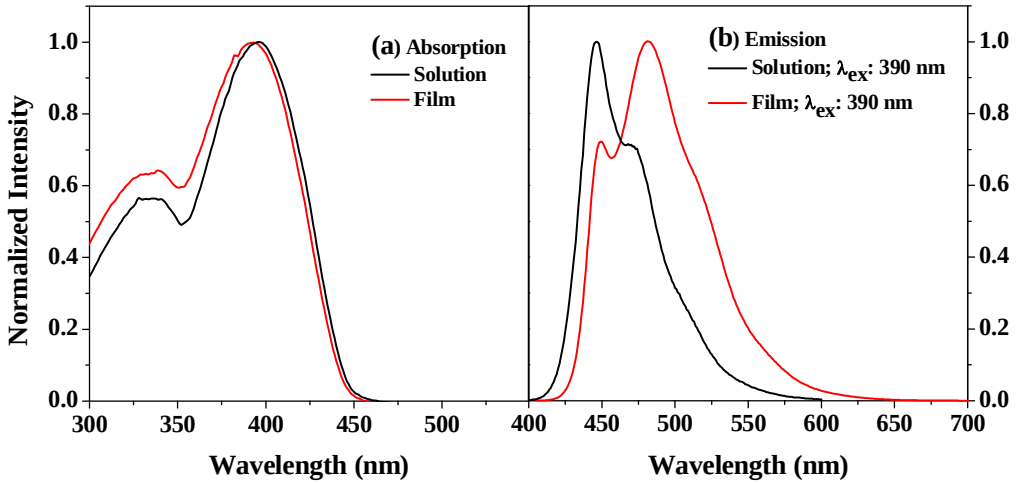

Figure 2.11. *Normalized (a) absorption and (b) emission of* ***BOPV-4-PCCD*** *prepared by high-temperature solution-blending in the solution (chloroform) as well as in film spin-coated from chloroform.*

Figure 2.12 shows the normalized absorption and emission spectra of **BPer-3-OPV-5-PCCD** recorded in chloroform as well as in film spin-coated from chloroform. The absorption spectra did not give any indication of electronic interaction between OPV and perylene units in the ground state as the peak maxima of absorption were exactly identical to that of the individual components as earlier report.[38] Excitation at 390 nm resulted in both OPV emission at 445 nm as well as weak emission corresponding to perylene as shoulder peaks at 535 and 578 nm. It could be concluded that the peaks at 535 nm and beyond was due to sensitized emission from perylene upon excitation of OPV units at 390 nm. In the solid state the absorption peaks were shifted to higher wavelength and the intensity of vibronic transitions change drastically as reported in literature.[39] Incorporation of PBI into the donor polymer backbone resulted in the quenching of both donor and acceptor emission by monitoring the PL emission from OPV unit. Energy transfer is excluded from the mechanism of the OPV luminescence quenching in donor-acceptor polymer because the characteristic emission of PBI was not observed when the **BPer-3-OPV-5-PCCD** polymer was excited at 395 nm. The observed quenching of photoluminescence that occurred in **BPer-3-OPV-5-PCCD** could be attributed to photoinduced electron-transfer from donor (OPV unit) to acceptor (PBI unit).

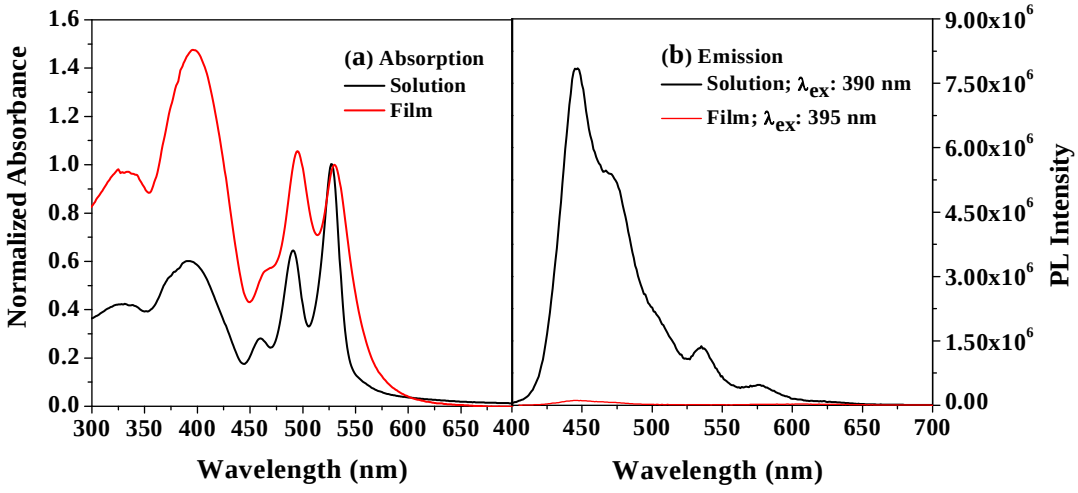

Figure 2.12. *Normalized (a) absorption and (b) emission of* ***BPer-3-OPV-5-PCCD*** *prepared by high-temperature solution-blending in the solution (chloroform) as well as in film spin-coated from chloroform.*

2.3.6. Electrochemical Properties

The electrochemical behaviour of the **BPer-3-PCCD, BOPV-4-PCCD** and **BPer-3-OPV-5-PCCD** were investigated by cyclic voltammetry (CV), which were performed in dichloromethane containing 0.1 M $TBAPF_6$ (tetra-n-butylammonium hexafluorophosphate) as electrolyte. Table 2.4 gives their redox behaviour and figure 2.13 shows the stack plot of their cyclic voltametry curves. Normally perylene bisimides show two reduction peaks corresponding to the formation of the mono and dianion respectively.[40] But the perylene copolymer **BPer-3-PCCD** had only one reversible reduction at -1.33 V because of the low content of PBI in the polymer backbone.[41] The OPV copolymer **BOPV-4-PCCD** had two reversible oxidation at 0.59 V and 1.23 V corresponding to mono and dication of OPV unit.[42] The redox behaviour of **BPer-3-OPV-5-PCCD** in dichloromethane indicated both oxidative and reductive processes. A reversible reduction peak was observed at -1.23 V corresponding to the reduction of the perylene moiety and a quasi reversible oxidation peak was observed at 0.81 V corresponding to the OPV moiety although in the cathodic scan it resolved as two peaks.[43] However, in **BPer-3-PCCD** and **BPer-3-OPV-5-PCCD**, the perylene showed only a single two electron peak. The HOMO energy value for the OPV was estimated from the onset potentials of oxidation, while the LUMO energy values for the perylene was estimated from the onset of reduction event. After calibration of the measurements against Fc/Fc^+, the oxidation potential of which is assumed at 4.8 eV below the vacuum level, the HOMO and LUMO energy levels were calculated according to the following equations,[44]

$$E_{HOMO}(eV) = -\left[E_{ox}^{onset} - E_{1/2}(F_c/F_c^+) + 4.8\right]$$

$$E_{LUMO}(eV) = -\left[E_{red}^{onset} - E_{1/2}(F_c/F_c^+) + 4.8\right]$$

where $E^{1/2}(Fc/Fc^+)$ is the half-wave potential of the ferrocene/ferrocenium couple measured relatively to Ag/Ag^+. The HOMO energy levels of perylene moiety and LUMO energy levels of OPV moiety were estimated from the optical band gap and cyclic voltammetry data. The optical energy gap E_g^{opt} was determined from the onset of absorption in the solid state using the equation $E_g^{opt} = 1240/\lambda_{onset}$.

The HOMO-LUMO values and the observation of electron transfer in these systems suggested that they were suitable materials for application as active components in photovolataic devices. The optimization of the energy transfer could be attained by varying

the extent of incorporation of the donor and acceptor units and also by designing different donor and acceptor combinations with the required functionality for transesterification.

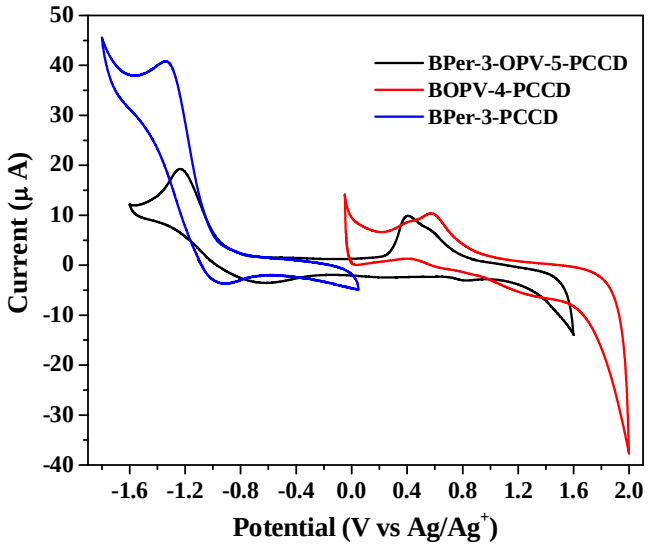

Figure 2.13. *Cyclic Voltammograms of* ***BPer-3-PCCD***, ***BOPV-4-PCCD*** *and* ***BPer-3-OPV-5-PCCD.***

Table 2.4. *Cyclic Voltammogram data of* ***BPer-3-PCCD***, ***BOPV-4-PCCD*** *and* ***BPer-3-OPV-5-PCCD****. Measurement was calibrated with ferrocene/ferrocenium redox system Vs Ag/Ag*$^{+}$.

Polymer	E_{ox} (V) OPV	E_{red} (V) PBI	LUMO (eV)	HOMO (eV)	E_g (optical) (Film) (eV)
BPer-3-PCCD	-	-1.33	-3.88	-6.05	2.17
BOPV-4-PCCD	0.59, 1.23	-	-2.30	-5.11	2.81
BPer-3-OPV-5-PCCD	0.81	-1.23	-3.86	-5.38	2.17

2.3.7. Thin Film Formation

Free-standing films could be formed for polymers synthesized using high-temperature solution-blending approach signifying their high mechanical stability. Figure 2.14 a, b, c shows the free standing films prepared from 1 wt % $CHCl_3$ solution of **BPer-3-PCCD**, **BOPV-4-PCCD** and **BPer-3-OPV-5-PCCD** respectively. The polymer synthesized by melt condensation method formed only brittle films which could not be peeled off. Figure 2.14 d, e and f shows the image of the three polymer films upon observation under 365 nm hand-held UV lamp. The emission from **BOPV-4-PCCD** showed bluish green emission whereas the emission from the other two samples was completely quenched in the solid state.

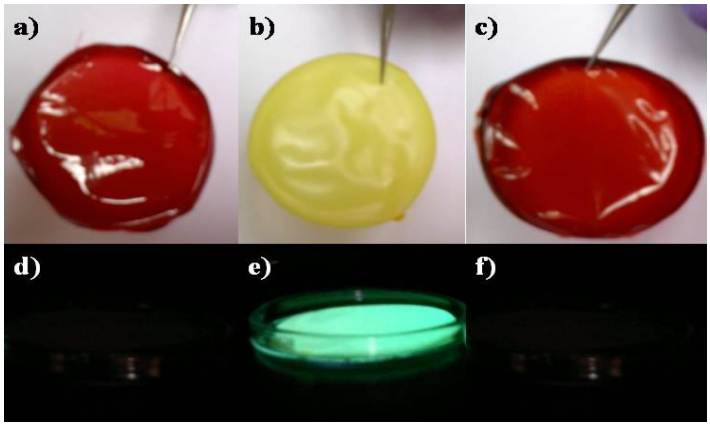

Figure 2.14. *Photograph of a)* ***BPer-3-PCCD****, b)* ***BOPV-4-PCCD*** *and c)* ***BPer-3-OPV-5-PCCD*** *drop cast from a 1 weight % solution in chloroform. The respective films upon observation under UV lamp (365 nm) [d)* ***BPer-3-PCCD****, e)* ***BOPV-4-PCCD*** *and f)* ***BPer-3-OPV-5-PCCD****].*

2.4. Conclusion

In conclusion we have demonstrated a successful strategy for incorporation of fluorescent chromophores like perylenebisimide (PBI) and oligo(*p*-phenylenevinylene) (OPV) into the backbone of an engineering thermoplastic polyester [Poly(1,4-cyclohexylenedimethylene-1,4-cyclohexanedicarboxylate)] (**PCCD**). This approach is extendable to a variety of chromophores after suitable end functionalization for transesterification. The chemical incorporation of these chromophores into the polyester backbone was also proved by carrying out the melt condensation of the polymers from the monomers 1,4-cyclohexanedimethanol (CHDM) and 1,4-dimethylcyclohexane dicarboxylate (DMCD) with varying mole ratios of terminal hydroxyl functionalized PBI and OPV derivatives. The advantages of solution blending over melt condensation are its ease of synthesis, high incorporation (> 30 mole % of PBI) of the desired chromophore while still retaining high molecular weight and solubility in common organic solvents. Commercial **PCCD** is semicrystalline with a glass transition temperature (T_g) around 69 °C, while the laboratory synthesized **PCCD** and its copolymers with PBI or OPV derivative were amorphous with a much lower T_g (< 50 °C). This packing difference was also reflected in their photophysical properties with the polymers developed via the solution blending approach showing less aggregation tendency compared to melt condensation polymers and higher fluorescence quantum yield for polymers of similar perylene incorporation. Polymers synthesized using solution blending approach also possesses the required thin film

processability for organic solar cell. The covalent incorporation of both donor and acceptor moieties are also expected to improve the morphology of the resultant polymer. Thus the reactive solution blending approach to covalently incorporate the desired chromophores into high molecular weight polymer backbones has the potential to develop polymers for applications like organic solar cells and luminescent solar collectors.

2.5. References

1) Facchetti, A. *Mater. Today* **2007**, *10*, 28.
2) Horowitz, G. *Adv. Mater*. **1998**, *10*, 365-377.
3) Horowitz, G. *J. Mater. Res*. **2004**, *19*, 1946 -1962.
4) Katz, H. E.; Bao, Z. *J. Phys. Chem. B* **2000**, *104*, 671-678.
5) Würthner, F. *Angew. Chem. Int. Ed*. **2001**, *40*, 1037-1039.
6) Dimitrakopoulos, C. D.; Malenfant, P. R. L. *Adv. Mater*. **2002**, *14*, 99-117.
7) Sun, Y.; Liu, Y.; Zhu, D. *J. Mater. Chem*. **2005**, *15*, 53-65.
8) Chabinyc, M.; Loo, Y.-L. *J. Macromol. Sci., Poly*. **2006**, *46*, 1-5.
9) Dodabalapur, A. *Nature* **2005**, *434*, 151-152.
10) Sirringhaus, H. *Adv. Mater*. **2005**, *17*, 2411-2425.
11) Malliaras, G.; Friend, R. *Physics Today* **2005**, *58*, 53-58.
12) Meyer, J.-P.; Schlettwein, D.; Wöhrle, D.; Jaeger, N. I. *Thin Solid Films* **1995**, *258*, 317-324.
13) Horowitz, G.; Kouki, F.; Spearman, P.; Fichou, D.; Nogues, C.; Pan, X.; Garnier, F. *Adv. Mater*. **1996**, *8*, 242-245.
14) Würthner, F. *Chem. Commun*. **2004**, 1564-1579
15) Rachford, A. A.; Goeb, S.; Castellano, F. N. *J. Am. Chem. Soc*. **2008**, *130*, 2766-2767.
16) Guoqiang, R.; Eilaf, A.; Jenekhe, S. A. *Adv. Energy Mater*. **2011**, *1*, 946-953.
17) Wang, Z. Y.; Qi, Y.; Gao, J. P. *Macromolecules* **1998**, *31*, 2075-2079.
18) Ghassemi, H.; Hay, A. S. *Macromolecules* **1994**, *27*, 4410-4412.
19) Chen, H. Y.; Hou, J.; Zhang, S.; Liang, Y.; Yang, G.; Yang, Y.; Yu, L.; Wu, Y.; Li, G. *Nat. Photonics* **2009**, 3, 649-653.
20) Zhou, H.; Yang, L.; Stuart, A. C.; Price, S. C.; Liu, S.; You, W. *Angew. Chem. Int. Ed*. **2011**, 50, 2995-2998.
21) Dou, L.; You, J.; Yang, J.; Chen, C. C.; He, Y.; Murase, S.; Moriarty, T.; Emery, K.; Li, G.; Yang, Y. *Nat. Photonics* **2012**, 6, 180-185.
22) Jiang, X.; Burgoyne Jr, W. F.; Robeson, L. M. *Polymer* **2006**, *47*, 4124-4131.
23) Montgomery, S. J.; Kannan, G.; Galperin, E.; Kim, S. D. *Macromolecules* **2010**, *43*, 5238-5244.
24) Liu, Y.; Turner, S. R.; Wilkes, G. *Macromolecules* **2011**, *44*, 4049-4056.
25) Kollodge, J. S.; Porter, R. S. *Macromolecules* **1995**, *28*, 4089-4096.
26) Ma, D.; Zhang, G.; He, Y.; Ma, J.; Luo, X. *J. Polym. Sci., Part B: Polym. Phys.* **1999**, *37*, 2960-2972.

27) Turner, S. R.; Seymour, R. W.; Dombroski, J. R. *Mordern Polyesters: Chemistry and Technology of Polyesters and Copolyesters*; John Wiley & Sons, Ltd., **2003**.

28) Jayakannan, M.; AnilKumar, P. *J. Polym. Sci., Part A: Polym. Chem.* **2004**, *42*, 3996-4008.

29) Bhavsar, G. A.; Asha, S. K. *Chem. Eur. J.* **2011**, *17*, 12646-12658.

30) Jayakannan, M.; Deepa, P. *J. Polym. Sci., Part A: Polym. Chem.* **2008**, *46*, 5897-5915.

31) Brunelle, D. J.; Jang, T. *Polymer* **2006**, *47*, 4094-4104.

32) Colonna, M.; Berti, C.; Binassi, E.; Celli, A.; Fiorini, M.; Marcheses, P.; Messori, M. *Polym. Int.* **2011**, *60*, 1607-1613.

33) Berti, C.; Binassi, E.; Celli, A.; Colonna, M.; Fiorini, M.; Marchese, P.; Marianucci, E.; Gazzano, M.; Credico, F. D. *J. Polym. Sci., Part B: Polym. Phys.* **2008**, *46*, 619-630.

34) Balakrishnan, K.; Datar, A.; Naddo, T.; Huang, J.; Oitker, R.; Yen, M.; Zhao, J.; Zang, L. *J. Am. Chem. Soc.* **2006**, *128*, 7390-7398.

35) Thelakkat, M.; Pösch, P.; Schmidt, H. *Macromolecules* **2001**, *34*, 7441-7447.

36) Jonkheijm, P; Jeroen K.J. van Duren, Kemerink, M.; René A. J. Janssen; Schenning, A. P. H.; Meijer, E. W. *Macromolecules* **2006**, *39*, 784-788.

37) Ajayaghosh, A.; Praveen, V. K.; Srinivasan, S.; Vargese, R. *Adv. Mater*. **2007**, *19*, 411-415.

38) Edda, E. N.; Paul, A. H.; Janssen, R. A. J. *Chem. Eur. J*. **2004**, *10*, 3907-3918.

39) Bauer, P.; Wietasch, H.; Lindner, S. M.; Thelekkat, M. *Chem. Mater*. **2007**, *19*, 88-94.

40) Lee, S. K.; Zu, Y.; Herrmann, A.; Geerts, Y.; Müllen, K.; Bard, A. J. *J. Am. Chem. Soc.* **1999**, *121*, 3513-3520.

41) Chuang, C. Y.; Ping-I Shih, Chen-Han Chien, Fang-Iy Wu, and Ching-Fong Shu, *Macromolecule* **2007**, *40*, 247-252.

42) Meng, H.; Wang-Lin Yu; Huang, W. *Macromolecules* **1999**, *32*, 8841-8847.

43) Mikroyannidis, J. A.; Stylianakis, M. M.; Sharma, G. D.; Balraju, P.; Roy, M. S. J. *Phys. Chem. C* **2009**, *113*, 7904-7912.

44) Grisorio, R.; Allegretta, G.; Romanazzi, G.; Suranna, G. P.; Mastrorilli, P.; Mazzeo, M.; Cezza, M.; Carallo, S.; Gigli, G. *Macromolecule* **2012**, *45*, 6396-6404.

Chapter 3

Chiral Poly(L-lactic acid) Driven Helical Self-Assembly of Oligo(p-phenylenevinylene)

Chapter 3

Chiral Poly(L-lactic acid) Driven Helical Self-Assembly of Oligo(p-phenylenevinylene)

The synthesis and self-assembly of a series of copolyesters incorporating varying mol ratios of an achiral oligo(*p*-phenylenevinylene) (OPV) into the backbone of a chiral poly(L-lactic acid) (**PLLA**) via high-temperature solution-blending is reported. The polymers were characterized by ^{1}H NMR spectroscopy and size exclusion chromatography (SEC) and their bulk properties were investigated by differential scanning calorimetry (DSC) and wide-angle X-ray diffraction (WXRD). DSC and WXRD analysis confirmed the crystallinity and π-π stacking of the OPV units in the **PLLA-OPV** copolyester. Absorption, emission and lifetime-decay studies showed that OPV chromophore was highly aggregated in the solid state. The solid powder samples of the copolyesters exhibited intense red shifted aggregate emission beyond 470 nm. Circular dichroism (CD) spectroscopy, scanning electron microscopy (SEM) and atomic force microscopy (AFM) studies revealed that the **PLLA-OPV** copolyester formed self-assembled architecture in which the helical organization of the achiral OPV segments was dictated by the chiral **PLLA** segments. The observed CD signal and AFM image accounted for right-handed helical self-assembly of OPV chromophore in the solid state. These results confirmed the effect of chiral **PLLA** segment on tuning the OPV chromophore packing and supramolecular chirality in molecular aggregates. The methodology illustrated here provides opportunities for the design of a new class of hierarchical self-assembled architectures based on organic π-conjugated materials and the manipulation of their optical properties. The nanofibers of copolyester of **PLLA** incorporating OPV chromophore were successfully constructed by electrospinning technique and the fluorescence microscopy images of these fibers showed both blue and green emission upon excitation at different wavelengths.

3.1. Introduction

Supramolecular π-conjugated materials based on organic molecules and polymers have been widely studied due to their potential applications in electronic devices like photovoltaics, light emitting diodes and chemical and biosensors.[1-4] Nature controls the architecture of supramolecular assemblies, such as the DNA double helix, the photosynthetic reaction centres and the collagen triple helix etc, which are vital for sustaining life.[5] Both covalent and noncovalent chemistry play important roles in this creativity and chemists try to mimic the molecular architectures of such functional assemblies. Over the past decade, several noncovalent interactions such as hydrogen bonding, electrostatic interactions, π-π stacking, dipolar interactions, chirality, and so forth, have been identified as enabling the construction of various hierarchical architecture from specially engineered small molecule building blocks.[6-9] The chiral self assembly of linear π-conjugated systems makes them interesting as optical probe molecules for various applications.[10-12] The optical and electronic properties of devices made up of these π-conjugated materials are sensitive to conformational changes upon intermolecular interactions.[13-15] Oligofluorenes, oligothiophenes, oligophenylenes and oligophenylenevinylenes were reported for chiral self-organization in π-conjugated materials.[16-18] High luminescent characteristics, thermal and optical stability, film forming tendency and solubility in organic solvents make oligo(*p*-phenylenevinylene) (OPV) chromophore very unique compared to other π-conjugates.[19, 20]

The self organization of oligo(*p*-phenylenevinylene) (OPV) chromophore via hydrogen bonding, π-π stacking and metal-ion interactions etc has been reported and the resultant structure were tested successfully as active layer in electronic devices.[21-24] In most of the cases, helicity has been achieved by the use of chiral monomers. Meijer and co-workers have made significant contributions to the helical self-assembly of π-conjugated oligomers derived from phenylenevinylenes where the chirality of the attached side chains was translated to the conjugated oligomer backbone at a supramolecular level.[25, 26] However, the lack of control over the chirality outcome and tedious asymmetric synthesis make the design of chiral monomers a challenging task. A different approach towards helical system is to use host-guest chemistry to induce tunable chirality to the achiral host by specific recognition of appropriate chiral guest molecules, for which a careful design is needed.[27] Yet another category that has received lot of attention is the helical self-assembly of the achiral π-conjugated oligomers by the chiral peptide segments. Examples are the solid state self-assembly of peptide-functionalized tetrathiophene and the aqueous supramolecular

aggregates of L-lysine branched phenylvinylene derivative.[28, 29] Synthesis and self-assembly of oligo(*p*-phenylenevinylene)-peptide conjugates in solution and at the solid-liquid interface was also reported. [30]

Inspired by the concept of chiral information transfer from the molecular level to macroscopic features, we have designed a series of copolyesters composed of a chiral poly(L-lactic acid) (**PLLA**) and an achiral oligo(*p*-phenylenevinylene). Poly(L-lactic acid) (**PLLA**) is a chiral semicrystalline aliphatic polyester derived from renewable resources such as corn and rice.[31] **PLLA** is the depsipeptide counterpart to polyalanine wherein each amide linkage is replaced by an ester. The $n\rightarrow\pi^*$ interactions between sequential ester carbonyl groups contribute to the conformational stability of **PLLA** helix.[32] The helical molecular conformation in **PLLA** produces large optical activity and this phenomenon is promising for new optical applications utilizing their optical activity.[31] In the current chapter, we describe the synthesis of a series of **PLLA-OPV** random copolyesters incorporating varying amounts of oligo(*p*-phenylenevinylene) (OPV) by high-temperature solution-blending approach and the helical self-assembly of the achiral OPV segments by the chiral **PLLA** segment was studied. The structure and bulk properties of the **PLLA-OPV** copolyesters were studied using ^{1}H NMR spectroscopy, size exclusion chromatography (SEC), differential scanning calorimetry (DSC) and wide-angle X-ray diffraction (WXRD). The photophysical properties were studied using steady-state UV-vis absorption and fluorescence spectroscopy as well as fluorescence lifetime-decay measurements. The helical self-assembly of OPV segments by chiral **PLLA** was monitored via CD spectroscopy and the morphological features were revealed by scanning electron microscopy (SEM) and atomic force microscopy (AFM). The **PLLA** induced self-assembly of OPV chromophore is reflected in their packing structure, optical properties and morphology. This molecular design can be applied to other π-conjugated chromophores to diversify their self-assembly pattern, morphologies, optical and electronic properties.

Nanofibers of random copolyester incorporating OPV has been successfully produced using the electrospinning technique. Electrospinning is a simple but advanced technique, which has attracted widespread attention for fabrication of micro-/nano fibers in recent years.[33] Electrospinning possesses great advantages including simplicity of use, potential scale up and versatility in spinning a wide variety of polymeric fibers. This method involves the application of a high voltage source to obtain fibers whose diameters range from several nanometers to microns. These fibers were analyzed using microscopic techniques like scanning electron microscopy (SEM) and fluorescence microscopy.

3.2. Experimental Methods

3.2.1. Materials: (3S)-cis-3,6-Dimethyl-1,4-dioxane-2,5-dione (L-lactide), tin(II) 2-ethylhexanoate ($Sn(Oct)_2$), 4-methoxyphenol, 2-ethylhexylbromide, triethylphosphite, 4-hydroxybenzaldehyde, potassium-tert-butoxide, titanium(IV) butoxide ($Ti(OBu)_4$), and ortho-dichlorobenzene (ODCB) were purchased from Aldrich and used without further purifications. HBr in glacial acetic acid, paraformaldehyde, 2-chloroethanol and all other solvents were purchased locally and purified with standard procedures.

3.2.2. Instrumentation: ^1H NMR spectra were recorded using a Bruker Avance 200 MHz spectrometer. Chemical shifts (δ) are reported in ppm at 25 ^oC with a small amount of tetramethylsilane (TMS) as internal standard. The mass spectral analysis of monomer was carried out using a Voyager-De-STR MALDI-TOF (Applied Biosystems, Framingham, MA, USA) instrument equipped with 337 nm pulsed nitrogen laser used for desorption and ionization. The molecular weight of synthesized polymers was determined using size exclusion chromatography (SEC). GPC measurements were carried on a Polymer Laboratories PL-GPC-220 at 25 ^oC using chloroform (Merck) as the mobile phase. The analysis was carried out at a flow rate of 1 mL/min using a set of three PLgel columns and a refractive index (RI) detector. This column set enabled the determination of a wide range of molecular weight from 10^2 to 10^6. Columns were calibrated with polystyrene standards and the molecular weights reported were with respect to polystyrene. The inherent viscosity (η_{inh}) of the polymers was measured for 0.5 wt % polymer solutions in chloroform. The absorption spectra in a chloroform solution were recorded using a Perkin-Elmer Lambda 35 UV-Vis spectrophotometer. The absorption spectra of the powdered polymer samples were recorded using a JASCO model V-570 spectrophotometer in the reflectance mode. Steady-state fluorescence studies and fluorescence lifetime-decay measurements were performed using Horiba Jobin Yvon Fluorolog 3 spectrophotometer having a 450 W xenon lamp for steady-state fluorescence and nanoLED of 390 nm for fluorescence lifetime-decay measurements. For lifetime measurements, decay curves were obtained by the time-correlated single photon counting (TCSPC) technique. The fluorescence quantum yield of the polymers were determined in $CHCl_3$ using quinine sulphate in 0.1 M H_2SO_4 (ϕ = 0.54) as the standard by exciting at 360 nm. Solid state photoluminescence spectra were recorded using the front face scan mode with the same Fluorolog spectrofluorimeter. The thermal stability of the polymers was analyzed using a Perkin-Elmer thermogravimetric analyzer under nitrogen atmosphere at

heating rate of 10 ^{o}C/min. Differntial scanning colorimetry (DSC) was performed using TA Q10 differential scanning calorimeter at heating rate of 10 ^{o}C/min. Wide-angle X-ray diffraction (WXRD) were recorded by Phillips x'pertpro powder X-ray diffractometer using Cu Kα radiation, and the spectra were recorded in the range of 2θ = 5-35°. Circular dichroism (CD) spectra were measured in JASCO J815 spectrometer from 550-200 nm. Atomic force microscopy (AFM) images were taken by using a Multimode scanning probe microscope equipped with a Nanoscope IV controller from Veeco Instruments, Inc. in the tapping mode using a SiN probe. The electrospinning apparatus consists of a syringe pump, syringe needle, high voltage power supply and a grounded collector. Polymer solution was loaded into a syringe and positive electrode was clipped onto the syringe needle. The flow rate of the polymer solution to the needle tip was kept constant. Solutions were electrospun horizontally onto the target. Scanning electron microscopy (SEM) images were recorded using FEI, QUANTA 200 3D scanning electron microscope with a tungsten filament as electron source. The fluorescence microscopy images were recorded by Epi-fluorescence microscope Leitz Laborlux, Germany, and images were observes by a cannon power shot S80 camera [excitation wavelengths: 350-430 nm (blue) and 488-520 (green)].

3.2.3. Synthesis

Synthesis of poly(L-lactic acid) (PLLA): PLLA was synthesized by following the literature procedure.[34] L-Lactide was sealed in a silanized glass tube and placed in an oil bath at 180 °C for 3 h. The ring-opening polymerization of the L-lactide was catalyzed by $Sn(Oct)_2$ in a 1:10000 catalyst:monomer ratio. The polymer was dissolved in chloroform and poured into methanol to separate any residual L-lactide. The polymer was filtered and dried in oven at 60 ^{o}C. Yield: 95.60 %; ^{1}H NMR (200 MHz, $CDCl_3$) δ ppm: 5.16 (q, 1H, –C**H**(CH_3)–COO–), 1.56 (d, 3H, –C**H**$_3$).

Synthesis of copolyesters of PLLA incorporating OPV chromophore by high-temperature solution-blending (PLLA-OPV-x): PLLA (0.68 g, 9.5 mmol) and OPV-2-Diol (0.28 g, 0.5 mmol) were dissolved in ODCB (0.5 mL) by heating at 160 °C in an oil bath (for **PLLA-OPV-4**). The mixture was stirred for 30 min using an overhead mechanical stirrer at a constant rate of 100 rpm. To this mixture, $Ti(OBu)_4$ (34 mg, 1 mol %) solution in ODCB was added and the reactive blending was continued with stirring at 160 °C for 1 h. The product was dissolved in chloroform and precipitated into methanol. The polymer was

filtered and dried in oven at 60 ^{o}C. Yield: 70.00 %; ^{1}H NMR (200 MHz, $CDCl_3$) δ ppm: 6.89–7.51 (Ar–**H** and vinylic **H**), 5.16 (–C**H**(CH_3)–COO–), 4.33–4.51 (–COO–C$\mathbf{H}_2$–C$\mathbf{H}_2$–), 3.90–4.17 (Ar–O–C$\mathbf{H}_2$–, Ar–O–C$\mathbf{H}_3$, Ar–O–C$\mathbf{H}_2$–C$\mathbf{H}_2$–OH end group), 2.69 (–O**H**), 0.90–1.80 (–C$\mathbf{H}_3$ in **PLLA** part and aliphatic **H** from OPV part).

A similar procedure was employed to synthesize the **PLLA-OPV-x** series of polyesters by changing the molar ratio of OPV-2-Diol in the feed from 0.5 to 5 mol%.

Synthesis of nanofibers: Polymer solution was prepared by dissolving 100 mg of polymer in 1 mL of DCM (10 wt % solution). This solution was subjected to a high electric field of about 10 kV for electrospinning. The tip to collector distance was fixed at 12 cm and the feeding rate was 0.5 mL h^{-1}. The fibers thus obtained were dried in an oven at 60 ^{o}C for 2 h.

3.3. Results and Discussions

3.3.1. Synthesis and Characterization of Polymers

High molecular weight poly(L-lactic acid) (**PLLA**) was synthesized by the ring-opening polymerization (ROP) of (3S)-cis-3,6-Dimethyl-1,4-dioxane-2,5-dione catalyzed by $Sn(Oct)_2$ as shown in scheme 3.1.[34] The hydroxyl functionalized OPV derivative (**OPV-2-Diol**) was synthesized as discussed previously in chapter 2.[35] The high-temperature solution-blending of OPV-2-Diol with **PLLA** was carried out by dissolving **PLLA** and OPV-2-Diol in minimum amount of a high boiling solvent like ODCB and heating in presence of 1 mol % of transesterification catalyst $Ti(OBu)_4$ as shown in scheme 3.2. The blending was carried out in a cylindrical glass reactor at 160 ^{o}C for 1 h with constant stirring using mechanical stirrer, under continuous nitrogen flow. For workup, the polymer was dissolved in chloroform and precipitated into methanol.

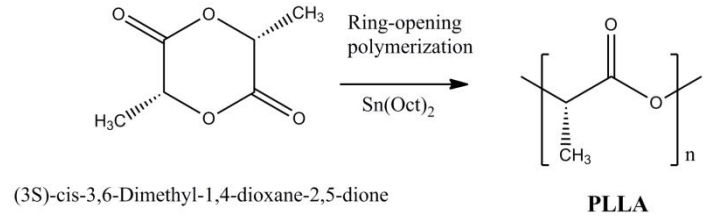

Scheme 3.1. *Synthesis of poly(L-lactic acid) (**PLLA**) using ring-opening polymerization of (3S)-cis-3,6-Dimethyl-1,4-dioxane-2,5-dione.*

The copolyesters obtained were named as **PLLA-OPV-x** where x represented the actual mole % incorporation of OPV calculated from integration of ^{1}H NMR signal. Table 3.1 gives the sample name, amount of hydroxyl functionalized OPV taken in the feed, the actual

incorporation determined using ^{1}H NMR spectroscopy, molecular weight determined using size exclusion chromatography (SEC) in $CHCl_3$ using polystyrene standard, the 10 % weight loss temperature obtained from thermal gravimetric analysis (TGA) as well as the yield of the various copolyesters.

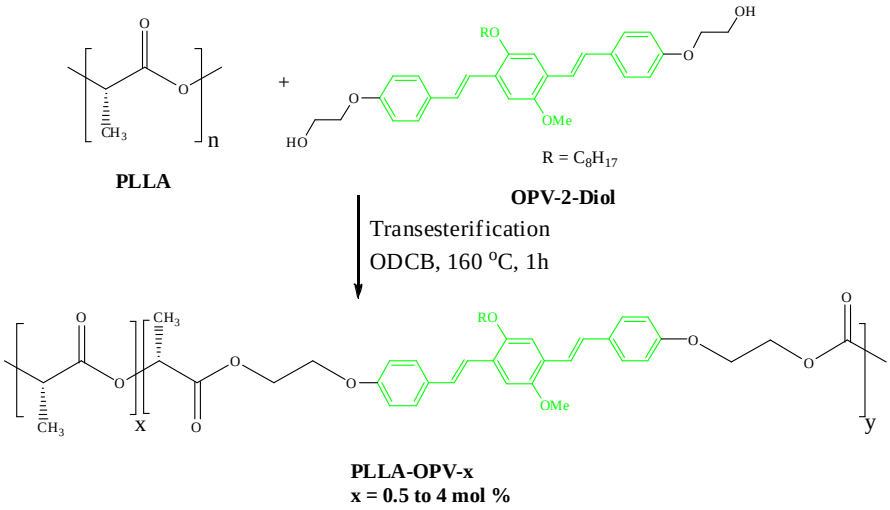

Scheme 3.2. *Synthesis of* ***PLLA-OPV-x*** *copolyesters by high-temperature solution-blending of OPV-2-Diol with* ***PLLA****.*

The structures of polymers were confirmed by ^{1}H NMR spectroscopy and molecular weights were determined using size exclusion chromatography (SEC). Figure 3.1 compares the ^{1}H NMR spectra of **PLLA** and OPV-2-Diol with that of the copolyester **PLLA-OPV-4**. The structure of the molecules is given and the different types of protons are assigned by alphabets. In OPV-2-Diol, the Ar–O–C**H**$_2$–CH$_2$– and Ar–O–CH$_2$–C**H**$_2$– protons appeared at δ = 4.11 and 3.95 ppm (labelled e and f) respectively. In OPV incorporated **PLLA**, a new peak at 4.33–4.51 ppm (labelled e' and f') corresponding to –COO–C**H**$_2$–C**H**$_2$– was observed [figure 3.1 (c)]. The formation of new trans-ester linkage involving OPV was confirmed by the shift of the Ar–O–C**H**$_2$–C**H**$_2$– proton in the proton NMR spectra, which transformed into the new –COO–C**H**$_2$–C**H**$_2$–O–Ar linkage. An attempt was made to determine the mol% incorporation of OPV in the different copolyesters by by comparing the integration of peaks corresponding to the OPV aromatic protons (labelled c) with that of –C**H**(CH$_3$)–COO– proton (labelled a) of the **PLLA**. The mol % incorporation of OPV unit in **PLLA-OPV-x** was determined as 0.5, 1, 2, 3 and 4 mol % corresponding to the intake feed of 0.5, 1, 2, 3 and 5 mol % respectively. Beyond this the molecular weight of the obtained polymer was drastically reduced, so higher incorporation of OPV beyond 4 mol% was not pursued. It was very difficult to accurately determine the low OPV content in the polymers by NMR. More

accurate information regarding the mol% incorporation of OPV into the **PLLA** backbone was obtained using Beer-Lamberts Law, using the molar extinction coefficient of OPV-2-Diol as 32059 L M^{-1} cm^{-1} in chloroform. The mol % incorporation of OPV unit in **PLLA-OPV-x** was determined as 0.79, 1.27, 2.36, 3.44 and 3.93 mol % corresponding to the intake feed of 0.5, 1, 2, 3 and 5 mol % respectively. These results are well agreement with the mol % incorporation of OPV units calculated from ^{1}H NMR.

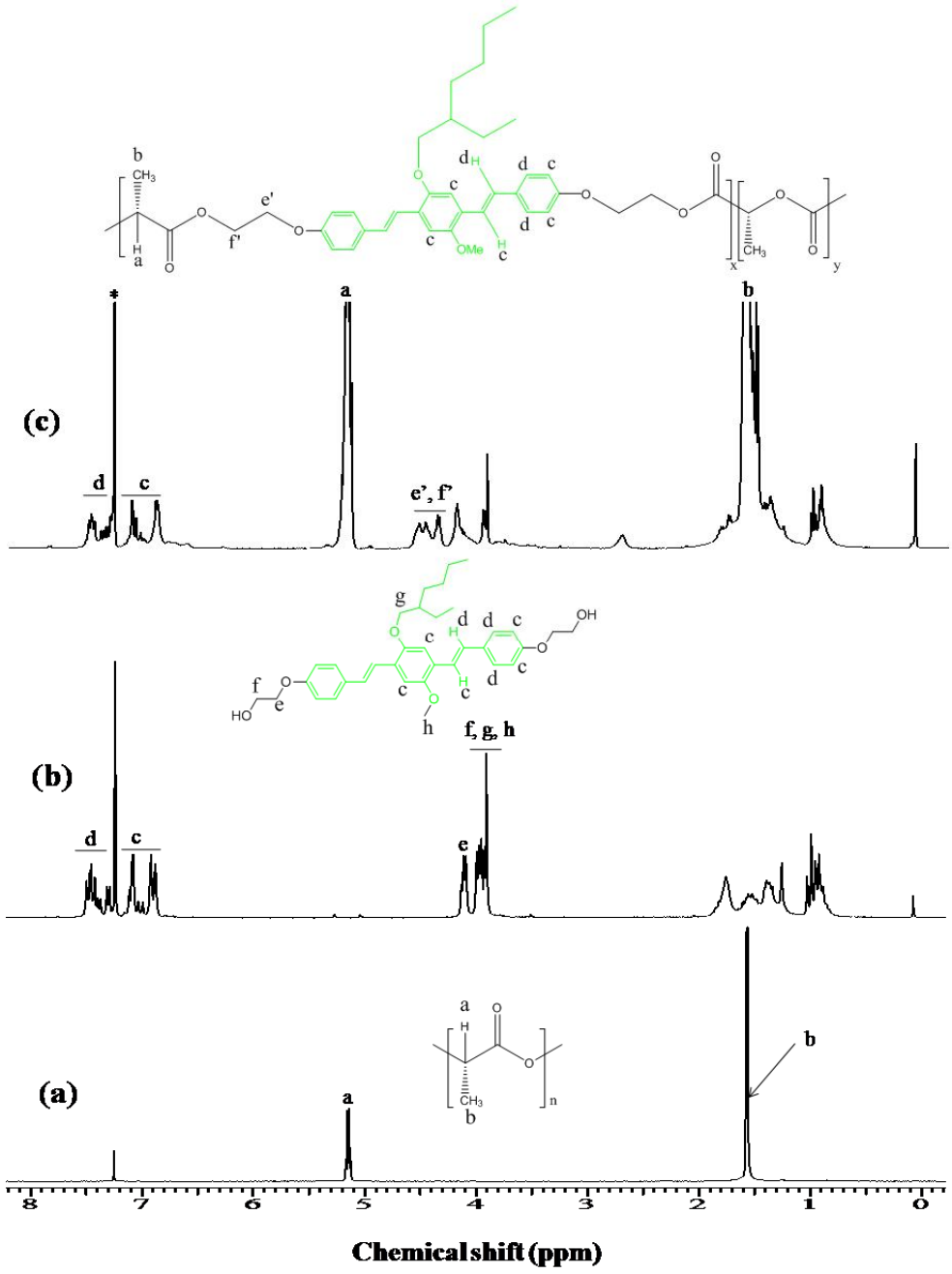

Figure 3.1. *^{1}H NMR spectra of (a)* ***PLLA****, (b) OPV-2-Diol and (c)* ***PLLA-OPV-4*** *recorded in chloroform.*

Table 3.1. *Polymer designation, feed ratio, actual incorporation determined from ^{1}H NMR and absorption spectra, molecular weight (M_w), polydispersity index, 10 % weight loss temperature (T_D) and yield of polymers.*

Sample	Feed Ratio (PLLA: OPV)	Composition (**PLLA**: OPV) (^{1}H NMR) (mol %)	Mol % incorporation of OPV from absorption specrtra[a]	Mw (g/ mol)[b]	Poly dispersity index ($Đ_M$)	η_{inh} (dL/ g)[c]	T_D (^oC)[d]	Yield (%)
PLLA	-	-	-	100600	1.8	1.01	268	96
PLLA-OPV-0.5	99.5:0.5	99.5:0.5	0.79	45700	1.6	0.42	260	92
PLLA-OPV-1	99:1	99:1	1.27	18100	1.6	0.29	229	85
PLLA-OPV-2	98:2	98:2	2.36	8500	1.2	0.22	209	81
PLLA-OPV-3	97:3	97:3	3.44	7700	1.2	0.18	205	75
PLLA-OPV-4	95:5	96:4	3.93	6100	1.1	0.17	202	70
OPV-2-Diol	-	-	-	-	-	-	368	61

a. Measured in chloroform solution.
b. Measured by size exclusion chromatography (SEC) in chloroform ($CHCl_3$), calibrated with linear, narrow molecular weight distribution polystyrene as standards.
c. Determined in chloroform.
d. Determined by TGA.

3.3.2. Molecular Weights of Polymers

The polymers were soluble in common organic solvents such as chloroform and dichloromethane at room temperature. The molecular weights of the polymers were determined by size exclusion chromatography (SEC) in $CHCl_3$ using polystyrene standards. Figure 3.2 shows the size exclusion chromatogram of the copolyesters along with that of the parent **PLLA** polymer and corresponding molecular weights are given in table 3.1. Molecular weights of polyesters decreased with increasing OPV content which was a consequence of the chopping of the **PLLA** chains to incorporate OPV units by transesterification. Exchange reactions can occur inter- or intramolecularly, and can involve ester, hydroxyl and carboxyl

groups.[36] These inter- and intramolecular exchanges lead to the formation of low molecular weight oligomers also. Due to the reversibility of these reactions, the oligomers concentration will be very low. The GPC traces of **PLLA-OPV-0.5** and **PLLA-OPV-1** showed a peak around 26 min with low intensity is corresponding to these oligomers. Table 3.1 gives the inherent viscosity measured in chloroform solution for all the polymers. The inherent viscosities of the polymer also decreased with increasing mol % of **OPV-2-Diol** in feed.

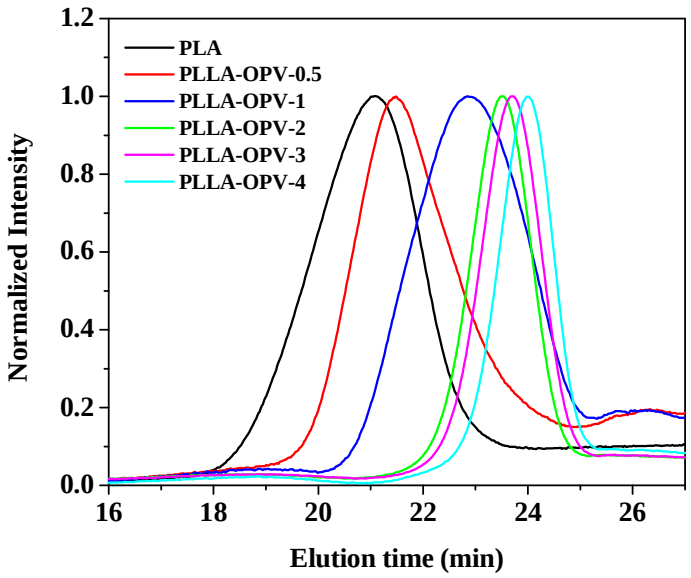

Figure 3.2. *Size exclusion chromatogram of copolyesters recorded in chloroform using polystyrene as standard.*

3.3.3. Thermal Properties of Polyesters

Figure 3.3 (a) shows the TGA thermograms for the series of polymers and OPV-2-Diol. The 10 % weight loss temperature is given in the table 3.1. All polyesters were thermally stable up to 200 ^{o}C. Figure 3.3 (b) compares the second heating DSC thermograms of **PLLA**, OPV-2-Diol, **PLLA-OPV-0.5**, **PLLA-OPV-1** and **PLLA-OPV-4** heated at a rate of 10 ^{o}C/min. All polymers exhibited both glass transitions (T_g) and melting transition. **PLLA** exhibited a T_g around 63 ^{o}C, an exothermic crystallization at 108 ^{o}C followed by a melting at 181 ^{o}C whereas OPV-2-Diol showed a melting transition at 109 ^{o}C. The **PLLA-OPV-0.5** copolyester showed a T_g around 57 ^{o}C, an exothermic crystallization at 101 ^{o}C followed by a melting transition at 168 ^{o}C. The DSC thermogram of **PLLA-OPV-1** exhibited T_g around 46 ^{o}C, an exothermic crystallization at 103 ^{o}C and multiple-melting transitions around 150 ^{o}C. Multiple-melting behaviour has been observed for many semicrystalline polymers, which are

explained by the melt-recrystallization model.[37] **PLLA-OPV-2** and **PLLA-OPV-3** also exhibited both T_g and multiple-melting. **PLLA-OPV-4** showed T_g around 39 ^oC and two melting transitions at 110 and 122 ^oC. The sharp endotherm at 110 ^oC and the broad endotherm around 122 ^oC are ascribed to the melting of OPV and PLLA segments respectively. The temperature corresponding to the melting transition of **PLLA-OPV-x** copolyesters decreased with increasing mol % incorporation of OPV chromophore into the **PLLA** backbone. This trend is well understood in literature also i.e higher incorporation of rigid units resulted in reduction in the melting point of **PLLA** copoyester.[31]

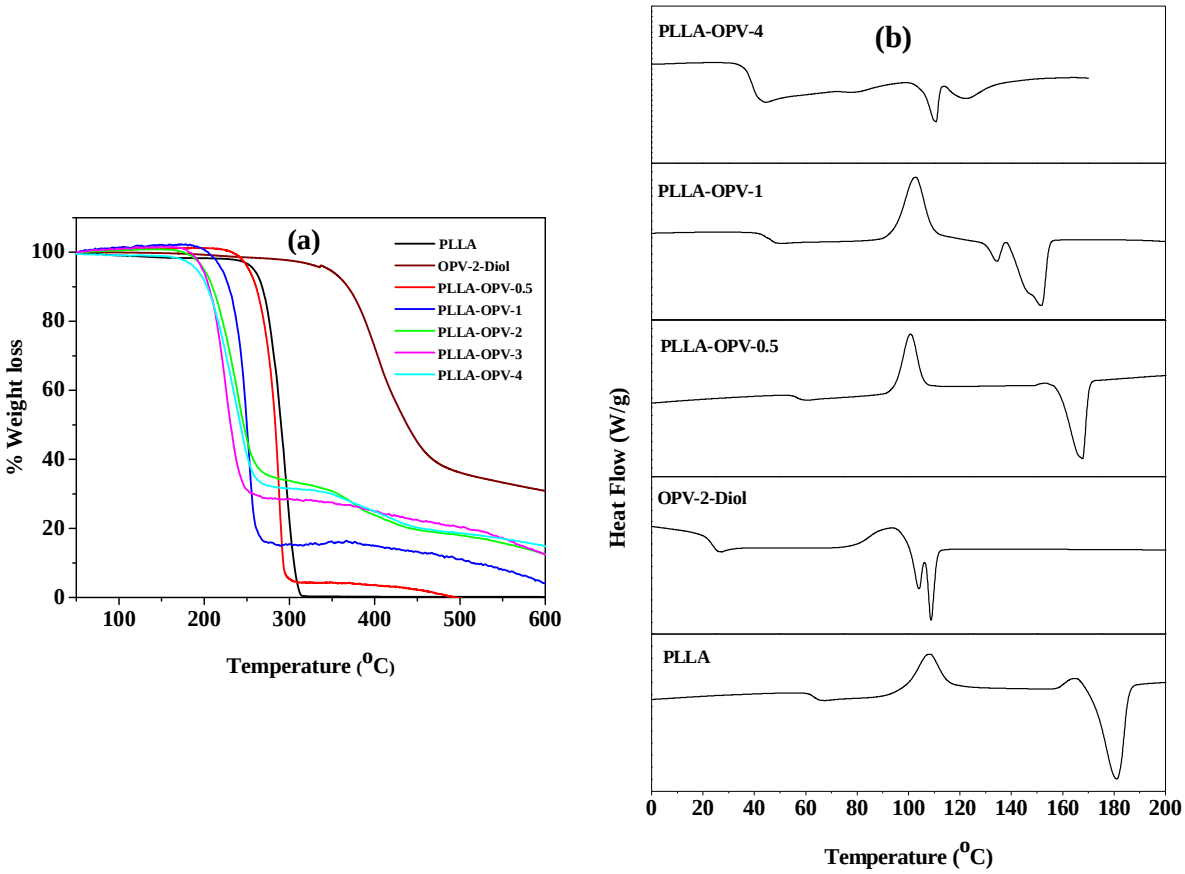

Figure 3.3. *(a) TGA thermograms of polymers and (b) the second heating DSC thermograms of* ***PLLA****, OPV-2-Diol,* ***PLLA-OPV-0.5****,* ***PLLA-OPV-1*** *and* ***PLLA-OPV-4*** *at the heating rate of 10 ^oC/min.*

3.3.4. Wide-angle X-ray Diffraction (WXRD)

The polyesters were analyzed for their bulk packing using wide-angle X-ray diffraction (WXRD) in the range of 2θ = 5-35° at room temperature (25 ^oC). Figure 3.4 compares the WXRD patterns of **PLLA-OPV-x** copolyesters along with that of **PLLA**. The

diffraction peaks at 2θ = 12.5°, 15.0°, 16.9°, 19.1° and 22.6° were assigned to the (103), (010), (200 or 110), (203) and (015) diffractions of the α-form crystal of **PLLA** respectively according to the literature report.[38] The peak around 2θ = 24.1 (3.69 A°), (circled in figure 3.4) visible only for the highest OPV incorporated copolyesters (**PLLA-OPV-2**, **PLLA-OPV-3** and **PLLA-OPV-4**) was attributable to the average π-π stacking distance of the OPV aromatic core.[39] This result was in agreement with the observation of melting transition at 110 °C corresponding to the melting of OPV chromophore in the DSC curve of the highest OPV incorporated **PLLA-OPV-x** copolyester (**PLLA-OPV-4**). Such an evidence for crystallinity and π-π stacking of the OPV units in a main chain polymer scaffold is very rare in literature. The **PLLA** segment could be expected to play a role in helping the OPV units to align properly resulting in improved π-π stacking.

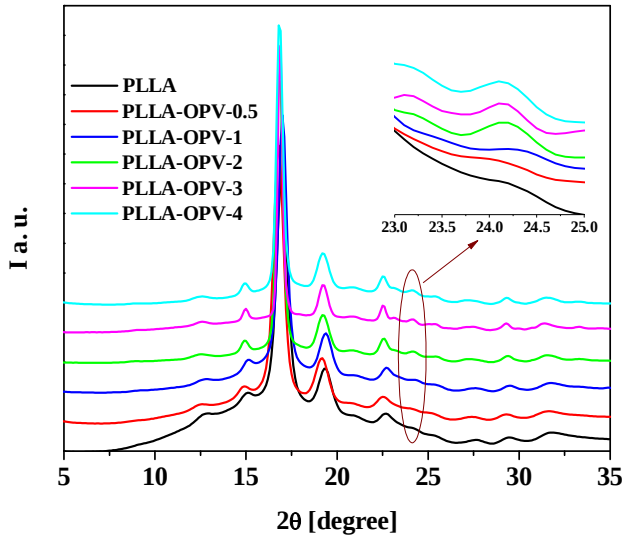

Figure 3.4. *WXRD patterns of polymers in powder form at room temperature.*

3.3.5. Photophysical Properties

The optical properties of the polymers were investigated by UV-Vis and fluorescence spectroscopy in both solution and solid state, which are summarised in table 3.2. Figure 3.5 (a) and (b) shows the normalized absorption spectra of **PLLA-OPV-x** copolyesters in chloroform solution and in powder state respectively. The copolyesters exhibited λ_{max} ~ 390 nm in chloroform solution indicating that all polymers were molecularly dissolved. Similar optical characteristics have been reported for other molecularly dissolved OPVs.[26] The absorption spectra in the solid state was broad and the absorption maxima was red shifted from 390 to ~ 430 nm, which was an indication of the strong aggregation of OPV

chromophore.[35] This was in accordance with the OPV aromatic core π-π stacking observed in WXRD.

Table 3.2. *Absorption and emission data of polymers in solution and solid state (powder form) along with fluorescence quantum yields Φ_{FL} in solution.*

Polymer	Absorption λ_{max} (nm) (In $CHCl_3$)	Emission λ_{max} (nm) (In $CHCl_3$)[a]	Absorption λ_{max} (nm) (In powder)	Emission λ_{max} (nm) (In powder)[a]	ϕ_{FL}[b] (In solution)
PLLA-OPV-0.5	390	445	431	476	0.62
PLLA-OPV-1	391	445	434	485	0.58
PLLA-OPV-2	388	445	432	489	0.57
PLLA-OPV-3	388	445	434	490	0.54
PLLA-OPV-4	387	445	431	494	0.41

a. Excitation at 390 nm.

b. The fluorescence quantum yield for polymers in $CHCl_3$ was obtained upon excitation at 360 nm and was measured using quinine sulphate in 0.1 M H_2SO_4 solution as standard.

Figure 3.5 (c) and (d) shows the emission spectra of **PLLA-OPV-x** copolyesters in solution and solid state respectively. All polymers emitted strongly with emission maximum at 445 nm with a shoulder peak at 470 nm in chloroform solution.[26] These **PLLA-OPV** copolyesters were highly fluorescent with quantum yields of 0.62, 0.58, 0.57, 0.54 and 0.41 for **PLLA-OPV-0.5**, **PLLA-OPV-1**, **PLLA-OPV-2**, **PLLA-OPV-3** and **PLLA-OPV-4** respectively in chloroform solution (see table 3.2). The quantum yield decreased with increasing incorporation of OPV suggesting aggregation induced self quenching. In the solid (powder) state, the OPV monomer emission at 445 nm was suppressed and a red shifted intense aggregate emission was observed. The copolyesters **PLLA-OPV-0.5**, **PLLA-OPV-1**, **PLLA-OPV-2**, **PLLA-OPV-3** and **PLLA-OPV-4** showed emission maximum at 476, 485, 489, 490 and 494 respectively. The strong π-π stacking of the OPV aromatic units in the solid state was responsible for the strongly red shifted emission.[35]

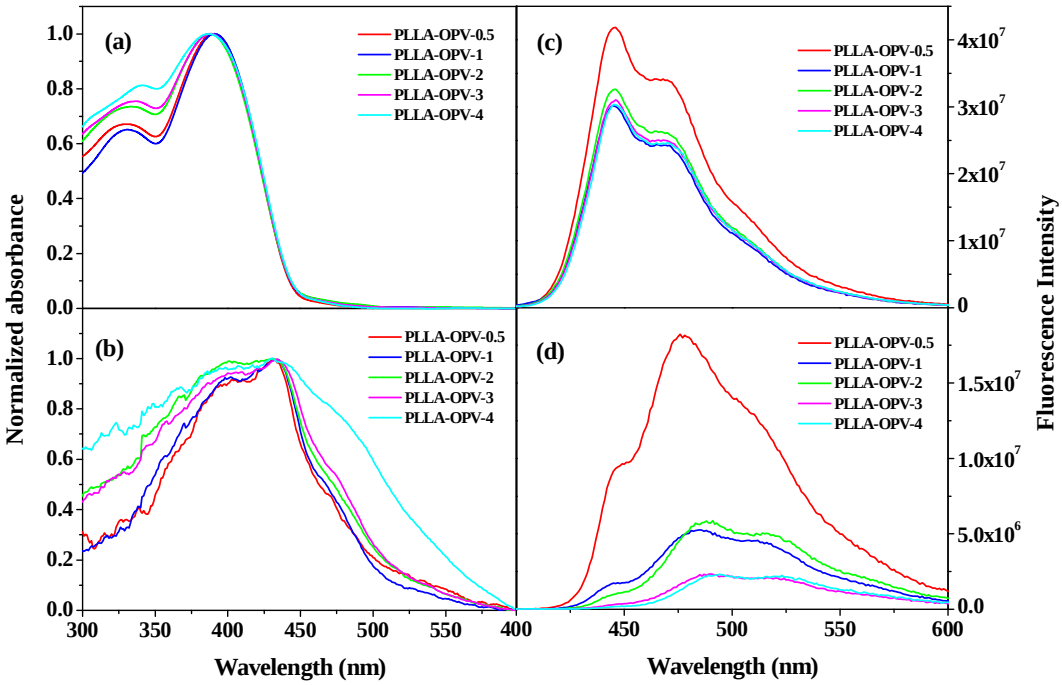

Figure 3.5. *Normalized absorption spectra of copolyesters (a) in the solution (chloroform) and (b) in the powder form; emission spectra of polymers (c) in the solution (chloroform) [0.1 OD at 390 nm, λ_{ex} = 390 nm] and (d) in the powder form [λ_{ex} = 390 nm].*

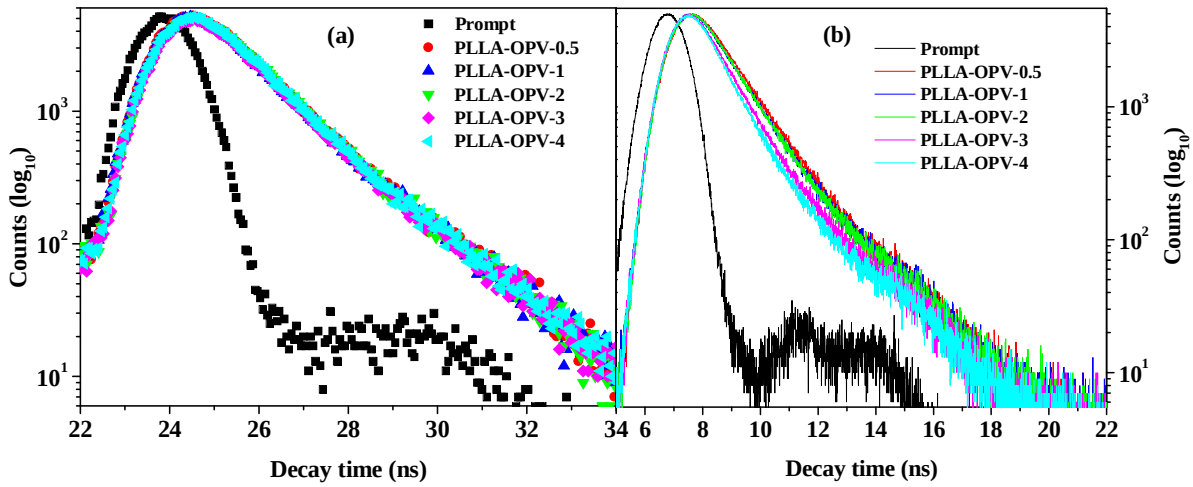

Figure 3.6. *Fluorescence lifetime-decay profiles of polymers in (a) chloroform at room temperature (0.1 OD at 390 nm, λ_{ex} = 390 nm, monitored at 445 nm) and (b) solid state (λ_{ex} = 390 nm, monitored at emission maxima) at room temperature.*

The aggregation of OPV chromophore in the solid state was further supported by fluorescence lifetime-decay studies. The fluorescence lifetime-decay profiles of all the polymers in chloroform solution are given in figure 3.6 (a). The fluorescence lifetime-decay profiles of **PLLA-OPV-x** copolyesters (λ_{ex} = 390 nm) in chloroform exhibited mono-

exponential decay with lifetime of 1.29 ns when monitored at 445 nm (see table 3.3).[35] The fluorescence lifetime-decay profiles of all the polymers in powder state are given in figure 3.6 (b). In the solid state, the fluorescence lifetime-decay profile of **PLLA-OPV-0.5** (λ_{ex} = 390 nm) also could be fitted to a mono-exponential decay with lifetime of 1.33 ns when monitored at 476 nm. This suggested the existence of a single luminescent species. On the other hand, all the other copolyesters (**PLLA-OPV-1**, **PLLA-OPV-2**, **PLLA-OPV-3** and **PLLA-OPV-4**) exhibited biexponential decay confirming the existence of two types of luminescent species corresponding to the aggregated and isolated chains.[35] The dominant fluorescence lifetime in the solid state decreased with increasing mol % incorporation of OPV chromophore in the copolyesters (see table 3.3). The fluorescence lifetime-decay measurements confirmed the presence of strong aggregation in solid state and also the enhancement of aggregation with increase in OPV content in the random copolyester.

Table 3.3. *Fluorescence lifetime-decay data of polymers in solution as well as in powder state using nanoLED 390 nm for excitation.*

Polymer	In chloroform[a]		In powder state[b]					
	Lifetime (τ) (ns)	χ^2	$\lambda_{monitored}$ (nm)	Lifetime (ns)		α_1	α_2	χ^2
				τ_1	τ_2			
PLLA-OPV-0.5	1.29	1.24	476	1.33	-	-	-	1.12
PLLA-OPV-1	1.29	1.20	485	1.13	2.23	0.92	0.08	1.08
PLLA-OPV-2	1.29	1.24	489	1.10	2.14	0.91	0.09	1.02
PLLA-OPV-3	1.29	1.07	490	0.99	1.98	0.86	0.14	0.98
PLLA-OPV-4	1.29	1.05	494	0.78	1.86	0.88	0.12	0.99

a. Parameters (τ: decay time and χ2: chi-squared value) retrieved from the mono-exponential fit for polyesters in chloroform solution (0.1 OD at 390 nm). The decay was collected at 445 nm.

b. Parameters (τ: decay time, α: pre-exponential factor and χ2: chi-squared value) retrieved from the biexponential fit for polyesters in powder state. The decay was collected at the emission maxima of polymers.

3.3.6. Helical Self-assembly of Copolyesters

Circular dichroism (CD) spectra of the polymers were recorded in both solution (chloroform) and solid state (powder form) to gain more insight into the self-assembly of OPV chromophore. It is reported that **PLLA** is a depsipeptide analogue of polyalanine which has a helical structure that resembles a polyproline II helix.[32] The n→π* interactions directs the folding of **PLLA** chain into a helical conformation. In an n→π* interaction, the filled *p*-type lone pair of carbonyl oxygen overlaps with the empty π* antibonding orbital of a nearby carbonyl group. This overlap allows for orbital mixing and the subsequent release of energy contributes to the conformational stability of the **PLLA** helix. [32] **PLLA** exhibited a strong, positive CD band with a maximum at 231 nm corresponding to the ester n–π* transition in chloroform solution [figure 3.7 (a)]. The large positive cotton effect exhibited by **PLLA** has been correlated with the helical conformation of **PLLA** chain in chloroform solution.[40] No CD signal was observed for all other copolyesters (**PLLA-OPV-X**) in chloroform solution where the polymers were molecularly dissolved.[30]

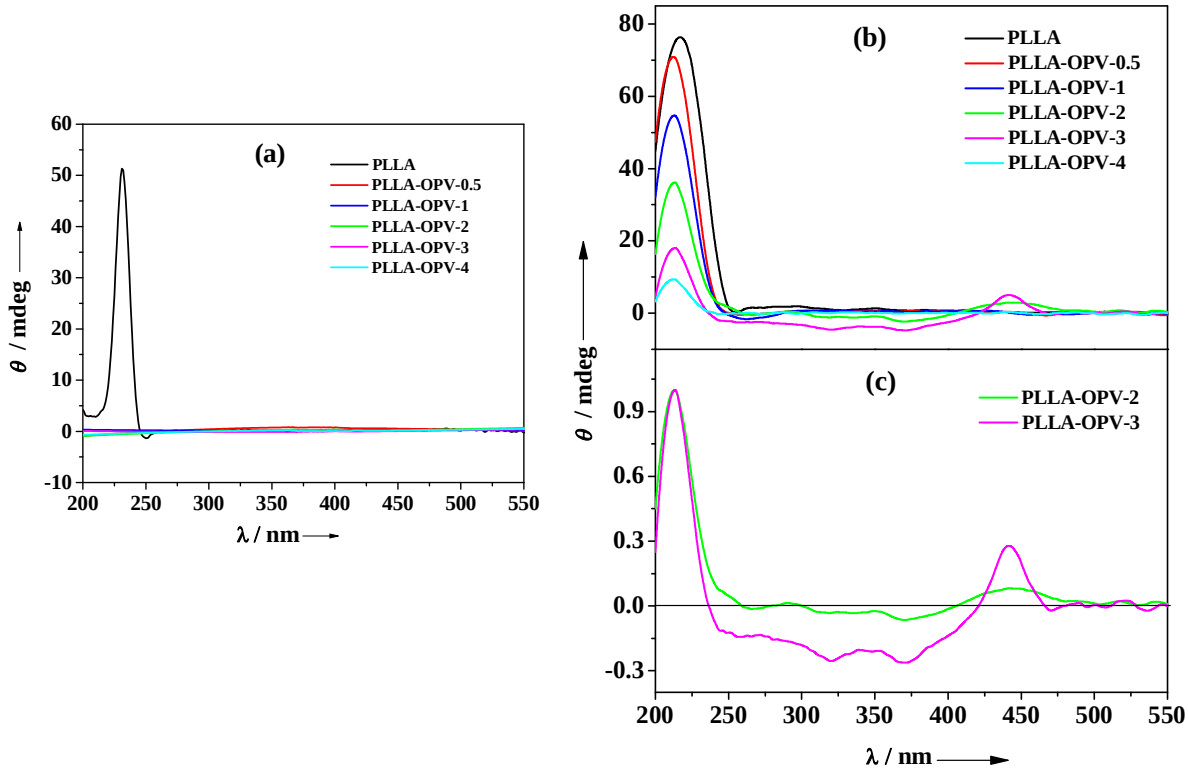

Figure 3.7. *(a) CD spectra of copolyesters in solution state (2 mg/mL) recorded in chloroform at 25 °C; (b) CD spectra of copolyesters and (c) normalized (at 213 nm) CD spectra of* ***PLLA-OPV-2*** *and* ***PLLA-OPV-3*** *in solid state recorded at 25 °C.*

In the solid state (powder), all the polymers showed a positive CD band with a maximum at 213 nm corresponding to the ester n–π^* transition [Figure 3.7 (b)]. Interestingly, one more sharp exciton-coupled bisignated CD signal with a first positive cotton effect with a maximum at 441 nm and a second negative cotton effect with maximum at 370 nm, through a zero crossing close to the absorption maximum (421 nm) of OPV chromophore was observed for **PLLA-OPV-3** corresponding to the π–π^* transition indicating the right-handed helical self-assembly of achiral OPV segments [figure 3.7 (c)].[23,41-45] The chirality information of the **PLLA** segment was transferred to the self-assembled OPV chromophore as evidenced by the exciton-coupled CD signal corresponding to the absorption maximum of the OPV chrompohore. These results confirmed the effect of chiral **PLLA** segment on tuning the OPV chromophore packing and supramolecular chirality in molecular aggregates. The right-handed self-assembly of OPV segment by the chiral **PLLA** segment was further confirmed by the morphology of **PLLA-OPV-3** observed by SEM and AFM analysis. **PLLA-OPV-2** also showed weak exciton-coupled bisignated CD signal. No bisignated Cotton effect was observed in the case of **PLLA-OPV-0.5** and **PLLA-OPV-1** because of the low mol % incorporation of OPV chromophore in the **PLLA** backbone. In the case of **PLLA-OPV-4**, the chain length of **PLLA** segment may not be sufficient enough to induce helical arrangement to OPV chromophore because of chopping of **PLLA** backbone to incorporate more OPV chromophore.

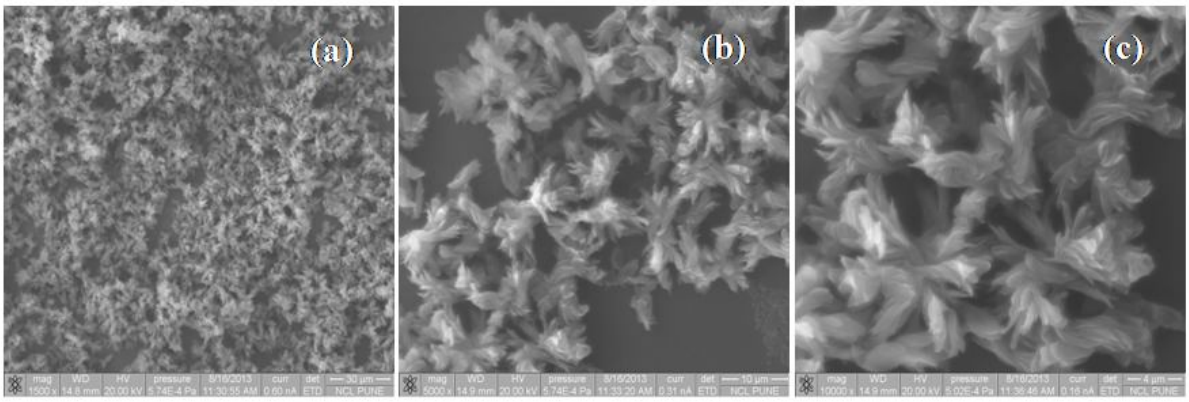

Figure 3.8. *Scanning electron microscope images of the solution-precipitated aggregate of* ***PLLA-OPV-3*** *in different magnifications.*

The morphology of the solution-precipitated aggregates of **PLLA-OPV-3** was examined by scanning electron microscopy (SEM) and atomic force microscopy (AFM). The solution-precipitated aggregate was prepared by injecting 1 mL of the polymer solution (1 mg/mL) in dichloromethane (DCM) into 10 mL of methanol. The resulting mixture was aged

at room temperature for overnight and the suspension of the aggregate was transferred to silicon wafer by a dropper. After the solvent was evaporated at room temperature, the sample was examined for its morphology. The SEM images of **PLLA-OPV-3** (figure 3.8) showed the formation of self-assembled bundles of twisted 'leaf-like' structures. The AFM height image of **PLLA-OPV-3** (figure 3.9) showed right-handed helical structure, in agreement with the observed CD spectrum.

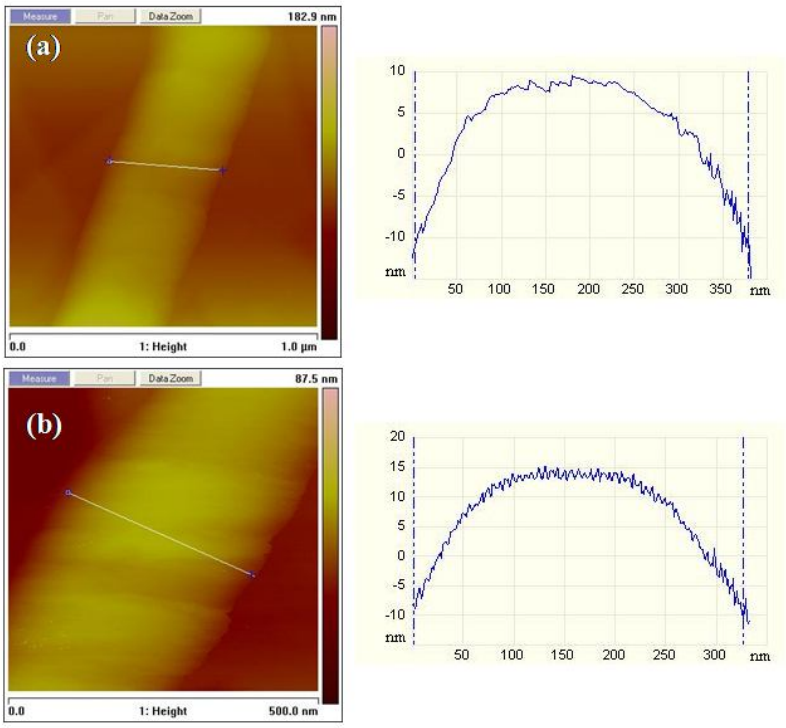

Figure 3.9. *Tapping mode AFM height images of the solution-precipitated aggregate of* ***PLLA-OPV-3*** *under different magnifications. The corresponding height section analysis is also shown.*

3.3.7. Microscopic Characterization of Electrospun Nanofibers

Electrospinning is a very versatile technique for making 1D elongated structure.[33] Figure 3.10 shows the scanning electron microscopy (SEM) and fluorescence microscopy images of the electrospun fibres of **PLLA-OPV-0.5.** SEM images revealed the presence of nanofibers of 150-500 nm diameters. Fluorescence microscopy images of this polymer showed strong blue and green emission upon excitation at 350-430 nm (blue filter) and 488-520 nm (green filter) respectively.

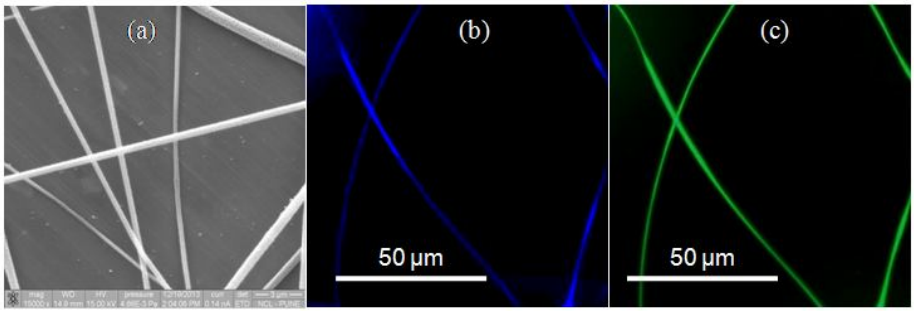

Figure 3.10. *(a) SEM; (b) and (c) fluorescent microscopy image of* ***PLLA-OPV-0.5*** *with excitation at wavelength of 350-430 nm and 488-520 nm respectively.*

3.4. Conclusion

A novel series of copolyesters incorporating varying mol ratios of an achiral oligo(*p*-phenylene vinylene) (OPV) into the backbone of a chiral poly(L-lactic acid) (**PLLA**) was synthesized by high-temperature solution-blending of **PLLA** with hydroxyl group functionalized OPV molecule (OPV-2-Diol). This approach is extendable to a variety of chromophores after suitable end functionalization for transesterification. The chemical incorporation of OPV chromophore into the polyester backbone was proved by ^{1}H NMR spectroscopy. The differential scanning calorimetry (DSC), wide-angle X-ray diffraction (WXRD), absorption, emission and lifetime-decay studies showed that OPV chromophore was aggregated in the solid state. The right-handed helical self-assembly of the achiral OPV segments driven by the chiral **PLLA** segments in the solid state was proved by CD investigation and AFM analysis. The chemistry described here is applicable as a general method to create helical self-assemblies of a variety of π-conjugated system, which have applications in organic electronic devices. Blue and green fluorescent nanofibers of random copolyester incorporating OPV were successfully constructed by electrospinning technique.

3.5. References

1) Kraft, A.; Grimsdale, A. C.; Holmes, A. B. *Angew. Chem. Int. Ed.* **1998**, *37*, 402-428.
2) Zgierski, M. Z.; Fujiwara, T.; Lim, E. C. *Acc. Chem. Res.* **2010**, 43, 506-517.
3) Chen, G.; Jiang, M. *Chem. Soc. Rev.* **2011**, *40*, 2254-2266.
4) Hoeben, F. J. M.; Jonkheijm, P.; Meijer, E. W.; Schenning, A. P. H. J. *Chem. Rev.* **2005**, *105*, 1491-1546.
5) Klug, A. *Angew. Chem. Int. Ed.* **1983**, *22*, 565-582.
6) Engelkamp, H.; Middelbeek, S.; Nolte, R. J. M. *Science* **1999**, *284*, 785-788.
7) Oda, R.; Huc, I.; Schmutz, M.; Candau, S. J.; MacKintosh, F. C. *Nature* **1999**, *399*, 566-569.
8) Sakai, N.; Matile, S. *Chem. Commun*. **2003**, 2514-2523.
9) Sautter, A.; Schmid, D. G.; Jung, G.; Würthner, F. *J. Am. Chem. Soc.* **2001**, *123*, 5424-5430.
10) Rubio-Magnieto, J.; Thomas, A.; Richeter, S.; Mehdi, A.; Dubois, P.; Lazzaroni, R.; Clément, S.; Surin, M. *Chem. Commun*. **2013**, *49*, 5483-5485.
11) Nilsson, K. P. R.; Inganäs, O. *Nat. Mater*. **2003**, *2*, 419-424.
12) Björk, P.; Herland, A.; Hamedi, M.; Inganäs, O. *J. Mater. Chem*. **2010**, *20*, 2269-2276.
13) Verswyvel, M.; Koeckelberghs, G. *Polym. Chem*. **2012**, 3, 3203-3216.
14) Langeveld-Voss, B. M. W.; Waterval, R. J. M.; Janssen, R. A. J.; Meijer, E. W. *Macromolecules* 1999, **32**, 227.
15) Lemaire, M.; Delabouglise, D.; Garreau, R.; Guy, A.; Roncali, J. *J. Chem. Soc., Chem. Commun*. **1988**, 658-661.
16) Geng, Y.; Trajkovska, A.; Katsis, D.; Ou, J. J.; Culligan, S. W.; Chen, S. H. *J. Am. Chem. Soc.* **2002**, *124*, 8337-8347.
17) Digennaro, A.; Wennemers, H.; Joshi, G.; Schmid, S.; Mena-Osteritz, E.; Bäuerle, P. *Chem. Commun.* **2013**, *49*, 10929-10931.
18) García, F.; Aparicio, F.; Marenchino, M.; Campos-Olivas, R.; Sánchez, L. *Org. Lett.* **2010**, *12*, 4264-4267.
19) Jørgensen, M.; Krebs, F. C. *J. Org. Chem*. **2004**, *69*, 6688-6696.
20) Guerlin, A.; Dumur, F.; Dumas, E.; Miomandre, F.; Wantz, G.; Mayer, C. R. *Org. Lett*. **2010**, *12*, 2382-2385.
21) Kimura, M.; Miki, N.; Adachi, N.; Tatewaki, Y.; Ohtaa, K.; Shirai, H. *J. Mater. Chem*. **200**9, *19*, 1086-1092.

22) Hirai, Y.; Babu, S. S.; Praveen, V. K.; Yasuda, T.; Ajayaghosh, A.; Kato, T. *Adv. Mater*. **2009**, *21*, 4029-4033.

23) Ajayaghosh, A.; Praveen, V. K. *Acc. Chem. Res*. **2007**, *40*, 644-656.

24) Balamurugan, A.; Reddy, M. L. P.; Jayakannan, M. *J. Phys. Chem. B* **2009**, *113*, 14128-14138.

25) Schenning, A. P. H. J.; Jonkheijm, P.; Peeters, E.; Meijer, E. W. *J. Am. Chem. Soc.* **2001**, *123*, 409-416.

26) Jonkheijm, P.; Hoeben, F. J. M.; Kleppinger, R.; Herrikhuyzen, J. V.; Schenning, A. P. H. J.; Meijer, E. W. *J. Am. Chem. Soc.* **2003**, *125*, 15941-15949.

27) Yamauchi, M.; Kubota, S.; Karatsu, T.; Kitamura, A.; Ajayaghosh, A.; Yagai, S. *Chem. Commun.* **2013**, *49*, 4941-4943.

28) Klok, H. –A.; Rösler, A.; Götz, G.; Mena-Osteritzc, E.; Bäuerle, P. *Org. Biomol. Chem*. **2004**, *2*, 3541-3544.

29) Harrington, D. A.; Behanna, H. A.; Tew, G. N.; Claussen, R. C.; Stupp, S. I. *Chem. Biol*. **2005**, *12*, 1085-1091

30) Matmour, R.; De Cat, I.; George, S. J.; Meijer, E. W.; Schenning, A. P. H. J. *J. Am. Chem. Soc*. **2008**, *130*, 14576-14583.

31) Auras, R.; Lim, L, -T.; Selke, S. E. M.; Tsuji, H.; *Poly(lactid acid): Synthesis, Structures, Properties, Processing, and Applications*; J. Wiley & Sons, **2010**.

32) Newberry, R. W.; Raines, R. T. *Chem. Commun*. **2013**, *49*, 7699-7701.

33) Wendorff, J. H.; Agarwal, S.; Greiner, A. *Electrospinning: Materials, Processing, and Applications*; Wiley-VCH, **2012**.

34) Thakur, K. A. M.; Kean, R. T.; Hall, E. S.; Kolstad, J. J.; Lindgren, T. A. *Macromolecules* **1997**, *30*, 2422-2428.

35) Jayakannan, M.; Deepa, P. *J. Polym. Sci. A Polym. Chem*. **2008**, *46*, 5897-5915.

36) Fakirov, S.; *Transreactions in Condensation Polymers*; Wiley-VCH, **1999**.

37) Lorenzo, M. L. D. *J. Appl. Polym. Sci*. **2006**, *100*, 3145-3151.

38) Li, X.-j.; Zhong, G. -j.; Li, Z. -m. *Chin. J. Polym. Sci*. **2010**, *28*, 357-366.

39) Percec, V.; Aqad, E.; Peterca, M.; Imam, M. R.; Glodde, M.; Bera, T. K.; Miura, Y.; Balagurusamy, V. S. K.; Ewbank, P. C.; Würthner, F.; Heiney, P. A. *Chem. Eur. J.* **2007**, *13*, 3330-3345.

40) Matsuo, S.; Iwakura, Y. *Macromol. Chem. Phys*. **1972**, *152*, 203.

41) Zhou, J.; Xue, L.; Shi, Y.; Li, X.; Xue, Q.; Wang, S. *Langmuir* **2012**, *28*, 14386-14394.

42) Berova, N.; Bari, L. D.; Pescitelli, G. *Chem. Soc. Rev*. **2007**, *36*, 914-931.

43) Mason, S. F.; *Molecular Optical Activity and the Chiral Discrimination*; University Press, **1982**.

44) Harada, N.; Nakanishi, K. *Circular Dichroic Spectroscopy - Exciton Coupling in Organic Stereochemistry*; Oxford University Press, **1983**.

45) George, S. J.; Ajayaghosh, A.; Jonkheijm, P.; Schenning, A. P. H. J.; Meijer, E. W. *Angew. Chem. Int. Ed*. **2004**, *43*, 3422-3425.

Chapter 4

Random copolyesters containing Perylenebisimide: Flexible Films and Fluorescent Fibers for Advanced Photonic Applications

Chapter 4

Random copolyesters containing Perylenebisimide: Flexible Films and Fluorescent Fibers for Advanced Photonic Applications

A series of high molecular weight random copolyesters of **PLLA** and **PCCD** incorporating varying mol ratios of perylenebisimide (PBI) was synthesized via high-temperature solution-blending. The polymers were characterized by ^{1}H NMR spectroscopy and size exclusion chromatography (SEC) and their bulk properties were investigated by differential scanning calorimetry (DSC) and wide-angle X-ray diffraction (WXRD). These polymers showed good solubility in common organic solvents and formed free-standing transparent and flexible films. Bright red photoluminescence was observed for all these films upon irradiation with ultraviolet radiation. The photophysical properties were studied using steady-state UV-vis absorption and fluorescence spectroscopy in solution as well as in solid state. Strong red fluorescent nanofibers of these polymers were successfully constructed by electrospinning technique. The nanofiber fabricated from random copolyester of **PLLA** and **PCCD** incorporating both OPV and PBI exhibited blue, green and red emission upon excitation at different wavelengths. The luminescent colour of the nanofibers can thus be tuned by the suitable choice of chromophores. The approach described here is easily adoptable for a wide range of π-conjugated chromophores to achieve the goal of easy fabrication to 1D nanostructure with strong photoluminescence.

4.1. Introduction

One-dimensional (1D) nanostructures (such as nanofibers) of semiconductor materials have attracted increased interest in recent years due to their promising applications in optical and electronic nanodevices.[1-4] Most nanofibers reported are based on inorganic materials. Rational design of semiconducting π-conjugated molecules, leading to desired nanostructures, is crucial for the success of organic electronics on the nanoscale.[5-8] 1D nanostructures have received a great deal of attention due to growing requirements in-unidirectional charge transport for miniaturized electronic devices.[9-11] Such 1D nanostructures are appealing in the view of photovoltaic applications because they provide a large interface area upon mixing with charge transporting materials suitable for photo-induced charge separation.[12] Nanowires have feasibly been fabricated from conducting polymers such as polyacetylene, polyaniline, polypyrrole and poly(pheneylenevinylene).[13-18] However, most of these materials are p-type semiconductors. Therefore, the fabrication and characterization of 1D nanostructures with n-type semiconductor would provide more insight to the development of organic material based devices.

Recently, it was shown that self-assembly through strong π-π stacking is an effective approach to 1D nanostructure for aromatic organic molecules and this implies a potential way to enhance the charge carrier mobility.[5, 19-21] Perylenebisimides represent a robust class of n-type organic semiconductor with high thermal and photostability, and have long been used in various optoelectronic devices.[5, 22, 23] The main challenge of 1D self-assembly of PBIs lies in controlling and optimizing the strong π-π interaction between the perylene planes in cooperation with the hydrophobic interactions between the side chains linked at the two imide positions. A sufficient solubility is crucial for the solution processing of individual molecules, and this requires appropriate side-chain modification to hinder the π-π stacking of perylene backbones, but on the other hand, such a weakened π-π stacking prevents the effective packing of PBI molecules.[24] One way to enhance the molecular packing is to increase the size of the core aromatic system, i.e., to change the PBI monomer to a trimer, tetramer, or pentamer.[25, 26] The twisting between the PBI units due to energy minimization in the supramolecules weakens the π-π interaction between molecules and thus distorts the molecular packing from the co-facial conformation, leading to a molecular assembly deviated from 1D morphology.

The current chapter deals with the synthesis of a strongly fluorescent PBI based polymer, which could be fabricated into well-defined nanofibers over a large length scale. An aliphatic hydroxyl functionalized perylenebisimide (PBI) derivative was synthesized and incorporated into the backbone of [poly(1,4-cyclohexylenedimethylene-1,4-cyclohexanedicarboxylate)] (**PCCD**) by melt condensation (**PCCD-PBI-3.4**). This copolymer showed low mechanical stability because of its low molecular weight. Poly(L-lactic acid) (**PLLA**) is a thermoplastic aliphatic polyester derived from renewable resources such as corn and rice.[27] It has similar mechanical properties to PETE (polyethylene terephthalate) polymer and it can be processed like most thermoplastics into fiber and film. The reactive blends of **PLLA** with **PCCD-PBI-3.4** were synthesized by a facile high-temperature solution-blending method. The ester-exchange reaction in the reactive blends of **PLLA** with **PCCD-PBI-3.4** was confirmed using size exclusion chromatography (SEC) and differential scanning colorimetry (DSC). The mol % incorporation of PBI in the copolyester was calculated by using Beer-Lamberts Law. The bulk properties of these polymers were studied using wide-angle X-ray diffraction (WXRD). These polymer formed transparent and flexible films with high luminescent efficiencies. The photophysical properties were studied using steady-state UV-vis absorption and fluorescence spectroscopy in solution as well as in solid state. Nanofibers of these polymers have been successfully produced using the electrospinning technique.[28-30] These fibers were analyzed using microscopic techniques like scanning electron microscopy (SEM) and fluorescence microscopy.

Random copolyester incorporating both the donor (OPV) and acceptor (PBI) moieties were also developed, and fluorescent nanofibers of this polymer were constructed by electrospinning. Emission spectra and fluorescence microscopy images showed that one could access different emission regions (blue, green and red) from the nanofibers of PBI-OPV random copolyester just by exciting at the appropriate wavelength. This simple and powerful approach described here is easily adoptable for a wide range of π-conjugated chromophores for generating fluorescent nanofibers.

4.2. Experimental Methods

4.2.1. Materials: Perylene-3,4,9,10-tetracarboxylic dianhydride (PTCDA), 6-aminohexan-1-ol, zinc acetate, 1,4-cyclohexanedimethanol (CHDM) (cis + trans), 1,4-dimethylcyclohexane dicarboxylate (DMCD) (cis + trans), titanium(IV) butoxide [$Ti(OBu)_4$], (3S)-cis-3,6-Dimethyl-1,4-dioxane-2,5-dione (L-lactide), tin(II) 2-ethylhexanoate ($Sn(Oct)_2$), 4-methoxyphenol, 2-ethylhexylbromide, triethylphosphite, 4-hydroxybenzaldehyde, potassium-tert-butoxide and ortho-dichlorobenzene (ODCB) were purchased from Aldrich and used without further purifications. HBr in glacial acetic acid, paraformaldehyde, potassium carbonate, potassium iodide, tetrahydrofuran (THF), 2-chloroethanol and all other solvents were purchased locally and purified with standard procedures.

4.2.2. Instrumentation: ^1H NMR spectra were recorded using a Bruker Avance 200 MHz and 500 MHz spectrometer. Chemical shifts (δ) are reported in ppm at 25 ^oC with a small amount of tetramethylsilane (TMS) as internal standard. The mass spectral analysis of monomer was carried out using a Voyager-De-STR MALDI-TOF (Applied Biosystems, Framingham, MA, USA) instrument equipped with 337 nm pulsed nitrogen laser used for desorption and ionization. The molecular weight of synthesized polymers was determined using size exclusion chromatography (SEC). SEC measurements were carried on a Polymer Laboratories PL-GPC-220 at 25 ^oC using chloroform (Merck) as the mobile phase. The analysis was carried out at a flow rate of 1 mL/min using a set of three PLgel columns and a refractive index (RI) detector. Columns were calibrated with polystyrene standards and the molecular weights reported were with respect to polystyrene. The inherent viscosity (η_{inh}) of the polymers was measured for 0.5 wt % solutions in chloroform as solvent. Absorption spectra were recorded using Perkin-Elmer Lambda 35 UV-spectrophotometer. Steady-state fluorescence studies and fluorescence lifetime-decay measurements were performed using Horiba Jobin Yvon Fluorolog 3 spectrophotometer having a 450 W xenon lamp for steady-state fluorescence and nanoLED of 390 nm for fluorescence lifetime-decay measurements. For lifetime measurements, decay curves were obtained by the time-correlated single photon counting (TCSPC) technique. Solid state photoluminescence spectra were recorded using the front face scan mode with the same Fluorolog spectrofluorimeter. The fluorescence quantum yields of PBI polymer were determined in $CHCl_3$ using rhodamine 6G in ethanol (ϕ= 0.95) as the standard by exciting at 490 nm and OPV polymer was determined in $CHCl_3$ using quinine sulphate in 0.1 M H_2SO_4 (ϕ=0.54) as the standard by exciting at 360 nm. The solid state

quantum yield was measured using a Model F-3029, Quanta-Phi 6'' Integrating Sphere connected with Horiba Jobin Yvon Fluorolog 3 spectrophotometer. The thermal stability of the polymers was analyzed using a Perkin-Elmer thermogravimetric analyzer under nitrogen atmosphere at heating rate of 10 ^{o}C/min. Differntial scanning colorimetry (DSC) was performed using TA Q10 differential scanning calorimeter at heating rate of 10 ^{o}C/min. Wide-angle X-ray diffraction (WXRD) were recorded by Phillips x'pertpro powder X-ray diffractometer using Cu Kα radiation, and the spectra were recorded in the range of 2θ = 5-35°. The electrospinning apparatus consists of a syringe pump, syringe needle, high voltage power supply and a grounded collector. Polymer solution was loaded into a syringe and positive electrode was clipped onto the syringe needle. The flow rate of the polymer solution to the needle tip was kept constant. Solutions were electrospun horizontally onto the target. Scanning electron microscopy (SEM) images were recorded using FEI, QUANTA 200 3D scanning electron microscope with a tungsten filament as electron source. The fluorescence microscopy images were recorded by Epi-fluorescence microscope Leitz Laborlux, Germany, and images were observes by a cannon power shot S80 camera [excitation wavelengths: 350-430 nm (blue), 488-520 (green) and 500-550 nm (red) filters].

4.2.3. Synthesis

Synthesis of hydroxyl functionalized perylenebisimide (PBI-6-Diol): 6-Aminohexan-1-ol (0.65 g, 5.61 mmol), zinc acetate (0.001 g, 0.006 mmol) in N, N-dimethylacetamide (DMAc) (25 mL) was heated to 110 °C under a nitrogen atmosphere. PTCDA (1.00 g, 2.55 mmol) was added, and the reaction mixture was stirred at 110 °C for 3 h and then continued at 160 °C for 15 h under nitrogen atmosphere. The excess solvent was distilled off, and the slurry was washed several times with hexane and precipitated into acetone. The reddish-black precipitate was filtered and dried in oven at 60 ^{o}C. Yield: 86.00 %; ^{1}H NMR (200 MHz, $CDCl_3$ + TFA) δ ppm: 8.85 (s, 8H, perylene), 4.32–4.46 (s, 8H, imide –C**H**$_2$– and –C**H**$_2$OH), 1.56–1.86 (m, 16H, –C**H**$_2$–**)**; MALDI-TOF (dithranol matrix): m/z calcd for $C_{35}H_{44}O_6$: 590.66; found: 591 $[M]^+$; elemental analysis calcd (%): C 73.20, H 5.80, N 4.74; found: C 72.87, H 5.69, N 4.36.

Synthesis of copolyesters of PCCD incorporating PBI chromophore through melt polycodensation (PCCD-PBI-x): DMCD (2.00 g, 10 mmol), CHDM (1.29 g, 9 mmol) and PBI-6-Diol (0.59 g, 1 mmol) were weighed into a tubular glass reactor (for **PCCD-PBI-3.4**). The reaction mixture was melted at 160 ^{o}C, cooled and $Ti(OBu)_4$ (3.4 mg, 0.1 mol % of diester) solution in ODCB was added to the mixture. The reaction was heated from 160 to

180 ^{o}C over 2 h with stirring 100 rpm and then from 180 to 230 ^{o}C over 2 h, allowing methanol to distil. Vacuum was applied and the pressure was gradually reduced to 0.4 mm Hg over 20 min, while the temperature was raised from 230 to 250 ^{o}C. The reaction was continued at 250 ^{o}C for 2 h. The product was cooled, chloroform was added, and the polymer solution was poured into methanol. The polymer was dried in oven at 60 ^{o}C. Yield: 76.03%; ^{1}H NMR (500 MHz, $CDCl_3$) δ ppm: 8.42–8.53 (perylene **H**), 3.86–4.15 (–CH_2–C**H**$_2$–O–CO–, imide –C**H**$_2$**–**, cis and trans –C**H**$_2$– in **PCCD**), 3.64 (–CO–O–C**H**$_3$ end group), 3.42 and 3.50 (–C**H**$_2$**–**OH end group), 2.24 and 2.43 (cis and trans –C**H**–CO– in **PCCD** part), 0.97–2.02 (cyclic **H** in **PCCD** and –C**H**$_2$**–** in PBI part).

Synthesis of random copolyesters of PLLA and PCCD incorporating PBI chromophore by high-temperature solution-blending (PLLA-PCCD-PBI-x).

PLLA (0.5 g, 50 wt %) and **PCCD-PBI-3.4** (0.5 g, 50 wt %) were dissolved in ODCB (0.5 mL) by heating at 180 °C in an oil bath (for **PLLA-PCCD-PBI-1.7**). The mixture was stirred for 30 min using an overhead mechanical stirrer at a constant rate of 100 rpm. To this mixture, $Ti(OBu)_4$ (2.9 mg, 0.1 mol %) solution in ODCB was added and the reactive blending was continued with stirring at 180 °C for 6 h. The product was dissolved in chloroform and precipitated into methanol. The polymer was filtered and dried in oven at 60 ^{o}C. Yield: 98.00%; ^{1}H NMR (500 MHz, $CDCl_3$) δ ppm: 8.61–8.66 (perylene **H**), 5.17 (–C**H**(CH_3)–COO– from **PLLA** unit), 3.87–4.19 (–CH_2–C**H**$_2$–O–CO–, imide –C**H**$_2$–, cis and trans –C**H**$_2$– in **PCCD**), 3.66 (–CO–O–C**H**$_3$ end group), 3.43 and 3.53 (–C**H**$_2$**–**OH end group), 2.26 and 2.45 (cis and trans –C**H**–CO– in **PCCD** part), 0.99–2.02 (–C**H**$_3$ in **PLLA** part, cyclic–**H** in **PCCD** and –C**H**$_2$– in PBI part).

A similar procedure was employed to synthesize the **PLLA-PCCD-PBI-x** series of polyesters by changing the wt % of **PCCD-PBI-3.4** in the feed from 10 to 90 wt%. The yield of the polymers is reported in table 4.2.

Synthesis of random copolyester of PLLA and PCCD incorporating both PBI and OPV chromophores through high-temperature solution-blending (PLLA-PCCD-PBI-0.3-OPV-0.7): **PLLA** (0.85 g, 85 wt %), **PCCD-PBI-3.4** (0.1 g, 10 wt %) and OPV-2-Diol (0.05 g, 5 wt %) were dissolved in ODCB (0.5 mL) by heating at 180 °C in an oil bath. The mixture was stirred for 30 min using an overhead mechanical stirrer at a constant rate of 100 rpm. To this mixture, $Ti(OBu)_4$ (4.1 mg, 0.1 mol %) solution in ODCB was added and the

reactive blending was continued with stirring at 180 °C for 6 h. The product was dissolved in chloroform and precipitated into methanol. The polymer was filtered and dried in oven at 60 ^{o}C. Yield: 96%.

Synthesis of nanofibers: Polymer solution was prepared by dissolving 100 mg of polymer in 1 mL of DCM (10 wt % solution). This solution was subjected to a high electric field of about 10 kV for electrospinning. The tip to collector distance was fixed at 12 cm and the feeding rate was 0.5 mL h^{-1}. The fibers thus obtained were dried in an oven at 60 ^{o}C for 2 h.

4.3. Results and Discussions

4.3.1. Synthesis and characterization of monomers and polymers

Hydroxyl group functionalized pentadecyl phenol substituted perylenebisimide derivative (Per-PDP-2-Diol) was used for the reactive blending with [poly(1,4-cyclohexylenedimethylene-1,4-cyclohexanedicarboxylate)] (PCCD) in chapter 2. The fluorescence quantum yield of this molecule was very low (Φ_{FL} = 0.057) due to the photo-induced electron transfer from the electron-rich pentadecyl phenoxy substituents to electron-deficient perylenebisimide unit.[5] Therefore, we synthesized new hydroxyl functionalized perylenebisimide derivative without pentadecyl phenoxy group. The new hydroxyl functionalized perylenebisimide derivative (PBI-6-Diol) was synthesized through the 6-aminohexan-1-ol coupling of PTCDA as shown in scheme 4.1. The ^{1}H NMR spectrum and MALDI-TOF data verifying the structural characterization of the PBI-6-Diol is given in figure 4.1.

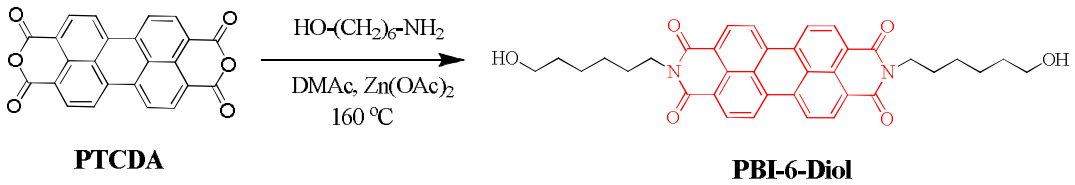

Scheme 4.1. *Synthesis of hydroxyl group functionalized perylenebisimide derivative (PBI-6-Diol) by the 6-aminohexan-1-ol coupling of PTCDA.*

The melt polycondensation of varying mol % of PBI-6-Diol with 1,4-cyclohexanedimethanol (CHDM) and 1,4-dimethylcyclohexane dicarboxylate (DMCD) was carried out as shown in scheme 4.2. The percentage of the monomer DMCD was kept fixed at 100 mol % and that of PBI-6-Diol: CHDM was varied from 5:95 to 30:70. The melt condensation was carried out in a cylindrical glass reactor in a two step process. The first step

was at atmospheric pressure with a temperature ramp and continuous nitrogen flow to remove the methanol that was eliminated, while the second step was under vacuum (0.4 mm Hg) at 250 ^{o}C. The polymers were dissolved in chloroform and precipitated into methanol. The copolyesters obtained by the melt polycondensation were named as **PCCD-PBI-x**, where x represented the actual mole % incorporation calculated from absorption spectra. Table 4.1 gives the sample name, amount of PBI-6-Diol taken in the feed, the actual incorporation of PBI chromophore determined using absorption spectra, molecular weight determined by SEC in $CHCl_3$ using polystyrene standards, the inherent viscosity measured in chloroform, the 10% weight loss temperature obtained from thermogravimetric analysis (TGA) as well as the yield of the various copolyesters.

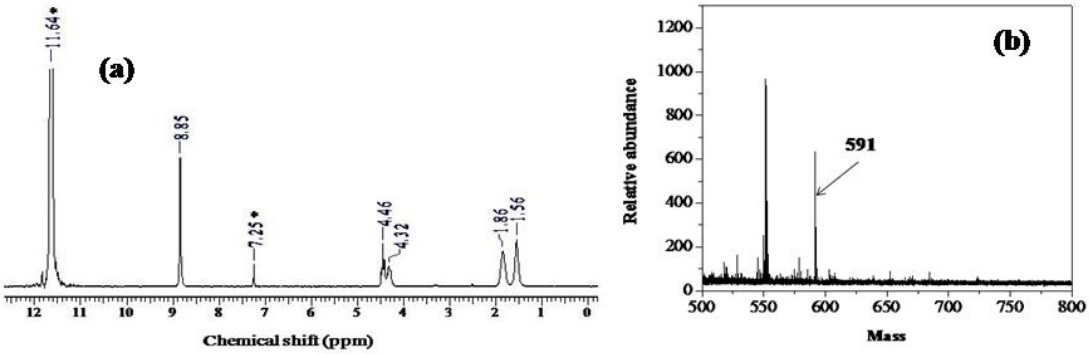

Figure 4.1. *(a) ^{1}H NMR spectrum of PBI-6-Diol recorded in $CDCl_3$ / CF_3COOH and (b) MALDI-TOF of PBI-6-Diol using dithranol matrix in $CHCl_3$ / CF_3COOH.*

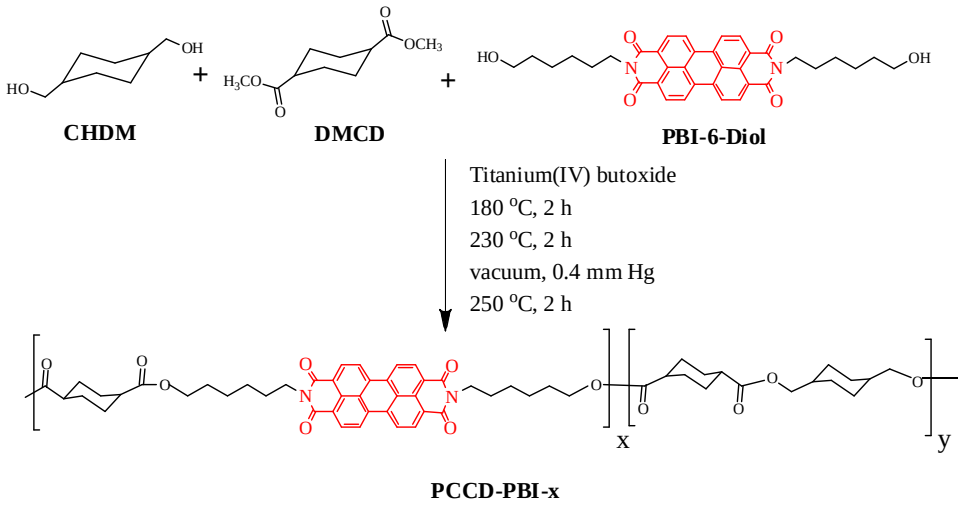

Scheme 4.2. *Synthetic route for the melt polycondensation of PBI-6-Diol with DMCD and CHDM.*

Table 4.1. *Polymer designation, feed ratio, actual incorporation of PBI chromophore determined from absorption spectra, molecular weight (Mn), polydispersity index, viscosity data (η_{inh}), 10 % weight loss temperature (T_D) and yield of polymers.*

Polymer	Feed Ratio (PCCD: PBI)	Mol % incorporation of PBI (from absorption spectra)[a]	Mn (g/ mol)[b]	Poly dispersity index ($Đ_M$)	η_{inh} (dL/ g)[a]	Yield (%)	T_D (^oC)[c]
PCCD-PBI-2.3	95:5	2.26	16100	2.2	0.36	83	383
PCCD-PBI-3.4	90:10	3.42	12500	1.9	0.30	76	420
PCCD-PBI-5.0	80:20	5.02	5500	2.4	0.15	75	393
PCCD-PBI-9.3	70:30	9.31	3100	2.3	0.11	71	388

a. Measured in chloroform.
b. Measured by size exclusion chromatography (SEC) in chloroform ($CHCl_3$), calibrated with linear, narrow molecular weight distribution polystyrene as standards.
c. Determined by TGA.

The structure of the polymers was confirmed by ^{1}H NMR spectroscopy and molecular weight was determined using size exclusion chromatography (SEC). The ^{1}H NMR spectrum of one of the representative polymer **PCCD-PBI-3.4** recorded in chloroform solution is shown in figure 4.2 (a). The mol % incorporation of the PBI in copolyesters was calculated from absorption spectra by using the molar extinction coefficient of symmetrical N,N'-bis(2-ethylhexyl)perylene-3,4,9,10-tetracarboxylic diimide as 83006 L M^{-1} cm^{-1}.[31] The mol % incorporation of PBI unit was determined as 2.3, 3.4, 5.0, and 9.3 mol % corresponding to the intake feed of 5, 10, 20, and 30 mol % respectively. Figure 4.2 (b) shows the size exclusion chromatogram of the polymers and the molecular weights are shown in table 4.1. The molecular weight and inherent viscosity of the polymers decreased with increasing the mol % incorporation of PBI in the copolyester, which could be attributed to the increase in the rigidity of the polymer backbone. This trend is well understood in the literature also, i.e., higher incorporation of rigid units resulted in reduction in the molecular weight.[32] None of

these polymers formed free standing film due to their low mechanical stability. We have selected **PCCD-PBI-3.4** from these polymer series, which has reasonably high molecular weight with high PBI incorporation and subjected it for high-temperature solution-blending with high molecular weight **PLLA**.

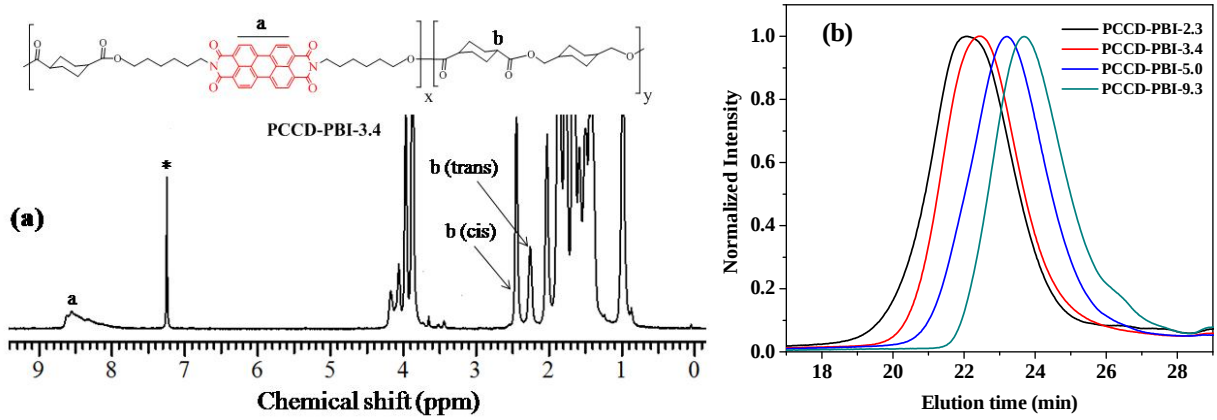

Figure 4.2. *(a) ^{1}H NMR spectrum of* ***PCCD-PBI-3.4*** *recorded in chloroform and (b) size exclusion chromatogram of the* ***PCCD-PBI-x*** *series of polymers recorded in chloroform using polystyrene as standard.*

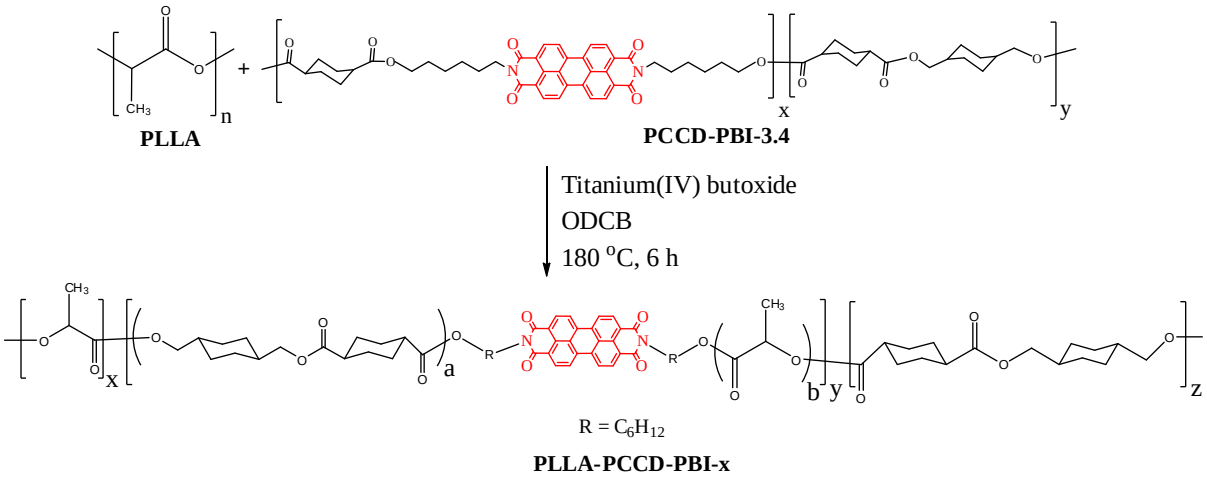

Scheme 4.3*. Synthesis of* ***PLLA-PCCD-PBI-x*** *polymer series by the high-temperature solution-blending of* ***PLLA*** *with* ***PCCD-PBI-3.4****.*

The high-temperature solution-blending of **PLLA** with varying amounts of **PCCD-PBI-3.4** was carried out by dissolving **PLLA** and **PCCD-PBI-3.4** in minimum amount of a high boiling solvent like ODCB and heating in presence of 0.1 mol % of transesterification catalyst $Ti(OBu)_4$ as shown in scheme 4.3. The blending was carried out in a cylindrical glass

reactor at 180 ^{o}C for 6 h with constant stirring using mechanical stirrer, under continuous nitrogen flow. For workup, the polymer was dissolved in chloroform and precipitated into methanol. The copolyesters obtained by the reactive blending of **PLLA** with **PCCD-PBI-3.4** were named as **PLLA-PCCD-PBI-x** where x represented the mol % incorporation of PBI in the copolyester calculated by using the molar extinction coefficient of symmetrical N,N'-bis(2-ethylhexyl)perylene-3,4,9,10-tetracarboxylic diimide as 83006 L M^{-1} cm^{-1}.

Table 4.2. *Polymer designation, feed ratio, actual incorporation of chromophores determined from absorption spectra, molecular weight (Mw), polydispersity index, viscosity data (η_{inh}), 10 % weight loss temperature (T_D) and yield of polymers.*

Polymer	Feed Ratio (**PLLA**: **PCCD-PBI-3.4/OPV-2-Diol**) (weight %)	Mol % of PBI/OPV incorporation from absorption spectra[a]	Mw (g/mol)[b]	Poly dispersity index ($Đ_M$)	η_{inh} (dL/g)[c]	T_D (^{o}C)[d]	Yield (%)
PLLA	-	-	100600	1.8	1.01	268	95
PCCD-PBI-3.4	-	3.42	23700	1.9	0.30	420	76
PLLA-PCCD-PBI-0.3	90:10	0.33	99100	1.7	0.90	299	98
PLLA-PCCD-PBI-1.0	70:30	1.02	79400	1.9	0.75	300	98
PLLA-PCCD-PBI-1.7	50:50	1.69	56600	1.7	0.68	296	98
PLLA-PCCD-PBI-2.9	30:70	2.92	35700	2.2	0.37	307	98
PLLA-PCCD-PBI-3.3	10:90	3.29	18400	2.2	0.22	307	98
PLLA-PCCD-PBI-0.3-OPV-0.7	85:10:5	0.32 (PBI) 0.67 (OPV)	79200	2.0	0.74	252	96

a. Measured in chloroform solution.
b. Measured by size exclusion chromatography (SEC) in chloroform ($CHCl_3$), calibrated with linear, narrow molecular weight distribution polystyrene as standards.
c. Determined in chloroform.
d. Determined by TGA.

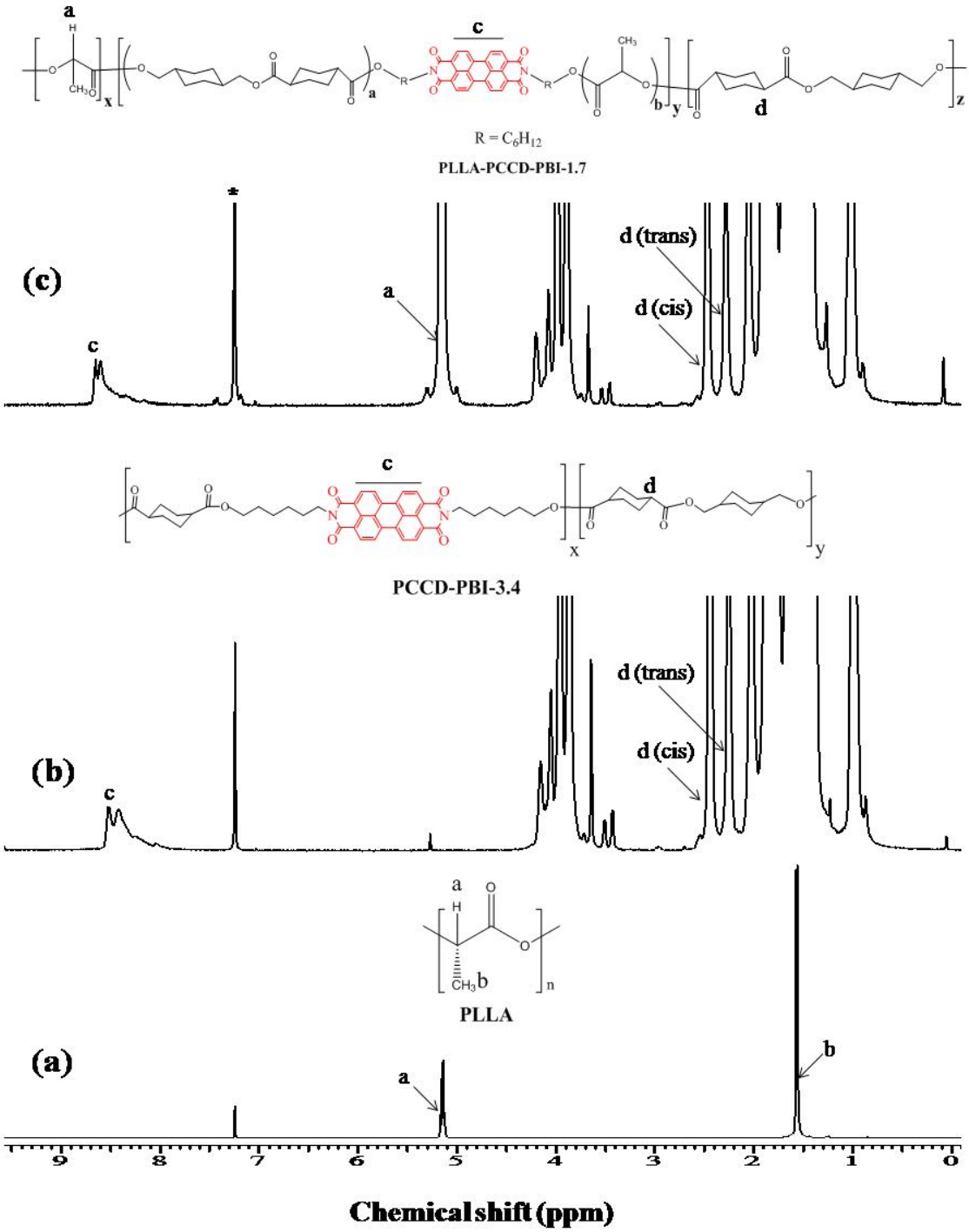

Figure 4.3. *^{1}H NMR spectra of (a)* ***PLLA****, (b)* ***PCCD-PBI-3.4*** *and (c)* ***PLLA-PCCD-PBI-1.7*** *recorded in chloroform.*

Table 4.2 gives the sample name, weight % of **PLLA** and **PCCD-PBI-3.4** taken in the feed, the actual incorporation of PBI units determined by Beer-Lamberts Law, molecular weight determined using size exclusion chromatography in $CHCl_3$ using polystyrene standards, the inherent viscosity measured in chloroform solution, the 10 % weight loss

temperature obtained from TGA as well as the yield of the various polymers. The structures of the polymers were confirmed by ^{1}H NMR and molecular weights were determined using size exclusion chromatography (SEC). Figure 4.3 compares the ^{1}H NMR spectra of **PLLA**, **PCCD-PBI-3.4** and **PLLA-PCCD-PBI-1.7**. The structure of the polymers is given and the different types of protons are assigned by alphabets.

The random copolyester of **PLLA** containing 0.7 mol % of OPV (calculated from absorption spectrum), named **PLLA-OPV-0.7** was synthesized by the reactive blending of **PLLA** with 5 wt % of OPV-2-Diol as discussed previously in chapter 3. One random copolyester incorporating both PBI and OPV was also synthesized by the reactive blending of **PLLA** (85 wt %) with **PCCD-PBI-3.4** (10 wt %) and OPV-2-Diol (5 wt %) (scheme 4.4). The actual incorporation of PBI unit in the polymer was calculated using the molar extinction coefficient of symmetrical N,N'-bis(2-ethylhexyl)perylene-3,4,9,10-tetracarboxylic diimide as 83006 L M^{-1} cm^{-1} and that of OPV unit was calculated using the molar extinction coefficient of OPV-2-Diol as 32059 L M^{-1} cm^{-1} in chloroform. The mol % incorporation of OPV and PBI units in the donor-acceptor random copolyester was calculated as 0.67 and 0.32 mol % respectively and this polymer was named as **PLLA-PCCD-PBI-0.3-OPV-0.7**. Figure 4.4. shows the ^{1}H NMR spectrum of **PLLA-PCCD-PBI-0.3-OPV-0.7** recorded in chloroform solution. The peaks corresponding to the OPV and PBI chromophores are not clear in the ^{1}H NMR spectrum due to their very low mol % incorporation in the polyester backbone. The characterization data of these polymers are given in table 4.2.

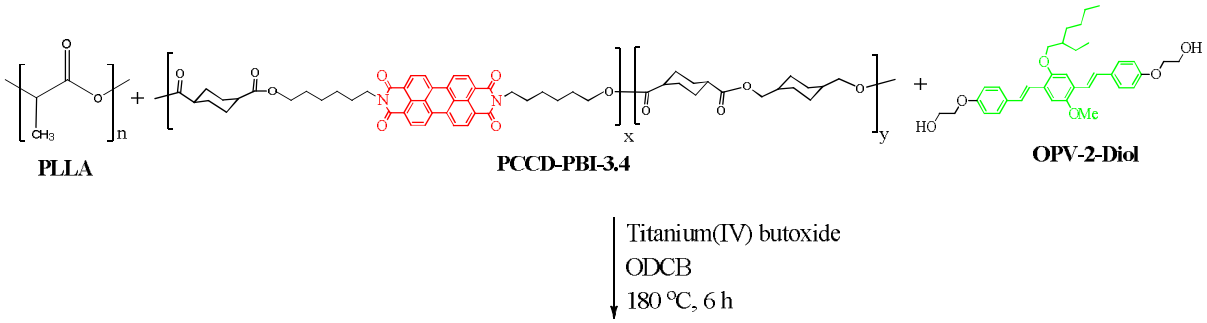

***Scheme 4.4**. Synthesis of **PLLA-PCCD-PBI-0.3-OPV-0.7** by the reactive blending of **PLLA** with **PCCD-PBI-3.4** and **OPV-2-Diol**.*

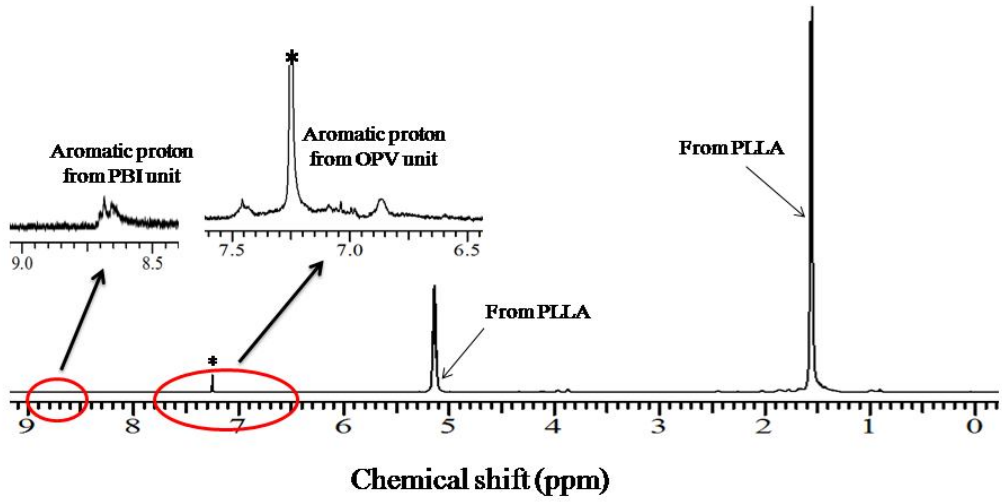

Figure 4.4. *^{1}H NMR spectra of* ***PLLA-PCCD-PBI-0.3-OPV-0.7*** *recorded in chloroform.*

4.3.2. Molecular Weights of Polymers

The polymers were soluble in common organic solvents such as dichloromethane and chloroform at room temperature. The molecular weights of the polymers were determined by size exclusion chromatography (SEC) in $CHCl_3$ using polystyrene standards. Figure 4.5 shows the SEC plots of the polymers and the molecular weights are shown in table 4.2.

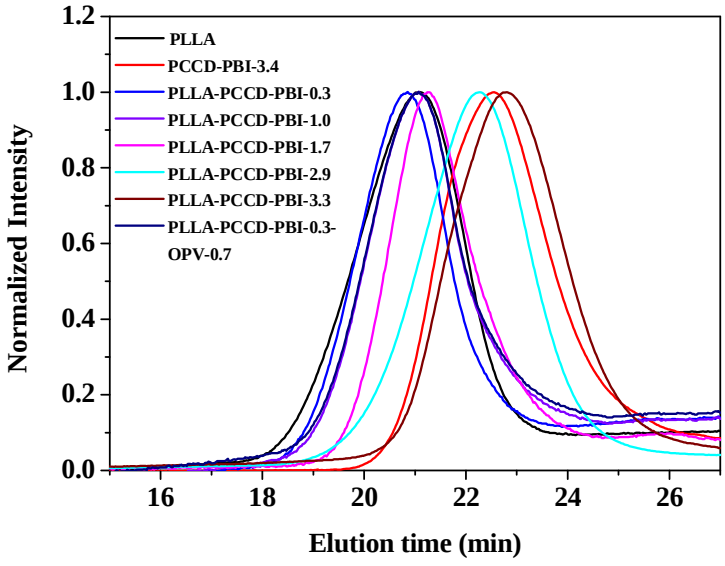

Figure 4.5. *Size exclusion chromatogram of the copolyesters recorded in chloroform using polystyrene as standard.*

The Mw of **PLLA** was 100600 and that of **PCCD-PBI-3.4** was 23700. The Mw of **PLLA-PCCD-PBI-0.3**, **PLLA-PCCD-PBI-1.0**, **PLLA-PCCD-PBI-1.7**, **PLLA-PCCD-PBI-2.9** and **PLLA-PCCD-PBI-3.3** were 99100, 79400, 56600, 35700 and 18400 respectively. The molecular weight of the **PLLA-PCCD-PBI-x** series of polymers decreased with increasing weight % of **PCCD-PBI-3.4** in feed. The copolyesters all eluted slowly compared to **PLLA** indicating their lower molecular weights which was a consequence of the chopping of the polymer chains to incorporate PCCD and perylenebisimide chromophore.[33] Table 4.2 gives the inherent viscosity measured in chloroform solution for all the polymers. The inherent viscosities of the polymer also decreased with increasing weight % of **PCCD-PBI-3.4** in feed. The Mw of **PLLA-PCCD-PBI-0.3-OPV-0.7** was determined as 79200.

4.3.3. Thermal Properties of Polymers

The thermal properties of the polymers are summarized in table 4.2. Figure 4.6 shows the TGA thermograms for the series of polymers. The 10 % weight loss temperature for **PLLA** was around 268 ^{o}C, while that for the **PCCD-PBI-3.4** was higher at around 420 ^{o}C. The 10 % weight loss temperatures of **PLLA-PCCD-PBI-x** series of polymers were around 300 ^{o}C, in between that of **PLLA** and **PCCD-PBI-0.3**. TGA thermograms of **PLLA-PCCD-PBI-x** series of polymers showed step wise degradation between 275 to 450 ^{o}C, but which was absent in **PLLA**. These steps wise degradations originate from the scission of aliphatic and cyclic aliphatic polyester segment of the copolyesters.[34]

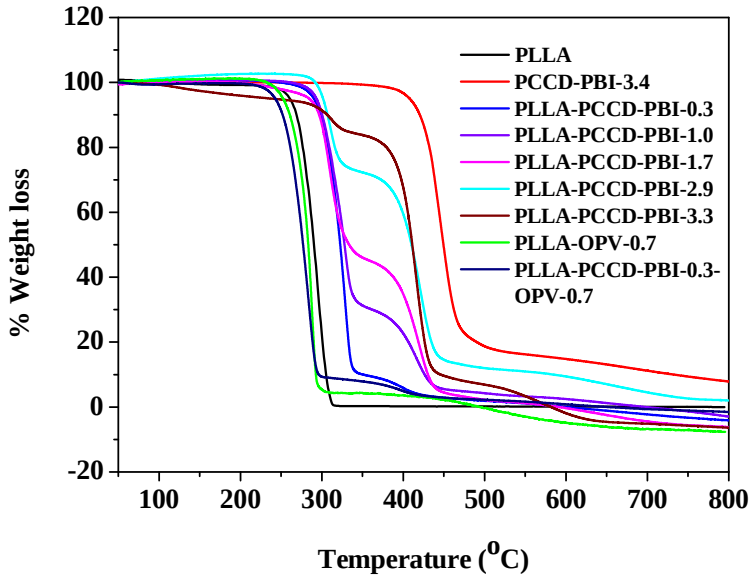

Figure 4.6. *TGA thermograms of the copolyesters recorded under nitrogen atmosphere at heating rate of 10 ^{o}C/min.*

Figure 4.7 (a) shows the stack plot of the second heating scans in the DSC thermograms of the **PLLA**, **PCCD-PBI-3.4**, **PLLA-PCCD-PBI-x** series of polymers and **PLLA-PCCD-PBI-0.3-OPV-0.7**. The step transition at 63 ^{o}C attributed to the glass transition temperature (T_g) of **PLLA** with a crystallization peak at 108 ^{o}C and a melting peak at 181 ^{o}C. **PCCD-PBI-3.4** was characterized by only T_g around 46 ^{o}C due to its amorphous nature. All **PLLA-PCCD-PBI-x** series of polymers showed T_g, crystallization and melting transition (see table 4.3). The second heating DSC thermogram of **PLLA-PCCD-PBI-0.3-OPV-0.7** polymer showed glass transition (T_g) at 53 ^{o}C, crystallization peak at 98 ^{o}C and melting at 168 ^{o}C. A single T_g was observed for **PLLA-PCCD-PBI-x** series of polymers and **PLLA-PCCD-PBI-0.3-OPV-0.7**, indicative of miscible blends formed by ester-ester exchange reaction.[33]

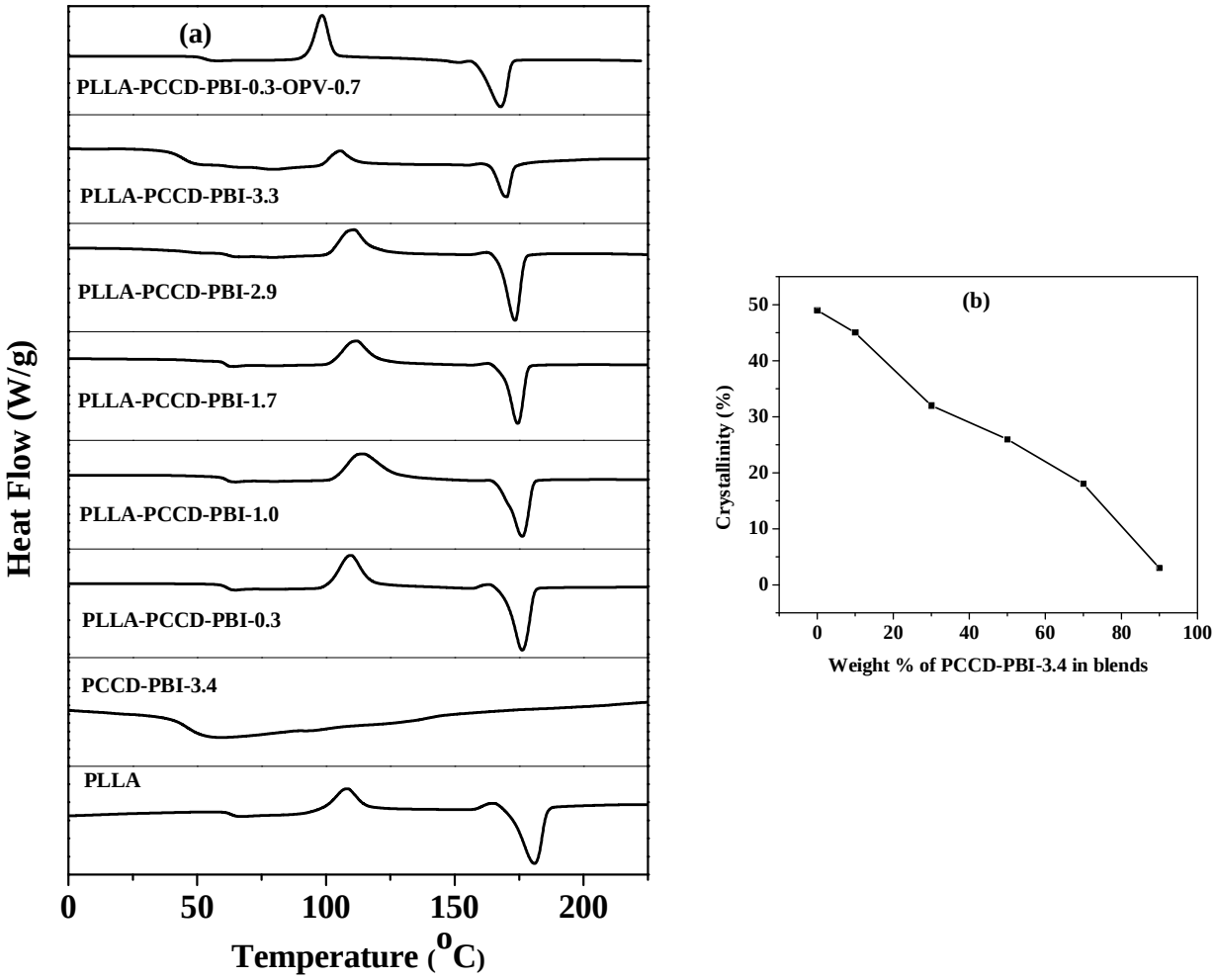

Figure 4.7*. (a) The second heating DSC thermograms of polymers at the heating rate of 10 ^{o}C/min and (b) plot comparing the crystallinity (%) of* ***PLLA-PCCD-PBI-x*** *series of polymers as a function of increased weight % of* ***PCCD-PBI-3.4****.*

The degree of crystallinity of **PLLA** and **PLLA-PCCD-PBI-x** series of polymers were calculated using the equation:

$$Crystallinity\ (\%) = \left(\Delta H_f / \Delta H_f^0\right) X\ 100$$

where ΔH_f is the melting enthalpy and ΔH_f^0 = 93 J/g is the heat of fusion for 100 % crystalline **PLLA** reported in literature.[35] The ΔH_f values were obtained from the melting curves of the second heating scans of the DSC. The crystallinity (%) of the synthesized **PLLA** and **PLLA-PCCD-PBI-x** series of polymers were summarized in table 4.3. Figure 4.7 (b) compares the crystallinity (%) of **PLLA-PCCD-PBI-x** series of polymers as a function of increasing weight % of **PCCD-PBI-3.4**. The crystallinity (%) of synthesized **PLLA** was calculated as 49 % and it was observed that the crystallinity (%) decreased with increasing weight % of **PCCD-PBI-3.4** in the blend.

Table 4.3*. The glass transition temperature (T_g), melting temperature (T_m), crystallisation temperature (T_c) and crystallinity (%) of the polymers.*

Polymer	T_g (^oC)[a]	T_m (^oC)[a]	T_c (^oC)[a]	Crystallinity (%)[b]
PLLA	63	181	108	49
PCCD-PBI-3.4	46	-	-	-
PLLA-PCCD-PBI-0.3	61	176	109	45
PLLA-PCCD-PBI-1.0	61	176	114	32
PLLA-PCCD-PBI-1.7	61	174	112	26
PLLA-PCCD-PBI-2.9	62	173	111	18
PLLA-PCCD-PBI-3.3	45	170	105	3
PLLA-PCCD-PBI-0.3-OPV-0.7	53	168	98	41

a. Determined by DSC.

b. Calculated from 100 % crystalline PLLA reported in literature.

4.3.4. Wide-angle X-ray Diffraction (WXRD)

The polyesters were analyzed for their bulk packing using wide-angle X-ray diffraction (WXRD) in the range of 2θ = 5-35° at room temperature (25 ^{o}C). Figure 4.8 compares the WXRD patterns of **PLLA-PCCD-PBI-x** series of polymers along with that of the parent **PLLA** and **PCCD-PBI-3.4** polyester. **PLLA** showed the diffraction peaks at 2θ = 12.5^{o}, 15.0^{o}, 16.9^{o}, 19.1^{o} and 22.6^{o} which were assigned to the (103), (010), (200 or 110), (203) and (015) diffractions of the α-form crystal of **PLLA** respectively as reported in literature.[36] The **PCCD-PBI-3.4** copolyester had reflections at 2θ = 9.49°, 12.41° and 24.94° corresponding to the d spacing of 9.31 Å, 7.12 Å and 3.57 Å respectively. The intensity of all the peaks corresponding to the α-form crystal of **PLLA** decreased with increasing weight % of **PCCD-PBI-3.4** in the **PLLA-PCCD-PBI-x** series of polymer, in conformation with observed from DSC.

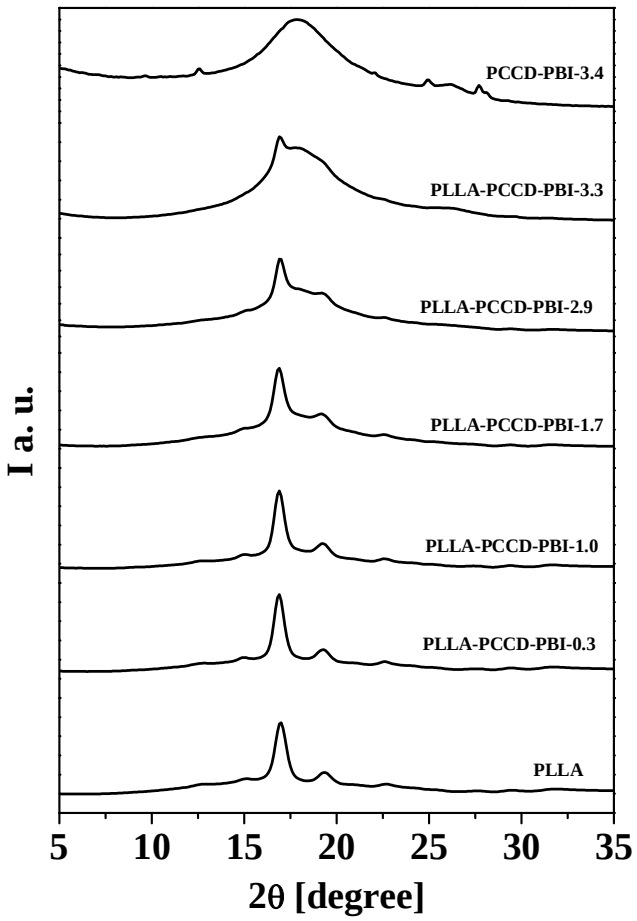

Figure 4.8. *WXRD patterns of* ***PLLA***, ***PCCD-PBI-3.4*** *and* ***PLLA-PCCD-PBI-x*** *series of polymers in powder form at room temperature.*

4.3.5. Thin Film Formation

Free-standing films could be formed from polymers signifying their high mechanical stability. Figure 4.9 shows photograph of the free standing films prepared from 0.5 wt % $CHCl_3$ solutions of **PLLA-PCCD-PBI-0.3**, **PLLA-PCCD-PBI-1.0** and **PLLA-PCCD-PBI-1.7** respectively and these films were transparent and flexible. The polymers, **PLLA-PCCD-PBI-2.9** and **PLLA-PCCD-PBI-3.3** formed only brittle films which could not be peeled off because of their low mechanical stability. Figure 4.9 also shows the image of these three polymer films upon observation under 365 nm hand-held UV lamp. All polymer films showed strong red colour emission under UV lamp. PBIs are well-known for their tendency to aggregate and lead to quenching of fluorescence in solid state.[37-39] Our current report is one of the few reports where PBI has been successfully incorporated into a polymer scaffold with intense red emission in solid state.

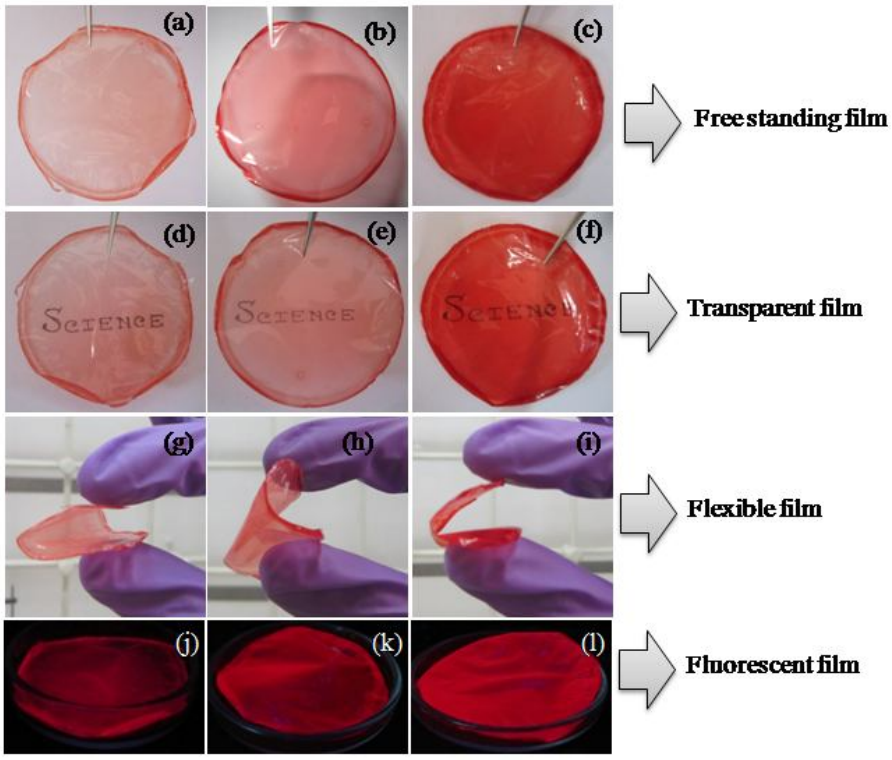

Figure 4.9*. Photographs of the free standing films of* ***PLLA-PCCD-PBI-0.3*** *(a, d, g),* ***PLLA-PCCD-PBI-1.0*** *(b, e, h) and* ***PLLA-PCCD-PBI-1.7*** *(c, f, i) drop casted from 0.5 wt % solution in chloroform. The respective films upon observation under UV lamp (365 nm) [(j)* ***PLLA-PCCD-PBI-0.3****, (k)* ***PLLA-PCCD-PBI-1.0*** *and (l)* ***PLLA-PCCD-PBI-1.7****].*

4.3.6. Microscopic Characterization

Among diverse range of approaches, chemical methods and physical deposition methods tend to produce short rods or wires and often incapable of making longer fibers. Electrospinning is a very versatile technique for making 1D elongated structure.[28-30] Figure 4.10 shows the scanning electron microscopy (SEM) (top) and fluorescence microscopy images (bottom) of the electrospun fibres of **PLLA-PCCD-PBI-0.3**, **PLLA-PCCD-PBI-1.0** and **PLLA-PCCD-PBI-1.7**. SEM images revealed the presence of nanofibers of 150-500 nm diameters. Red emission was observed from the nanofibers of **PLLA-PCCD-PBI-0.3**, **PLLA-PCCD-PBI-1.0** and **PLLA-PCCD-PBI-1.7** as seen from the fluorescence microscopy images, upon excitation at wavelength of 500-550 nm. The formation of beaded fibers was observed from the SEM images of **PLLA-PCCD-PBI-2.9** and **PLLA-PCCD-PBI-3.3** due to the low viscosity of polymer solutions. The nanofiber fabricated from **PLLA-PCCD-PBI-0.3-OPV-0.7** showed blue, green and red emission with excitation at three different wavelength regions (figure 4.11). Therefore, one can access three different emission regions from the nanofiber of **PLLA-PCCD-PBI-0.3-OPV-0.7** just by exciting at the appropriate wavelength.

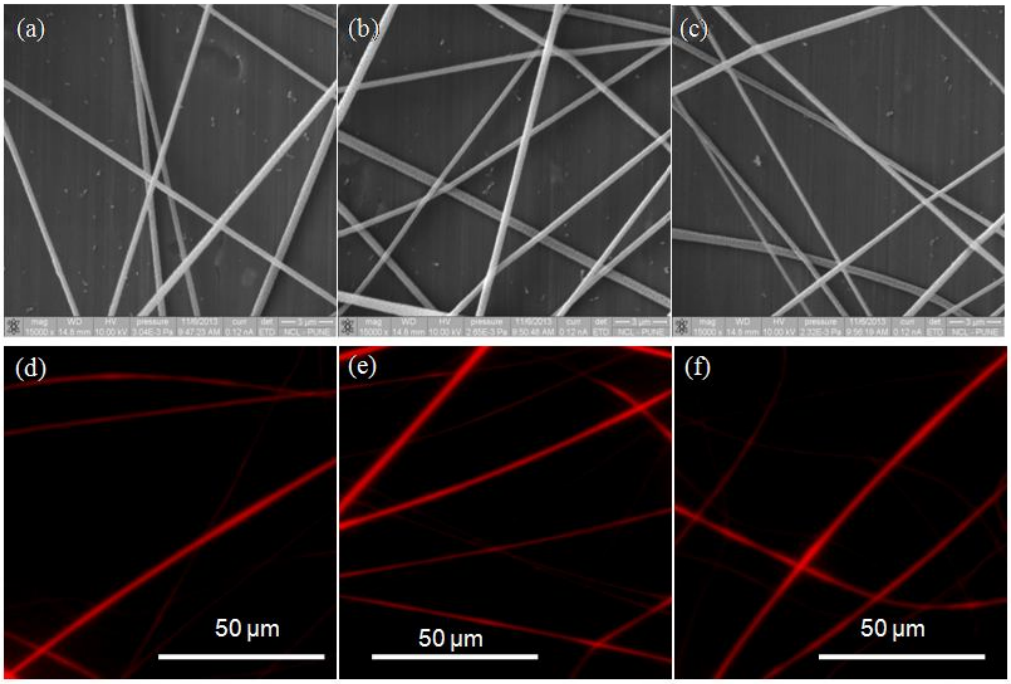

Figure 4.10. *SEM images of the electrospun fibers of (a)* ***PLLA-PCCD-PBI-0.3****, (b)* ***PLLA-PCCD-PBI-1.0*** *and (c)* ***PLLA-PCCD-PBI-1.7*** *(top) and the respective fluorescent microscopy images (bottom) with excitation at wavelength of 500-550 nm.*

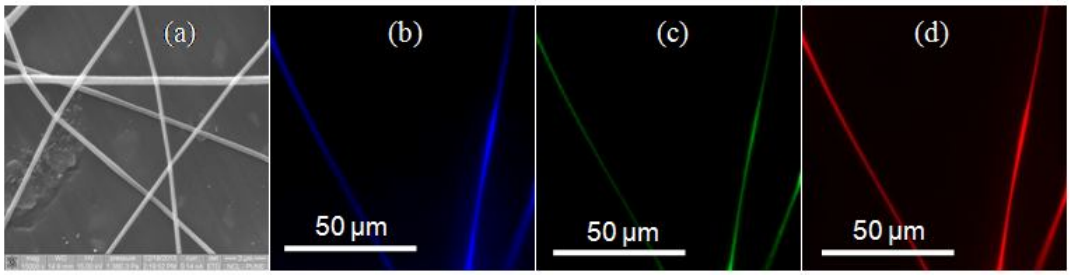

Figure 4.11. *(a) SEM; (b), (c) and (d) fluorescent microscopy image of* ***PLLA-PCCD-PBI-0.3-OPV-0.7*** *with excitation at wavelength of 350-430 nm, 488-520 nm and 500-550 nm respectively.*

4.3.7. Photophysical Properties

The optical properties of the polymers were investigated by UV-Vis and fluorescence spectroscopy in both solution and solid state, which are summarised in table 4.4.

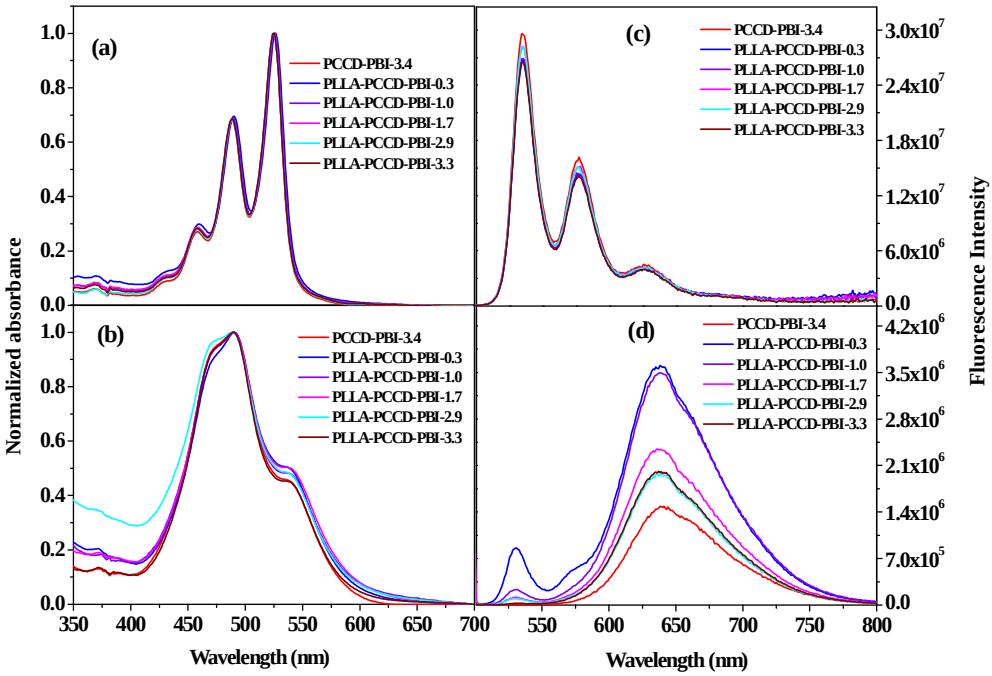

Figure 4.12. *Normalized absorption spectra of polymers (a) in the solution (chloroform) and (b) in the film spin-coated from chloroform solution; emission spectra of polymers (c) in the solution (chloroform) [0.1 OD at 490 nm, λ_{ex} = 490 nm] and (d) in film state [0.1 OD at 490 nm, λ_{ex} = 490 nm].*

Figure 4.12 (a) and (b) shows the normalized absorption spectra of **PCCD-PBI-3.4** and **PLLA-PCCD-PBI-x** series of polymers in chloroform solution as well as in film state. All polymers showed the typical absorption of PBI chromophore with peaks in the range of

400-530 nm, corresponding to the 0-0, 0-1, 0-2, and 0-3 electronic transitions, respectively, in chloroform solution.[39] The absorption spectra in the solid state was broad with $\lambda_{max} \approx 490$ nm, a new band emerging at 538 nm, and the ratios of peak intensities were different compared to that in solutions, indicative of aggregation.[39]

Emissions from the polymers were studied by exciting at 490 nm, which is shown in figure 4.12 (c) and (d). In solution, typical emission of PBI with peaks at 534, 576, and 625 nm was observed, whereas in the solid state, PBI monomer emission at 534 nm was hugely suppressed, and a red-shifted intense broad excimer emission was observed at 638 nm indicating **J** type of aggregate formation.[39, 40] It can be seen from the figure that the aggregate emission intensity of all the **PLLA-PCCD-PBI-x** series of polymers were higher compared to **PCCD-PBI-3.4** where the PBI units were segmented by the blocks of **PLLA** units. The emission intensity of **PLLA-PCCD-PBI-x** series of polymers decreased with increasing weight % of **PCCD-PBI-3.4**, which could be attributed to aggregation-induced quenching.[39, 40]

Table 4.4 gives the fluorescence quantum yield data for all the polymers in both solution and solid state. The relative fluorescence quantum yields of PBI polymer were determined in $CHCl_3$ using rhodamine 6G in ethanol (ϕ= 0.95) as the standard by exciting at 490 nm. The absolute solid state quantum yield of polymers was measured using Integrating Sphere. All **PLLA-PCCD-PBI-x** series of polymers were highly fluorescent in chloroform solution with quantum yields of ~ 82%. All polymers showed low fluorescence quantum yield in solid state as compared to solution state due to aggregation-induced quenching. **PCCD-PBI-3.4** had solid state quantum yield of 2%, whereas **PLLA-PCCD-PBI-0.3** had a high quantum yield of 10%. The solid state fluorescence quantum yields of **PLLA-PCCD-PBI-1.0**, **PLLA-PCCD-PBI-1.7**, **PLLA-PCCD-PBI-2.9** and **PLLA-PCCD-PBI-3.3** were 9%, 7%, 6% and 2% respectively. The solid state fluorescence quantum yields of **PLLA-PCCD-PBI-x** series of polymers decreased with increasing weight % of **PCCD-PBI-3.4** in the blend. In contrast to the weak fluorescence emission (with quantum yield < 1%) previously observed for the self-assembled materials of PBIs in the literature, the polymer reported herein demonstrated drastically increased solid state emission (with quantum yield of 10%).

Table 4.4. *Absorption and emission of polymers in solution as well as in solid state (film spin-coated from chloroform solution) along with fluorescence quantum yields (Φ_{FL}).*

Polymer	Absorption λ_{max} (nm) (In $CHCl_3$)	Emission λ_{max} (nm) (In $CHCl_3$)	Absorption λ_{max} (nm) (In film)	Emission λ_{max} (nm) (In film)	ϕ_{FL} (solution)	ϕ_{FL}[f] (%) (In powder)
PCCD-PBI-3.4	526	534[a]	490	638[a]	0.84[d]	2
PLLA-PCCD-PBI-0.3	526	534[a]	490	638[a]	0.80[d]	10
PLLA-PCCD-PBI-1.0	526	534[a]	490	638[a]	0.82[d]	9
PLLA-PCCD-PBI-1.7	526	534[a]	490	638[a]	0.82[d]	7
PLLA-PCCD-PBI-2.9	526	534[a]	490	638[a]	0.81[d]	6
PLLA-PCCD-PBI-3.3	526	534[a]	490	638[a]	0.82[d]	2
PLLA-OPV-0.7	390	445[b]	392	440, 469[c]	0.62[e]	63
PLLA-PCCD-PBI-0.3-OPV-0.7	390, 526	445[b] 534[a]	392, 490	441[c], 467[c] 638[a]	-	23 (OPV)[c] 8 (PBI)[a]

a. Excitation at 490 nm.
b. Excitation at 390 nm.
c. Excitation at 392 nm.
d. The fluorescence quantum yield for polymers in $CHCl_3$ was obtained upon excitation at 490 nm and was measured using rhodamine-6G in ethanol as standard.
e. The fluorescence quantum yield for polymers in $CHCl_3$ was obtained upon excitation at 360 nm and was measured using quinine sulphate in 0.1 M H_2SO_4 solution as standard.
f. Absolute fluorescence quantum yields in the solid state were determined with an integrating sphere.

The photophysical characteristics of **PLLA-PCCD-PBI-0.3-OPV-0.7** were determined by recording the absorption and emission spectra in solution as well as in film state and compared with that of **PLLA-PCCD-OPV-0.7** and **PLLA-PCCD-PBI-0.3**. Figure 4.13 (a) compares the normalized absorption spectra of **PLLA-OPV-0.7**, **PLLA-PCCD-PBI-0.3** along with **PLLA-PCCD-PBI-0.3-OPV-0.7** in chloroform solution. **PLLA-OPV-0.7** had absorption maximum at 390 nm. The absorption spectrum of the **PLLA-PCCD-PBI-0.3-OPV-0.7** was a linear addition of the characteristic absorption bands of both OPV and PBI

moiety, indicating no charge transfer occurring in the ground state.[41] Figure 4.13 (b) compares the normalized absorption spectra of thin films of the polymers spin coated from chloroform. The absorption spectrum of **PLLA-PCCD-PBI-0.3-OPV-0.7** was broad, especially for the PBI region and the ratios of peak intensities were different compared to that in solution, indicating aggregation tendency.[42]

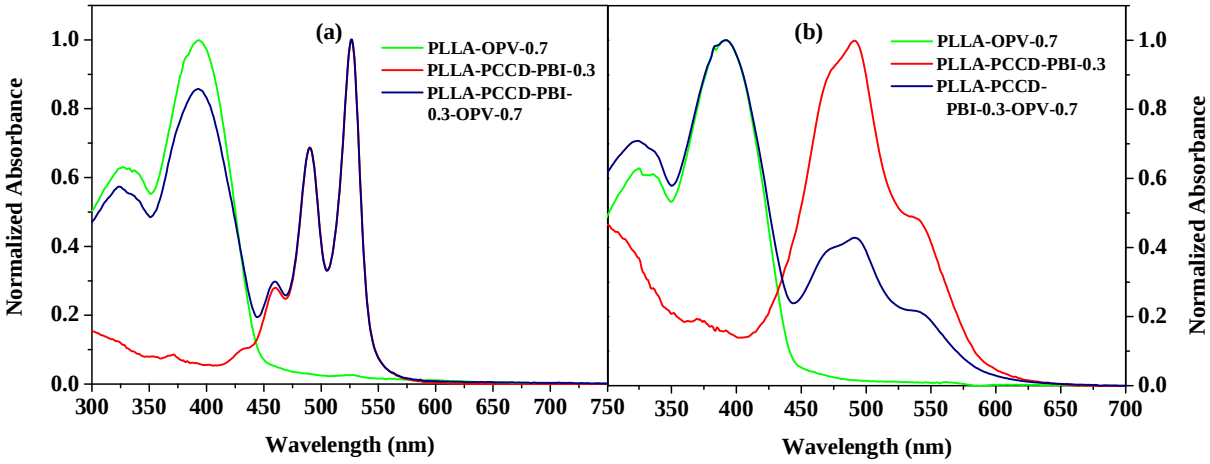

***Figure 4.13**. Normalized absorption spectra of **PLLA-OPV-0.7**, **PLLA-PCCD-PBI-0.3** and **PLLA-PCCD-PBI-0.3-OPV-0.7** in (a) chloroform solution and (b) film spin coated from chloroform.*

To investigate the photophysics and especially address the possibility of photo-induced energy transfer between the donor (OPV) and acceptor (PBI) moieties of the copolyester **PLLA-PCCD-PBI-0.3-OPV-0.7**, their emission was measured in chloroform solution. The energy transfer from OPV unit to PBI unit was monitored in the solution state by recording the emission of OPV in the absence and presence of acceptor after excitation of OPV at 390 nm. Figure 4.14 (a) compares the emission of the donor alone polymer **PLLA-OPV-0.7**, acceptor alone polymer **PLLA-PCCD-PBI-0.3**, along with that of the D-A polymer **PLLA-PCCD-PBI-0.3-OPV-0.7** upon excitation at 390 nm. **PLLA-OPV-0.7** and **PLLA-PCCD-PBI-0.3-OPV-0.7** were prepared with 0.1 OD at 390 nm and **PLLA-PCCD-PBI-0.3** was made to have 0.1 OD at 490 nm. When excited at 390 nm, **PLLA-OPV-0.7** emitted strongly with emission maximum at 445 nm. **PLLA-PCCD-PBI-0.3** did not exhibit noticeable emission upon excitation at the donor wavelength maximum of 390 nm. Excitation of donor-acceptor polyester (**PLLA-PCCD-PBI-0.3-OPV-0.7**) resulted in 27.82% quenching of the OPV emission at 445 nm as compared to that of donor alone polymer (**PLLA-OPV-0.7**). Excitation of the donor-acceptor polymers (**PLLA-PCCD-PBI-0.3-OPV-0.7**) at the acceptor absorption maximum of 490 nm resulted in a slight (16.96%) quenching of emission

from PBI compared to that of the acceptor alone polymer **(PLLA-PCCD-PBI-0.3)** [figure 4.14 (b)]. The inset in figure 4.14 (a) compares the excitation spectra collected while monitoring the PBI emission at 575 nm for **PLLA-PCCD-PBI-0.3** as well as **PLLA-PCCD-PBI-0.3-OPV-0.7.** The OPV absorption band is not observed in the excitation spectrum while monitoring the PBI emission in **PLLA-PCCD-PBI-0.3-OPV-0.7** suggested the absence of energy transfer channels between OPV and PBI units. This was also confirmed by fluorescence lifetime-decay studies of **PLLA-PCCD-PBI-0.3-OPV-0.7** in the presence and absence of the acceptor. Fluorescence lifetime-decay profiles were collected for the **PLLA-OPV-0.7** and **PLLA-PCCD-PBI-0.3-OPV-0.7** copolymers using LED 390 nm and by probing at 445 nm [figure 4.16 (a)]. Both polymers exhibited similar fluorescence lifetime decay values of 1.3 ns, indicating that energy transfer did not play a major role. The reason for this quenching of donor emission could be radiative transfer by the trivial mechanism where the emission of the donor is absorbed by the acceptor.[43]

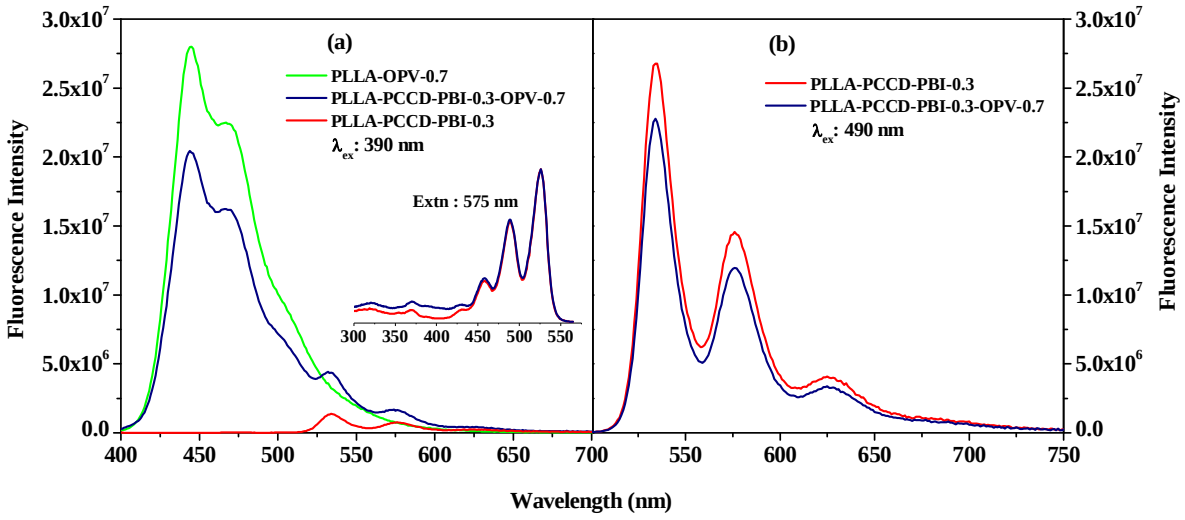

Figure 4.14*. Emission spectra of* ***PLLA-PCCD-PBI-0.3****,* ***PLLA-OPV-0.7*** *and* ***PLLA-PCCD-PBI-0.3-OPV-0.7*** *in the chloroform solution (a) λex = 390 nm [0.1 OD at 490 nm for* ***PLLA-PCCD-PBI-0.3*** *and 0.1 OD at 390 nm for other two polymers]; (b) λex = 490 nm [0.1 OD at 490 nm for both polymers]. Inset of (a) compares the normalized (at 526 nm) excitation (*λ_{em} *= 575 nm) spectra of* ***PLLA-PCCD-PBI-0.3*** *and* ***PLLA-PCCD-PBI-0.3-OPV-0.7****.*

Figure 4.15 compares the emission of the donor alone polymer **PLLA-OPV-0.7**, acceptor alone polymer **PLLA-PCCD-PBI-0.3**, along with that of the D-A polymers **PLLA-PCCD-PBI-0.3-OPV-0.7** in film state. Donor-acceptor polymer (**PLLA-PCCD-PBI-0.3-OPV-0.7**) exhibited strong emission intensity for OPV and PBI unit upon excitation at 392

nm (absorption maximum of OPV unit) and 490 nm (absorption maximum of PBI unit) respectively. As compared to donor alone polymer (**PLLA-OPV-0.7**), D-A polymer exhibited 36.14% quenching of donor emission by monitoring the PL emission from OPV unit. The inset in figure 4.15 compares the excitation spectra collected while monitoring the PBI emission at 638 nm for **PLLA-PCCD-PBI-0.3** as well as **PLLA-PCCD-PBI-0.3-OPV-0.7.** The OPV absorption band is not observed in the excitation spectrum while monitoring the PBI emission in **PLLA-PCCD-PBI-0.3-OPV-0.7** suggested the absence of energy- and electron transfer channels between OPV and PBI units and it is further confirmed by fluorescence lifetime-decay studied in film state. Fluorescence lifetime-decay profiles were collected for the **PLLA-OPV-0.7** and **PLLA-PCCD-PBI-0.3-OPV-0.7** copolymers using LED 390 nm and by probing at 440 nm [figure 4.16 (b)]. Both polymers exhibited similar fluorescence lifetime decay values of 1.28 ns, confirmed that energy- or electron transfer did not play a major role.[43] The solid state (powder form) quantum yield of OPV and PBI emission in **PLLA-PCCD-PBI-0.3-OPV-0.7** was 23 % and 8 % respectively. **PLLA-PCCD-PBI-0.3-OPV-0.7** could be excited independently without energy transfer occurring between them, and therefore one can access two different emission regions from **PLLA-PCCD-PBI-0.3-OPV-0.7** just by exciting at appropriate wavelength and it is confirmed by fluorescence microscopy studies.

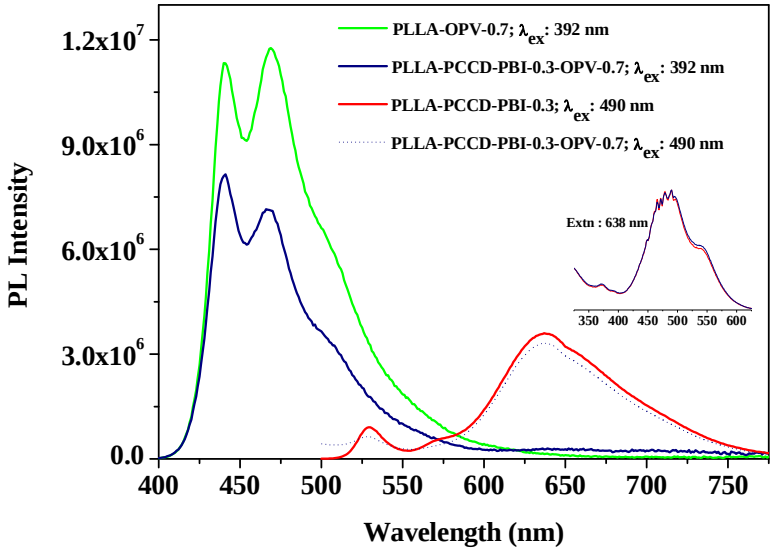

Figure 4.15. *Emission spectra of* ***PLLA-PCCD-PBI-0.3***, ***PLLA-OPV-0.7*** *and* ***PLLA-PCCD-PBI-0.3-OPV-0.7*** *in the film spin-coated from chloroform solution. Inset compares the normalized (at 490 nm) excitation (λ_{em} = 638 nm) spectra of* ***PLLA-PCCD-PBI-0.3*** *and* ***PLLA-PCCD-PBI-0.3-OPV-0.7.***

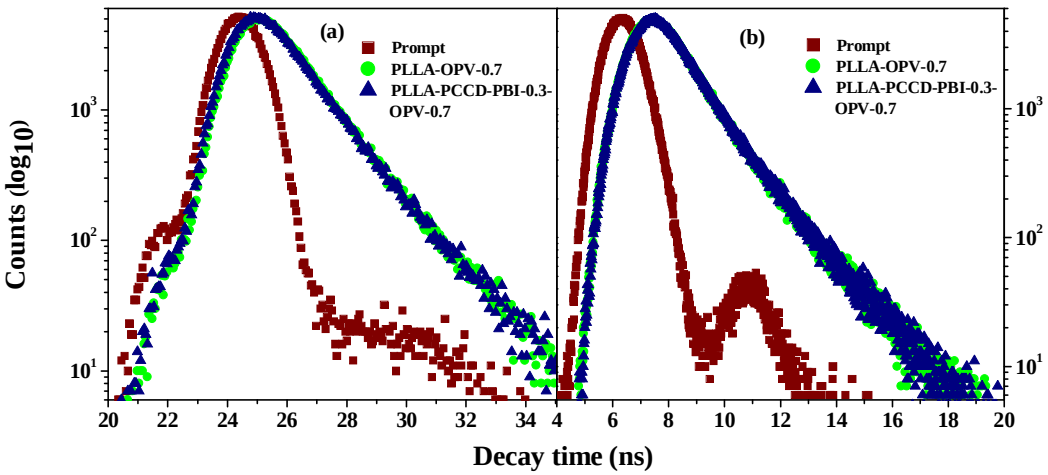

Figure 4.16. *(a) Fluorescence life-time decay profiles (0.1 OD at 390 nm, monitored at 445 nm) of* ***PLLA-OPV-0.7*** *and* ***PLLA-PCCD-PBI-0.3-OPV-0.7*** *in chloroform and (b) fluorescence life-time decay profiles (0.1 OD at 392 nm, monitored at 440 nm) of* ***PLLA-OPV-0.7*** *and* ***PLLA-PCCD-PBI-0.3-OPV-0.7*** *in film spin-coated from chloroform solution.*

4.4. Conclusions

Random copolyesters of **PLLA** and **PCCD** incorporating varying mol % of perylenebisimide (PBI) was successfully synthesized by high-temperature solution-blending. All the polyesters were characterized by ^{1}H NMR, SEC, viscosity, TGA, DSC and WXRD analyses. The chemical incorporation of PBI chromophore in the backbone of the polyester was confirmed by SEC and DSC analysis. These polymers showed good solubility, film-forming properties and displayed strong red photoluminescence. The photophysical properties were studied using steady-state UV-vis absorption and fluorescence spectroscopy in solution as well as in solid state. All polymers were highly fluorescent in solution state. The solid state fluorescence quantum yield of the polymers decreased with increasing mol % incorporation of PBI units. Red fluorescent nanofibers of these polymers were successfully constructed by electrospinning technique. These interesting emission properties make them potential candidates in various nanodevice applications including laser, waveguide and polarized emission. This approach was extended for the construction of the nanofibers of copolyester of **PLLA** and **PCCD** incorporating both OPV and PBI chromophore. Blue, green and red emission from this polymer was observed under fluorescence microscopy upon excitation at different wavelengths.

4.5. Reference

1) Law, M.; Goldberger, J.; Yang, P. *Annu. Rev. Mater. Res.* **2004**, *34*, 83-122.
2) Xia, Y.; Yang, P.; Sun, Y.; Wu, Y.; Mayers, B.; Gates, B.; Yin, Y.; Kim, F.; Yan, H. *Adv. Mater*. **2003**, *15*, 353-389.
3) Huang, M. H.; Mao, S.; Feick, H.; Yan, H.; Wu, Y.; Kind, H.; Weber, E.; Russo, R.; Yang, P. *Science* **2001**, *292*, 1897-1899.
4) Law, M.; Sirbuly, D. J.; Johnson, J. C.; Goldberger, J.; Saykally, R. J.; Yang, P. *Science* **2004**, *305*, 1269-1273.
5) Würthner, F. *Chem. Commun*. **2004**, 1564-1579.
6) Pisula, J. W. W.; Müllen, K. *Chem. Rev*. **2007**, *107*, 718-747.
7) Ajayaghosh, A.; Praveen, V. K. *Acc. Chem. Res.* **2007**, *40*, 644-656.
8) Zang, L.; Che, Y.; Moore, J. S. *Acc. Chem. Res.* **2009**, *4*, 1596-1608.
9) Schenning, A. P. H. J.; Meijer, E. W. *Chem. Commun*. **2005**, 3245-3258.
10) Grimsdale, A. C.; Müllen, K. *Angew. Chem. Int. Ed*. **2005**, *44*, 5592-5629.
11) Zang, L.; Che, Y.; Moore, J. S. *Acc. Chem. Res.* **2009**, *41*, 1596-1608.
12) Wicklein, A.; Ghosh, S.; Somme, M.; Würthner, F.; Thelakkat, M. *ACS Nano* **2009**, *3*, 1107-1114.
13) Huang, J. X.; Virji, S.; Weiller, B. H.; Kaner, R. B. *J. Am. Chem. Soc*. **2003**, *125*, 314-315.
14) Virji, S.; Huang, J.; Kaner, R. B.; Weiller, B. H. *Nano Lett*. **2004**, *4*, 491-496.
15) Lee, H. J.; Jin, Z. X.; Aleshin, A. N.; Lee, J. Y.; Goh, M. J.; Akagi, K.; Kim, Y. S.; Kim, D. W.; Park, Y. W. *J. Am. Chem. Soc*. **2004** , *126*, 16722-16723.
16) Zhang, X.; Manohar, S. K. *J. Am. Chem. Soc*. **2005**, *127*, 14156-14157.
17) Luo, Y. H.; Liu, H. W.; Xi, F.; Li, L.; Jin, X. G.; Han, C. C.; Chan, C. M. *J. Am. Chem. Soc*. **2003**, *125*, 6447-6451.
18) Jeukens, C. R. L. P. N.; Jonkheijm, P.; Wijnen, F. J. P.; Gielen, J. C.; Christianen, P. C. M.; Schenning, A. P. H. J.; Meijer, E. W.; Maan, J. C. *J. Am. Chem. Soc*. **2005**, *127*, 8280-8281.
19) Nguyen, T.-Q.; Martel, R.; Avouris, P.; Bushey, M. L.; Brus, L.; Nuckolls, C. *J. Am. Chem. Soc.* **2004**, *126*, 5234-5242.
20) Kastler, M.; Pisula, W.; Wasserfallen, D.; Pakula, T.; Mullen, K. *J. Am. Chem. Soc*. **2005**, *127*, 4286-4296.
21) Guillon, D. *Struct. Bonding* **1999**, *95*, 41-82.

22) Law, K. -Y. *Chem. Rev.* **1993**, *93*, 449-406.

23) Jones, B. A.; Ahrens, M. J.; Yoon, M.; Facchetti, A.; Marks, T. J.; Wasielewski, M. R. *Angew. Chem. Int. Ed*. **2004**, *43*, 6363-6366.

24) Langhals, H. *Heterocycles* **1995**, *40*, 477-500.

25) Yan, P.; Chowdhury, A.; Holman, M. W.; Adams, D. M. *J. Phys. Chem. B* **2005**, *109*, 724-730.

26) Ahrens, M. J.; Sinks, L. E.; Rybtchinski, B.; Liu, W.; Jones, B. A.; Giaimo, J. M.; Gusev, A. V.; Goshe, A. J.; Tiede, D. M.; Wasielewski, M. R. *J. Am. Chem. Soc.* **2004**, *126*, 8284-8294.

27) Auras, R.; Lim, L, -T.; Selke, S. E. M.; Tsuji, H. *Poly(lactid acid): Synthesis, Structures, Properties, Processing, and Applications*; J. Wiley & Sons, **2010**.

28) Wu, J.; Wang, N.; Zhao, Y.; Jiang, L. *J. Mater. Chem. A* **2013**, *1*, 7290-7305.

29) Wendorff, J. H.; Agarwal, S.; Greiner, A. *Electrospinning: Materials, Processing, and Applications*; Wiley-VCH, **2012**.

30) Li, Z.; Wang, C. *One-Dimensional nanostructures: Electrospinning Technique and Unique Nanofibers*; Springer, **2013**.

31) Monk, P.; Munro, L. J. *Maths for Chemistry: A Chemist's Toolkit of Calculations*; Oxford University Press Inc., **2010**.

32) Liu,Y.; Turner, S. R.; Wilkes, G. *Macromolecules* **2011**, *44*, 4049-4056.

33) Fakirov, S. *Transreactions in Condensation Polymers*; Wiley-VCH, **1999**.

34) Pielichowski, K.; Njuguna, J. *Thermal Degradation of Polymeric Materials*; Rapra Technology Limited, **2005**.

35) Haynes, D.; Abayasinghe, N. K.; Harrison, G. M.; Burg, K. J.; Smith, D. W. *Biomacromolecules* **2007**, *8*, 1131-1137.

36) Li, X. -J.; Zhong, G.; Li, Z. *Chin. J. Polym. Sci*. **2010**, *28*, 357-366.

37) Che, Y.; Datar, A.; Balakrishnan, K.; Zang, L. *J. Am. Chem. Soc*. **2007**, *129*, 7234-7235.

38) Balakrishnan, K.; Datar, A.; Oitker, R.; Chen, H.; Zuo, J.; Zang, L. *J. Am. Chem. Soc.* **2005**, *127*, 10496-10497.

39) Balakrishnan, K.; Datar, A.; Naddo, T.; Huang, J.; Oitker, R.; Yen, M.; Zhao, J.; Zang, L. *J. Am. Chem. Soc.* **2006**, **128**, 7390-7398.

40) Würthner, F.; Kaiser, T. E.; Saha-Möller, C. R. *Angew. Chem. Int. Ed*. **2011**, *50*, 3376-3410.

41) Neuteboom, E. E.; van Hal, P. A.; Janssen, R. A. *Chem. Eur. J*. **2004**, 10, 3907-3918.

42) Bauer, P.; Wietasch, H.; Lindner, S. M.; Thelakkat, M. *Chem. Mater*. **2007**, 19, 88-94.
43) Lakowicz, J. R. *Principles of Fluorescence Spectroscopy*; Springer, **2010**.

Chapter 5

Donor-Acceptor Random Copolyesters containing Perylenebisimide (PBI) and Oligo(p-phenylenevinylene) (OPV) by Melt Condensation Polymerization: Energy Transfer Studies

Chapter 5

Donor-Acceptor Random Copolyesters containing Perylenebisimide (PBI) and Oligo(p-phenylene vinylene) (OPV) by Melt Condensation Polymerization: Energy Transfer Studies

Novel copolyesters consisting of oligo(*p*-phenylenevinylene) (OPV) as donor (D) and perylenebisimide (PBI) as acceptor (A) were synthesized by melt polycondensation. Photo-induced energy transfer and photo-induced charge separation in these polyesters were studied in solution as well as in the solid state. Selective excitation of OPV moiety resulted in the energy transfer efficiency of > 90% from OPV to PBI chromophore in the solution state. The direct excitation of PBI in the D-A copolyester resulted in reduced fluorescence emission of acceptor, indicating electron transfer between the D and A moieties. The photo-induced energy transfer process in solution state was supported by fluorescence lifetime decay studies. The HOMO and LUMO values of polyesters were calculated from cyclic voltammetry. A strong fluorescence quenching (~100%) of both chromophores in solid state indicated an efficient photo-induced charge transfer after photoexcitation of either donor or acceptor. The optical characteristics revealed a short distance and strong interaction between the donor and the acceptor chromophores. Reactive blend of donor/acceptor copolyester was also prepared by the transesterification reaction between donor and acceptor alone copolyesters. The energy transfer efficiency from donor to acceptor moiety upon selective excitation of donor chromophore in the donor/acceptor copolyester blend was four times higher compared to a physical mixture of donor and acceptor alone copolyesters, which gives the direct proof for the transesterification reaction in polyester/polyester reactive blending.

5.1. Introduction

Semiconducting polymers have been attracting considerable attention in organic electronics owing to their mechanical properties and solution processability.[1-4] Energy-transfer and electron-transfer processes between a donor and an acceptor play a fundamental role in most of the applications such as organic light-emitting diodes (OLEDs) and solar cells as well as in basic biological processes such as photosynthesis.[5-15] Therefore, a systematic design and study of D-A systems is required for understanding these key processes. In most of these cases, energy transfer is considerably influenced by the supramolecular ordering and spacial relationship of the donor and acceptor chromophores.[16-21] One of the way to control the distance between donor and acceptor is by covalently linking the D and A in a single polymer chain, either as random D-A copolymers or as block copolymers D-*b*-A.[12, 22] Although synthetically more challenging compared to simple random copolymerization processes, the block copolymer approach has received more attention due to the expectation that they would produce ordered morphologies with domain sizes on the order of tens of nanometers favourable for better device performance. But contrary to expectations, literature reports on D-A based block copolymers have shown that the desired structural orientation of the D and A units on the device substrate was rather unpredictable.[23] A D-A polymer design – random, block or graft which can give rise to crystalline domains of the D and/or A is the need of the hour. In this regard, the recent literature reports on the positive influence of presence of insulating polymer in donor-acceptor semiconductor blends on their solar cell device parameters is very encouraging.[24, 25] It has recently been shown by Wu et al that small amounts of insulating polymer like poly(methylmethacrylate) (PMMA) in P3HT:PCBM blends can improve the fill factor (FF) and open circuit voltage (V_{OC}) of solar cells by causing the P3HT chain conformations to become more homogeneous and suppress the formation of vacancies and leakage pathways. [26]

In the second chapter, we had reported a simple high-temperature solution-blending approach whereby suitably designed donor and acceptor small molecules based on perylenebisimides (PBI; A) and oligo(*p*-phenylenevinylene) (OPV; D) could be incorporated into the backbone of [poly(1,4-cyclohexylenedimethylene-1,4- cyclohexanedicarboxylate)] (**PCCD**). [27] This simple approach not only afforded polymers of a semicrystalline nature with blocks of **PCCD** separating the PBI units but also was able to produce free-standing films of

hitherto nonprocessable polymers. The current chapter deals with the synthesis of a series of random copolymers of **PCCD** incorporating varying amounts of suitably modified PBI as acceptor and oligo(*p*-phenylenevinylene) (OPV) as the donor by melt polycondensation, where all the copolymers retained the crystallinity of the PBI. The combination of oligo(*p*-phenylenevinylene) (OPV) as donor and perylenebisimides (PBI) as acceptor along a polymer backbone has been reported previously also.[28-30] None of these main chain copolymers were reported to retain the crystalline nature of the donor or acceptor units. Almost all the reported PBI polymers – whether side chain polymers or main chain polymers, were amorphous in nature.[31, 32] Perylenebisimides (PBI) although widely studied for its unique combination of high electron mobility, large molar absorption coefficients, excellent self-assembling ability as well as good thermal and photochemical stabilities, have the inherent problem of not retaining its crystalline nature upon incorporation into polymer backbone.[33-38]

Reactive blending is a very promising technology for preparing new polymeric materials from existing polymers. The presence of active functional groups such as ester, amide and urethane etc. groups in the polymers makes the post reactions possible.[39, 40] The reactive blend of donor/acceptor copolyester was also prepared by the transesterification reaction between donor and acceptor alone copolyesters. The structure and bulk properties of the D-A polyesters were studied using ^{1}H NMR, size exclusion chromatography (SEC), differential scanning calorimetry (DSC) and wide-angle X-ray diffraction (WXRD). The photophysical properties were studied using steady-state UV-vis absorption and fluorescence spectroscopy as well as fluorescence lifetime decay measurements. The successful occurrence of transesterification between the donor and acceptor alone polyesters in the reactive blend was confirmed by comparing the photophysical behaviour with a physical mixture of donor and acceptor alone copolyesters. These D-A polyesters combine the electronic and optical properties of semiconductors and the attractive mechanical properties and processing advantages of polyesters.

5.2. Experimental Methods

5.2.1. Materials: Perylene-3,4,9,10-tetracarboxylic dianhydride (PTCDA), 6-aminohexan-1-ol, zinc acetate, 1,4-cyclohexanedimethanol (CHDM) (cis + trans), 1,4-dimethylcyclohexane dicarboxylate (DMCD) (cis + trans), titanium(IV) butoxide [$Ti(OBu)_4$],

4-methoxyphenol, 2-ethylhexylbromide, triethylphosphite, 4-hydroxy benzaldehyde, potassium-tert-butoxide, and ortho-dichloro benzene (ODCB) were purchased from Aldrich and used without further purifications. HBr in glacial acetic acid, paraformaldehyde, potassium carbonate, potassium iodide, tetrahydrofuran (THF), 2-chloroethanol and all other solvents were purchased locally and purified with standard procedures.

5.2.2. Instrumentation: ^{1}H NMR spectra were recorded using a Bruker Avance 200 MHz spectrometer. Chemical shifts (δ) are reported in ppm at 25 ^{o}C with a small amount of tetramethylsilane (TMS) as internal standard. The molecular weight of synthesized polymers was determined using size exclusion chromatography (SEC). SEC measurements were carried on a Polymer Laboratories PL-GPC-220 at 25 ^{o}C using chloroform (Merck) as the mobile phase. The analysis was carried out at a flow rate of 1 mL/min using a set of three PLgel columns and a refractive index (RI) detector. Columns were calibrated with polystyrene standards and the molecular weights reported were with respect to polystyrene. The inherent viscosities were measured with an ubbelodhe viscometer at 30 °C in the mixture of phenol/1,1,2,2-tetrachloroethane (60/40) at a concentration of 0.5 g/dL. Absorption spectra were recorded using Perkin-Elmer Lambda 35 UV-spectrophotometer. Steady-state fluorescence studies and fluorescence lifetime measurements were performed using Horiba Jobin Yvon Fluorolog 3 spectrophotometer having a 450 W xenon lamp for steady-state fluorescence and nanoLED of 390 nm and 460 nm for fluorescence lifetime measurements. For lifetime measurements, decay curves were obtained by the time-correlated single photon counting (TCSPC) technique. The fluorescence quantum yields of PBI polymer were determined in $CHCl_3$ using rhodamine 6G in ethanol (ϕ= 0.95) as the standard by exciting at 490 nm and OPV polymer were determined in $CHCl_3$ using quinine sulphate in 0.1 M H_2SO_4 (ϕ=0.54) as the standard by exciting at 360 nm. Solid state photoluminescence spectra were recorded using the front face scan mode with the same Fluorolog spectrofluorimeter. The thermal stability of the polymers was analyzed using a Perkin-Elmer thermogravimetric analyzer under nitrogen atmosphere at heating rate of 10 ^{o}C/min. Differntial scanning colorimetry (DSC) was performed using TA Q10 differential scanning calorimeter at heating rate of 10 ^{o}C/min. Wide-angle X-ray diffraction (WXRD) were recorded by Phillips x'pertpro powder X-ray diffractometer using Cu Kα radiation, and the spectra were recorded in the range of 2θ = 5-30°. Electrochemical properties of polymers were studied using a BAS-Epsilon potentiostat.

5.2.3. Synthesis

Synthesis of copolyester of PCCD incorporating OPV chromophore by melt polycondensation (MCOPV-13): DMCD (2.00 g, 10 mmol), CHDM (1.15 g, 8 mmol) and OPV-2-Diol (1.12 g, 2 mmol) were weighed into a tubular glass reactor. The reaction mixture was melted in a salt bath at 160 ^{o}C, cooled and $Ti(OBu)_4$ (3.4 mg, 0.1 mol % of diester) solution in ODCB was added to the mixture. The reaction was heated from 160 to 180 ^{o}C over 2 h with stirring 100 rpm and then from 180 to 230 ^{o}C over 2 h, allowing methanol to distil. Vacuum was applied and the pressure was gradually reduced to 0.4 mm Hg over 20 min, while the temperature was raised from 230 to 250 ^{o}C. The reaction was continued at 250 ^{o}C for 2 h. The product was cooled, DCM was added, and the polymer solution was poured into methanol. The resultant material was filtered and dried in oven at 60 ^{o}C. Yield: 74.94%; ^{1}H NMR (200 MHz, $CDCl_3$) δ ppm: 6.86–7.45 (Ar–**H** and vinylic **H**), 4.43 (–CH_2–C**H**$_2$–O–CO–R), 4.17 (–C**H**$_2$–CH_2–O–CO–R), 3.96 (cis –C**H**$_2$ in **PCCD**), 3.90 (trans –C**H**$_2$ in **PCCD**), 3.66 (–CO–O–C**H**$_3$ end group), 0.97–2.45 (aliphatic **H** in OPV unit and cyclic–**H** in **PCCD**).

Synthesis of copolyesters of PCCD incorporating both OPV and PBI chromophores (MCOPV-13-Per-x): DMCD (2.00 g, 10 mmol), CHDM (1.00 g, 7 mmol), OPV-2-Diol (1.12 g, 2 mmol) and PBI-6-Diol (0.59 g, 1 mmol) [for **MCOPV-13-Per-7**] were weighed into a tubular glass reactor. The reaction mixture was melted in a salt bath at 160 ^{o}C, cooled and $Ti(OBu)_4$ (3.4 mg, 0.1 mol % of diester) solution in ODCB was added to the mixture. The reaction was heated from 160 to 180 ^{o}C over 2 h with stirring 100 rpm and then from 180 to 230 ^{o}C over 2 h, allowing methanol to distil. Vacuum was applied and the pressure was gradually reduced to 0.4 mm Hg over 20 min, while the temperature was raised from 230 to 250 ^{o}C. The reaction was continued at 250 ^{o}C for 2 h. The product was cooled, DCM was added, and the polymer solution was poured into methanol. The resultant material was filtered and dried in oven at 60 ^{o}C. Yield: 76.01%; ^{1}H NMR (200 MHz, $CDCl_3$) δ ppm: 8.58 (perylene **H**), 6.86–7.44 (Ar–**H** and vinylic **H** in OPV part), 4.42 (–CH_2–C**H**$_2$–O–CO– in OPV part), 3.86–4.17 (–C**H**$_2$–CH_2–O–OC– in OPV part, –CH_2–C**H**$_2$–O–OC– in PBI part, cis and trans –C**H**$_2$ – in **PCCD** and imide –C**H**$_2$**–**), 3.66 (–CO–O–C**H**$_3$ end group), 0.97–2.45 (cyclic–**H** in **PCCD**, aliphatic **H** in OPV unit and –C**H**$_2$**–** in PBI part).

Synthesis of MCOPV-13/MCPer-7 blend by high-temperature solution-blending approach: MCOPV-13 (1.58 g, 5 mmol) and **MCPer-7** (1.52 g, 5 mmol) were weighed into a cylindrical polymerization tube and added 5 mL of ODCB. The tube was immersed in a preheated oil bath at 180 ^{o}C, and the mixture was stirred for 30 min with stirring rate of 100 rpm. To this, $Ti(OBu)_4$ (34 mg, 1 mol %) solution in ODCB was added and the reactive blending was continued with stirring at 180 °C for 3 h. The product was cooled, DCM was added, and the polymer solution was poured into methanol. The resultant material was filtered and the polymer was dried in oven at 60 ^{o}C. Yield: 86.13%; ^{1}H NMR (200 MHz, $CDCl_3$) δ ppm: 8.58 (perylene **H**), 6.86–7.44 (Ar–**H** and vinylic **H** in OPV part), 4.42 (–CH_2–C**H**$_2$–O–CO– in OPV part), 3.86–4.17 (–C**H**$_2$–CH_2–O–OC– in OPV part, –CH_2–C**H**$_2$–O–OC– in PBI part, cis and trans –C**H**$_2$ – in **PCCD** and imide –C**H**$_2$**–**), 3.66 (–CO–O–C**H**$_3$ end group), 0.97–2.45 (cyclic–**H** in **PCCD**, aliphatic **H** in OPV unit and –C**H**$_2$**–** in PBI part).

5.3. Results and Discussions

5.3.1. Synthesis and Characterization of Monomers and Polymers

The hydroxyl functionalized perylenebisimide derivative (PBI-6-Diol) was synthesized through the 6-aminohexan-1-ol coupling of PTCDA as discussed previously in chapter 4. Similarly, the hydroxyl functionalized OPV derivative (OPV-2-Diol) was synthesized as discussed previously in chapter 2.[41] The melt condensation polymerization of the PBI-6-Diol and/or OPV-2-Diol with 1,4-cyclohexanedimethanol (CHDM) and 1,4-dimethylcyclohexane dicarboxylate (DMCD) was carried out as shown in scheme 5.1. 0.1 mol % of $Ti(OBu)_4$ dissolved in ODCB was added as the catalyst. The melt condensation was carried out in a cylindrical glass reactor in a two step process. The first step was at atmospheric pressure with a temperature ramp and continuous nitrogen flow to remove the methanol that was eliminated, while the second step was under dynamic vacuum (0.4 mm Hg) at 250 ^{o}C. The polymers were dissolved in DCM and precipitated into methanol. The copolyesters obtained by the melt condensation were named as **MCOPV-x**, **MCPer-x** or **MCOPV-x-Per-x**, where x represented the mole % incorporation.

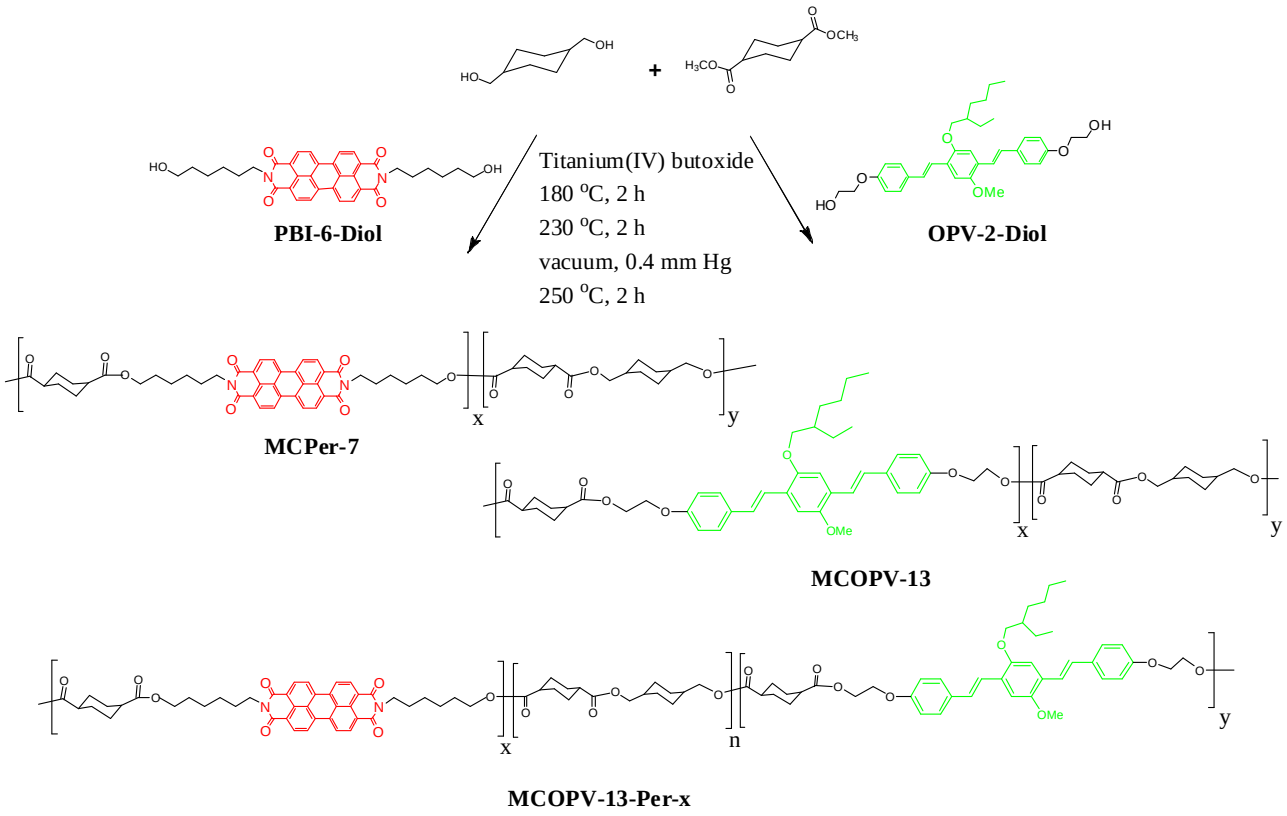

Scheme 5.1. *Synthetic route for the melt polycondensation of* ***PBI-6-Diol/OPV-2-Diol*** *with DMCD and CHDM.*

Table 5.1 gives the sample name, amount of hydroxyl functionalized PBI or OPV taken in the feed, the actual incorporation determined using ^{1}H NMR, molecular weight determined by SEC in $CHCl_3$ using polystyrene standards, the inherent viscosity measured in the mixture of phenol/1,1,2,2-tetrachloroethane (60/40 v/v), the 10 % weight loss temperature obtained from TGA, the glass transition temperature (T_g) obtained from differential scanning calorimetry (DSC) as well as the yield of the various copolyesters. The structure of all the copolyesters is shown in scheme 5.1. The transesterification reaction between **MCOPV-13** (donor polymer) and **MCPer-7** (acceptor polymer) was carried out by dissolving **MCOPV-13** and **MCPer-7** in minimum amount of a high boiling solvent like ODCB and heating in presence of 1 mol % of transesterification catalyst $Ti(OBu)_4$. The copolyester obtained by the reactive blending was named as **MCOPV-13/MCPer-7 blend**.

Table 5.1. *Polymer designation, feed ratio, actual incorporation determined from ^{1}H NMR, molecular weight (Mw), polydispersity index, viscosity data (η_{inh}), yield, glass transition (T_g) and 10% weigh loss temperature (T_D) of polymers.*

Polymer	Feed Ratio (PCCD: PBI/ OPV)	Composition (PCCD: OPV/PBI) (from ^{1}H NMR) (mol %)	Mw (g/ mol)[a]	Poly dispersity index ($Đ_M$)	η_{inh} (dL/ g)[b]	Yield (%)	T_g (^oC)	T_D (^oC)
MCPer-7	90:10	93:7	23700	1.9	0.31	76	46	420
MCOPV-13	80:20	87:13	45900	2.7	0.41	75	50	393
MCOPV-13-Per-4	75:20:5	83:13:4	35500	2.5	0.37	77	55	424
MCOPV-13-Per-7	70:20:10	80:13:7	17000	2.3	0.29	76	56	428
MCOPV-13-Per-11	60:20:20	76: 13:11	16800	2.4	0.27	77	64	424
MCOPV-13-Per-18	50:20:30	69:13:18	13500	2.3	0.21	75	76	403
PBI-6-Diol	-	-	-	-	-	86	-	439
OPV-2-Diol	-	-	-	-	-	61	-	368

a. Measured by size exclusion chromatography (SEC) in chloroform ($CHCl_3$), calibrated with linear, narrow molecular weight distribution polystyrene as standards.
b. Determined in a mixture of phenol/1,1,2,2-tetrachloroethane (60/40) as solvent.

The structures of the polymers were confirmed by ^{1}H NMR and molecular weights were determined using size exclusion chromatography (SEC). Figure 5.1 compares the ^{1}H NMR spectra of **MCOPV-13**, **MCPer-7** and **MCOPV-13-Per-7**. The incorporation of the OPV or PBI in the different copolyesters were calculated from the ^{1}H NMR spectra by comparing the integration of peaks corresponding to the OPV aromatic protons (labelled 'c') or PBI aromatic protons (labelled 'd') with that of the cis and trans-isomeric protons in –C**H**CO– attached to DMCD (labelled 'a'). The incorporation of OPV and PBI was determined to be 13 and 7 mol % for a feed intake of 20 and 10 mol % in OPV containing polyester (**MCOPV-13**) and PBI containing polyester (**MCPer-7**) respectively.

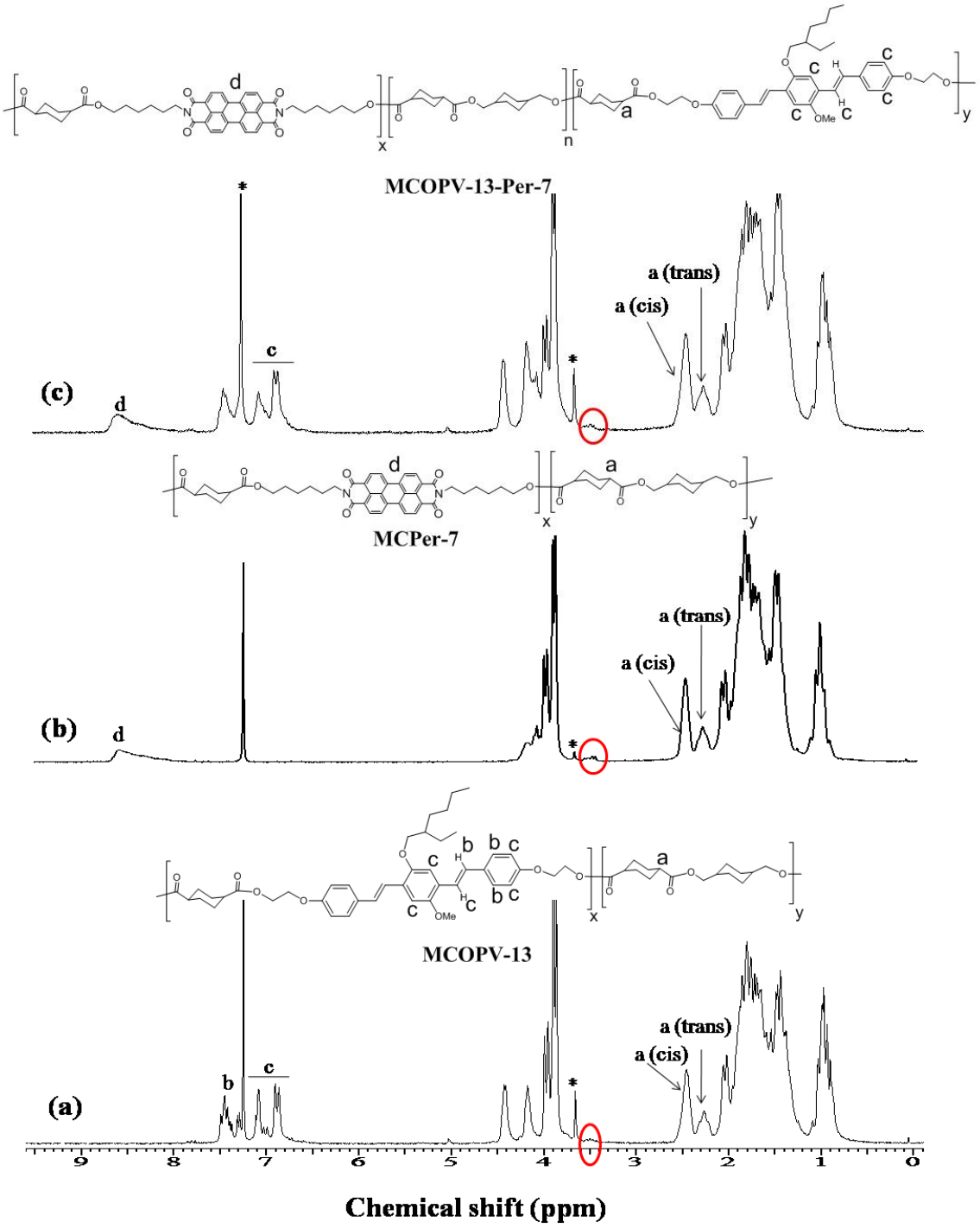

Figure 5.1. *Stack plot of ^{1}H NMR spectra of* ***MCOPV-13***, ***MCPer-7*** *and* ***MCOPV-13-Per-7*** *in $CDCl_3$.*

In the copolyester containing both PBI and OPV, the mol % feed of OPV-2-Diol was kept constant at 20 mol % and the mol % feed of PBI-6-Diol was varied from 5 to 30 mol %. The aromatic units (labelled 'c' and 'd') and protons in –C**H**CO– attached to DMCD (labelled 'a') were used to calculate the extent of incorporation of the donor and acceptor with respect to PCCD. The mol % incorporation of OPV unit was determined to be the same

for all polyesters ~ 13 mol % incorporation for an intake feed of 20 mol % and the mol % incorporation of PBI unit was determined as 4, 7, 11 and 18 mol % corresponding to the intake feed of 5, 10, 20 and 30 mol % respectively. The ^{1}H NMR spectra of all polymers showed the presence of two sets of doublets around 3.48 and 3.55 ppm (encircled in figure 5.1). This corresponded to the methylene proton of the C**H**$_2$OH end group.[42] The polyesters also showed a singlet at 3.66 ppm (figure 5.1, asterisk), which corresponded to the methyl ester (–CO–O–C**H**$_3$) end group from the DMCD component.[42]

5.3.2. Molecular Weights of Polymers

The polymers were soluble in common organic solvents such as dichloromethane and chloroform at room temperature. The molecular weights of the polymers were determined by size exclusion chromatography (SEC) in $CHCl_3$ using polystyrene standards. Figure 5.2 (a) shows the SEC plots of the polyesters. The Mw of **MCOPV-13** was 45900 and that of **MCPer-7** was 23700. Molecular weights of polyesters decreased with increasing PBI content. Table 5.1 also gives the solution viscosity measured in a solvent mixture of phenol/1,1,2,2,-tetrachloroethane of composition (60/40) for all the polymers.

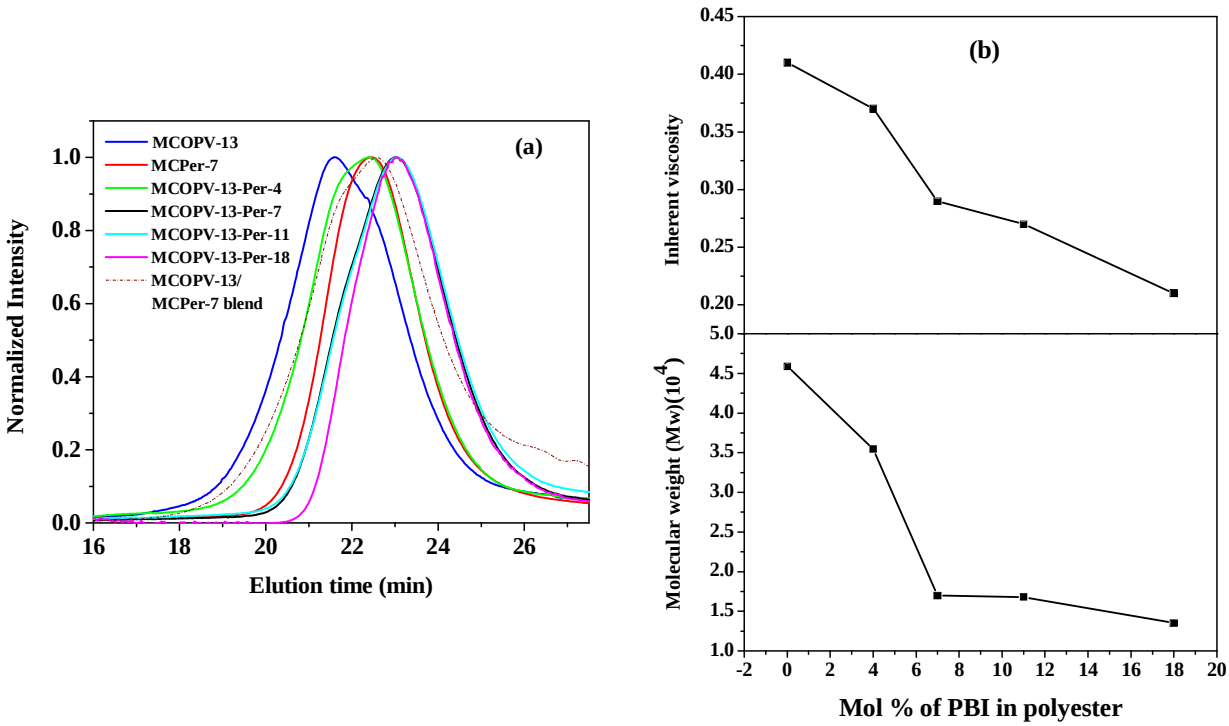

Figure 5.2. *(a) Size exclusion chromatography (SEC) of copolyesters in chloroform using polystyrene as standard; (b) plot comparing the molecular weight (Mw) and inherent viscosity (η_{inh}) of copolyesters as a function of increased PBI.*

Figure 5.2 (b) compares the molecular weight (Mw) and inherent viscosity (η_{inh}) of copolyesters as a function of increasing incorporation of PBI. Both the plots were consistent with each other and showed decrease in molecular weight and viscosity with more PBI incorporation which could be attributed to the increase in the rigidity of the polymer backbone. This trend is well understood in literature also i.e higher incorporation of rigid units resulting in reduction in the molecular weight.[43] As shown in figure 5.2 (a), the molecular weight distribution of **MCOPV-13/MCPer-7 blend** was different from that of **MCOPV-13** and **MCPer-7** copolyesters. Polydispersity index (ĐM = Mw/Mn) of **MCOPV-13** and **MCPer-7** were 2.7 and 1.9 respectively whereas the reactive blending of these two polyesters resulted in a drastic change in polydispersity index to 3.7. This illustrated the very wide molecular weight ranges present in the **MCOPV-13/MCPer-7 blend** which was a consequence of the transesterification reaction between these polyesters.

5.3.3. Thermal Properties of Polyesters

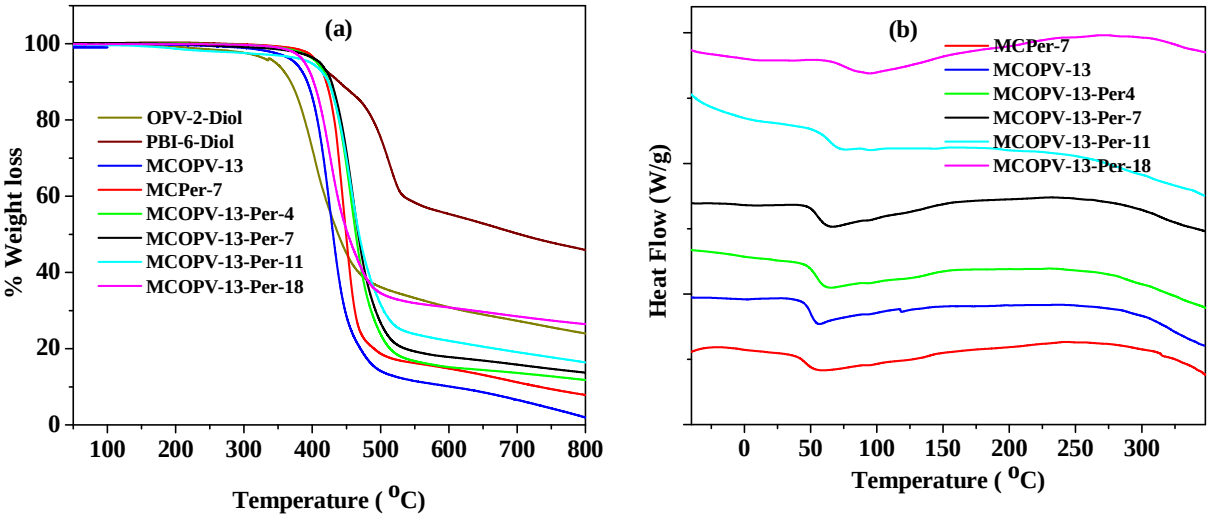

Figure 5.3. *(a) TGA thermograms of PBI-6-Diol, OPV-2-Diol and copolyesters under nitrogen atmosphere at heating rate of 10 °C/min; (b) DSC thermograms of copolyesters showing second heating cycle at heating rate of 10 °C/min.*

The thermal properties of the polymers and the two diols – PBI-6-Diol and OPV-2-Diol are summarized in table 5.1. Figure 5.3 (a) shows the TGA analysis for the series of polymers. All polyesters were thermally stable up to 390 °C. The 10% weight loss temperature for OPV-2-Diol was around 368 °C, while that for the more rigid PBI-6-Diol was higher at around 440 °C. As shown in the table 5.1, the 10% weight loss temperature for all

the **MCOPV-13-Per-x** polyesters were higher than those of OPV containing polyester (**MCOPV-13**) as expected from the highly rigid structure of PBI. Figure 5.3 (b) compares the second heating DSC thermogram of all the polyesters. The T_gs of polyesters increased with increasing mol % incorporation of PBI. The T_g of **MCOPV-13** was 50 ^oC where as 18 mol % incorporation of PBI resulted in copolyester with T_g of 76 ^oC indicating the increased stiffness upon incorporation of rigid PBI units into the polyester backbone.[43]

5.3.4. Wide-angle X-ray Diffraction (WXRD)

The polyesters were analyzed for their bulk packing using wide-angle X-ray diffraction (WXRD) in the range of 2θ = 5-30° at room temperature (25 ^oC). The diols, PBI-6-Diol and OPV-2-Diol were highly crystalline as indicated by the large number of sharp reflections in the entire range of 2θ (figure 5.4).

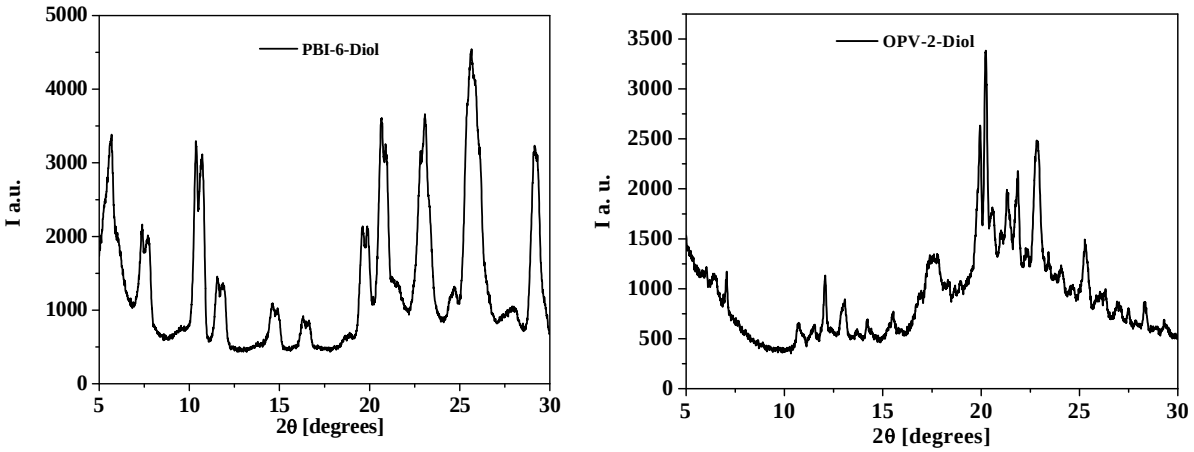

Figure 5.4. *WXRD traces of PBI-6-Diol and OPV-2-Diol at room temperature.*

Figure 5.5 compares the WXRD patterns of **MCOPV-13-Per-x** polyesters along with that of **MCPer-7** and **MCOPV-13** polyester. The OPV alone polyester **MCOPV-13** showed a broad peak indicating the absence of crystallinity. The PBI alone polyester **MCPer-7**, on the other hand had sharp reflections at 2θ = 9.49°, 12.41° and 24.94° corresponding to the d spacing of 9.31 Å, 7.12 Å and 3.57 Å respectively. The sharp peak in the wide angle region (circled in figure 5.5) corresponding to 3.57 Å is attributable to the average π-π stacking distance of the PBI aromatic core.[44] The copolyesters containing both OPV and PBI, **MCOPV-13-Per-x** all had sharp crystalline peaks at 2θ = 9.49° (9.31 A^o), 12.41° (7.12 A^o) and 24.94° (3.57A^o). The intensity of all the sharp peaks with respect to the broad amorphous peak around 2θ = 15-20° increased with

increasing mol % incorporation of PBI, suggesting increased crystalline packing. The peak around 2θ = 24.94 (3.57 A^{o}) was visible even for the lowest incorporation of PBI i.e 4 mol %, but the intensity was quite high beyond 11 mol % incorporation of PBI units. Such an evidence for crystallinity and π-π stacking of the PBI units in a main chain polymer scaffold is very rare in literature. The insulating PCCD matrix could be expected to play a role in helping the PBI units to align properly resulting in improved π stacking.[24-26]

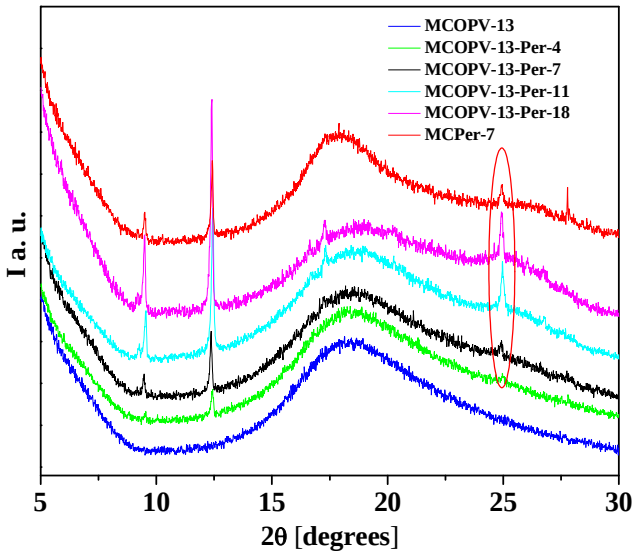

Figure 5.5. *WXRD patterns of thin films of the polymers at room temperature.*

5.3.5. Electrochemical Properties

The electrochemical behaviour of the **MCOPV-13**, **MCPer-7** and **MCOPV-13-Per-7** were investigated by cyclic voltammetry (CV), which was performed in dichloromethane containing 0.1 M $TBAPF_6$ (tetra-n-butylammonium hexafluorophosphate) as electrolyte. Table 5.2 gives their redox behaviour and figure 5.6 shows the stack plot of their cyclic voltammetry curves. Normally perylenebisimides show two reduction peaks corresponding to the formation of the mono and dianion respectively.[45] But the perylene copolymer **MCPer-7** had one broad reduction peak at -1.23 V in the cathodic scan indicating that the two reduction peaks had merged together to give one broad peak. But in the anodic scan it resolved as two peaks at -0.91 and -1.13 V. The OPV copolymer **MCOPV-13** had two irreversible oxidation at 0.53 V, 0.81 V corresponding to mono and dication of OPV unit.[28] The redox behaviour of **MCOPV-13-Per-7** in dichloromethane indicated both oxidative and reductive processes. Two reversible reduction peaks were observed at -1.00 and -1.19 V corresponding to the

reduction of the perylene moiety and two irreversible oxidation peak were observed at 0.53, 0.81 V corresponding to the OPV moiety.

Table 5.2. *Cyclic Voltammogram data of* ***MCPer-7****,* ***MCOPV-13*** *and* ***MCOPV-13-Per-7*** *performed in dichloromethane containing 0.1 M* $TBAPF_6$ *(tetra-n-butylammonium hexafluorophosphate) as electrolyte at 100 mV* s^{-1}*. Measurement was calibrated with ferrocene/ferrocenium redox system Vs* Ag/Ag^+*.*

Polymer	E_{ox}^{onset}(V) OPV	E_{red}^{onset} (V) PBI	LUMO (eV)	HOMO (eV)	E_g^{opt} (eV) ($E_g^{electro}$)
MCPer-7	-	-0.83	-3.90	-5.64	1.74
MCOPV-13	0.42	-	-2.83	-5.15	2.32
MCOPV-13-Per-7	0.44	-0.82	-3.91	-5.17	1.65 (1.26)

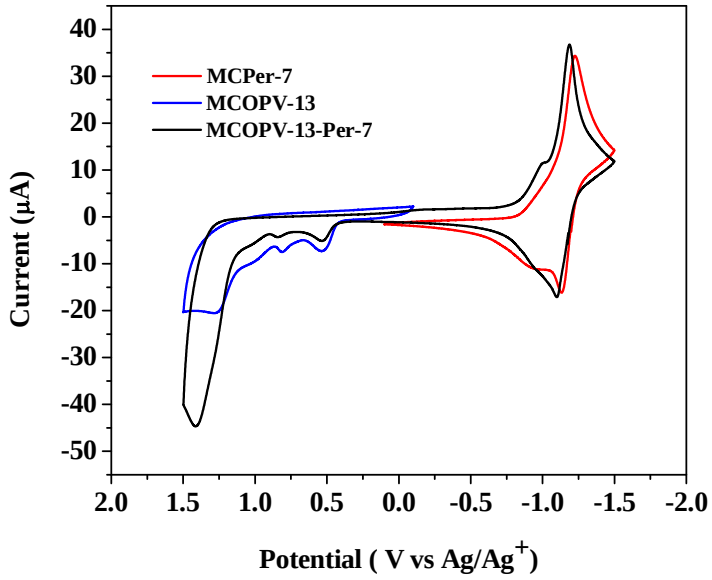

Figure 5.6. *Cyclic Voltammogram of* ***MCPer-7****,* ***MCOPV-13*** *and* ***MCOPV-13-Per-7*** *performed in dichloromethane containing 0.1 M* $TBAPF_6$ *(tetra-n-butylammonium hexafluorophosphate) as electrolyte at 100 mV* s^{-1}*. Measurement was calibrated with ferrocene/ferrocenium redox system Vs* Ag/Ag^+*.*

The HOMO energy value for the OPV was estimated from the onset potentials of oxidation, while the LUMO energy values for the PBI was estimated from the onset of reduction event. After calibration of the measurements against Fc/Fc^+, the oxidation potential of which is assumed at 4.8 eV below the vacuum level, the HOMO and LUMO energy levels were calculated according to the following equations.[46]

$$E_{HOMO}(eV) = -\left[E_{ox}^{onset} - E_{1/2}(F_c/F_c^+) + 4.8\right]$$

$$E_{LUMO}(eV) = -\left[E_{red}^{onset} - E_{1/2}(F_c/F_c^+) + 4.8\right]$$

where $E_{1/2}(F_c/F_c^+)$ is the half-wave potential of the ferrocene/ ferrocenium couple measured relatively to Ag/Ag+. The HOMO energy levels of PBI moiety and LUMO energy levels of OPV moiety were estimated from the optical band gap and cyclic voltammetry data. The electrochemical band gap $E_g^{electro} = E_{LUMO} - E_{HOMO}$ for **MCOPV-13-Per-7** was estimated as 1.26 eV. The optical energy gap E_g^{opt} was determined from the onset of absorption in thin film (given in table 5.2) using the equation $E_g^{opt} = 1240/\lambda_{onset}$. The energy values suggested the possibility of photoinduced energy- and/or electron- transfer from OPV moiety to PBI moiety.

5.3.6. Photophysical Properties

The optical properties of the polymers were investigated by UV-Vis and fluorescence spectroscopy in both solution and solid state, which are summarised in table 5.3. Figure 5.7 (a) shows the normalized absorption and emission of **MCPer-7** in chloroform solution as well as film state. The copolyester, **MCPer-7** showed the typical absorption of perylenebisimide with peaks in the range of 400-530 nm, corresponding to the 0–0, 0–1, 0–2, and 0–3 electronic transitions respectively in chloroform.[47] The absorption spectrum in the solid state was broad with $\lambda_{max} \approx 495$ nm, and the ratios of peak intensities were different compared to that in solution which is characteristic of π-π stacking of PBI aromatic core with rotational offset.[47, 48] This was in accordance with the observation of PBI aromatic core stacking in thin films studied using WXRD. Emission from **MCPer-7** was studied by exciting at the absorption wavelength of 490 nm. In solution, typical emission of PBI with peak maxima at 533, 575, 625 nm was observed whereas in the solid state, PBI monomer emission at 533 nm was hugely suppressed and a red shifted intense broad aggregate emission was observed at 641 nm.[47] Figure 5.7 (b) shows the normalized absorption and emission of **MCOPV-13** in solution as well as film state. **MCOPV-13** exhibited absorption maximum at 392 nm and emission maximum at 445 nm with a shoulder peak at 470 nm in chloroform.[49] In the solid state, the absorption spectrum was slightly red shifted with absorption maximum at 396 nm. The lower extent of organization of the OPV moieties compared to the PBI units was evident from the very short (4 nm) shift of the absorption

spectra in the solid state compared to that in solution. The OPV monomer emission at 445 nm was suppressed and a red shifted intense aggregate emission was observed at 493 nm in the solid state.[50] Both polymers, **MCOPV-13** and **MCPer-7** were highly fluorescent with quantum yields of 0.58 and 0.87 in chloroform respectively.

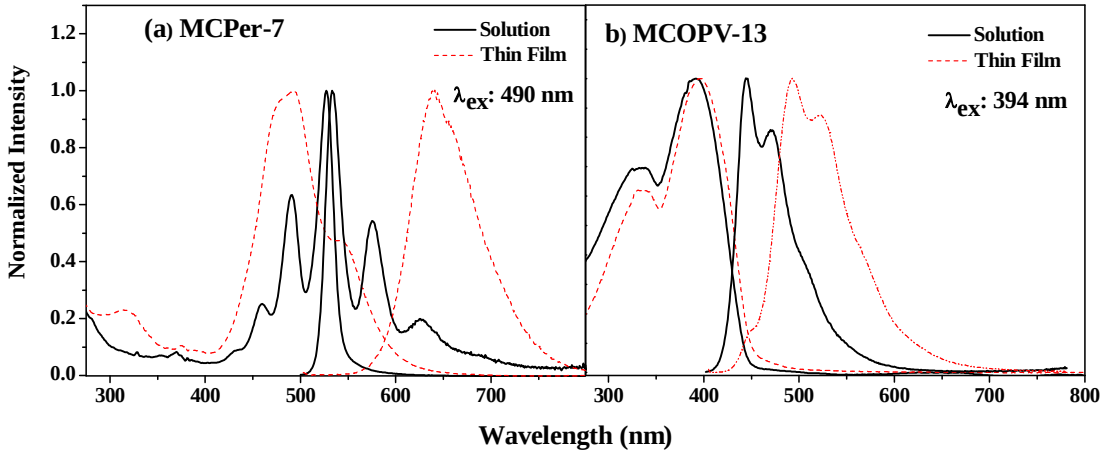

Figure 5.7. *Normalized absorption and emission spectra of (a)* ***MCPer-7*** *and (b)* ***MCOPV-13*** *in the solution (chloroform) and in film spin-coated from chloroform [0.1 OD at 490 nm, λ_{ex} = 490 nm for* ***MCPer-7*** *and 0.1 OD at 394 nm, λ_{ex} = 394 nm for* ***MCOPV-13****].*

Table 5.3. *Absorption and emission of polymers in solution and solid state along with fluorescence quantum yields Φ_{FL} in solution.*

Polymer	Absorption λ_{max} (nm) (In $CHCl_3$)	Emission λ_{max} (nm) (In $CHCl_3$)	Absorption λ_{max} (nm) (In film)	Emission λ_{max} (nm) (In film)	ϕ_{FL} (solution)
MCPer-7	527	533[a]	493	641[a]	0.87[c]
MCOPV-13	392	445[b]	396	493[b]	0.58[d]
MCOPV-13-Per-4	527, 394	445, 533[b]	396, 497	-	-
MCOPV-13-Per-7	527, 394	445, 533[b]	398, 497	-	-
MCOPV-13-Per-11	527, 394	445, 533[b]	399, 497	-	-
MCOPV-13-Per-18	527, 394	445, 533[b]	402, 497	-	-

a. Excitation at 490 nm
b. Excitation at 394 nm
c. The fluorescence quantum yield for **MCPer-7** in $CHCl_3$ was obtained upon excitation at 490 nm and was measured using rhodamine-6G in ethanol as standard.

d. The fluorescence quantum yield for **MCOPV-13** in $CHCl_3$ was obtained upon excitation at 360 nm and was measured using quinine sulphate in 0.1 M H_2SO_4 solution as standard.

Figure 5.8. compares the normalized (at the OPV absorption wavelength maxima of 394 nm) absorption spectra of **MCOPV-13** and **MCPer-7** along with donor-acceptor random copolyesters (**MCOPV-13-Per-x**) in chloroform. The absorption spectra of the random copolyesters, **MCOPV-13-Per-x** was a linear addition of the characteristic absorption bands of both OPV and PBI moiety indicating no charge transfer occurring in the ground state .[30]

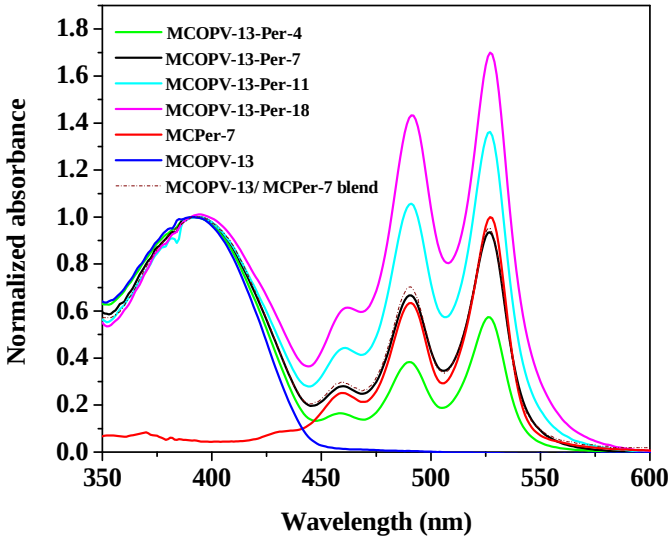

Figure 5.8. *Normalized absorption spectra of polymers in chloroform.*

The primary condition for energy transfer from donor to acceptor is the spectral overlap of the donor emission and acceptor absorption.[51] Figure 5.9 shows the overlap in the emission spectra of **MCOPV-13** with the absorption band of **MCPer-7** indicating possible transfer of excitation energy from donor (OPV moiety) to acceptor (PBI moiety). The absorption of OPV and PBI unit did not have any considerable overlap, which made them suitable for selective excitation and energy-transfer studies. The overlap integral [J(λ)] which expresses the degree of spectral overlap between the donor emission and the acceptor absorption is determined as follows.[51]

$$J(\lambda) = \int_0^\infty F_D(\lambda)\varepsilon_A(\lambda)\lambda^4 d\lambda$$

Here, $F_D(\lambda)$ is the corrected fluorescence intensity of the donor in the wavelength range λ to $\lambda + \Delta\lambda$ with the total intensity (area under the curve) normalized to unity. $\varepsilon_A(\lambda)$ is the extinction coefficient of the acceptor at λ. The overlap integral calculated for **MCOPV-13** (donor) and **MCPer-7** (acceptor) was 13.3 x 10^{14} $M^{-1}cm^{-1}(nm)^4$. The distance at which energy transfer is 50 % efficient is called the Förster distance (R_0), which is given by,

$$R_0 = 0.211[k^2 n^{-4} Q_D J(\lambda)]^{1/6}$$

The Förster distances (R_0) are usually reported for an assumed value of k^2; typically $k^2 = 2/3$. The quantum yield of the donor (Q_D) is determined by comparison with standard fluorophores. The Förster distance calculated for **MCOPV-13** (donor) and **MCPer-7** (acceptor) was 45.73 Å.

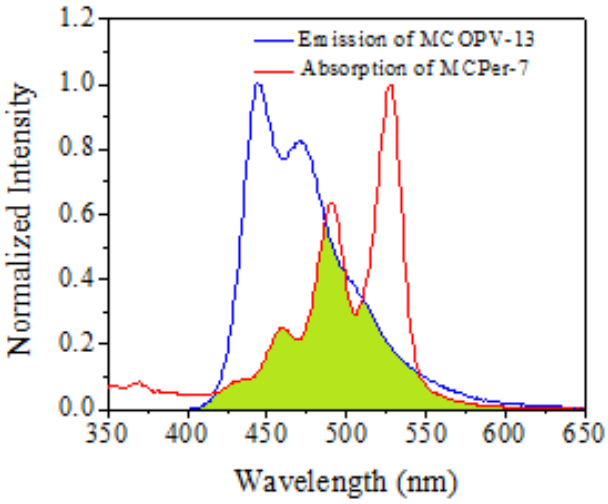

Figure 5.9. *Normalized absorption spectrum of* ***MCPer-7*** *and emission spectrum of* ***MCOPV-13*** *in the solution (chloroform).*

To investigate the photophysics and especially address the possibility of photo-induced energy transfer between the donor (OPV) and acceptor (PBI) moieties of the copolyester, their fluorescence was measured in chloroform solution. The energy transfer from OPV unit to PBI unit was monitored in the solution state by recording the emission of OPV in the absence and presence of acceptor after excitation of OPV at 394 nm. Figure 5.10 (a) compares the emission of the donor alone polymer **MCOPV-13,** acceptor alone polymer **MCPer-7**, along with that of the D-A polymers **MCOPV-13-Per-x** upon excitation at 394 nm. All polymers were prepared with 0.1 OD at 394 nm except for **MCPer-7** which was made to have 0.1 OD at 490 nm. When excited at 394 nm, **MCOPV-13** emitted strongly with emission maximum at 445 nm. **MCPer-7** did not exhibit noticeable emission upon excitation at the donor wavelength maximum of 394 nm. Excitation of donor-acceptor polyesters having

different amount of acceptor (4–18 mol %) resulted in gradual quenching of the OPV emission at 445 nm with simultaneous emission at 533, 575 and 625 nm corresponding to the emission of the acceptor, indicating the efficient energy transfer from donor to acceptor.[52] The intensity of emission peak corresponding to the acceptor increased with increasing mol % incorporation of acceptor, which could be clearly observed from figure 5.10 (b) which was obtained by normalizing the emission spectra at the OPV emission maximum of 445 nm. Excitation of the polymers at the acceptor absorption maximum of 490 nm resulted in a quenched emission from PBI compared to that of the acceptor alone polymer. Since photoexcitation of PBI cannot result in energy transfer to the energetically high OPV, the reason for the PBI quenched emission could be attributed to occurrence of charge separation.[28]

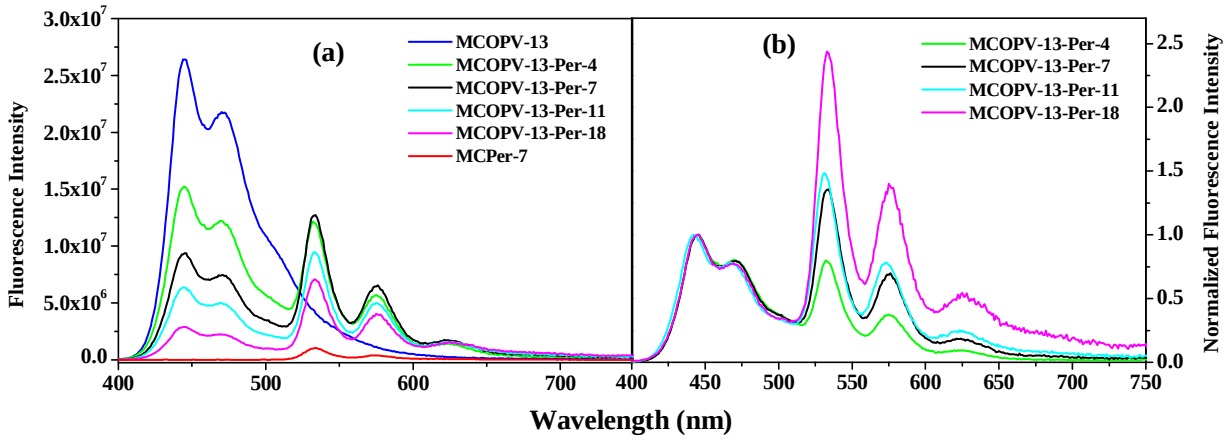

Figure 5.10. *(a) Emission spectra of polymers in the solution (chloroform) [0.1 OD at 490 nm for* ***MCPer-7*** *and 0.1 OD at 394 nm for all other polymers,* λ_{ex} *= 394 nm] and (b) normalized (at* λ_{ex} *= 445 nm) emission spectra.*

The energy transfer efficiency from donor to the acceptor can be measured using the relative fluorescence intensity of the donor, in the absence (F_D) and presence (F_{DA}) of acceptor:

$$E = 1 - \frac{F_{DA}}{F_D}$$

The energy transfer efficiencies from OPV moiety to PBI moiety for **MCOPV-13-Per-4**, **MCOPV-13-Per-7**, **MCOPV-13-Per-11** and **MCOPV-13-Per-18** were calculated as 51.47, 70.00, 79.67 and 90.75 % respectively, which is showed in table 5.4.

Table 5.4. *Spectral overlap integral J(λ), Förster radii (R_0) and energy transfer efficiency together with the calculated donor-acceptor distance (r) of the polymers.*

Polymer			J (λ)10^{14} [M^{-1} $cm^{-1}(nm)^4$]	Förster radii Ro (A^0)	Energy transfer efficiency (%)	Donor-acceptor distance (r) A^0
Donor	Acceptor	Donor/ acceptor polymer				
MCOPV-13	**MCPer-7**		13.3	45.73	17.15	59.46
		MCOPV-13-Per-4			51.47	42.28
		MCOPV-13-Per-7			70.00	39.70
		MCOPV-13-Per-11			79.67	36.42
		MCOPV-13-Per-18			90.75	31.25
		MCOPV-13/MCPer-7 blend			77	37.39

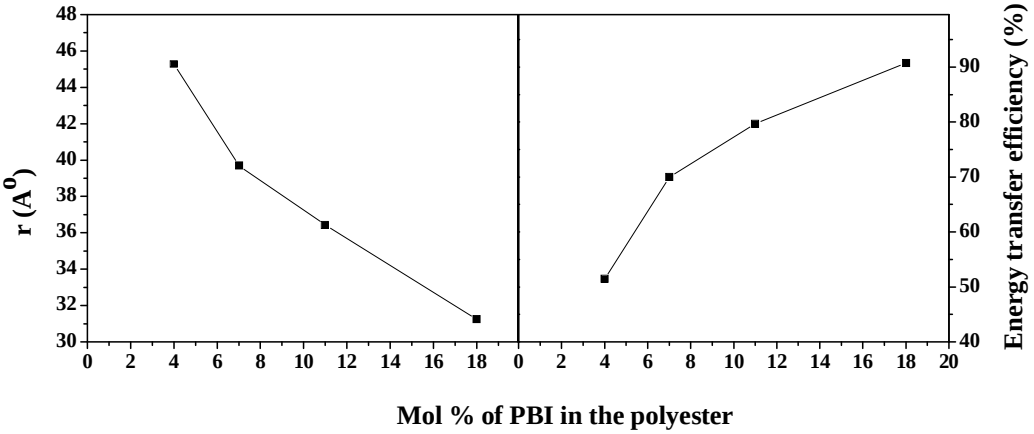

Figure 5.11*. Plot comparing the energy transfer efficiency and D-A distance (r) of the polymers as a function of increased mol % incorporation of PBI.*

The distance between donor and acceptor (r) in each polymer was calculated using the equation,

$$r = R_0 \left[\frac{1-E}{E}\right]^{1/6}$$

The D-A distance for **MCOPV-13-Per-4**, **MCOPV-13-Per-7**, **MCOPV-13-Per-11** and **MCOPV-13-Per-18** were 45.28, 39.70, 36.42 and 31.25 Å respectively. Figure 5.11 compares the energy transfer efficiency and D-A distance for **MCOPV-13-Per-x** polymers as a function of increasing mol % incorporation of PBI. The energy transfer efficiency increased with increasing mol % of PBI since it depended strongly on D-A distance, which decreased with increasing mol % of PBI.

The influence of covalent linking of D and A on the energy transfer process from D to A was investigated by comparing the emission spectra of the donor-acceptor polymer - **MCOPV-13-Per-7** and a 1:1 physical mixture of **MCOPV-13** (donor polymer) with **MCPer-7**(acceptor polymer). Therefore, emission spectra of donor copolyester **MCOPV-13**, D-A polymer **MCOPV-13-Per-7** and a 1:1 physical mixture of **MCOPV-13** and **MCPer-7** in $CHCl_3$ were recorded at concentration of 0.1 OD at 394 nm, excited at 394 nm and given in figure 5.12. Compared with 70 % energy transfer efficiency from OPV moiety to PBI moiety in **MCOPV-13-Per-7,** only 17 % was observed in the 1:1 physical mixture. Thus the covalent linkage of D and A had a drastic influence on the energy transfer in the D-A copolyester. The excitation of **MCOPV-13/MCPer-7 blend** at 394 nm resulted in the energy transfer efficiency of 77 % from OPV to PBI moiety with simultaneous emission at 533, 575 and 625 nm corresponding to the emission of the acceptor, which is also showed in figure 5.12. The energy transfer efficiency from OPV to PBI in **MCOPV-13/MCPer-7 blend** was 4 times more than in the physical mixture of **MCOPV-13** (donor polymer) with **MCPer-7** (acceptor polymer). This gives the direct proof for the ester exchange reaction in the reactive blend of **MCOPV-13** with **MCPer-7**.

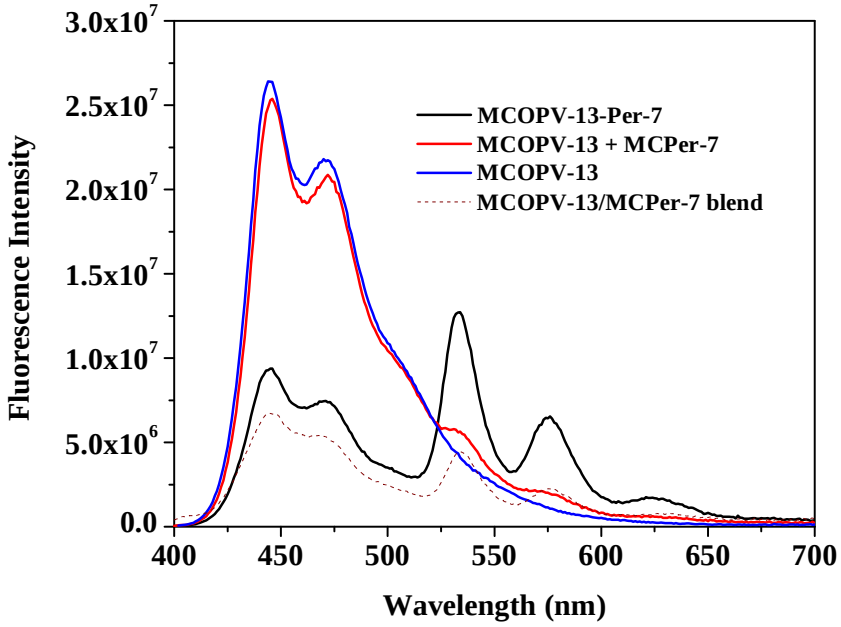

Figure 5.12. *Emission spectra of* ***MCOPV-13****,* ***MCOPV-13-Per-7****,* ***MCOPV-13/MCPer-7 blend*** *and a 1:1 physical mixture of* ***MCOPV-13*** *with* ***MCPer-7*** *(****MCOPV-13*** *+* ***MCPer-7****) in solution (chloroform) [0.1 OD at 394 nm,* λ_{ex} *= 394 nm].*

The photoinduced energy transfer was further supported by fluorescence decay studies. Fluorescence decays were collected at 445 nm (donor emission) with excitation at 390 nm in chloroform at 25 °C. The fluorescence decay profiles of **MCOPV-13** in $CHCl_3$ (λ_{ex} = 390 nm) exhibited biexponential decay with a dominant lifetime of 1.17 ns (α = 0.87) and 1.80 ns (α = 0.13) when monitored at 445 nm (figure 5.13 and table 5.5). In the D-A polymers **MCOPV-13-Per-x**, the decay become fast, with the dominant lifetime of 0.60 ns for **MCOPV-13-Per-4**, which reduced further to 0.35 ns for **MCOPV-13-Per-18**. Such acceleration in decay dynamics of donor in the presence of acceptor provides clear evidence of nonradiative energy transfer, and rule out the possibility of trivial radiative mechanism.[51] The 1:1 physical mixture also exhibited biexponential decay with lifetimes of 1.11 ns (α = 0.81) and 1.71 ns (α = 0.19) when monitored at 445 nm. Noticeably, the fluorescence decay of the 1:1 physical mixture of **MCOPV-13** with **MCPer-7** was found to be almost same as that observed for **MCOPV-13** indicating poor efficiency of energy transfer from donor to acceptor in the physical mixture. The fluorescent decay profile of **MCOPV-13/MCPer-7 blend** exhibited biexponential (χ2 = 1.04) decay with reduced lifetime of 0.44 ns (α = 0.63) and 1.25 ns (α = 0.37) provides the evidence for the energy transfer from OPV to PBI moiety.

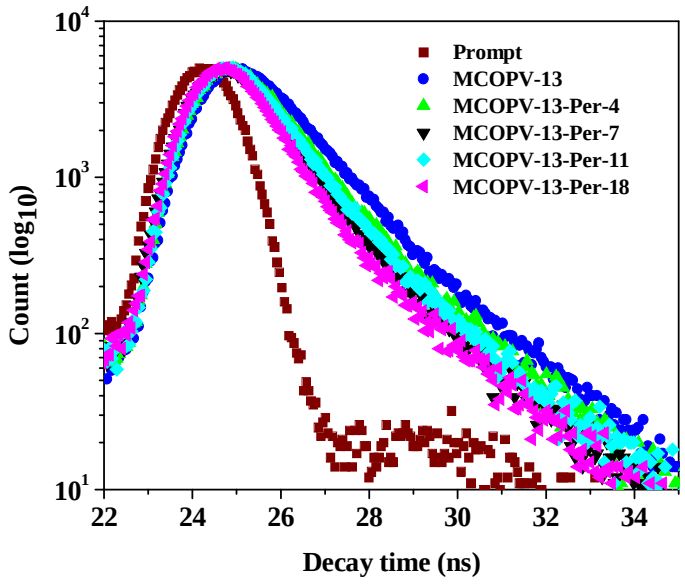

***Figure 5.13**. Fluorescence decay profiles (0.1 OD at 394 nm, λ_{ex} = 390 nm, monitored at 445 nm) on the addition of increasing amount of PBI (from 4 to 18 mol %) in chloroform at room temperature.*

Table 5.5. *Parameters (τ: decay time, α: pre-exponential factor, χ2: chi-squared value) retrieved from the biexponential fit for polyesters in solution (chloroform, 0.1OD at 394 nm). The decay time was collected at 445 nm by using nano LED 390 nm for excitation.*

Polymer	Life Time (ns)				
	τ_1	τ_2	α_1	α_2	χ^2
MCOPV-13	1.17	1.80	0.87	0.13	1.00
MCOPV-13-Per-4	0.60	1.34	0.51	0.49	1.00
MCOPV-13-Per-7	0.47	1.27	0.62	0.38	1.00
MCOPV-13-Per-11	0.42	1.24	0.64	0.36	1.00
MCOPV-13-Per-18	0.35	1.23	0.78	0.22	1.00
Physical mixture of MCOPV-13 with MCPer-7	1.11	1.71	0.81	0.19	1.00
MCOPV-13/MCPer-7 blend	0.44	1.25	0.63	0.37	1.04

The fluorescence decay of **MCOPV-13-Per-7** was also collected at 533 nm (acceptor emission) with excitation at 460 nm in chloroform and compared with that of the acceptor alone polymer **MCPer-7** (figure 5.14). The lifetime at the PBI emission in **MCPer-7** could be fitted to monoexponential (χ2 = 1.06) with lifetime of 3.71 ns and in **MCOPV-13-Per-7,** the decay become fast (χ2 = 1.20) with lifetime of 3.09 ns. This is an indication of presence of electron transfer process resulting in reduced lifetime in the donor-acceptor polymer.

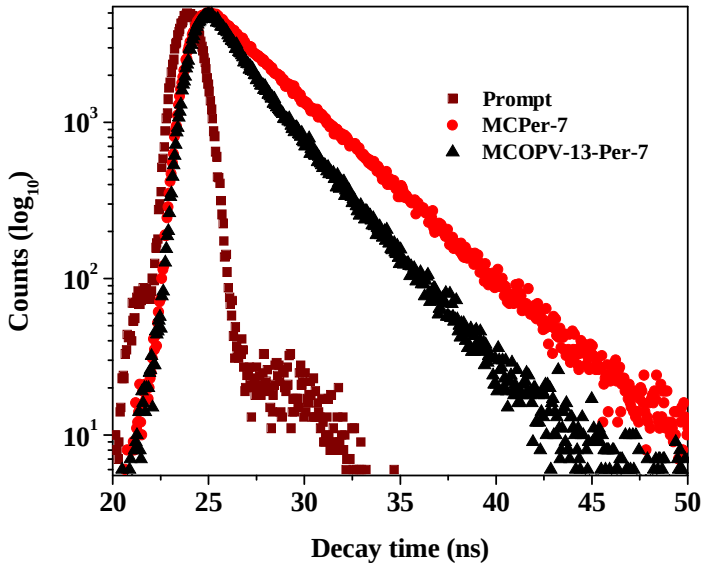

Figure 5.14*. Fluorescence decay profiles (0.1 OD at 490 nm, λ_{ex} = 460 nm, monitored at 533 nm) of* ***MCOPV-13-Per-7*** *and* ***MCPer-7*** *in chloroform.*

Photoexcitation studies were carried out in the solid state for **MCOPV-13**, **MCOPV-7** and **MCOPV-13-Per-x.** Figure 5.15 (a) compares the normalized absorption spectra of thin films of the polymers (0.1 OD at 394 nm) spin-coated from chloroform. The absorption spectra in the solid state, especially for the PBI region was broad and the ratios of peak intensities were different compared to that in solution indicating aggregation tendency.[13] The absorption band of donor–acceptor polymers covered the range from 300-650 nm, suggesting good prospects for complementary solar light harvesting in heterojunctions.[53] The result of photoluminescence (PL) quenching experiments are shown in figure 5.15 (b). The donor polymer, **MCOPV-13** was highly fluorescent even in the solid state. Incorporation of PBI into the donor polymer backbone resulted in ~ 100 % quenching of donor emission by monitoring the PL emission from OPV unit. Energy transfer is excluded from the mechanism of the OPV luminescence quenching in donor–acceptor polymer because the characteristic emission of PBI was not observed when the **MCOPV-13-Per-x** polymers were excited at 394 nm. The observed quenching of photoluminescence that occured in **MCOPV-13-Per-x** could be attributed to photoinduced electron-transfer between donor (OPV unit) to acceptor (PBI unit). Extensive prior studies of donor poly(p-phenylene vinylene) (PPV) and acceptor C_{60} and other fullerene derivatives in blends have clearly established that ultrafast photoinduced electron-transfer from excited PPV to fullerene molecule accounts for PL emission quenching in the combined material.[11, 54, 55]

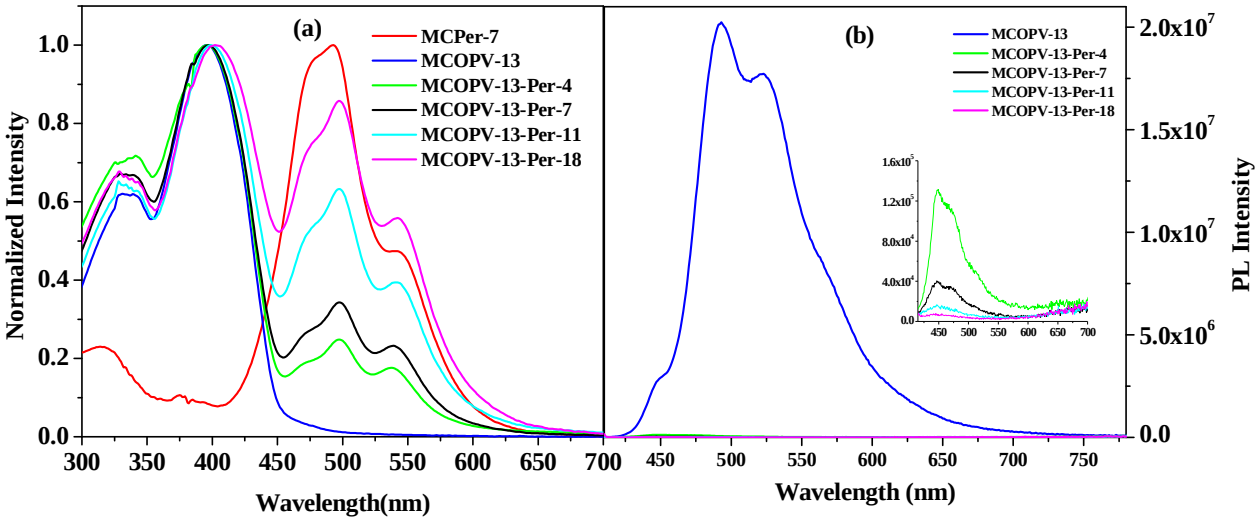

Figure 5.15*. Normalized (a) absorption spectra of polymers in film spin-coated from chloroform and (b) emission spectra of polymers in film spin-coated from chloroform [0.1 OD at 394 nm, λ_{ex} = 394 nm]. Inset shows the quenched emission.*

When the PBI unit of **MCOPV-13-Per-7** were selectively excited at 490 nm, the PBI emission in the polymer was ~ 100 % quenched compared to that of acceptor alone polymer **MCPer-7** indicating a very efficient deactivation of its singlet excited state by charge separation (figure 5.16).

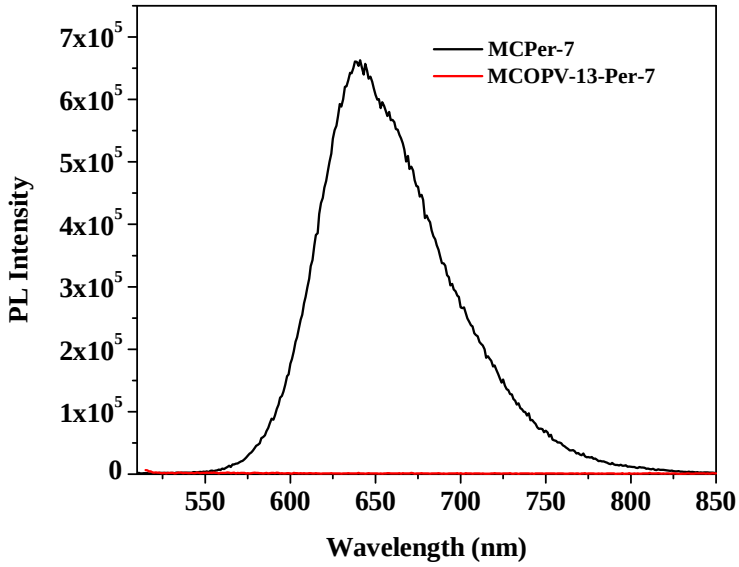

***Figure 5.16**. Emission spectra of **MCPer-7** and **MCOPV-13-Per-7** spin-coated from chloroform [0.1 OD at 490 nm, λ_{ex} = 490 nm].*

The difference in emission properties of **MCOPV-13-Per-x** in solution and solid state was explained by the conformation of polymers. Figure 5.17 shows the schematic representation of the probable packing of the OPV and PBI units in the solution and solid state. In solution state, OPV and PBI units are far apart than in solid state and face-to-face orientation of OPV and PBI chromophores are not efficient to cause electron transfer from donor to the acceptor. The electron transfer from D to A in film state may be due to the face-to-face orientation of OPV and PBI moiety. The thin film X-ray diffraction data in figure 5.5 also supported π-π stacking interactions, which was indicated by the increased intensity of the diffraction at 3.57 Å with increased incorporation of PBI. The driving force for such orientations is the π-stacking in combination with electrostatic or weak charge-transfer interaction.[56]

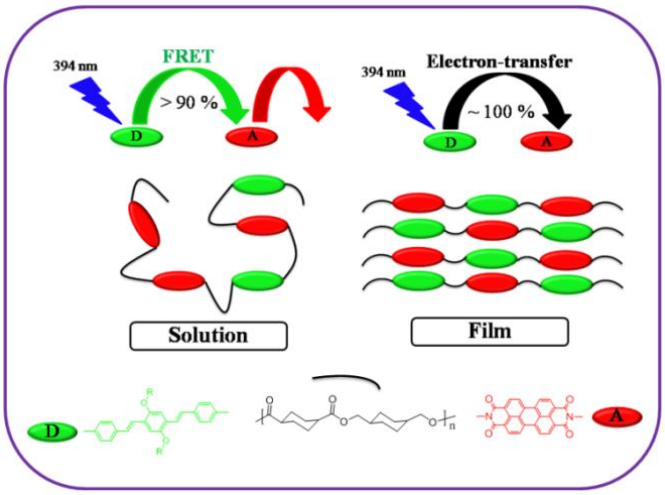

Figure 5.17. *Schematic representation of packing of donor (OPV) and acceptor (PBI) units in the solution and solid state highlighting the energy and electron transfer processes.*

5.4. Conclusion

Random copolyesters of **PCCD** incorporating oligo(*p*-phenylenevinylene) (OPV) as donor (D) and perylenebisimide (PBI) as acceptor (A) were successfully synthesized by melt polycondensation. All the polyesters were characterized by ^{1}H NMR, SEC, viscosity, TGA, DSC and WXRD analyses. In solution state, the selective excitation of the OPV chromophore led to the energy transfer efficiency of > 90% from OPV to the PBI moiety and the energy transfer efficiency increased with increasing mol % incorporation of PBI in the copolyester. The efficiency of energy transfer from OPV to PBI moiety was four times more in donor/acceptor copolyester blend than in the physical mixture of donor and acceptor alone polymer after selective excitation of donor chromophore gives the direct proof for the ester exchange reaction in polyester/polyester reactive blending. The donor polymer, **MCOPV-13** was highly fluorescent even in solid state. Incorporation of ~ 4 mol % of PBI as in **MCOPV-13-Per-4** resulted in ~ 100% quenching of donor emission. The observed quenching of photoluminescence of OPV chromophore in the thin films was assigned to photoinduced electron transfer between donor (OPV unit) to the acceptor (PBI unit). The difference in emission properties of D-A polyesters in solution and solid state was explained by the conformation of polymers. The photoluminescence and the wide angle X-ray scattering in film revealed better packing of chromophore in the polyester backbone. The HOMO and LUMO values of polymers were calculated using cyclic voltammetry and these energy values fulfil the energetic condition required for the electron transfer in solid state from donor to the acceptor.

5.5. References

1) Skotheim, T. A.; Reynolds, J. R. *Handbook of Conducting Polymers*; CRC Press, **2007**.
2) Leclerc, M.; Morin, J.-F. *Design and Synthesis of Conjugated Polymers*; Wiley-VCH, **2010**.
3) Osaka, I.; Sauvé, G.; Zhang, R.; Kowalewski, T.; McCullough, R. D. *Adv. Mater*. **2007**, *19*, 4160-4165.
4) Zhang, M.; Tsao, H. N.; Pisula, W.; Yang, C.; Mishra, A. K.; Müllen, K. *J. Am. Chem. Soc*. **2007**, *129*, 3472-3473.
5) Kavarnos, G. J. *Fundamentals of Photoinduced Electron Transfer*; Wiley-VCH, **1993**.
6) Balzani, V. *Electron Transfer in Chemistry*; Wiley-VCH, **2001**.
7) Fox, M. A.; Chanon, M. *Photoinduced Electron Transfer*; Elsevier, **1988**.
8) Warman, J. M.; De Haas, M. P.; Verhoeven, J. W.; Paddon-Row, M. N. *Adv. Chem. Phys.* **1999**, *106*, 571-601.
9) Wasielewski, M. R. *Chem. Rev.* **1992**, *92*, 435-461.
10) Guldi, D. M. *Chem. Soc. Rev*. **2002**, *31*, 22-36.
11) Yu, G.; Gao, J.; Hummelen, J. C.; Wudl, F.; Heeger, A. J. *Science* **1995**, *270*, 1789-1791.
12) Günes, S.; Neugebauer, H.; Sariciftci, N. S. *Chem. Rev.* **2007**, *107*, 1324-1338.
13) Bauer, P.; Wietasch, H.; Lindner, S. M.; Thelakkat, M. *Chem. Mater*. **2007**, *19*, 88-94.
14) Dudek, S. P.; Pouderoijen, M.; Abbel, R.; Schenning, A. P. H. J.; Meijer, E. W. *J. Am. Chem. Soc*. **2005**, *127*, 11763-11768.
15) Alam, M. M.; Jenekhe, S. A. *Chem. Mater.* **2004**, *16*, 4647-4656.
16) Ward, M. D. *Chem. Soc. Rev.* **1997**, *26*, 365-375.
17) Devadoss, C.; Bharathi, P.; Moore, J. S. *J. Am. Chem. Soc.* **1996**, *118*, 9635-9644.
18) Wang, P. -W.; Liu, Y. -J.; Devadoss, C.; Bharathi, P.; Moore, J. S. *Adv. Mater*. **1996**, *8*, 237-241.
19) Schultze, X.; Serin, J.; Adronov, A.; Fréchet, J. M. J. *Chem. Commun*. **2001**, *13*, 1160-1161.
20) Dutton, P. J.; Conte, L. *Langmuir* **1999**, *15*, 613-617.
21) Stewart, G. M.; Fox, M. A. *J. Am. Chem. Soc.* **1996**, *118*, 4354-4360.
22) Sommer, M.; Huettner, S.; Thelakkat, M. *J. Mater. Chem.* **2010**, *20*, 10788-10797.
23) Barrau, S.; Heiser, T.; Richard, F.; Brochon, C.; Ngov, C.; van de Wetering, K.; Hadziioannou, G.; Anokhin, D. V.; Ivanov, D. A. *Macromolecules* **2008**, *41*, 2701-2710.

24) Wu, F.-C.; Cheng, H.-L.; Chen, Y.-T.; Jang, M.-F.; Chou, W.-Y. *Soft Matter* **2011**, *7*, 11103–11110.

25) Wu, F.-C.; Huang, Y.-C.; Cheng, H.-L.; Chou, W.-Y.; Tang, F.-C. *J. Phys. Chem. C* **2011**, *115*, 15057-15066.

26) Wu, F. -C.; Hsu, S. -W.; Cheng, H. -L.; Chou, W. -Y.; Tang, F. -C. *J. Phys. Chem. C* **2013**, *117*, 8691-8696.

27) Nisha, S. K.; Asha, S. K. *J. Polym. Sci. A Polym. Chem.* **2013**, *51*, 509–524.

28) Neuteboom, E. E.; Meskers, S. C. J.; Van Hal, P. A.; van Duren, J. K. J.; Meijer, E. W.; Janssen, R. A. J.; Dupin, H.; Pourtois, G.; Cornil, J.; Lazzaroni, R.; Brėdas, J. -L.; Beljonne, D. *J. Am. Chem. Soc.* **2003**, *125*, 8625-8638.

29) Mikroyannidis, J. A.; Stylianakis, M. M.; Sharma, G. D.; Balraju, P.; Roy, M. S. *J. Phys. Chem. C* **2009**, *113*, 7904–7912.

30) Neuteboom, E. E.; van Hal, P. A.; Janssen, R. A. J. *Chem. Eur. J.* **2004**, *10*, 3907-3918.

31) Rao, K. V.; Haldar, R.; Kulkarni, C.; Maji, K. T.; George, S. J. *Chem. Mater*. **2012**, *24*, 969-971.

32) Lang, A. S.; Thelakkat, M. *Polym. Chem.* **2011**, *2*, 2213-2221.

33) Würthner, F. *Chem. Commun.* **2004**, *14*, 1564-1579.

34) Hüttner S.; Sommer M.; Thelakkat M. *Appl. Phys. Lett.* **2008**, *92*, 093302/1-3.

35) Li, J.; Dierschke, F.; Wu, J.; Grimsdale, A. C.; Müllen, K. *J. Mater. Chem.* **2006**, *16*, 96-100.

36) Horowitz, G.; Kouki, F.; Spearman, P.; Fichou, D.; Nogues, C.; Pan, X.; Garnier, F. *Adv. Mater.* **1996**, *8*, 242-245.

37) Struijk, C. W.; Sieval, A. B.; Dakhorst, J. E. J.; van Dijk, M.; Kimkes, P.; Koehorst, R. B. M.; Donker, H.; Schaafsma, T. J.; Picken, S. J.; van de Craats, A. M.; Warman, J. M.; Zuilhof, H.; Sudhölter, E. J. R. *J. Am. Chem. Soc.* **2000**, *122*, 11057-11066.

38) Ling, M. M.; Erk, P.; Gomez, M.; Koenemann, M.; Locklin, J.; Bao, Z. *Adv. Mater.* **2007**, *19*, 1123-1127.

39) Legros, A.; Carreau, P. J.; Favis, B. D. *Polymer* **1994**, *35*, 758-764.

40) Fakirov, S. *Transreactions in Condensation Polymers*; Wiley-VCH, **1999**.

41) Jayakannan, M.; Deepa, P. *J. Polym. Sci. A Polym. Chem.* **2008**, *46*, 5897-5915.

42) Colonna, M.; Berti, C.; Binassi, E.; Celli, A.; Fiorini, M.; Marcheses, P.; Messori, M.; Brunelle, D. J. *Polym Int* **2011**, *60*, 1607-1613.

43) Liu,Y.; Turner, S. R.; Wilkes, G. *Macromolecules* **2011**, *44*, 4049-4056.

44) Percec, V.; Aqad, E.; Peterca, M.; Imam, M. R.; Glodde, M.; Bera, T. K.; Miura, Y.; Balagurusamy, V. S. K.; Ewbank, P. C.; Würthner, F.; Heiney, P. A. *Chem. Eur. J.* **2007**, *13*, 3330-3345.

45) Lee, S. K.; Zu, Y.; Herrmann, A.; Geerts, Y.; Müllen, K. u.; Bard, A. J. *J. Am. Chem. Soc.* **1999**, *121*, 3513-3520.

46) Grisorio, R.; Allegretta, G.; Romanazzi, G.; Suranna, G. P.; Mastrorilli, P.; Mazzeo, M.; Cezza, M.; Carallo, S.; Gigli, G. *Macromolecules* **2012**, *45*, 6396-6404.

47) Balakrishnan, K.; Datar, A.; Naddo, T.; Huang, J.; Oitker, R.; Yen, M.; Zhao, J.; Zang, L. *J. Am. Chem. Soc.* **2006**, *128*, 7390-7398.

48) Lin, X.; Hirono, M.; Seki, T.; Kurata, H.; Karatsu, T.; Kitamura, A.; Kuzuhara, D.; Yamada, H.; Ohba, T.; Saeki, A.; Seki, S.; Yagai, S. *Chem. Eur. J.* **2013**, *19*, 6561-6565.

49) Jonkheijm, P.; van Duren, J. K. J.; Kemerink, M.; Janssen, R. A. J.; Schenning, A. P. H. J.; Meijer, E. W. *Macromolecules* **2006**, *39*, 784-788.

50) Ajayaghosh, A.; Praveen, V. K.; Srinivasan, S.; Vargese, R. *Adv. Mater.* **2007**, *19*, 411-415.

51) Lakowicz, J. R. *Principles of Fluorescence Spectroscopy*; Springer, **2010**.

52) Abbel, R.; Grenier, C.; Pouderoijen, M. J.; Stouwdam, J. W.; Leclére, P. E. L. G.; Sijbesma, R. P.; Meijer, E. W.; Schenning A. P. H. J. *J. Am. Chem. Soc.* **2009**, *131*, 833-843.

53) Thompson, B. C.; Fréchet J. M. J. *Angew. Chem. Int. Ed*. **2008**, *47*, 58-77.

54) Sariciftci, N. S.; Smilowitz, L.; Heeger, A. J. Wudl, F. *Science* **1992**, *258*, 1474-1476.

55) Smilowitz, L.; Sariciftci, N. S.; Wu, R.; Gettinger, C.; Heeger, A. J.; Wudl, F. *Phys. Rev. B*. **1993**, *47*, 13835-13842.

56) Hill, D. J.; Mio, M. J.; Prince, R. B.; Hughes, T. S.; Moore, J. S. *Chem. Rev.* **2001**, *101*, 3893-4011.

Chapter 6

Summary and Conclusions

Chapter 6

Summary and Conclusions

The thesis entitled '**Solution-Processable Random Copolyesters containing Perylenebisimide and Oligo(*p*-phenylenevinylene) by Reactive Blending'** deals with the design and development of new solution processable random copolyesters based on perylenebisimide and oligo(*p*-phenylenevinylene). These chromophores were incorporated into the backbone of commercially available polyesters using transesterification and thereby combined the electronic and optical properties of semiconductors with the attractive processing advantages of polyesters. The ability to combine existing polymers into new compositions offers the advantage of reduced research and development expense compared to the development of new monomers and polymers to yield a similar property profile.

A successful strategy for the incorporation of fluorescent chromophores like perylenebisimide (PBI) and oligo(*p*-phenylenevinylene) (OPV) into the backbone of an engineering thermoplastic polyester [Poly(1,4-cyclohexylenedimethylene-1,4-cyclohexanedicarboxylate)] (**PCCD**) has been demonstrated. The chemical incorporation of these chromophores into the polyester backbone was proved by carrying out the melt condensation of the polymers from the monomers 1,4-cyclohexanedimethanol (CHDM) and 1,4-dimethylcyclohexane dicarboxylate (DMCD) with varying mole ratios of terminal hydroxyl functionalized PBI and OPV derivatives. The packing difference between the polymers synthesized by high-temperature solution-blending and melt polycondensation was reflected in their photophysical properties with the polymers developed via the solution blending approach showing less aggregation tendency compared to melt condensation polymers and higher fluorescence quantum yield for polymers of similar perylene incorporation. Polymers synthesized using solution blending approach possessed thin film processability require for device applications.

A novel series of copolyesters incorporating varying mol ratios of an achiral oligo(*p*-phenylenevinylene) (OPV) into the backbone of a chiral poly(L-lactic acid) (**PLLA**) was synthesized by high temperature solution blending of **PLLA** with hydroxyl group functionalized OPV molecule (OPV-2-Diol). The chemical incorporation of OPV chromophore into the polyester backbone was proved by ^{1}H NMR spectroscopy. The

differential scanning calorimetry (DSC), wide-angle X-ray diffraction (WXRD), absorption, emission and lifetime-decay studies showed that OPV chromophore was aggregated in the solid state. The right-handed helical self-assembly of the achiral OPV segments driven by the chiral **PLLA** segments in the solid state was proved by CD investigation and AFM analysis. This methodology provides opportunities for the design of a new class of hierarchical self-assembled architectures based on organic π-conjugated materials and the manipulation of their optical properties. Nanofibers of random copolyester of **PLLA** incorporating OPV chromophore was constructed by electrospinning technique. Electrospun fibers of this polymer showed both blue and green emission upon excitation at different wavelengths.

High molecular weight random copolyesters of **PLLA** and **PCCD** incorporating varying mol % of perylenebisimide (PBI) were successfully synthesized by high-temperature solution-blending. All the polyesters were characterized by ^{1}H NMR, SEC, viscosity, TGA, DSC and WXRD analyses. The chemical incorporation of PBI chromophore in the backbone of the polyester was confirmed by SEC and DSC analysis. These polymers showed good solubility, film-forming properties and displayed strong red photoluminescence. The photophysical properties were studied using steady-state UV-vis absorption and fluorescence spectroscopy in solution as well as in solid state. All polymers were highly fluorescent in solution state. The solid state fluorescence quantum yield of the polymers decreased with increasing mol % incorporation of PBI units. Red fluorescent nanofibers of these polymers were successfully constructed by electrospinning technique. This approach was extended for the construction of the nanofibers of copolyester of **PLLA** and **PCCD** incorporating both OPV and PBI chromophore. Blue, green and red emission from this polymer was observed under fluorescence microscopy upon excitation at different wavelengths. These interesting emission properties make them potential candidates in various nanodevice applications including laser, waveguide and polarized emission.

Towards the end, random copolyesters consisting of oligo(*p*-phenylenevinylene) (OPV) as donor (D) and perylenebisimide (PBI) as acceptor (A) were successfully synthesized by melt polycondensation. All the polyesters were characterized by ^{1}H NMR, SEC, viscosity, TGA, DSC and WXRD analyses. In solution state, the selective excitation of the OPV chromophore led to the energy transfer efficiency of > 90% from OPV to the PBI moiety and the energy transfer efficiency increased with increasing mol % incorporation of PBI in the copolyester. The efficiency of energy transfer from OPV to PBI moiety was four

times more in donor/acceptor copolyester blend than in the physical mixture of donor and acceptor alone polymer after selective excitation of donor chromophore gives the direct proof for the ester exchange reaction in polyester/polyester reactive blending. The donor polymer, **MCOPV-13** was highly fluorescent even in solid state. Incorporation of ~ 4 mol % of PBI as in **MCOPV-13-Per-4** resulted in ~ 100 % quenching of donor emission. The observed quenching of photoluminescence of OPV chromophore in the thin films was assigned to photo-induced electron transfer from donor (OPV unit) to the acceptor (PBI unit). The difference in emission properties of D-A polyesters in solution and solid state was explained by the conformation of polymers. The photoluminescence and the wide angle X-ray scattering in film revealed better packing of chromophore in the polyester backbone. The HOMO and LUMO values of polymers were calculated using cyclic voltammetry and these energy values fulfil the energetic condition required for the proposed electron transfer in solid state from donor to the acceptor.

In short, this thesis work is focused on design and development of new solution processable semiconducting polymers based on perylenebisimide and oligo(*p*-phenylenevinylene) for optoelectronic applications. The transesterification by high-temperature solution-blending approach described here is easily adoptable for a wide range of suitably derivatised donor or acceptor molecules resulting in tunable photophysical properties with film forming ability. The polymers developed in the thesis can be explored for various applications in optoelectronics.

List of Publications in international journals

1. **Nisha, S. K.**; Asha, S. K. A Facile One-Pot Reactive Solution Blending Approach for Main-Chain Donor-Acceptor Polymeric Materials. *J. Polym. Sci. A: Polym. Chem.* **2013**, *51*, 509-524.
2. **Nisha, S. K.**; Asha, S. K. Donor-Acceptor Random Copolyesters Containing Perylenebisimide (PBI) and Oligo(*p*-phenylenevinylene) by Melt Condensation Polymerization: Energy Transfer Studies. *J. Phys. Chem. B.* **2013**, *117*, 13710-13722.
3. **Nisha, S. K.**; Asha, S. K. Chiral Poly(L-lactic acid) Driven Helical Self-Assembly of Oligo(*p*-phenylenevinylene. *J. Mater. Chem. C* **2014**, *2*, 2051-2060.
4. **Nisha, S. K.**; Asha S. K. Random copolyesters containing Perylenebisimide: Flexible Films and Fluorescent Fibers for Advanced Photonic Applications. ***Manuscript under preparation***.

Patent

5. **Kumari Nisha, S.**; Asha, S. K. Perylenebisimide-Polyester Blend. ***Patent Application*** **(2012) WO 2012/111026 A1.**

Papers published in conferences

6. **Nisha, S. K.**; Asha, S. K. Perylenebisimide-Polyester Blend Films for Photovoltaic Applications. Macro-2010, Delhi, **2010**.
7. **Nisha, S. K.**; Asha S. K. Solution Processable n-type Perylenebisimide Copolyesters for Photovoltaic Application. Science day -2011, NCL-Pune, **2011**.
8. **Nisha S. K.**; Asha S. K. A facile one-pot Reactive Blending Approach for Main Chain Donor-Acceptor Polymeric Materials. Poly Tech-2012, NCL-Pune, **2012** (oral presentation).
9. **Nisha S. K.**; Asha S. K. A facile one-pot Reactive Blending Approach for Main Chain Donor-Acceptor Polymeric Materials. Macro-2013, Bangalore, **2013**.